1 7™ International Mining Congress and Exhibition of Turkey- IMCET2001, © 2001, ISBN 975-395-417-4

Stability Analysis and Support Design of Glandroud Coal Mine Tunnel

K.G.Goshtasbi & S.F.Dehghan
Department of Mining Engineering, School of Engineering, Tarbiat Modares University, Tehran, Iran

ABSTRACT: This paper reports the results of a research study which was carried out in order to analyze the stability of a tunnel at Glandroud coal mine, which is situated in northern Iran. The tunnel, with dimensions of 3 x 3.2 meters, was excavated at a depth of 150 meters below the surface. A numerical method was used to analyze the stability of the tunnel. Due to the structural, features and geology of the area, the distinct element method was used and the code utilized according to this method was UDEC. The results obtained from the numerical analysis show that instability in the tunnel is due to block falls from the roof and sidewalls. In view of this, various support systems were analyzed. This analysis shows that a combination of grouted rock bolt and shotcrete is the most suitable support system in Glandroud coal mine tunnel.

1 INTRODUCTION

The excavation of tunnels in coal mines causes instability, which may occur as a result of roof falls, wall failures or a combination of both. Therefore, in order to conduct safe mining operations, the stability of such tunnels is very important The prime concern in excavations is the control of displacements in the rock surrounding the excavation. In each excavation the design objective is to ensure that displacements of the rock around the excavation do not interfere with specified engineering activities (Pan et al. 1991).

Computer modeling for strata control and in rock mechanics has developed significantly in recent years. There are various numerical methods and codes available for stability analysis of tunnels. One of these methods İs the distinct element method, which has been developed for deformation and stability analysis of multiple-jointed rock masses around underground structures. Due to the structural features and geology of the Glandroud area, the distinct element method was used for stability analysis. The code utilized according to this method was UDEC. Many researchers have found UDEC to be a very powerful code when analyzing underground structures in various rock masses.

2 GEOLOGY

The Glandroud coal mine is İn the northern part of the Alborz Mountains, situated in northern Iran. Exploration studies have revealed that there are 14 coal seams which can be extracted (Glandroud & coal deposit 1998). These seams range from 0.5 to 1 meter in thickness. The lithology mainly consists of roof siltstone, coal and floor siltstone.

Field investigations were carried out and the general trend and characteristics of the joint structure were then determined. The analyzed data show that there are two joint sets in the floor and roof siltstones and a bedding plane in the coal seam. Table I shows the dip and dip directions of these joint sets regarding the roof siltstone, floor siltstone and coal seam. These details were then used İn model generation.

Table I. Joint directions in roof siltstone, coat seam and floor siltstone.

Formation	Joint set	Dip O	Dipi direcnon O	Spacing (m)
Roof Siltstone	11	55	124	0.54
	J2	81	187	0.85
Coal Seam	J1	70	14	0.33
Floor Siltstone	J1	55	127	0.38
	J2	82	24	0.65

3 GEOMECHANICAL PROPERTIES

Laboratory investigations were carried out in order to determine the physical and mechanical properties of the rocks and joints. Mechanical and physical tests were carried out on samples from the roof siltstones, floor siltstone and coal seam. With this consideration, uniaxial, triaxial and shear strength tests were carried out İn accordance to lSRM suggested methods (Brown 1981). Table 2 shows the material properties used in model stability analysis.

Table 2. Geo mechanical properties

Property	Roof siltstone	Coal	Floor siltstone
U.C.S. (MPa)	11.3	5.85	10.7
Young's Modulus (MPa)	900	1300	850
Possion's ratio	031	0.28	0.33
Cohesion (MPa)	2.15	1.90	2.43
Friction angle (deg.)	25	30	23
Tensile strength (MPa)	1.65	1.15	1.4
Unit weight (KN/m^3)	26	13.1	27

4 NUMERICAL ANALYSIS

There are various numerical methods and programs available, each of which has its own applicabilities regarding the rock mass and discontinuités encountered in underground structures.

The universal distinct element code (UDEC, Itasca 1992) is a powerful numerical method for analyzing the stability of structures in jointed rock masses. In UDEC, the rock mass is presented as an assemblage of distinct blocks having joints between the blocks. Each block can be modeled with either rigid or deformabie materials. The rigid blocks represent me medium as a set of distinct blocks which do not change their geometry as a result of applied loading. Deformabie blocks are internally discretized into finite difference elements, with each element behaving according to a prescribed linear or non-linear stress-strain constitutive relationship. UDEC uses time-marching finite difference schemes to solve the force equations of morion in the system.

4.1 *Model simulation*

Glandroud coal mine tunnel no. 630, with dimensions of 3 x 3.2 meters, was excavated at a depth of 150 meters below the surface. The model geometry was built up in accordance with the joint dip and dip directions given in Table 1. All the models analyzed had dimensions of 17 x 17 meters. Figure 1 shows the model geometry of Glandroud coal mine tunnel. The block material properties were used from the properties given in Table 2.

The UDEC's Mohr Coulomb plasticity model was used to simulate the intact rock of the blocks. However, for simulating discontinuities the joint area contact-Coulomb slip model was used.

The main objective of the model simulation was to model effectively the important behavior mechanism and modes of rock failure occurring in the tunnel under study. Thus, numerical models were analyzed under various horizontal-to-vertical stress ratios (k), ranging from 0.5 to 2. The analyzed data show that the models with a horizontal-to-vertical stress ratio of 1.5 produced very close findings compared to the observations and measurements that were taken in the mine. Therefore, this stress ratio was utilized for stability analysis and support design.

The model simulation process was checked by die resulting unbalanced force. The model converged to an equilibrium state when the unbalanced force in the model reached an acceptable value.

5 STABILITY ANALYSIS

The results of the UDEC distinct element analysis are obtained in terms of stress and displacement contours. Many models were analyzed under various in-situ stress fields. The minimum and maximum displacements occurred in models wim k=0.5 and k=2 respectively. However, the displacements obtained from the model with k=1.5 were very close to those measured in the Glandroud coal mine tunnel. Therefore, the results below are from models withk=1.5.

Figure 2 and Figure 3 show the displacement vectors and principal stresses respectively after excavation of the tunnel. The maximum displacements in the roof and floor of the tunnel were 48 and 23.5 centimeters respectively. The maximum displacements in the left and right sidewalls were about 20 centimeters. The results also show that minor block falls occurred in the roof and sidewalls. Therefore, supports were needed in order to control the displacements and block falls. Many support systems were analyzed, and die most suitable support system was found to be a combination of reinforced shotcrete and rock bolts. The bolt spacing was 2 meters in tie roof and 1 meter in the sidewalls. The thickness of the reinforced shotcrete was 20 centimeters. Figure 4 shows displacement vectors after support installation, clearly indicating that very little displacement occurred in the model. Figure 5 and Figure 6 show me shear force and axial force on the support system. The forces on the structure clearly indicate that no yielding occurs and therefore the tunnel is stable with this support system.

6 CONCLUSIONS

This investigation has shown that the distinct element method and the UDEC code can successfully model and analyze the stability of tunnels in coal mines.

This can best be achieved if the in-situ stress, geomechanical properties and joint structure are properly measured. The numerical analysis showed that the stress ratio of k=1.5 produced displacements which were in close agreement with measurements from the Glandroud coal mine tunnel. The maximum displacement was 48 centimeters, which occurred in the roof. The UDEC code has the capacity to model various support systems. The designed support system was 20 centimeters of reinforced shotcrete and rock bolts in the roof and sidewalls. This support system proved to be suitable in controlling block falls and displacements in the tunnel. Therefore, this support system is recommended for stabilizing the tunnel in Glandroud coal mine.

REFERENCES

Brown, E.T. 19B1. *Rock characterization testing & monitoring. ISRM suggested methods.* Pergamon Press.

Glandroud & Coal deposits 1998. Preliminary exploration, *final report,* vol. 1.N1SC.

liasca Consulting Group, Inc. 1992. *Universal Distinct Element Code,* version 1.8, user manual, v. 1 & 2.

Pan, X.D. & Hudson, J.A [991. Large déformation Analysis for rock excavations. *Intt of Mining and Met. Trans.*

Pande, G.N., Beer, G. & Williams, J.R. 1990. *Numerical methods in rock mechanics* John Wiley & Sons.

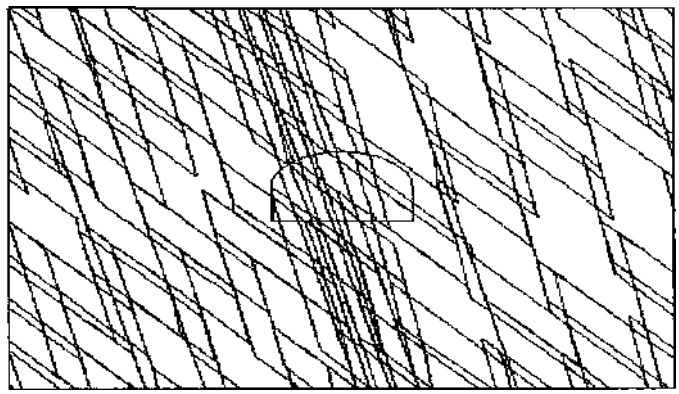

Figure İ. UDEC model geometry.

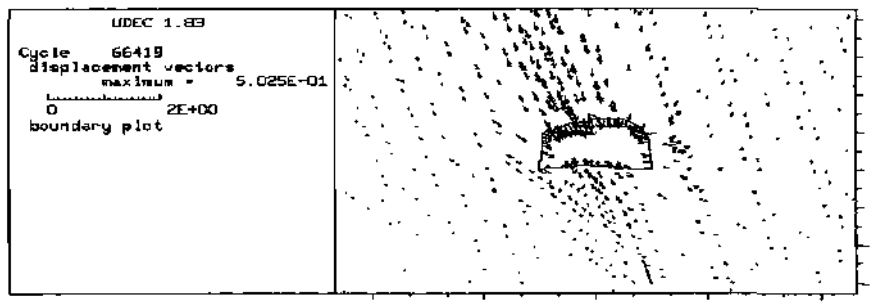

Figure 2. Model displacement vectors.

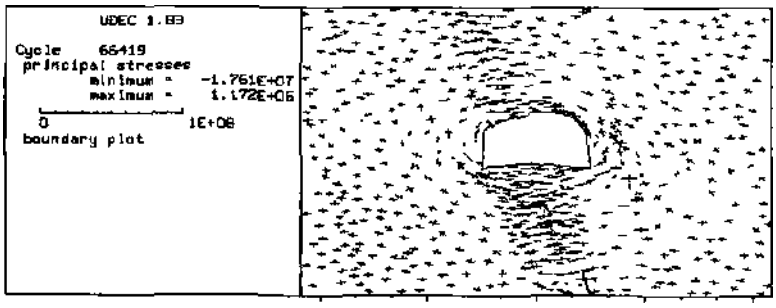

Fi Türe 3. Mode! principal stresses.

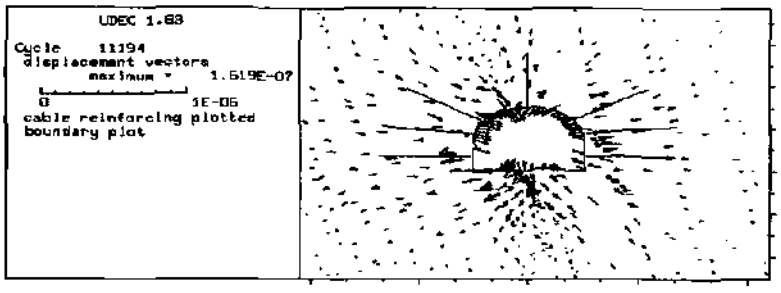

Figure 4. Displacement vectors after support installations.

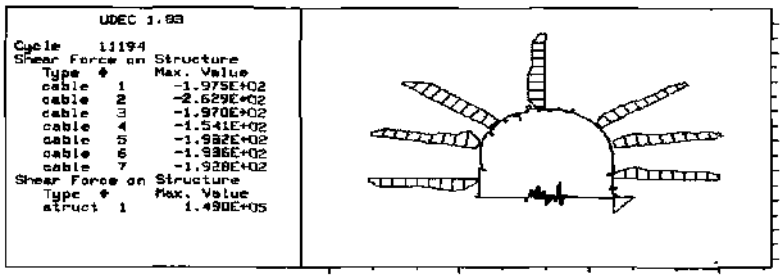

Figure 5. Shear forces on supports.

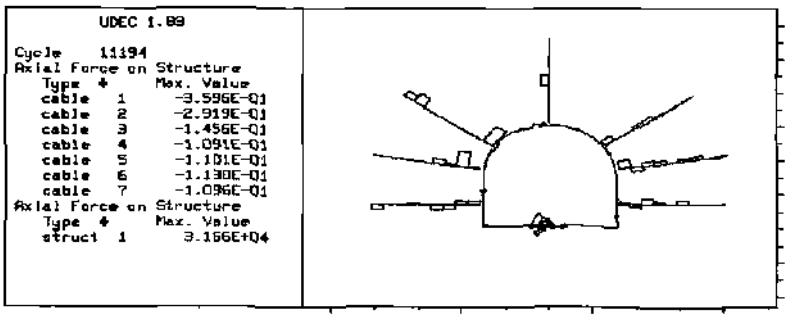

Figure 6. Axial forces on supports.

17* International Mining Congress and Exhibition of Turkey- IMCET2001, ©2001, ISBN 975-395-417-4

Some Considerations of Highwall Mining Systems in Coal Mines

K.Matsui & H.Shimada
Department of Earth Resources and Mining Engineering, Kyushu University, Fukuoka, Japan
S.Kramadibrata & M.S.Rai
Department of Mining Engineering, institute of Technology Bandung, Indonesia

ABSTRACT: The purpose of the highwall mining system is to extract coal with an auger machine or a continuous miner from exposed seams at the base of open pit or strip operations. The major factors in the highwall mining system are coal recovery and the stability of the highwall. A large amount of coal remains isolated and undeveloped as pillars due to previous indiscriminate mining operations performed by the use of the auger or the continuous miner. Therefore, it is necessary to increase the coal extraction ratio, and to reduce the threat of failure of the pillars and highwall and reduce damage caused by subsidence at the surface. This paper describes the background of the study, reviews the highwall mining system and discusses some considerations in the application of highwall mining systems with a view to increasing the extraction ratio and keeping the highwall stable.

1 INTRODUCTION

Final highwalls in open pit coal mines can form a starting point for other mining methods, such as highwall or underground mining. In its basic application, highwall mining is a technique utilized after the open pit portion of a reserve has been mined, sometimes prior to the introduction of underground mining (Seib, 1993).

However, a large amount of coal tends to remain isolated and undeveloped as pillars due to previous indiscriminate mining operations performed by the use of an auger machine or a continuous miner. Moreover, highwall mining may cause highwall instability and surface subsidence.

In this study, the background of the study is described, then the highwall mining system is reviewed, and finally, some considerations are discuseed with a view to increasing the extraction ratio and maintaining the stability of the highwalL

2 BACKGROUND

Indonesia produces over 70 million tons of clean coal annually and is the second largest coal exporter to Japan, with about 12 million tons annually. 99% of the total production of coal is from open pit mines. It is anticipated that more open pit mines will be developed and more coal will be mined underground in order to fulfill the great demand for coal in Indonesia and the rest of the world.

In order to maintain its confidence as the largest coal importer in the world, Japan has started a 'five-year plan for coal technology transfer'. Under the plan, Japanese coal technology will be transferred to coal-producing countries, especially Indonesia.

In the academic field, joint research work has, since 1998, been conducted by Kyushu University, Japan, Institute of Technology Bandung (ITB) and the Indonesian Institute of Sciences-LIPI at Ombilin Coal Mine, Indonesia. This work is directed primarily towards the optimal support system and the development of optimal underground mining systems in Indonesia. Some findings of the joint research project have already been reported (Anwar et al., 1998, 1999a, b; Matsui et al., 1999a; Kramadibrata et al., 2000; Matsui et al., 2000a, b).

Because almost all the coal is extracted from open pit mines in Indonesia, there are many sites where mining operations have developed long highwalls that have been abandoned due to the economics of the day. Mining operations have been transferred to lower stripping ratio blocks of coal or overlying seams. In some cases, coal lies buried beneath spoil heaps or is covered with mud and water. It is estimated that there is a great deal of coal beneath both abandoned and working highwalls. In light of this, it seems to be worth pursuing the possibility of the introduction of highwall mining systems into Indonesian open pit mines.

3 HIGHWALL MINING SYSTEMS

A highwall mining system extracts coal from exposed seams at the base of open pit or strip operations as shown in Figure 1. Auger machines and continuous miners are suited to ail applications where a seam of coal has been exposed as a result of open pit mining. Seams as thin as 1 meter can be highwall mined depending on the choice of system.

Final highwalls in open pit coal mines can form a starting point for other mining methods, such as highwall or underground mining. In its basic application, highwall mining is a technique utilized after the open pit portion of a reserve has been mined, sometimes prior to the introduction of underground mining.

Surface reclamation and/or rehabilitation costs after highwall mining are minimized due to the small bench required to gain access to the coal seam.

The narrow bench needed to operate the highwall mimng system is cot only economically attractive, but also offers minimal disturbance to the surrounding land, making mining possible on relatively small properties. The highwall mining system is extremely mobile and can be moved from pit to pit İn a matter of hours, or from one mine to another in a day or two.

Many coal seams that are presently uneconomical or technically unsuited to conventional mining techniques can be recovered using the highwall mining system.

3 A Auger Mining

Augers became part of the contour-mining cycle in hilly areas in the Appalachian coalfields during the 1950s. They allowed the recovery of additional coal that would have otherwise been left. They began growing in size and power in the 1960s, so that by the early 1970s some were being built with a diameter of as large as 2.1 m and were capable of drilling up to 60 m into the coal seam. New auger designs have boosted the use of augering. Some new designs are capable of boring almost square holes while others can back-ream the holes to pull out a higher percentage of coal.

The auger system works at right angles to the highwall, driving a 5 5-m long cutting head into the coal seam, as shown in Figure 2. The motion of the cutting process carries the coal back to the collar of the excavation.

The auger machine can excavate holes over 100 m long and 1.0 m in diameter and greater İn the coal seams from highwalls, depending on the method of application. Single or multiple pass operations are possible.

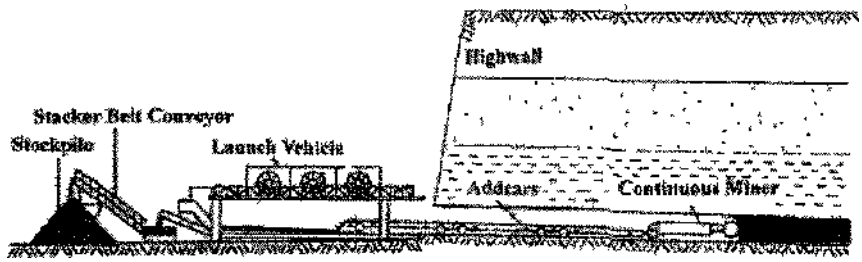

Figure 1. Highwall mining system


Figure 2. Auguer mining

In Australia, about 9000 tons of coal was produced by a three-person crew in a 12-hour-shift 5-day week. Its best performance is 13,200 tons.

The auger is more maneuverable than the continuous miner and can be applied when shorter lengths of highwall are present. It is also suitable for recovering open pit end walls and major pillars of coal remaining after continuous miner operation.

The auger cutting head drives directly from the auger into the coal seam. Additional 5.5-m long flights are added as the hole deepens. This process continues until the final depth of the auger hole is reached.

Once each flight is in place, tractive effort is provided by hydraulic rams. Each auger flight is connected via a latch pin assembly that operates by remote control from the operator's climate-controlled cabin. As the coal is extracted from the excavation, a side conveyor advances the coal onto a stacker belt for stockpiling.

The auger flights are retracted from the hole by reversing the mining sequence.

Operators are sheltered by a full-length Falling Objects Protective Structure (FOPS). They are also protected from possible methane initiation by a gas inactivation system. The system diffuses methane gas by injecting oxygen-starved air. This process provides a safer working environment and promotes greater productivity, since operations are able to continue in known gas areas.

A new-generation, higher-power auger is being designed and built, which will be more effective because of the addition of various controls. This new auger, however, does not overcome the inherent problems associated with augers, particularly that of diminishing power with increased augering depth. Augers also suffer from increasing size degradation with depth, a fixed cutting height and certain other operational attributes that diminish the percentage of coal actually recovered. Neither do augers have the ability to negotiate dips and rolls in the seam because of the ngid structure of the auger flights.

3.2 *Continuous Highwall Mining (CHM)*

3.2.1 *Addcar System*

The Addcar system consists of a continuous miner, launch vehicle, 30 conveyor belt cars (addcars), a stacker conveyor, and two loaders, as shown in Figures 1, 3 and 4.

The continuous miner is positioned at right angles to die highwall on the launch vehicle. Addcars are progressively linked from the launch vehicle to extract the coal from the advancing continuous miner. The system can currently handle seams ranging from as low as 0.97 m to as high as 5.2 m in thickness.

One week of production by a five-person crew (four crews) can produce between 20,000 and 30,000 tons of coal.

The addcar system provides a cost-effective and safe means of extracting coal from final open pit highwalls and purpose-built trenches, and is ideally suited to applications that have 500 m or more of exposed highwall.

The continuous miner is remote controlled and will reach up to 350 m into the wall. The addcars facilitate a continuous flow of coal from the cutting head of the continuous miner to the launch vehicle belly belt and stacker conveyor. Hydrauhcally powered push arms provide thrust in addition to the tractive effort of the continuous miner.

The removal of the system from a completed hole is simply the mining sequence in reverse.

A five-person crew operates the entire system under the protection of a full-length Falling Object Protective Structure (FOPS), and it is also sheltered by frontal blast doors. Methane monitors mounted on the continuous miner provide the operator with constant information for safe mining operations.

The system is operated from a comfortable air-conditioned cab located on the rear of the launch vehicle. Up to six remote monitors provide the operator with the visual information necessary to control the system. The quality of pictures obtained from the continuous miner is preserved by automatic jet washing of the camera boxes.

3.2.2 Archveyor System

The system consists of a continuous miner, chain conveyor (Archveyor conveyor) and a loadout vehicle. The loadout vehicle contains an onboard substation for power distribution and control of all three main system components.

The continuous miner mines in a cyclical fashion into the coal seam of the highwall. As the coal is mined, it is conveyed by the miner to the Archveyor conveyor. The Archveyor carries the coal to the loadout vehicle. The loadout vehicle receives the coal from the Archveyor and moves it from ground level to a height that is suitable for loading into open cut, mine-type haul trucks. The system requires just two employees per shift to safely mine coal from exposed highwalls.

One week of production will produce over 30,000 tons of coal depending on the strata and mining condition.

The current available length of die chain conveyor iş 350 m, being variable in excess of 350 m. As the miner advances, the Archveyor advances to the miner once every 1.85 m. The Archveyor does mis by lowering itself to the ground and bringing die return side conveyor chain in contact with the floor. The Archveyor conveyor chain is then reversed, which gives tractive effort to the complete length of

die chain conveyor system. The Archveyor advances to the miner in the manner of a large crawler truck. Thus, the Archveyor conveyor chain performs a dual role, by conveying coal as well as advancing the chain conveyor itself.

The multiple-drive motors {one every 7.5 m) make up the primary electrical drive components of the chain conveyor system. All the conveyor motors are started together to move the chain conveyor system. They are reversed and started together again to convey coal to the loadout vehicle. The loadout vehicle advances with the conveyor every other chain conveyor advance. This process is continually repeated until the full extent of mining in each particular hole is complete.

A variety of sensors keep the miner in the seam automatically. The sensors include a roof and floor passive gamma detector system, multiple inclinometers, a ring laser gyroscope, and a programmable logic controller.

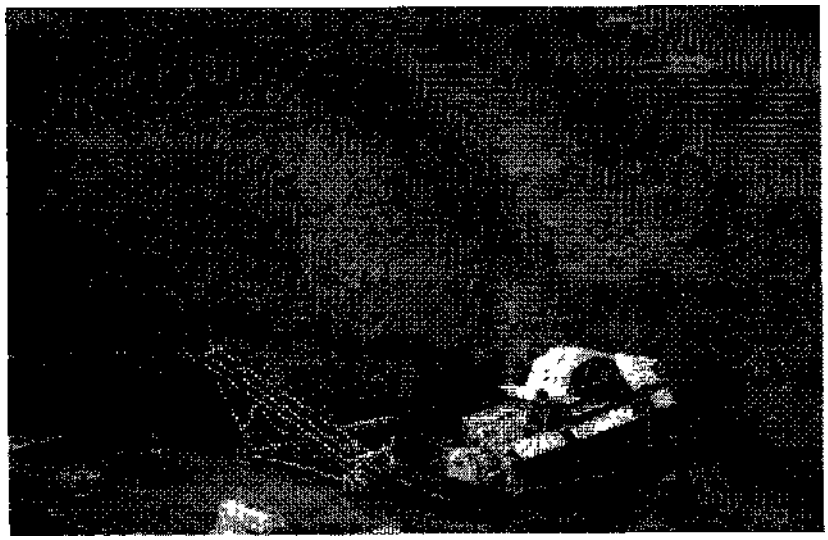

Figure 3 Addcar system.

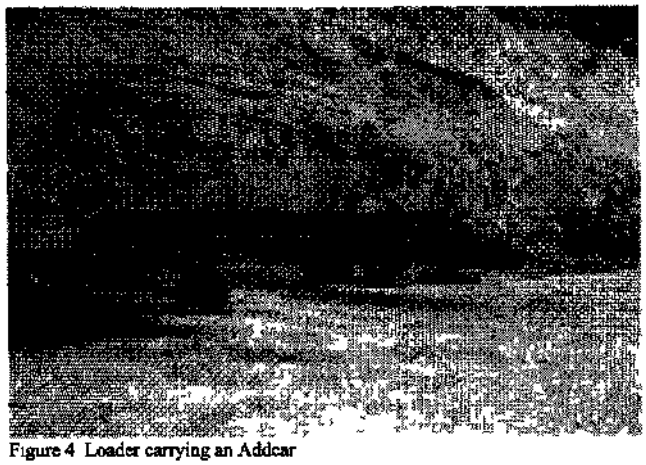

Figure 4 Loader carrying an Addcar

These components are of flameproof or intrinsically safe construction, or are located İnside flameproof enclosures.

This mining process is highly automated and controlled through the use of a programmable logic control (PLC) system. PLC technology has been m

use in processing and manufacturing facilities for the last two decades, and it has been used on underground coal mine conveyors and longwall systems for the last decade as well.

Operators are sheltered by a full length FOPS. They are also protected from possible mediane initiation by a gas inactivation system. The system diffuses methane gas by injecting oxygen-starved air. This process provides a safer working environment and promotes greater productivity, since operations are able to continue in known gas areas.

The system can be used in underground mines and is more productive and safer, with a lower cost than other mining methods.

4 OPERATIONAL AND GEOTECHNICAL CONSIDERATIONS

Highwall mining improves mining operations due to its safe mining system. The highwalls are generally along die strike of die seam, meaning that if the seams are extracted perpendicular to the highwall, as is normally the case, mining will be along the dip of the coal seam. Highwall mining in Australia has been carried *out on seam* dips ranging from 2-15°. Retraction is faster on lower grades, and therefore productivity İs affected by the seam dip. However, it is difficult or almost impossible to apply the system in steeper dip coal seams, over 15°. Therefore, another strand of system development is aimed at coal seams in me 16-25"dip range. There are currently no mining methods available for mining seams in this dip range beyond meir final economic highwall.

Use of an effective dip mining method with me basic highwall mining system is an alternative for steep coal seams. The machine is positioned at some angle off die perpendicular to the highwall to extract die coal with an effective dip within the limit of the machine.

Roof conditions have had a great influence on machine performance m certain seams. The rectangular geometry of the current excavations resulted from the lack of availability of suitable machines to mine more favorable shapes. Field trials of a machine tiiat will form an elliptical excavation with a short exposed roof span are now being conducted.

Mine water is another big problem. Any small amount of water tends to collect at tfie face in inclined seam excavations, interfering wiüi excavation work and decreasing the stability of the excavation. Stable loading and haulage operations should be established even with the existence of water in the face. It is necessary to control the water rush-in into the face on rainy days or during the rainy season in highwall mining, especially in Indonesia. Moreover, some coal measure rocks such as shale, siltstone and mudstone show excessive slaking behavior, leading to a severe deterioration of meir properties. The immediate roof tends to fall easily and the machine also tends to sink or slip on me softened floor. These problems make the controlling system difficult.

5 BACKFILLING SYSTEM

In highwall mining systems, a large amount of coal tends to remain isolated and undeveloped as pillars due to previous indiscriminate mining operations. Moreover, highwall mining causes highwall instability and surface subsidence. Specifically, the situation is more complicated in ÜıİcK seams. In order to cope with these problems, backfilling must be considered in a highwall mining system. Some considerations regarding backfillmg in highwall mining have already been reported {Matsui et al., 2000b).

Figure 5 shows die failure development around openings wim a narrow pillar in highwall mining. With a narrow pillar, die openings show less stability and the pillars fail much *more* severely than wide pillars. This situation leads to unstable work conditions, and in some cases, the cutting machine can be caught in *the* opening, making it impossible to withdraw.

Figure 6 shows the failure development around openings witii backfilling. It is clear that backfilling helps the openings remain stable when compared to die situation which İs shown in Figure 5.

Backfilling in underground mines is not a revolutionary concept. Waste rocks have been used throughout the world for many years as backfilling material to provide additional support to underground excavations in mines. Recently, due to the lack of dumping sites, the use of backfill for regional and local support has received increased attention in the mining industry.

According to previous research work (Afrouz, 1994), backfilling offers me following benefits to underground coal mines:

1) Fills me excavated areas, promoting better support and ground control.
2) Provides better environmental control of the waste rocks and coal preparation plant wastes.
3) Increases coal recovery, especially in room and pillar mining and highwall mining systems.
4) Reduces ventilation short-circuiting between adjacent mining sites.
5) Reduces cost of waste transportation to the mine surface dumping sites and tailing ponds, mus reducing the cost of associated up-keep and monitoring of these facilities.

The required strength of the backfill depends on the strata and mining conditions: cover depth, rock type and properties, mining method, etc. In a shallow mine, die required strength is not as critical when compared to that for a deep mine. According to research work done in South Africa, backfilling shallow underground room and pillar mines with pulverized flyash slurry could significantly improve the mine operating conditions by providing improved roof support and an increased extraction ratio {Wagner et al., 1979). The research also suggests that the complete filling of the rooms, up to roof level, is not necessary for improved roof control. Filling up to 70% of the pillar height provided adequate confinement, which constrained die lateral expansion of the pillar under concentrated compressive stresses. Moreover, by providing confinement to the pillars, thick coal seams have been successfully mined with a subsequent reduction of pillar height to width ratio and have improved the load-bearing capacity of the pillars.

Backfilling materials that are of concern to the mining industry can be broadly classified in the following three categories (Matsui et al., 1999b):

1) Waste originating from coal mines.

2) Waste originating from coal-burning power plants.

3) Waste originating from other industries.

In the USA, increased opposition from environmental groups is severely restricting the operation and planning of large-scale surface mines Some projects of mountaintop removal mining have had to be cancelled or downsized. In these situations, as discussed in the previous section, me highwall mining system would be applicable and useful for the protection of the environment and reclamation. Backfilling would increase the coal extraction ratio, keep the pillars and the highwall stable and control the subsidence at the surface.

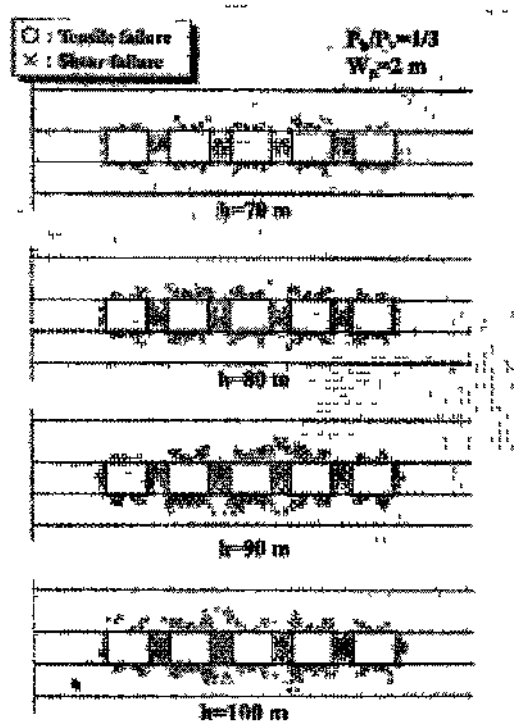

Figure 5 Failure development around the openings under the different initial stresses

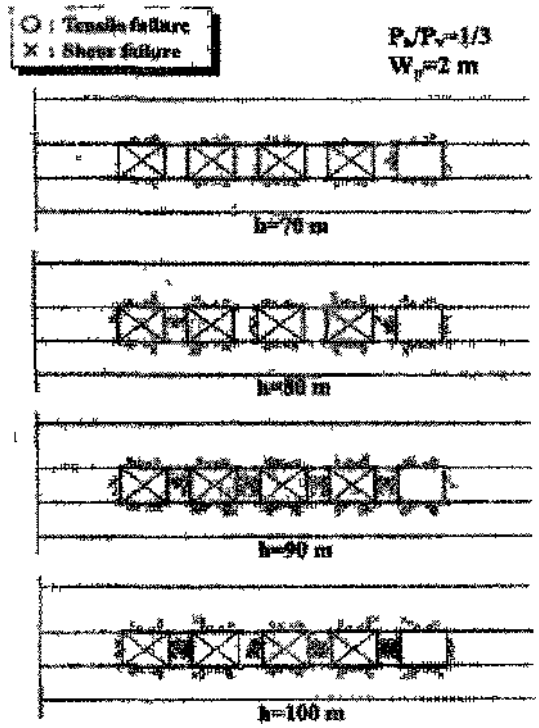

Figure 6 Failure development around the openings with backfilling

6 CONCLUSIONS

Highwall mining systems can sometimes be the final mining method used in open pit mines, or they can serve as a means of transition, with low capital cost, from surface mining to underground mining

Backfilling in the highwall mining system not only increases the coal extraction ratio and highwall stability, but also contributes to the protection of the environment around the mines However, the optimal backfilling system needs more intensive investigation, because there are many factors which need to be considered

The mining system also has to be improved so as to cope with steeper coal seams and water problems at the face m order to increase the extraction ratio and to maintain highwall stability

The highwall mining system will be introduced mto Indonesian open pit mines in order to improve productivity and to reduce environmental problems

ACKNOWLEDGEMENTS

This paper is the result of a joint research study between the Department of Earth Resources and Mining Engineering Kyushu University and the Department of Mining Engineering, Institute of Technology Bandung The joint research program started in 1998 concerning Ground Control Problems at Ombilin Coal Mine'

The authors are grateful to the managers and engineers of the Matsushima Coal Mining Co, Ltd and the Mitsui Matsushima Resources Co Ltd for their assistance in this study Many thanks should be given to the Japan Society for the Promotion of Science (JSPS), because their 'Ronpaku and 'Exchange Researcher' programs provided the opportunity to start this joint research program This academic relationship between our two countries will become stronger and help to advance the study and education of mining in both countries

REFERENCES

Afrouz, A A 1994 Placement of backfill *Mining Engmeei* February, pp 205-211

Anwar, H Z , Shimada, H , Ichinose M & Matsuı, K 1998 Fundamental studies of the improvement of coal mine shales behavior, *Proc of Regional S\mp on Sedtmentan Rock Engineering,* Taipei, Taiwan, 45 50

Anwar, H Z Shimada, H , Ichinose, M & Matsuı K 1999a Roof bolting application in longwall mining in Indonesia and Japan, *Proc of IS"' Int Conf on Ground Control in Mmmg* Morgantown, WV USA 256 262

Anwar, H Z, Shimada, H Ichinose, M & Matsuı, K 1999b Slakıng-durabılıty behavior of coal mine shales *Pioc of 99 Int Symp on Mining Science and Technology* Beijing China, 343-346

Kramadibrata S & Matsuı K 2000 *Rock engineering*

problems in Indonesian mining industry, Special Lecture at National Institute for Resources and Environment, Tsukuba, Japan, 20.

Seib, W. T. 1993. *Australasian Coal Mining Practice*, edited by Hargraves, A. J. & Martin, C. H., The Australasian Institute of Mining Metallurgy, pp. 238-242.

Matsui, K., Shimada, H., Ichinose, M. & Anwar, H. Z. 1999a. Reinforcement of slaking-prone mine tunnel floor by grouting, *Proc. of 8^ Int. Symposium on Mine Planning and Equipment Selection & the Int. Syntp. on Mine Environmental Economical Issues*, Dnipropetrovsk, Ukraine, pp. 253-260.

Matsui, K., Sasaoka, T., Shimada, H., Ichinose, M. & Kunota, S. 1999b. Disposal and utilization of mine waste rocks and flyash as a coal mine backfill, *Proc. of 6e Int. Conf. on Environmental Issues and Management of Waste in Energy and Mineral Production*, Calgary, Canada, pp. 219-224.

Matsui, K., Shimada, H., Ichinose, M Kramadibrata, S., Anwar, H. Z. & Furukawa, H. 2000a. Drivage of a new incline with a roadheader at Ombilin Coal Mine, Indonesia, *Proc. of P"1 Int. Symp. on Mine Planning & Equipment Selection*, Athens, Greece, pp.83-88.

Matsui, K., Shimada, H., Sasaoka, T., Ichinose, M. & Kubota, S. 2000b. Highwall mining system with backfilling, *Proc. of 9"" Int. Symp. on Mine Planning & Equipment Selection*, Athens, Greece, pp.333-338.

Wagner, H. & Galvin, J. M. 1979. Use of hydraülically placed PFA to improve stability in board and pillar workings in South African collieries, *Symp. on the Utilization of Pulverized Fuel Ash*, Pretoria, South Africa, Report No. CONF-7906215, pp.27.

1 7* Internationa! Mining Congress and Exhibition of Turkey- İMCET 2001, ©2001. ISBN 975-395-417-4

The Stability Assessment of a Large Underground Opening at Great Depth

Ö. Aydan
Tokai University, Department of Marine Civil Engineering, Shimizu, Japan
T.Kawamoto
Aichi Institute of Technology, Department of Cıvıl Engineering, Toyota, Japan

ABSTRACT: This article is concerned with the stability assessment of a large underground opening at great depth. The opening is planned as a power house cavem with dimensions of 24m wide, 45m high and 200m long at a depth of 500m in granitic rock mass The in-situ stress measurements indicated unusually high initial stresses act at the level of the underground cavern compared with other caverns constructed in Japan. The authors first outline the geological and laboratory and in-situ tests on rock mass and initial stress state. Then various stability analysis methods are briefly described. And then the results of the stability analysis methods are presented and their implications on the stability of the cavern are discussed.

1 INTRODUCTION

The stability of large underground caverns in civil engineering such as underground power-houses receives great attention and a very detailed geological exploration and rock mechanics investigations are carried out for the stability assessment studies. The stability assessments involve empirical methods and also analytical and numerical studies. A large underground opening for a pumped-storage scheme is planned at a depth of 500m in the Central Japan. The in-situ stress measurement showed that unusually high in-situ stresses exist in the site, which was not experienced at other underground power house constructions in Japan. The rock mass is granite and various laboratory and in-situ tests were carried out. After outlining geology, and rock mechanics investigations for the construction site, the fundamental concepts of the methods for stability assessments are briefly described. Then these methods used to assess the stability of the power house and they are compared with each other. Furthermore, the implications of results from each method are discussed.

2 GEOLOGY AND ROCK MECHANICS INVESTIGATIONS

2.1 *Geology*

Rock is granite and it belongs to the geologic era of cretaceous. Figure 1 shows the geology of the site. The grain size is classified a[r]. medium. Figure 2 shows the lower-hemisphere stereo projection of major discontinuities at the site of the cavem. The discontinuities are grouped into some sets as shown İn Figure 3. Figure 4 shows the appearance of discontinuities on me cross-section of the cavern.

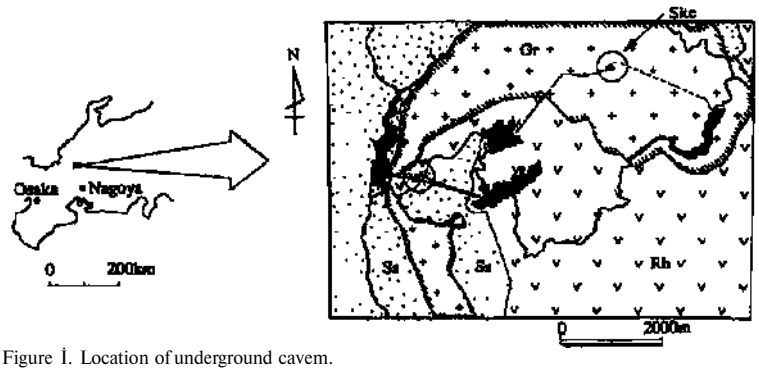

Figure İ. Location of underground cavem.

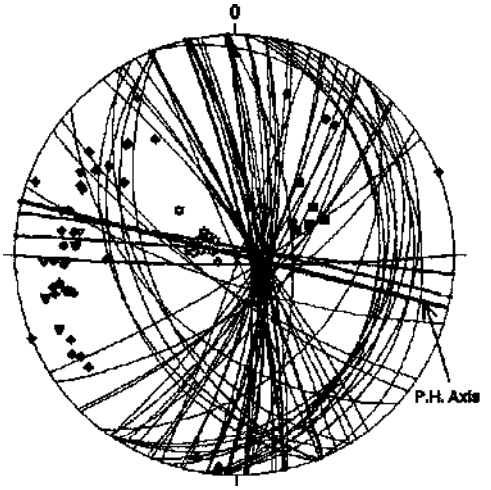

Equal angle projection, lower hemisphere

Figure 2. Stereo projection of discontinuities.

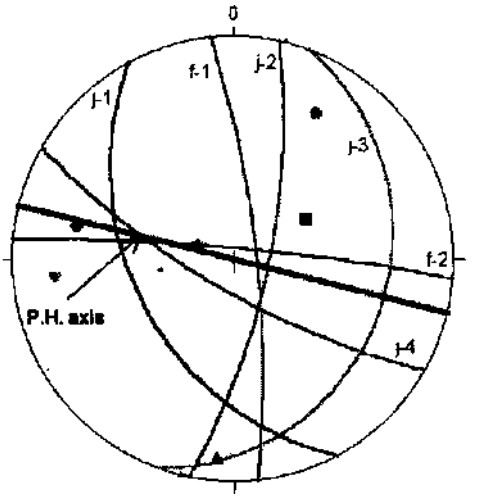

Equal angle projection, iower hemisphere

Figure 3. Grouping of discontinuity sets on a lower hemisphere stereo projection.

Table 1. Orientations of major discontinuity groups.

Discontinuity ÏH*	Dip Direction Q	Dip Q
f-l	84	78
f-2	5	84
j-l	242	41
j-2	102	72
j-3	20	20
j-4	210	74

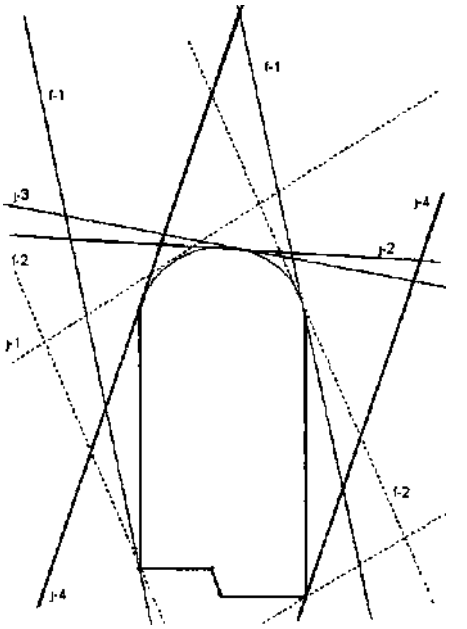

Figure 4. Traces of discontinuities on the cross-section of underground power house.

2.2 *Rock Mechanics Investigations*

2.2.1 *Classifications of Rock Mass*

Rock masses at the site were classified as B and CH on DENKEN classification system of Japan. B Class rock mass has less discontinuity sets with large spacing. Furthermore, rock is fresh and staining or weathering of discontinuity walls does not exist. On the other hand, CH Class rock mass has more discontinuities and its discontinuity spacing becomes smaller. Furthermore, staining and/or weathering of discontinuity walls exist. The relations among this classification system and the classifications of RMR and Q-system are given in Table 2. Figure 5 shows the relation between RMR and Q-value for this site together with overseas data. The staining of discontinuity walls in this site is due to thermal alteration resulted from volcanic dykes, which took place after the placement of granitic rock.

2.2.1 *Laboratory and In-situ Tests on Physical and Mechanical Properties*

Laboratory and in-situ tests are carried out to obtain physical and mechanical properties of rock mass. Tests involve physical properties such unit weight, porosity and wave velocity and mechanical properties such as elastic modulus, Poisson's ratio, uniaxial and biaxial compression tests, Brazilian tests and permeability tests. Cores are obtained from the sites,

which are classified as B Class rock and CH Class rock and they are tested in the laboratory. Table 3 gives the physical and mechanical properties of intact rock for each rock class.

No tests on the properties of discontinuities of this site were carried out. Nevertheless, the residual friction angle of the sheared samples was 55° and tilting tests on the rock joints at nearby projects yielded the friction angle between 36°-44°.

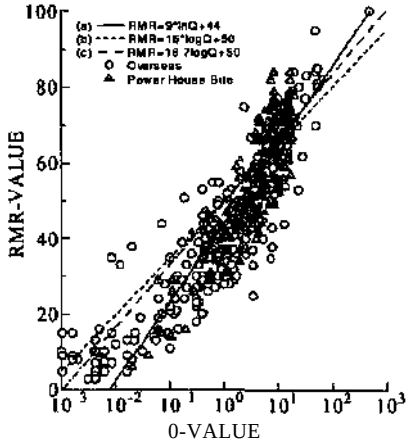

Figure 5 Relations between RMR and Q-value

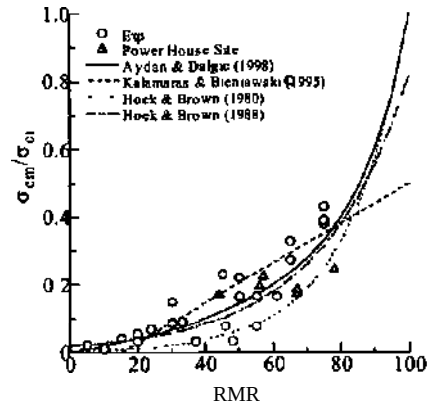

Figure 6. Relation between RMR and normalised uniaxial strength of rock mass

Table 2. Relation among DENKEN classes and RMR & Q-value

Class	RMR	Q-Value
B	67-79	16.7-20 0
CH	44-62	2.78-4.17

In-situ tests involve wave velocity measurements, permeability tests, shear tests and plate bearing tests at designated locations for each rock class. Shear test samples were 50cm wide, 50cm long and 20cm high. The nominal diameter of plate bearing tests was 30cm. However, some tests were also carried out by varying the diameter of the bearing plate from 15cm to 60cm. Table 4 gives the mechanical properties of rock mass for each rock class. Furthermore, Figures 6 to 8 show the relations between RMR and normalised mechanical properties of rock mass together with some empirical relations (Aydan and Kawamoto 2000).

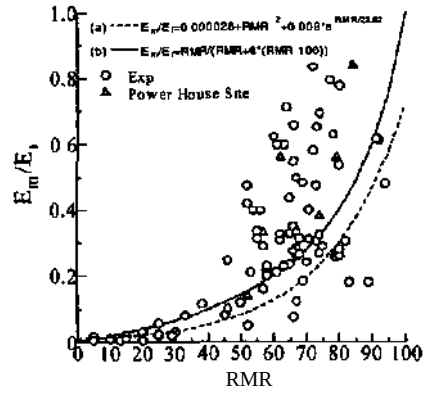

Figure 7 Relation between RMR and normalised elastic modulus of rock mass.

Table 3. Physical and mechanical properties of intact rock.

Class	γ (kN/m³)	E_i (GPa)	ν	σ_{ci} (MPa)	σ_{ti} (MPa)	ϕ_i O	V_{pi} (km/s)
B	26	25-t6	0 16-0 22	218-217	74.4-112	59-62	4 6-5.5
CH	26	5-21.4	0.18-0.27	110-153	46 8-92	53-58	3 9-5 1

Table 4 Rock mass properties.

Class	E_m (GPa)	C_m (MPa)		V_{pm} (km/s)
B	10-20	5-6	60-65	4 0-4 3
CH	5-13	3 8-4	54-56	2.3-4 0

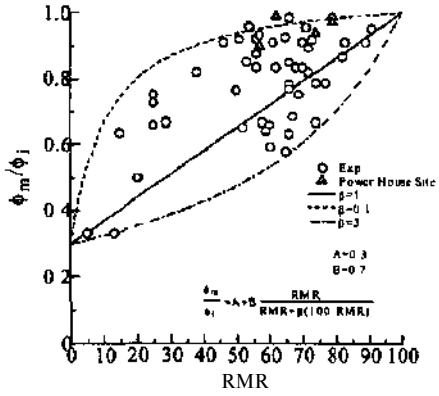

Figure 8. Relation between RMR and normalised fnclion angle of rock mass

2.2.2 *In-situ Stress Measurements*

An extensive in-situ stress measurements was carried out at this site since the preliminary in-situ stress measurement programme by overcoring method yielded unusually high in-situ stresses which were not observed previously at other power house construction sites in Japan (Ishiguro et al. 1998). In-situ stress measurements involve overcoring methods such borehole deformation method (BDM), conically ended-borehole method (CBT), hydro-fracturing method (HFM) and acoustic emission method (AE). In addition to these methods, a stress inference method (FSM) (Aydan 2000) based on fault striations was also used. The dominant fault on the she was denoted as F-1. Its dip direction and dip were 297 and 51, respectively. The rake angle (striation angle) was 240. The friction angle of the fault was set to 30° for the stress inference computations. Table 5 compares the inferred in-situ stress with the measurements obtained from various method.

3 STABILITY ANALYSIS METHODS

There are a number of methods to analyse the stability of underground methods. These methods can be classified as:

1) Analytical Methods,
2) Numerical Methods and
3) Block Analysis Methods.

These methods are briefly explained in the followings.

3.1 *Analytical Methods*

It is general difficult to derive closed form solutions for underground openings with complex geometry and complex material behaviour. Although there are some analytical solutions for openings excavated in elastic media with complex geometry, it is very difficult to have such solutions for openings behaving in elasto-plastic manner. The simple yet often used closed solutions are for openings with a circular geometry excavated in elasto-plastic media. Aydan et al. (1993) derived solutions for openings in elasto-plastic rock supported by rockbolts, shotcrete and steel ribs. Since the solutions are presented İn the articles referred no expressions are given here.

3.2 *Numerical Methods*

There are several numerical methods for underground openings depending upon the mechanical behaviour rock mass and its natural state. Among them, various types of finite element methods (FEM), discrete element methods (DEM), displacement discontinuity analysis (DDA), discrete finite element methods (DFEM) and displacement discontinuity method (DDM) are commonly used (Kawamoto and Aydan 1999). A brief outline of some of these methods İs presented below.

Table 5. Comparison of in-situ stress measurements by various methods

Method	σ_1			σ_2			σ_3					
	$\frac{\sigma_1}{\sigma_v}$	d_1	p_1	$\frac{\sigma_2}{\sigma_v}$	d_2	p_2	$\frac{\sigma_3}{\sigma_v}$	d_3	p_3	$\frac{\sigma_h}{\sigma_v}$	$\frac{\sigma_H}{\sigma_v}$	d_{σ_H}
FSM	2.30	90	16	1.59	187	23	0 76	329	62	1.44	2.21	84
BDM	3.02	105	16	1.69	197	6	0.83	307	73	1.67	2.86	104
CBT	2.49	89	25	1.01	353	13	0.66	239	62	0.99	2.18	91
HFM	2.70	89	1	1.59	179	28	0.84	358	63	1.43	2.70	88
AE										0.94	1.96	102

3.2.1 *Conventional Elastic and Elasto-plastic Finite Elemeni Methods*

Any numerical method must be solving the equation of moment of momentum for the stability assessment of any engineering structures. If inertia term İs negligible, the equation of moment of momentum takes the following form

$$\nabla \cdot \sigma + b = 0 \tag{1}$$

With the use of variational principles and adopting the conventional finite element discretization procedure together with Hookean type constitutive law, one easily gets the following simultaneous linear equation system:

$$[K]\{U\} = \{F\} \tag{2}$$

Where

$$[K] = \int_V [B]^T [D][B]dV$$

$$\{F\} = \int_V [N]^T \{b\}dV + \int_S [\overline{N}]^T \{t\}dS$$

When the material behaviour becomes elasto-plastic, then the incremental form of the above equation system is used. For two-dimensional case, it is common to use the Mohr-Coulomb yield criterion. Since the intermediate principal stress is indeterminate in this criterion and there is a comer-effect problem, the use of Drucker-Prager criterion is quite common, which is given by

$$\alpha I_1 + \sqrt{J_2} = k \tag{3}$$

Where

$$I_1 = \sigma_I + \sigma_{II} + \sigma_{III};$$

$$J_2 = \frac{1}{6}((\sigma_I - \sigma_{II})^2 + (\sigma_{II} - \sigma_{III})^2 + (\sigma_{III} - \sigma_I)^2$$

Nevertheless, it is possible to relate the Drucker-Prager yield criterion with the Mohr-Coulomb yield criterion. On n-plane, if the inner corners of the Mohr-Coulomb yield surface are assumed to coincide the Drucker-Prager yield criterion, the following relations may be derived

$$\alpha = \frac{2\sin\phi}{\sqrt{3}(3+\sin\phi)}; \; k = \frac{6c\cos\phi}{\sqrt{3}(3+\sin\phi)} \tag{4}$$

Where c,ϕ are cohesion and friction angle, respectively.

3.2.2 *No-tension Finite Element Method*

The no-tension finite element method is proposed by Valliappan in 1969(Zienkiewicz et al. 1969). The essence of this method lies with the assumption of no tensile strength for rock mass since it contains discontinuities. In the finite element implementation, the tensile strength of media is assumed to be nil. It behaves elastically when all principal stresses are compressive. The excess stress is re-distributed to the elastically behaving media using a similar procedure adopted in the finite element method with the consideration of elastic-perfectly plastic behaviour.

3.2.3 *Pseudo Discontinuum Finite Element Method*

This method was first proposed by Baudendistel et al. in 1970. In this method the effect of discontinuities in the finite element method is considered through me introduction of directional yield criterion in the elasto-plastic behaviour. Its effect on the deformation characteristics of the rock mass is not taken into account. If there is any yielding in a given element, the excess stress is computed and the iteration scheme for elastic-perfectly plastic behaviour is implemented. If there is more than one discontinuity set, the excess stress is computed for the discontinuity set which yields the largest value.

3.2.4 *Discrete Finite Element Method*

Aydan-Mamaghani proposed the discrete finite element method (DFEM) for the numerical analysis of discontinuous media (Aydan et al. 1996). In this method, discontinuities are modelled using contact element with a given thickness. The method basically follows the conventional finite element procedure togemer with implementation of the updated-Lagrangian scheme for large motions of blocks. There are several variations of this method during implementations, such as, elliptical, parabolic and hyperbolic schemes, depending upon *the* problem handled. In this article, the elliptical scheme is utilised.

3.3 *Block Analysis*

Block analysis methods are first proposed by Wittke (1967), and it was extended to several typical situations. A good description of this method was given by Hoek & Brown (1980) for underground excavations. In this model, the stability of blocks or layers of rock mass are assessed using the limiting equilibrium equations. For two-dimensional situations, Kawamoto et al. (1991) also presented limiting equilibrium methods for various forms of instability of potentially unstable blocks or layers in underground excavations.

4 RESULTS AND DISCUSSIONS

In diis section, the applications of various methods described in the previous sections are applied to assess the stability of an underground opening to be excavated at a depth of 500m below the ground surface as a powerhouse. Taking into account initial stress state, the original layout of the opening, which was determined by considering the topography and the optimum configuration for the hydraulic power scheme, and its variation to another configuration had to be examined. The rock mass around the cavern was classified as B and CH in DENKEN's rock classification system, which is commonly used in energy power projects in Japan. Computations for die stability assessment of the power house cavern are carried out by considering the variation of initial stress state and rock mass classes. The initial stress states for the original configuration and the present configuration are denoted as CASE-1 and CASE-2 (Table 6). For each initial stress state, computations are carried out for two rock classes by using different methods and are compared herein. In the numerical analysis, the maximum iteration number for each load increment was set to 200.

Table 6. Initial Siress slate for CASE-I & CASE-2.

Case No	a HI (MPa)	(MPa)	(MPa)
CASE-I	-24.7	-8.76	5.12
CASE-2	-14.7	-8.76	-0.79

4.1 *Closed Form Solution*

In this section, the results for the cavern computed by assuming that its shape İs circular with a diameter of 16m, situated hydrostatic stress state, which is equal to the largest horizontal stress, are presented. For CASE-1, the plastic zone is 0.5m when the material properties of rock class B is used (Figure 8). On the other hand, the plastic zone radius is 12.5m if the properties of rock mass class CH are used. Furthermore, the axial stresses of rock anchors and shotcrete are greater in the case of rock class CH as compared with those in the case of rock class B.

As for CASE-2, no plastic zone is observed around the cavern for rock class B, while the plastic zone radius is about 2.2m (Figure 9). Furthermore, the axial stresses in rockanchors and shotcrete are greater in the case of rock class CH as compared with those for rock class B.

4.2 *Elastic Finite Element Analyses*

Elastic finite element analyses were carried out to get a general idea on how the rock mass will deform and what regions may be over-stressed against shearing and tension around the cavern. Table 7 gives the material properties used in most of the finite element analyses reported herein and other sections. Figures 10-18 shows the deformation of rock mass and the over-stressed zone against tension and shearing around the cavern for rock class CH only. As expected, large deformations and over-stressed zone occur for rock class CH compared with rock class B for each in-situ stress regime. Furthermore, the expected overstressed zone against tension is larger than that against shearing. The expected over-stressed zones are about 9m on the pen-stock side (mountain side) of the cavern.

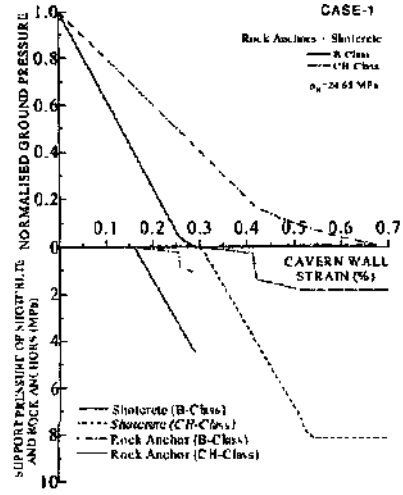

Figure 8 Ground reaction curve and axial stress development in support members.

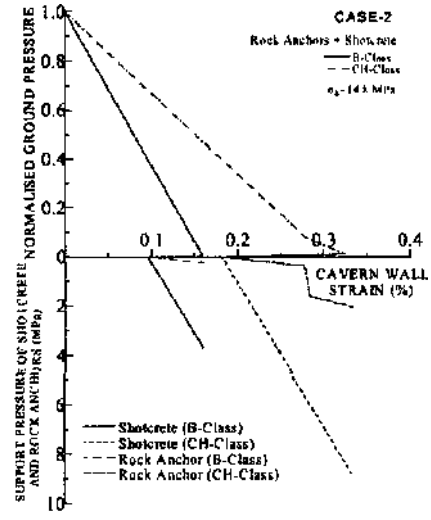

Figure 9. Ground reaction curve and axial stress development in support members.

Table 7 Mechanical Properties of rock mass classes used in computations

Rock Class	Unit Weight (kN/m^3)	Elastic Modulus (GPa)	Poisson Ratio	Cohesion (MPa)	Tensile Strength (MPa)	Friction Angle (°)
B	26	15	0 25	5	0 5	60
CH	26	9	0 25	2	0 2	55

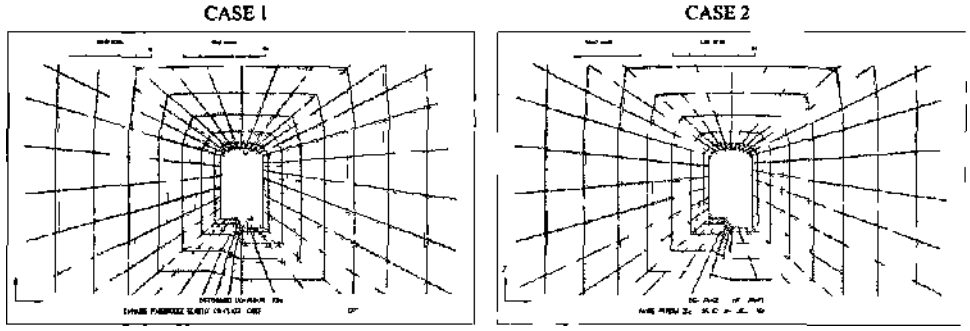

Figure 10 Deformed configurations around the cavern for rock class CH under different in-situ stress regimes

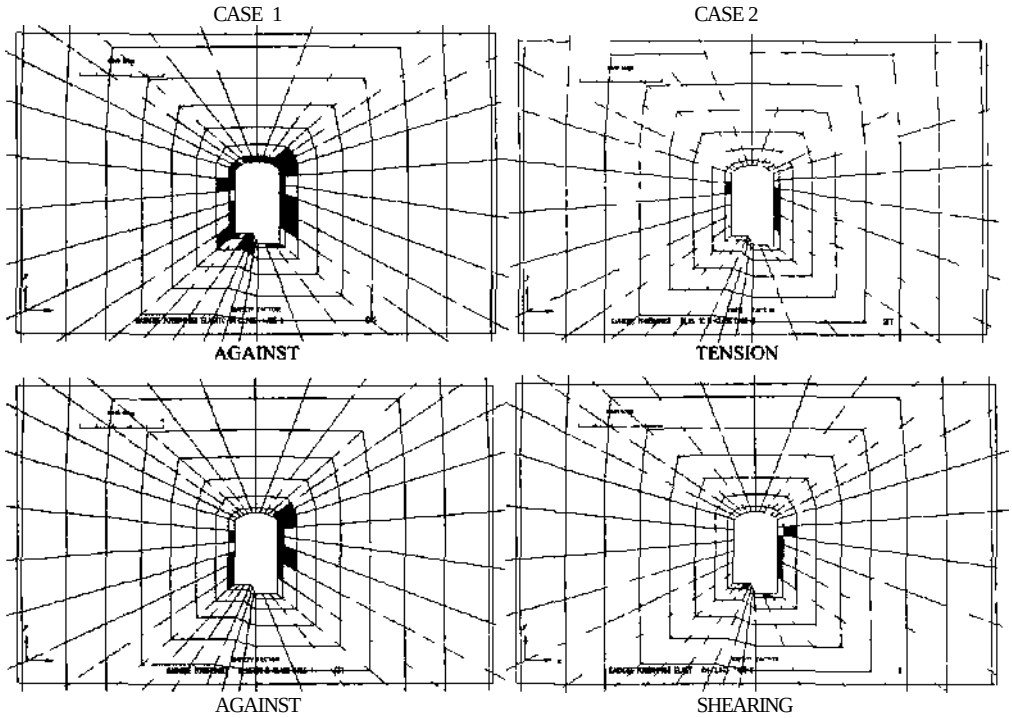

Figure 11 Over-stressed zones against tension shearing around the cavern for rock class CH under different m-situ stress regimes

4 2 *Elasto-plastic Finite Element Analyses*

Elasto-plastic finite element analyses were earned out to check the actual deformation and plastic zone development around the cavern and to compare with those obtained from preliminary elastic finite element analyses Figures 12 shows the deformation of and plastic zone development in rock mass around the cavern for rock class CH As expected large deformations and plasüc zone occur for rock class CH

around the cavem under the m-situ stress regime of CASE 1 Furthermore, the plastic zone development is smaller than the expected overstressed zone obtamed from elastic finite element analyses if rock mass behaves perfectly plastic after yielding The width of plastic zone is about 3m The plastic zone is larger on the pen stock side of the cavern

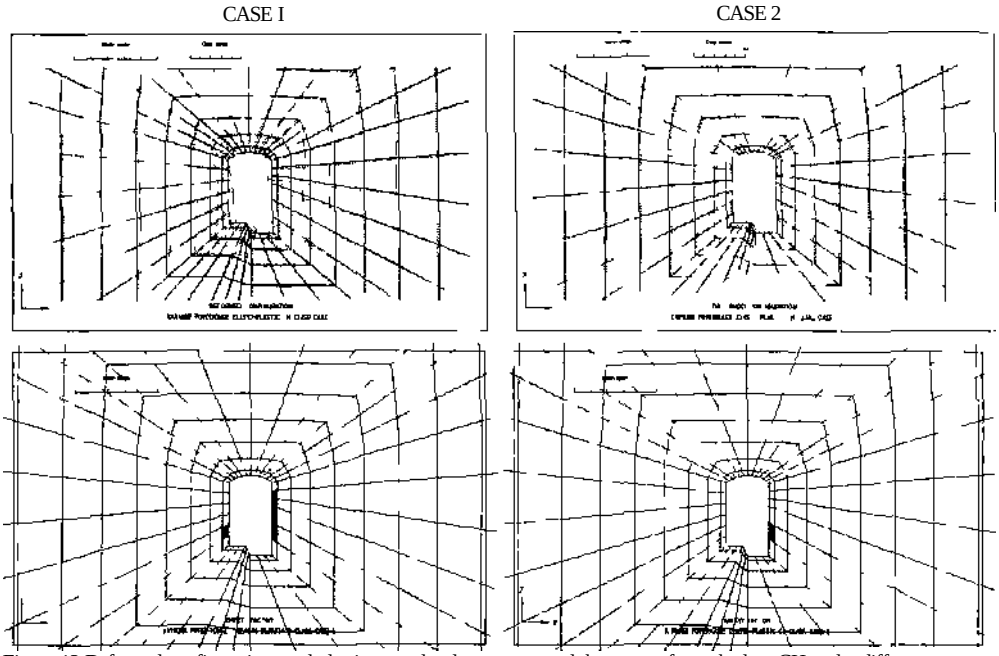

Figure 12 Deformed configurations and plastic zone development around the cavern for rock class CH under different tn-svtu stress regimes (elasto plastic analysis)

4 3 *No-tension Analysis*

A series of finite element analyses were earned out by using the no-tension method In the computations, the tensile strength of rock mass was assumed to be ml and behaving in an elastic-perfectly plastic manner Figure 13 shows the deformed configuration and plastic zone development around the cavern for rock class CH Except the final deformation configuration, the other results are the same

Although the maximum width of the plastic zone is about 9m for both CASE 1 and CASE-2, the failed zone in tension is greater for CASE-1 as compared with that for CASE-2 The deformation of the cavern is also greater for CASE-1 as compared with that for CASE-2

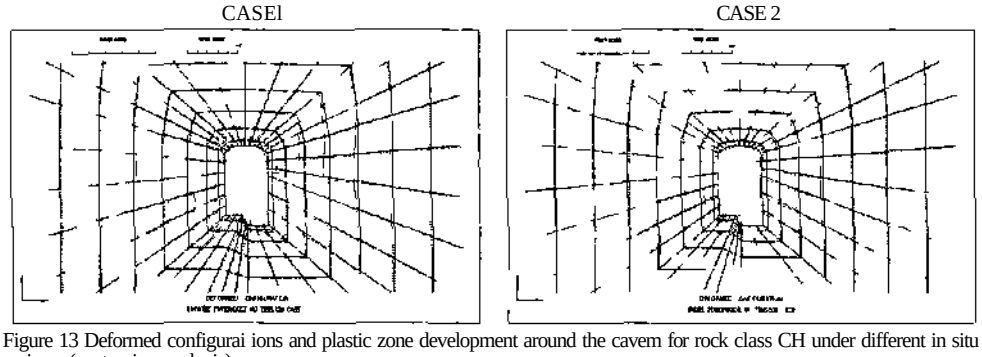

Figure 13 Deformed configurai ions and plastic zone development around the cavem for rock class CH under different in situ stress regimes (no tension analysis)

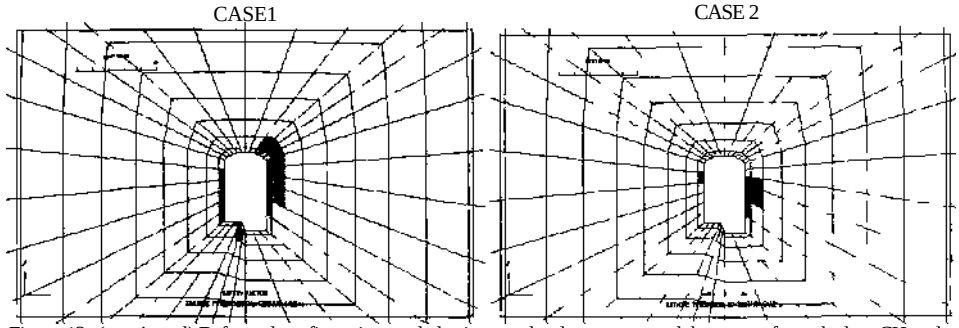

Figure 13 *(continued)* Deformed configurations and plastic zone development around the cavern for rock class CH under different in-sifu stress regimes (no-tension analysis)

4 4 *Pseudo-discontxnuum Finite Element Analysis*

In the computations, the yielding of discontinuity set at each Gauss point was checked and if the yielding occurs, the excess stress was evaluated and an iteration procedure similar to that for elastic-perfectly plasOc behaviour was employed The inclinations of discontinuity sets were set 60° and 120° with the consideration of discontinuity sets m rock mass around the" cavern The friction angle and cohesion of discontinuity sets were set to 40° and 0 MPa, respectively Figure 14 shows the deformed configuration and plastic zone development around the cavern for rock class CH Except the final deformation configuration, the other results are the same for both rock classes Although the maximum width of the plastic zone is about 18m for CASE-1 and CASE-2, the failed zone is greater for CASE-2 as compared with that for CASE-1 The deformation of the cavern is also greater for CASE-1 as compared with that for CASE-2

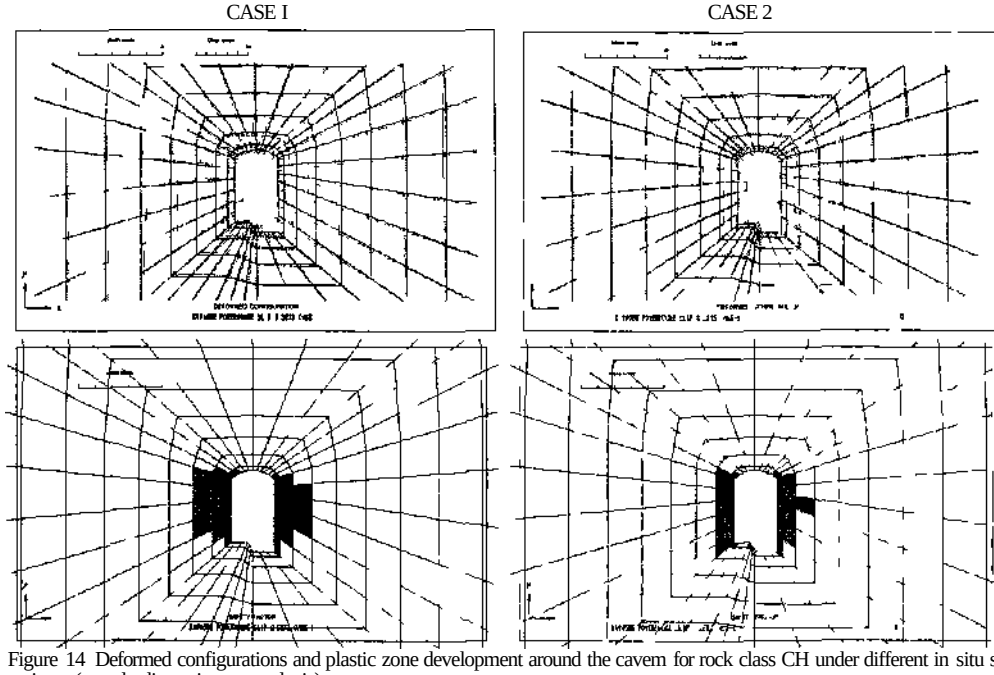

Figure 14 Deformed configurations and plastic zone development around the cavern for rock class CH under different in situ stress regimes (pseudo-discontinuum analysis)

4 5 *Discrete Finite Element Method Analyses*

In the computations, two discontinuity sets were considered Nevertheless, the explicitly modelled discontinuities were restricted to a region, m which discrete blocks could be formed The mechanical properties used in computations are given in Table 8 Figure 15 shows the computed results for the 10^{th} pseudo-time step for CASE-1 and CASE-2 As expected, the deformation of the blocks are greater for in-situ stress regime CASE-1 for the same computation step Furthermore, the blocks at both side-walls start to slide into the opemng whilg the one m Üıe crown remains stable This fact indicates the importance stress state acting on the blocky rock mass As will be shown later, the block in the roof compare^ to those in side-walls can easily fall into opening in conventional block analyses since the gravitational forces are only considered in such analyses

Table 8 Mechanical properties used in DFEM

Blocks			Discontinuity				
Unit Weight (kN/m^3)	λ (GPa)	μ (GPa)	λ (GPa)	μ (GPa)	σ_t (MPa)	c (MPa)	ϕ (°)
26	15	0 25	6	1	0 0	0 0	40

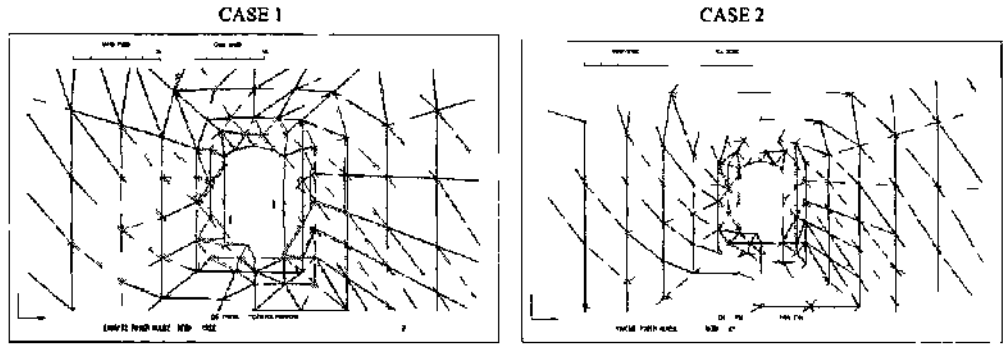

Figure 15 Deformed configurations of the cavern under different in situ stress regimes (DFEM)

4 6 *Block Analyses*

Block analyses method was also used to assess the stability of blocks, which may appear in the side-walls and in me roof of the cavern Figure 16 shows the most cnücal situation due to blocks formations as a result of discontinuous nature of the rock mass Figure 17 shows the required support pressure to prevent the fall of the block in the roof and the sliding of blocks in the side-walls by considering the gravity, only As a result, to prevent the block from falling into opening, the required support pressure is quite high Nevertheless, it should be noted that such analysis do not consider the stress state resulting from the cavem excavation Therefore, the design of support members under such circumstances may be sometimes over-designed

Since the two dimensional block analyses may be overestimating the required support load, the computations for individual blocks along the longıtudı rial axis of the caverns are also performed Figure 18 shows discontinuity traces at a location called "G-*hne"* for die cavern considered in the article as an example

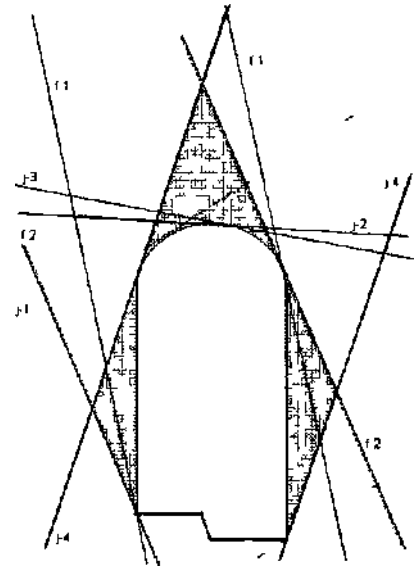

Figure 16 Critical block formations around the cavem

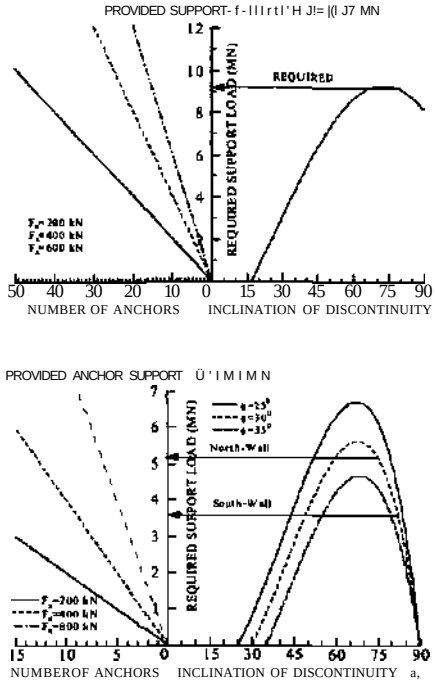

Figure 17. Required support pressure computed for roof and side-walls from block analysis.

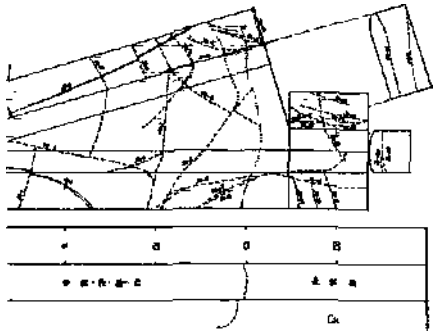

Figure 18. Traces of discontinuities at the G-line adit.

Table 9 gives the orientation data and properties of discontinuities used in block analysis. Figure 19 shows the stereo projections of the discontinuities at this location. For a block bounded by three discontinuity sets, there may be 8 different stability modes for a single block as listed in Table 10. Figure 20 and 21 shows the stability modes of blocks in the roof and side-walls for the respective location., Although the rock loads are not computed for such blocks, it is expected to be smaller than those shown in figure 17.

Table 9. Orientation data and properties of discontinuities.

Discontinuity	Strike	Dip	Friction Angle	Cohesion (kPa)
N1: JG-3	28	82	40	0
N2: JG-5	63	85	40	0
N3:JG-10	350	80	40	0

Table 10. Stability modes of a block

Failure Mode No	Explanation
1	Stable
2	Sliding along 1^
3	Sliding along lo
4	Sliding I«
5	Sliding on N3
6	Sliding on N2
7	Sliding on NI
8	Fall from roof

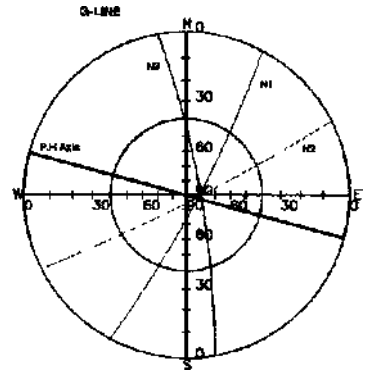

Figure 19. Stereo projections of discontinuities.

5 CONCLUSIONS

In this article, the authors described the applications of various methods for the stability assessment of a large underground power house opening and they discussed their implications. The maximum displacements of side-walls and crown, plastic zone width obtained from various methods are given in Table 11 for two different in-situ stress regimes.

Results indicated that the in-situ stress state, denoted as CASE-1, is understood to be the most unfavorable in view of the stability of the opening. On the other hand, the in-situ stress state, denoted as CASE-2, is favorable and it was right decision to change the longitudinal direction of the cavern so that the CASE-2 in-situ stress state will act on the cavern. For this case both displacements of side-walls and of the crown and plastic zone width are smaller.

Table 11. Comparison of the displacements of side-wall and of the crown and plastic zone width obtained from various methods.

Analysis Method	CASE NO	Rock Class	Crown	Displacement (mm) Side-walls		Plastic Zone Width
				Mountain side	Valley Side	
	İ	B	ÖÖ5	*6Ï1*	59~3	'•
Elastic Analysis	1	CH	0.07	105.4	99,0	
	2	B	5.7	35.6	34.4	
	2	CH	9.5	59.3	57J	-
	1	B	0.4	64.6	60,1	3.0
Elasto-plastic Analysis	I	CH	0.2	111.5	103.4	9.0
	2	B	5.7	35.6	35.0	
	2	CH	9.5	*59A*	57J	9J)
No-tension Analysis	I	CH	0.01	142.2	114.9	9.0
	2	CH	1,0	62.0	58.1	9.0
Pseudo-discontinuum	I	CH	3,2	188,8	160.2	18.0
Method	2	CH	28.5	98.5	86.8	18.0
DFEM	1	B	27.8	75.3	48.6	
	2	B	10,4	*TW>*	24^4	-

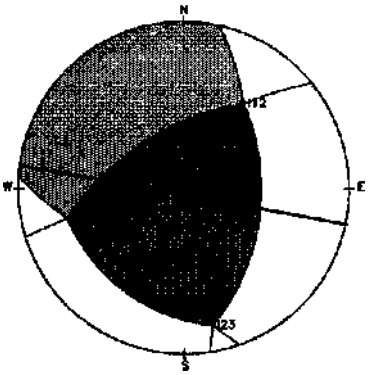

Figure 20. Predicted stability modes of a block in the roof.

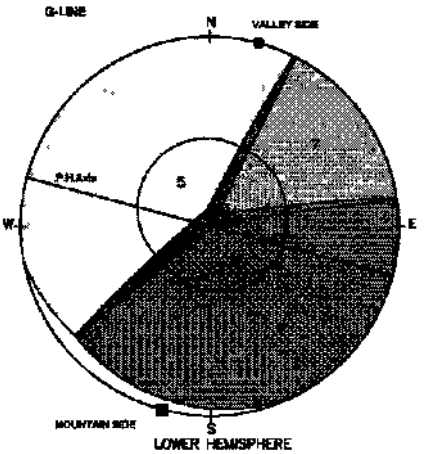

Figure 21. Predicted stability modes of a block in the side-walls.

REFERENCES

Aydan, Ö. 2000. A new stress inference method from the stress state of Earth's crust and its applications. Yerbilimleri, 22, 223-236, Ankara.

Aydan, O., I.H.P Mamaghani, T. Kawamoto (1996). Application of discrete finite element method (DFEM) to rock engineering structures. *NARMS'96,* 2039-2046.

Aydan, T. Akagi & T. Kawamoto (1993). Squeezing potential of rocks around tunnels; theory and prediction. *Rock Mechanics and Rock* Engineering, 26(2), 137-163

Aydan, Ö., & T. Kawamoto (2000). The assessment of mechanical properties of rock masses through RMR classification system. *GeoEng2000,* Melbourne.

Baudendistel, M., Malina, H., Müller, L. (1970). Einfluss von Discontinuitaten auf die Spannungen und Deformationen in der Umgebung einer Tunnelröhre, Rock Mechanics, 2, 17-40.

Hoek, E. and E.T. Brown 1980: Underground excavations in rock. Inst. Min. \& Metall,, London.

Ishiguro, Y., Nishino, K, Murakami, Sugawara, K., Kawamoto, T. (1999). In-situ initial rock stress measurement and design of deep underground powerhouse cavern. 9th Int. Congress on Rock Mechanics, Paris.

Kawamoto, T. and Aydan, O. (1999): A review of numerical analysis of tunnels in discontinuous rock masses. International Journal of Numerical and Analytical Methods in Geomechanics, Vol. 23, 1377-1391.

Kawamoto, T., Ö. Aydan, and S. Tsuchiyama (1991). A consideration on the local instability of large underground openings. Int. Conf. ,GEOMECHANICS'91,33-41.

Wittke, W. (1967): Influence of the shear strength of joints on the design of pre-stressed anchors to stabilize a rock slope Geotechnica] Conference, Oslo, Paper No. 4.11,311 -318.

Zienkiewicz,O.C, Valliappan, S. & King, LP. (1969). Elasto-plastic solutions of engineering problems. Initial stress finite element approach. Int. J. Num. Meths. Eng., 1,75-100.

17*[1] International Mining Congress and Exhibition of Turkey- IMCET 2001, ©2001, ISBN 975-395-417-4

The Next Atlas Copco Generation of Tunnel-Rigs and Some Experience

G.Nord
Senior Construction Advisor, Atlas Copco Rock Drills AB

J.Appelgren
Systems Manager, Atlas Copco Rock Drills AB

ABSTRACT: Now a new generation of computerised drill rigs has been launched and they are based on modern computer technology. The rigs have been well embraced by the market and more than 100 units have left the assembly line. The new generation has taken a quantum leap forward with respect to drilling accuracy, logging capabilities, reduction of manpower İn some types and serviceability. The Can bus technology, well proven in the automobile products, is an integrated part in the computerisation.

1 INTRODUCTION

From 1998 and up to today Atlas Copco has introduced a number of new drill rigs for underground excavation. These rigs are to a large extent the result a new design approach where Atlas Copco is working in close relation with skilled contractors and mining companies. This construction and mining business is generally considered as conservative. Only few of the advantages brought in by computerisation and atomisation other business have prospered from has been brought underground.

Atlas Copco introduced the so-called Robot rig already 1987. The sales of this rig indicate that it was not as good as we thought or the launching was too early. The arguments for this rig 1987 were to reduce manpower and possibly to improve production. The rigs that now have been launched will still require people for the operations and they will give a reasonably nice working environment but also a high and reliable good quality production. The drilling of the holes has turned out to constitute an ever-smaller share of the direct tunnelling cost and so time as well of the all the activities at the tunnel face. However the result of the drilling has a major impact on the other activities up at the tunnel face. The drilling has influence on the fragmentation as well as the over/under- break, required support etc. Although great attention is paid to penetration rate wear of drill steel and bits atlas Copco is paying an ever-greater interest in drilling can do to improve the tunnelling process as a whole. The input in this ongoing process is coming from our customers.

2 THE NEW RIGS

All the new rigs have been launched and consequently they are properly documented on video, CD-ROM and still also on paper. Still the paper will present a few pictures of the rigs. This time it has been possible to adopt a modern design of the ngs differing from the latest launches of what were called new rigs. In fact they are better characterised as upgrading of existing rigs as new features were added where space was available. In this case all components have been in the planning process right from the beginning. They are however to some extent based on old but competitive components like the BUT 35, which has been modified and reinforced. The hydraulic and the electric systems are completely different. The design-ambition has been in all details to go for simplicity in service and good ergonomics. Air condition in the cabin can operate both during drilling and tramming and not as before only during drilling. The new L2 rigs are shown in the pictures below.

Photo 1. Rocket Boomer L2 C.

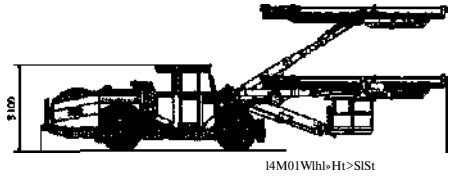

Figure 1 Rocket Boomer L2 C

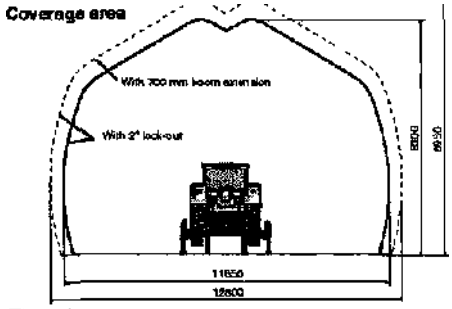

Figure 2.

Modular System - Rocket Boomer L2 C

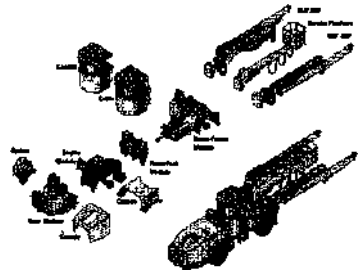

Figure 3.

3 THE RIG CONTROL SYSTEM

3.1 *History*

With exception for the former Robot rig all Atlas rigs have in principle been based on the so-called PLC system. The large radial net-work systems that were used could handle both analogue high speed signals but hosted also many processors for advanced digital communication plus man machine communication. Parallel interfaces were used meaning that the computer was centrally located and hooked up to each sensor and transmitters. The cable is supplying analogue signals that are converted digital and vice versa. When automating a process hosting a single or only few steps this is probably still the fastest way to meet the requested target. The draw back is in cases where the system can manage a defined application it will in practise mean overkill. This means that the system will be large and expensive. Some signals require high precision (14 to 16 bits) and some requires high speed while others do not demand any of that. This mixture is difficult to optimise in commercial systems and makes standardisation difficult for different rig-types. Beside this the radial nets requires intense cabling.

3.2 *The new rig control system*

The car manufacturing industry faced the control system problems discussed above especially for the luxurious cars that were equipped with very high numbers of electrical motors giving weight of the cables in the range of 100 kg per car. The ultimate solution would be one power-cable servicing all the electric units plus a switch analogue or digital ruling the use of the electric power. The digital signal should be superimposed on the power-line. A computer would than listen to superimposed signals and sent out instruction in the same manner. This ultimate solution almost came true. The single cable had to be expanded to three as two tiny wires had to be added to cope with the signalling but they are hooked up as a chain like the power line. There are cases where one power-line is unacceptable due to safety aspects and this means that the 3 lmes will be 4 (four), it would have been convenient if the industry had agreed on "one" language for communications in the signalling lines. The result was a number of dialects but luckily many components can deal with the majority of the dialects. The system was given the name CAN Bus (Controlled Area Network). A system of this kind is flexible easily expandable. Anywhere a new unit can be added without adding another cable. It İs foreseen that most passenger-cars, trucks and construction vehicles will have this system within a ten-year period.

The system described above is now implemented on the new generation of Atlas Copco CAN Bus drill rigs. The so-called DCS rigs where the rig activities are controlled by direct activation of the hydraulic valves are though still available for customers looking for simpler rigs.

For tunnelling rigs the flexibility of the system is highly utilised. The system can be adapted to the number of booms, the level of automation and adding new functions without being forced to install a heavy and expensive computer in the small and less complex rigs. To improve the reliability of the system, needed for a multiple boom rig operating İn the full automation mode, a two level circuit communication system has been implemented. The upper level talks to the whole rig and the identical lower one is talking to the boom. That means also that each boom has its own circuit. The advantage of

this set up is that a lower level fault affecting one boom will not have any consequences for the other booms. All the signalling on angles in the joints is restricted to the boom circuit and the upper level system advises only on the basic position of each boom.

A failure in the cables due to rock-fall or squeezing against the wall of a boom will not hamper the activities of the other booms.

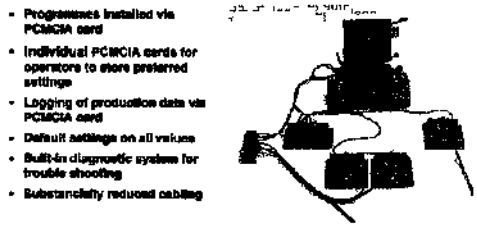

Figure 6.

The modules are all developed solely for the rigs and they are exposed in figure 6 above. It is believed that the figure shows how small the units are. It has been possible to give them a very good protection towards magnetic and electric disturbing influence. Below in figure 7 and 8 is shown in the form of a block-diagram the hardware of the Bus system for a standard 2-boom rig and a 3-boom rig with a service platform and rod adding system (RAS).

The software is split into a number of units (blocks) and the individual blocks can be added, deleted or modified. Figure 9 shows an access menu and a service menu. Access is given by pressing buttons on the screen.

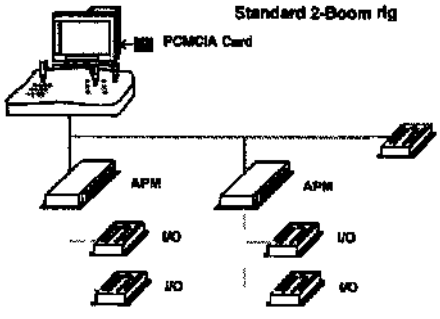

Figure 7. Block diagram for a standard two boom ng

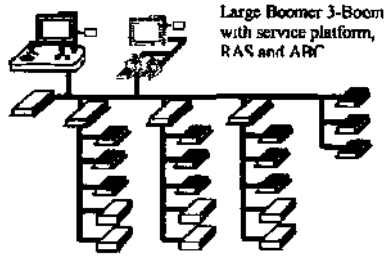

Figure 8. Block diagram for a three boom rig equipped with a service platform and rod adding system (RAS).

Our knowledge on how to start the drilling of the hole, means to avoid to get stuck with the drill steel and to get loose if stuck is incorporated in the system. The combination of this and the double dampened drill machines 1838 and 1432 is the explanation to the experienced favourable drill steel costs.

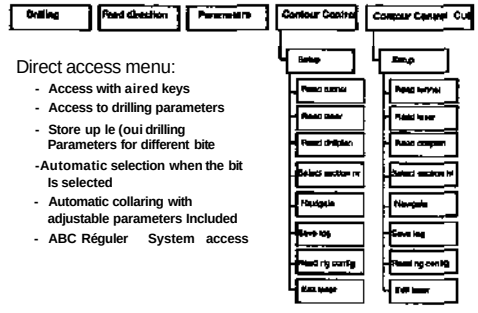

Figure 9

The operator's menu

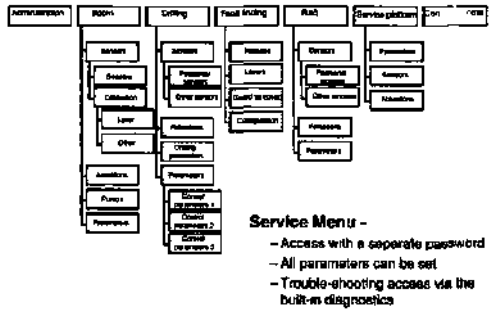

Figure 10. The service menu.

3.3 *The advanced boom control system. "ABC"*

ABC İs a shortage for advanced boom control. It is an important part the new rig control system "RCS" and ABC is available in three levels of automation and what these levels means will be described below.

ABC Basic: The operator is moving Booms and feeds and the orientation of the feed is shown on the screen placed in the cabin of the rig

ABC regular: This mode was earlier called "Contour control". Drill pattern, laser lines are being designed by use of a PC software tool named "Tunnel Manager". The result of the design work is loaded into the tunnel rig by use of a PC card. During drilling the operator is informed on where each boom İs located and where each blasthole has to be drilled. He will than guide the boom and feed into the correct position. During the drilling of the hole monitored drill data are collected without being shown on the screen. The recorded data can then be plotted or stacked in another form for later evaluation.

ABC total: This mode was earlier called "Auto" or "Robot". The planning of the round as well as the monitoring of the drill data is the same as for ABC Regular and is carried out using the same PC tool. The difference İs in the automation of the drilling process. The movements of booms and feeds is controlled by the RCS-technique (rig control system). The operator does not necessarily have to participate in the drilling process. There is built in extensive checking to ensure that collision of booms won't occur.

4 THE PURPOSE OF THE "NEXT GENERATION RIGS"

The new rigs will mean numerous improvements in the drilling and quality of the drilling result, which eventually will lead to lower overall cost. Some of the advantages are listed below.

-The operator can master the whole rig from one panel and that means that he can communicate with any of the booms

This means that only one operator is needed for both or all three booms if ABC Total is used. This statement is valid even for short holes as the moving of the boom and feed to a new position is done without any activity from the operator. The saving in this case İs one-operator times three shift. This is in a normal tunnelling situation a considerable saving. Another saving is the fast positioning in the Total mode, which also will be shown below. Positioning of the perimeter holes may result in skidding of the drill-bits on the rock-surfaces and the Total mode may have to be changed to Regular and requesting action from the operator.

The two drilling functions "Rotation pressure controlled feed force and Feed pressure controlled impact works even better in the digitised form as the fine tuning of the function is far easier done. A number of sites have indicated that jamming of the drill steel no occurs and this is certainly a time saving result and the drilled holes are expected to be straighter.

-There is a high degree of repeatability at positioning of the booms, as the digital system does not allow any drifting of the signals.

There are a number of factors that will contribute to the faulty placing of the boom, like the ambition of the crew and management, the quality of the survey work, acceptance of the new system, flexibility of booms and feeds, the boomer signalling system, and the character of the rock,. The digitised signalling will eliminate the drifting in the drifting and this gives a better accuracy. Furthermore the Total mode gives better accuracy in the positioning as the booms and feeds are automatically heading for a pre-set position and not moved by lever to a spotted point on a display.

Some results on overbreak is discussed in the cases below.

-Higher availability of the drill rig is expected.

The running costs are expected to be lower as the proper follow up of the machine performance and direct fault finding will improve the availability of the rig. The fault tracing İs simply made in the software. When operating in ABC Total the moving of booms and feeds are to a large extent controlled by the computer and that should result in a lower frequency of collisions between booms and wall and other objects. Consequently this would contribute to a higher availability.

-Monitoring of the ground ahead of the face

The ABC-system in Regular and Total means that the MWD (Measuring While Drilling) parameters can be logged without input of any extra efforts. This is valuable for those capable of interpreting the results of the parameter monitoring.

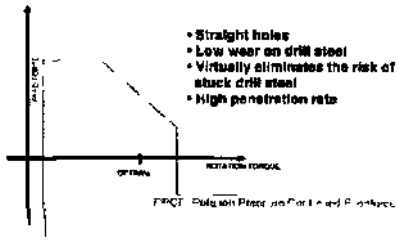

Figure 11 The principle performance of the RPCF system. The feed force is depending on the rotation torque according to the function as shown.

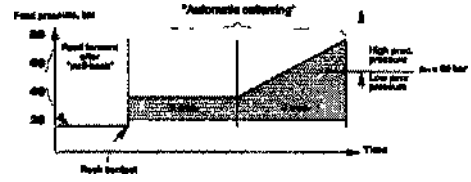

Figure 12 The sequences at the drill start and restart after a pull back of the drill-steel.

5 EXPERIENCE FROM THE CAN BUS RIGS BEING USED FOR TUNNELLING WORKS FOR MTRC IN CONTRACT 611 AND THE WEST RAIL PROJECT CONTRACT DB 350

5.1 *MTRC Pak Shing kok Tunnels*

The Hong Kong MTRC Pak shing Kok Tunnels comprise a complex of 5 interconnected tunnels driven as 9 tunnels totalling 6 km. The tunnels have a cross-section of some 35 m2. They are located in crystalline pyroclastic rocks resulting in a high wear of the bits.

For the drill and blast operations the Contractor Hyundai-Kier Joint venture had employed three (3) units of the Atlas Copco drill rig L2C, which is a two-boom ng with a Can-bus based control system. The rigs are equipped with the boom navigation ABC regular, meaning that the operator guides the booms and feeds to the correct position using the pre set drill pattern that is presented on the display. "The feeds are given a length to host up to 14 feet rods resulting in a max hole depth of 4,20 m.

What results have been achieved on this tunnel project over the monitored reaches? As said above the rock İs hard abrasive and not as brittle as regular hard crystalline basement rock. That means that the penetration will not be the best and the wear will be high. The average penetration is in the range of 2,5 meters/min. The service life of bits, rods and shanks have been roughly estimated to 400 m, 8-9000 m, and 8-9000 m respectively. These results are considered as good taking into account the penetration rate.

There was one operator for the two booms and the total time for the rig including mob and demob for a 70 number of holes and 4 m round was 1,5 to 2 hrs. As the manual moving of the boom from one hole position to the next generally takes about 40 to 50seconds the operator was busy with the levers two thirds of the drilling time

The tunnels are to be concrete lined and İt is therefore very important to keep over-break at a low level. A summery of the results from all the tunnels are shown in the table below, which has been provided by the owner MTR. In order to simplify the reading a bar diagram has been produced on the given figures and is also shown below. The contour holes are placed 10 cm outside the theoretical line at the face and 30 cm at the bottom of the hole. The conclusion from reading this bar diagram is that there is a risk for embarrassing under-break if the ambition to squeeze overbreak to too low .Bar no 6 which represents tunnel no 6 has much larger under-break than the other tunnels.

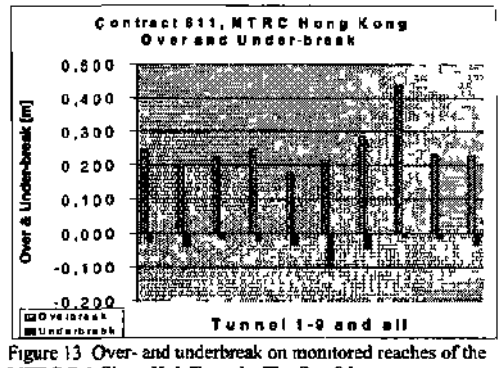

Figure 13 Over- and underbreak on monitored reaches of the MTRC Pak Shing Kok Tunnels The first 9 bars represent tunnels 1 through 9 and the tenth a summery of the 9 tunnels

Tunnel no 6 was die first to be excavated and the ambition was to keep overbreak low by allowing smaller margins than said above and the consequence was too much underbreak. Some of the underbreak is explained by apphcation of too much shotcrete for primary support.

Table 1. Overbreak and underbreak at the tunnel for Contract 611 Hong Kong *(Please note that the surveying is not yet complete)*

Tunnel no	Length [m]	Survey %	Over-break [m]	Under-break [m]
1	856	67	0,25	-0,027
2	504	73	0,20	-0,038
3	550	94	0,22	-0,017
4	1044	43	0,25	-0,022
5	1004	39	0,18	-0,029
6	324	45	0,22	-0,096
7	746	48	0,29	-0,042
8	380	3	0,44	-0,008
9	600	21	0,23	-0,014

Certainly better results with respect to overbreak has been achieved on other projects but it is always a matter of the ambition of the management and the incentive and skill of the labour. For tunnel 5 overbreak been is shown for a 150 meter long reach in the figure below. There are noticeable variations that may be explained by the geological conditions. Simply overbreak caused poor ground.

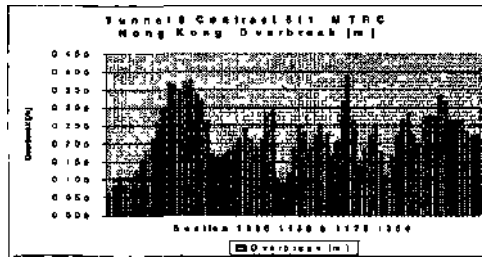

Figure 14 Overbreak, chainage by chatnage at 2 m centre for 150 metre reach of tunnel 5. The variation in over-break is noticeable.

5.2 *West rail contract DB 350*

The West rail contract DB 350 comprises a double track tunnel of 5 km located in the so-called Repulse bay formation, which mainly is built up of crystalline pyroclastic rocks. The joint venture companies Nishimatsu and Dragages split the tunnel in half-and-half. Nishimatsu is using the new generation WL3C Can-bus rigs for the drilling work.

The tunnel design, which is produced by the joint venture, is a double track tunnel with a cross-section of 110 m2. A concrete wall İn the centre separating the two tracks from each other. The cross-section somewhat distorted is shown in the figure 15 below.

The two WL3 Can-bus rigs are given feeds bo long that up to 5,8 deep holes can be drilled. The drilled length of the rounds varies generally from 5 to 5,8 meters. In poor rock these long rounds are shortened. This is important to bear in mind when overbreak is discussed below. This rig is equipped with ABC Total, which means that the holes are drilled and the booms and feeds are moved to a new position automatically.

For the drilling two rigs are positioned next to each other at the tunnel face and each rig drills 77 holes giving totally 154 for the 110-m2 face plus three 4 inch holes for the parallel cut.. The contour holes are than given a spacing of 35 to 40 cm. Generally all the holes but the contour and the bottom are being drilled in the "Total mode". The pull of the round is about 90 %. Two rounds per day, 25 days per month gives a production of 200-220 meters/month. If the contour is free from protruding rock the automatic drilling is applied also for the contour holes.

The wears of drilling tools are equal to the MTRC tunnels described above except for the bit life that is about 500 meters. Here again is concluded that the Can-rig is treating the drilling tools well.

One man operates the three-boom rig and when the "Total" mode is utilised the booms have no down time not even for shorter rounds. The time for the drilling operation including mob and demob is in the range of 2-2,5 hrs and the penetration rate for the 48-mm spherical button-bits 2,5 meters/minutes. The drill pattern and the travelling routes for the booms are shown for both ng< below. In cases where only one rig has been placed in front of the tunnel face the drilling of the rounds takes 3,5 to 4 hrs.

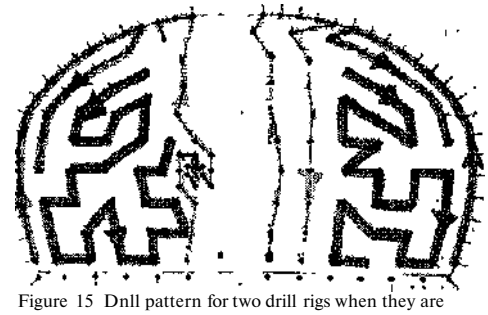

Figure 15 Dnll pattern for two drill rigs when they are working in parallel The path for each boom is shown in colours. Please noie that there is a overlap of about 1,5 meters in the centre

Considering firstly the length of the round secondly the length of the rounds with respect to partly poorer rock-quality, over-break cannot match the result from the MTRC tunnels. Without any

splitting on rock-classes the results from 450 meters of tunnel is shown in the histogram below. Here as well as in the MTRC-project the drilling of the contour starts 10 cm outside the theoretical line and the bottom is meant to be 30-cm outside the theoretical line.

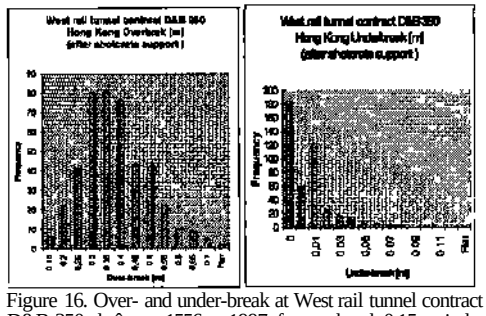

Figure 16. Over- and under-break at West rail tunnel contract D&B 350 chaînage 1556 to 1997, for overbreak 0,15 m isthe first mark on the x-axis and the first bar in the underbreak histogram covers all zero registrations.

What is surprisingly encouraging is that underbreak is found only in half the surveyed sections and where found only smaller quantities is registered. As the deviation is depending on the length of the hole with a power of more than one (I) possibly 1,5 -2 a 5,5 meter long would deviate 50 % more than for a 4 m long hole. ConsequenUy the underbreak ought to be more embarrassing than in the MTRC case as shown above.

Information the on the rock quality over the reach 1556 to 1999 has been provided by the contractor and it can be concluded that almost all excavation is done in rock having a Q-value higher than 10. That means that the rock quality can be considered as good speaking in general terms. Overbreak caused by geology should not have been dominating in this

6 FINAL WORDS

For a machine supplier it is very important to have good relations with skilled customers, as they to some extent become partners in the development work of new equipment. It is the believe in Atlas Copco that the new generation of rigs will a profitable tool when chasing costs in the tunnel construction. It has not been convincingly shown that overbreak is drastically improved. There are however many prerequisites that have to be fulfilled in order to achieve low overbreak result.The other improvements like better drill steel economy, savings on operator cost higher utilisation etc. have been easier to verify. This is also the reason for the well reception of the new generation.

if international Mining Congress and Exhibition of Turkey- IMCET2001, ©2001, ISBN 975-395-417-4

Evolution of Blasting Practices at the Ekati™ Diamond Mine

D.D.Tannant & J.Peterson
Department of Civil & Environmental Engineering, University of Alberta, Edmonton, Canada

ABSTRACT: A review of blast designs and improved blasting practices at the Ekati Diamond Mine is presented along with the results of three blast-monitoring experiments. Blast monitoring was undertaken to investigate blast damage mechanisms in the mine's well jointed rock mass. Rock mass damage caused by production, pre-shear and wall control blasts was measured. Ekati uses 270mm holes for production blasting, and 165mm holes loaded with a decoupled charge for pre-shearing. The production blasts are loaded with bulk emulsion / ANFO blends. The mine plan involves using 30m double benches. A 30m high pre-shear is drilled and blasted prior to the production blasting that İs done with sequential 15m benches. This paper summarizes the monitoring equipment and data gathered to date.

1 INTRODUCTION

The Ekati™ Diamond Mine is located about 300km northeast of Yellowknife, NWT, Canada. The mine is a joint venture of BHP Diamonds Inc. (51%), Dia Met Minerals Ltd. (29%) and geologists Charles Fipke and Stewart Blusson (10% each). The Ekati mine is Canada's first diamond mine and BHP is the operator. The mine is accessed by air and by a winter ice road.

The first kimberlite pipe mined at Ekati is known as the Panda pipe. The Panda open pit mine will have a total depth of 315m (Figure 1), width of about 600m, and a 50° overall slope. Initial ore production is 9,000 tonnes per day.

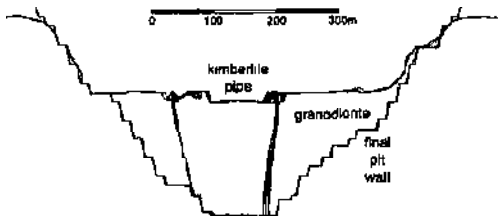

Figure t Cross-section of the final pit design

This paper summarizes the pre-strip blasting and the evolution of the production and wall control blast designs from 1997 to 2000. The initial blast designs and the rational behind subsequent changes that took place are presented along with the techniques currently m use.

The paper also briefly presents an experiment done to measure the rock mass response to blasting. Three blasts were instrumented with geophones, gas pressure sensors and time domain reflectometry cables. A brief summary of the instrumentation and data gathered is included.

2 BLAST DESIGNS

2.1 *Pre-strip Blasting*

During 1997 the Panda kimberlite pipe was prestripped to prepare for mining. The pit was initially stripped in 10m benches. Drilling was carried out with an Ingersoll-Rand DM-45 that drilled 165mm holes and an Ingersoll-Rand DM-M2 that drilled 270mm holes. The smaller unit was used for pioneering work due to the rough terrain encountered. The larger rig was used once level benches had been established. The blast patterns used were a 4m by 6m staggered pattern for 165mm holes and a 6m by 7m staggered pattern for the 270mm holes.

In the early stages of pre-stnpping it was found that the majority of the drilled holes contained water. This resulted in all of the holes being loaded with DYNOFLO Lite, a 70% emulsion / 30% Ammonium Nitrate and Fuel Oil (ANFO) chemicaUy gassed bulk explosive. The cup density of the product was 1.2g/cc. The product was manufactured on

site at a temporary plant during the pre-stripping phase.

All of the blasts were tied in using detonating cord and millisecond connectors. This system was chosen because of the reliability of a dual path tie-in. The blast patterns were designed to have hole-by-hole initiation to ensure the optimum fragmentation and displacement in the muck pile. Typically the inter-hole delays were from 17 to 50 milliseconds with the inter-row delays 100 to 135 milliseconds. Blasts were shot in V-patteras or en-echelon depending on the shot geometry.

The blast results were generally very good. The blasts were mucked with smaller equipment and finer material was required for road construction so the blasted material was smaller then would be typically expected İn a large mine.

2.2 *Production Blasting*

In the summer of 1998, BHP commissioned two D90KS drill rigs equipped for drilling 311 mm holes. At the same time, the mine plan increased to 15m bench heights. Between the summer of 1998 and spring of 1999 several blast designs were tested before arriving at the current design.

The first blast design with 31 lmm holes was a 7.5m by 7.5m square partem. The holes were loaded with 750 kg per hole of 70% emulsion / 30% ANFO blend at a density of I.2g/cc. The sub-drill on the pattern was 1.5m giving a 16.5m total depth. This design resulted in 8m of stemming in each hole and no explosives in the upper half of the bench. The resulting muck piles were poorly fragmented and very tight in die upper half of the bench and the shovel faces were standing close to vertical, resulting in lower productivity and increased shovel wear. A fragmentation study done on this material showed that the material was 90% passing 0.5m (Peterson 1998).

Several methods were tried to improve the blast performance. These included:

- dividing the explosive load into two decks to improve explosive distribution,
- loading the holes with lower density explosives to improve explosive distribution,
- increasing the total load per hole,
- adjustments to timing sequence, and
- switching to a 7m by 8m staggered pattern.

There were varying degrees of success in each method tried. The use of two decks noticeably improved the digging conditions, however the blast crew productivity and the accessory costs suffered as a result. During the winter of 1998 several blasts were loaded with ANFO in the top portion of the holes over a toe load of 70/30 emulsion/ANFO blend. By loading the upper part of the hole with ANFO at a density of 0.83g/cc, the kilograms per metre of borehole was lowered by close to 45%. This improved the explosive distribution and reduced the stemming length and gave excellent results, however water conditions did not allow for this practice to continue.

The blasthole layout was also switched from the 7.5m square pattern to a 7m by 8m staggered pattern to gave a better distribution of explosive for the same amount of drilling.

Problems with drill productivity as well as the desire to improve fragmentation and diggability led the operation to try using 270mm holes in the production patterns. Several patterns were tried on a 6m by 7m staggered pattern. The good results and increased drilling productivity led the mine to using 270mm holes on all production shots. The pattern was also slightly expanded to a 6.5m by 7.5m equilateral pattern.

The holes are presently loaded with 70% emulsion / 30% ANFO chemically gassed to a density of 1.15g/cc. Each production hole is loaded with 775kg of explosive and stemmed with I0-20mm crushed rock. The holes are toe primed with a 454-gram pentolite cast booster on a 17m long 500 millisecond non-electnc detonator.

The blast initiation sequence and timing was also adjusted before the current design was adopted. Earlier blasts were shot faster using 35 to 50 millisecond delays along the rows and 117 milliseconds between rows. The present design uses 65 millisecond delays between holes and 340 milliseconds between rows. It was found that die blast results improved when increasing the delay times.

2.3 *Wall Control Blasting*

Open pit development commenced at the 458 to 465m elevations above sea level, and will conclude at the 150m elevation giving a total pit depth of 315m. Contractors were used to excavate down to the 435m elevation. The pit design consists of 30m high double benches mined in 15m increments. Desired bench face angles range from 75° to 85°. Mine inspectors approved a minimum catch bench width of 11m.

The steep slopes in the pit require the final wall to be left as undisturbed as possible. Therefore, the blast patterns must be significantly altered when blasting against the final wall. During the pre-stripping phase there was little attention paid to wall control blasting. As the depth increased and the bench size increased to 30m it was imperative that the wall control blasting practices be implemented.

The first attempts at wall control blasting were done on the 435 bench as a test away from the final wall and involved the use of large diameter 31 lmm holes. The initial blasts were modified production blasts (7.5m by 7.5m, square pattern, 311 mm holes,

750kg/hole) with a reduced load in the final row of holes (460kg/hole). The final row of holes was offset from the desired wall by several metres. It was not possible to dig to the limits and there was blocky material in the buffer row. The next modification in the design was to place a trim row of unstemmed holes along the design toe with a toe load of 100kg on 5m spacing. These holes were 5.5m from the buffer row. This helped reduce the toe along the base of the final wall, however mere was still significant damage at the crest. Several minor modifications were made before arriving at the following design that was used on the 420 bench:

- trim row = 4m spacing, 5.5m burden, 70kg/hole - no stemming,
- buffer row = 7.5m spacing, 7.5m burden 400kg/hole with air-deck,
- delays = inter-hole = 35ms, inter-row = 167ms.

This design resulted in a low powder factor in the area of the buffer row, which caused excess confinement, greater vertical movement, and less forward movement during the blast as well as poor fragmentation and significant damage to the final wall. To improve the design, the burden was reduced on the buffer row.

The next evolution İn the design was to drill and blast a row of pre-shear holes prior to drilling and blasting the wall control blast. This was done in an attempt to eliminate penetration of the gases from the production holes into the rock mass of the final wall and to reduce the vibration levels beyond the final wall. The first pre-shear blasts were drilled with 311mm holes on 4m spacing and loaded with 70kg per hole. A crack did not form between all of the holes, therefore die spacing was reduced to 3m for the pre-shear holes.

The results from pre-shearing still did not provide the quality of wall that was desired. In many cases the buffer row was damaging the crest behind the pre-shear and loosening wedges (Figure 2). This resulted in a reduction of the catch bench width.

As the design continued to evolve, more changes were implemented. In several cases there were large toes left at the base of the final wall. These required secondary blasting for removal to allow drilling of the mid-bench pre-shear. Placing the buffer row 3m from the toe and reducing the spacing to 4m significantly reduced the incidence of these toes.

The second issue that faced the operation was being able to attain the toe of me final wall in the design location. It soon became apparent that the configuration of the DK90S drills did not allow for the final row of holes on the second pass of the double bench to be drilled in the proper location (Figure 3). The drill could not get close enough to the wall to collar the final hole of the second bench. This resulted in the loss of 2 to 3 metres of the catch bench in order to maintain the overall pit design. By doing two separate pre-shears there was also a lip mat developed at the middle of the bench face. This lip was a source of loose material, and could potentially deflect rocks falling from above over the catch bench below.

Figure 2. Blast damage to the bench walls, (a) increased fracturing near crest of bench and (b) loosening of rock wedges and loss of bench width.

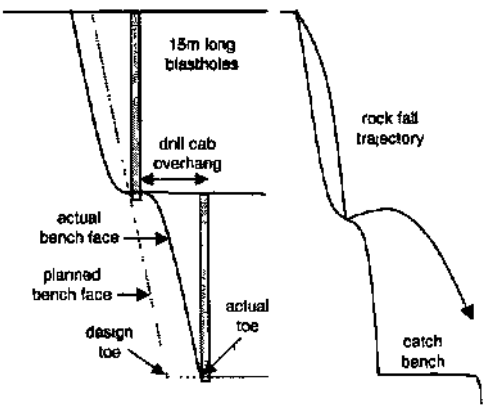

Figure 3 Small lip created by offset of 15m pre-shear holes used for 30m high benches.

In late 1999, a pre-sbear was attempted using 165mm holes on 2m spacing. The holes were loaded with 44mm Dynosplit C, a continuous watergel explosive. The buffer design was the same as for the large hole pre-shear. The wall conditions improved drastically. The time spent scaling was also reduced resulting in increased productivity. Success with the small hole pre-shear led the operation to try pre-shear blasting for the entire 30m bench using 165mm holes. This eliminated the small lip at mid-bench.

The current wall control blast design involves pre-shearing the entire 30m-bench height with smaller diameter (165mm) holes prior to drilling 15m high trim blasts. The trim blast is drilled with the production drills (270mm). The pre-shear holes are drilled 30m deep on 2m spacing. The holes are then loaded with a radially de-coupled charge. The product loaded is 44mm diameter Dynosplit C. This product is a continuous watergel explosive containing a 25 grain detonating cord running the length of the product. The toe of the hole is loaded with two 75mm chubbs of the packaged emulsion Blastex. The hole is loaded to within 3m of the collar and not stemmed to allow for further decoupling.

The trim or wall control blast fired next to the pre-shear has the closest two rows loaded lighter with reduced burden and spacing compared to the production rows (Figure 4). The buffer row closest to the final wall is 3m from the pre-shear line. The holes are drilled on 4m spacing. These holes are loaded with two 150kg decks. The second row of holes is drilled on 5m spacing with a 5m burden and loaded with 200kg and 250kg decks. The third row is a laid out the same as a standard production row.

The use of a smaller diameter hole for the pre-shear resulted in better quality walls, reduced time scaling the final wall, and a better catch bench (Figure 5).

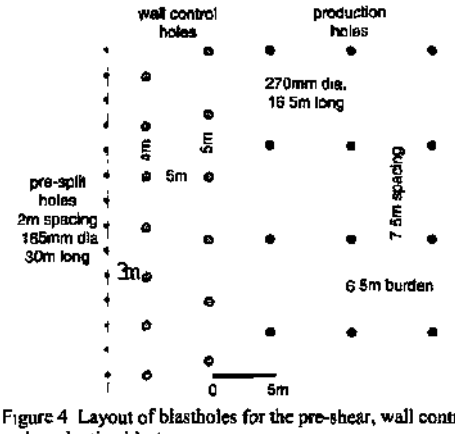

Figure 4 Layout of blastholes for the pre-shear, wall control, and production blasts.

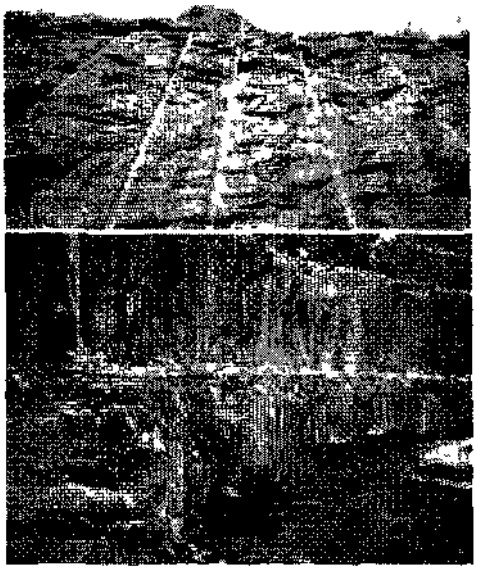

Figure S. Successful wall control blasts showing half barrels from pre-spht holes and stable benches

3 BLAST MONITORING EXPERIMENTS

Three blasts were monitored at the Ekati mine during August to October 2000. The blasts were the 345-38 production blast, 345-40 wall control blast, and the 330-45PS pre-shear. The 345-38 blast was the 38th blast on the 345 bench, and was drilled from the 360 bench. The 345-40 blast was also drilled from the 360 bench and was the 40 blast on the bench. The pre-shear blasts are drilled every second bench to accommodate the 30m double bench.

3.1 *Vibration Monitoring*

The peak particle velocity, PPV, is often related to a blast's ability to fracture rock, through the relationships between PPV and dynamic stress or strain. McKenzie et al (1992) identified two mechanisms by which blast vibrations can cause damage:

- generation of fresh fractures in intact rock, and
- promoting slip along unfavorably oriented joint and fracture surfaces.

The first is a near field effect, and the second can occur up to hundreds of metres from a blast.

The vibration amplitude is a function of the charge weight per delay, rock type, scaled distance and charge geometry. The vibration data can be used to develop a scaled distance law that relates the PPV to the charge distance (Dowding 1985).

Over the past ten years of blast monitoring, the consensus among the leading practitioners is that geophones are the best choice for vibration monitoring. Geophones that are robust and have a suitable dynamic range and are suitably grouted in place provide the best means of collecting vibration information. The vibration monitoring was carried out with uniaxial geophones (OYO 101LT 900ß 14Hz) grouted into boreholes at mid-level of the benches. The geophones were oriented with placing rods in the boreholes to point toward the blast before grouting.

3.2 *Gas Pressure Monitoring*

One of the objectives of the field tests was to assess whether explosive gases penetrated along induced or existing fractures to a significant distance beyond the blast perimeter. Research on gas penetration monitoring has been published by Preston & Tienkamp (1984), Williamson & Armstrong (1986), Lilly (1987), LeJuge et al. (1994), Bulow & Chapman (1994), Forsyth et al. (1997), Ouchterlony et al. (1996), and Brent & Smith (1996, 1999). It is difficult to collect reliable and reproducible gas penetration data. The difficulties involve the instrumentation design and the location of the instrument and the local geology.

The instrumentation used at Ekati was a sensitive Honeywell 18615PCDT pressure sensor installed in a sealed borehole a given distance from the blast. The borehole had a diameter of 100 or 165mm and was drilled to depth of 15m below the bench. A 2m long section of 50mm diameter ABS pipe with a threaded end cap was sealed by grout and cuttings over the upper 2m of the borehole. The pressure sensor, which is capable of reading 137kPa overpressures to 137kPa under-pressures, was installed inside the cap threaded onto the end of the ABS pipe and thus exposed to the pressure changes occurring in the borehole. The 18615PCDT Honeywell pressure sensor is designed to read relative pressure changes and a short tube was vented to the atmosphere through the top of the threaded cap for this purpose.

The pressure sensor has good dynamic response <1ms and gives direct output voltage in the 7 to 16 volt range. An Instantel Minimate logger was used to record the pressure signals at a sampling rate of 16kHz. When other researchers conducted borehole pressure monitoring near blasts to detect penetration of high-pressure explosive gasses, it was noted that that under-pressures or negative pressures with respect to atmospheric pressure often occurred. Work by Brent & Smith (1996, 1999) suggests that this phenomenon İs due to volume increase caused by crack formation and overall rock mass dilation. Their data are based on twelve free-face blasts where there were no instances of high-pressure gas penetration. Pressures were monitored at distances less than one burden. This was also supported in work done by Ouchterlony et al. (1996) where 10 of 13 blasts showed under-pressures, the three overpressures coming from pre-split blasts.

4 RESULTS

4.1 *Visual Observations*

The damage behind the production blasts typically follows this pattern: 5 to 7m back break from last row of holes, large cracks opened up to the 10m range and fine cracks as far as 25m behind the last row blasted. In all cases the cracking appears to be related to the jointing (Figure 6). There is often vertical offset on these cracks as well.

The wall control blasts typically resulted in small structurally controlled failures along the crest and some opening of horizontal joints is visible near the crest.

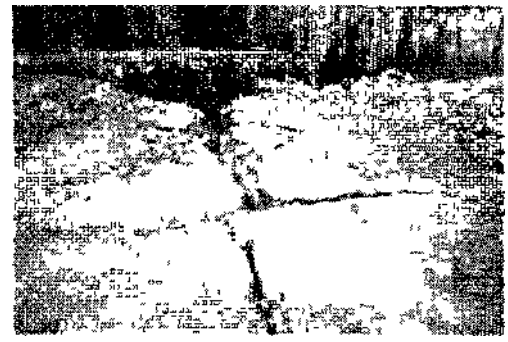

Figure 6. Cracking behind production blast at Ekati.

4.2 *PPV- Scaled Distance Relationships*

Two PPV - scaled distance relationships were used to process the recorded vibration data from the 345-38 production blast and the *345-40* wall control blast. A traditional square root scaling relationship was used. A square-root relationship assumes the explosive charge acts at a point and is best for condition involving near spherical concentrations of explosive or when monitoring relative far from the explosive column. In this approach, the square root of the charge weight is used to fit an equation of the form:

$$PPV = K\left(\frac{R}{\sqrt{W}}\right)^{-\beta} \quad (1)$$

where:

PPV = peak particle velocity (mm/sec)

R = distance from charge (m)

W= charge weight (kg)

K, ß = site specific constants.

The scaled distance is given *by R/sJ W* .

A second method to analyze the vibration data was proposed by Holmberg and Persson (1979). This method works best for near-field prediction of vibration amplitude since the method essentially integrates the effects of vibration generated over the length of the borehole. The PPV data were fit to an equation of the form:

$$PPV = K\left[\frac{l}{R_o}\right]^{\beta/2}\left[\phi - \arctan\left(\frac{R_o Tan\phi - H}{R_o}\right)\right]^{\beta/2} \quad (2)$$

with the Holmberg term defined as:

$$HolmbergTerm = \left[\frac{l}{R_o}\right]\left[\phi - \arctan\left(\frac{R_o Tan\phi - H}{R_o}\right)\right] \quad (3)$$

where:

PPV = peak particle velocity (mm/sec)

/ = linear charge density (kg/m)

K, a, ß = site specific constants

R_o, ϕ, x, H are defined in Figure 7.

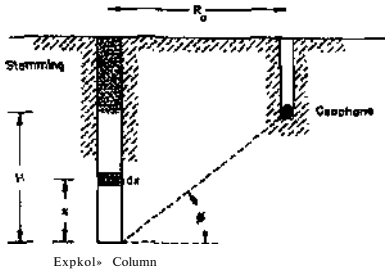

Figure 7. Definition of terms used in the Holmberg term.

The field data were plotted in two forms: log (PPV) vs. log (scaled distance) and log (PPV) vs. log (Holmberg term). On each plot linear regression lines were added. From each equation the site specific constants K and ß were calculated. The plots for each are shown in Figure 8 and Figure 9.

The square-root scaling relationship gave the constants K = 332 and ß = 1.53 for the production blast and K= 206 and ß = 1.14 for the wall control blast. The Holmberg relationship gave the constants K = 1650 and ß = 1.58 for the production blast and K = 7644 and ß = 1.20 for the wall control blast. In bom cases, the degree of fit on the production data was very good (R = 0.85), while the data from the wall control blast had a poor fit (R^2 = 0.26 or 0.29).

A value of K = 1686 was used by Holmberg & Persson (1979) for a large open pit scenario. This agrees well with the K value of 1650 from the

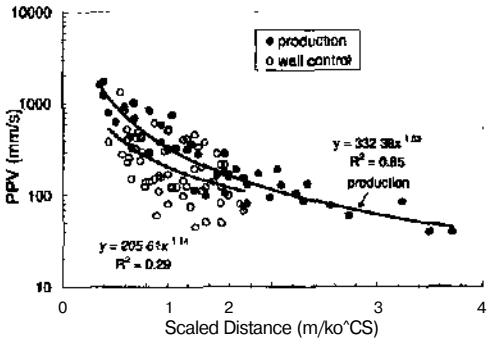

Figure 8. PPV versus scaled distance for the 345-38 production blast and the 345-40 wall control blast.

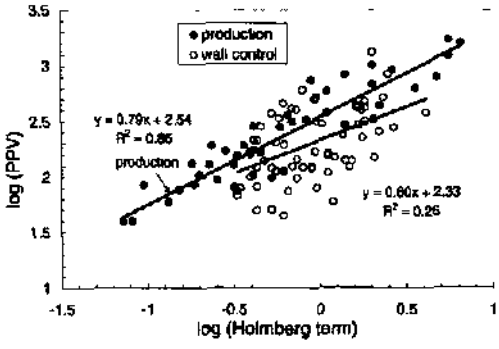

Figure 9. PPV versus Holmberg term for the 345-38 production blast and the 345-40 wall control blast.

production blasting. The ß value for the production shot monitored at Ekati was 1.58. The ß value in the study by Holmberg and Persson (1979) was 1.78. Both values are within the range of 1 to 2 that is commonly encountered. Due to die effects of the pre-shear and choked face (Figure 10) it İs difficult to compare the constants from the wall control blast to values from literature.

The increased scatter in the data from the wall control blast may be attributed to one or a combination of the following issues:

- me blast was choked on one free-face,
- large amounts of water were draining into the pre-shear fracture,
- larger variation in the charge weight per delay than the production blast, and
- the geophones were located behind a previously blasted pre-shear.

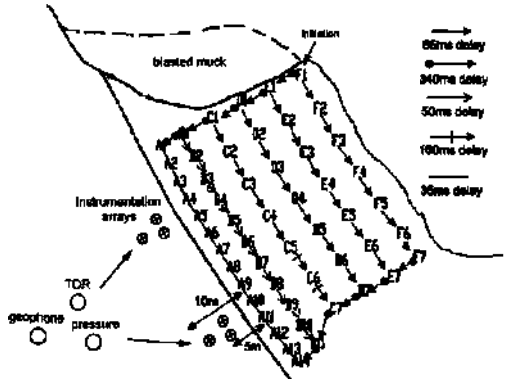

Figure 10. Layout of blastholes and instrumentation holes for the 345-40 wall control blast.

The choked free face on the wall control blast had a noticeable effect on the vibration levels in the final wall. The geophone located closest to the pre-existing pile of blasted muck recorded a PPV of 1300mm/s while the other location, which was near a better free face, only recorded a PPV of 600mm/s. This clearly illustrates the effect that a choked face can have on the damage to the final wall.

For the conditions monitored *at* Ekati Mine both the square-root scaled-distance and Holmberg methods gave similar degrees of fit to the data. Based on this observation it is recommended that the square-root scaled distance relationship be used for simplicity. It is difficult to back calculate distances for the Hohnberg equation, and no significant improvement in quality of PPV prediction İs realized.

4.3 *Borehole Pressures During the Production and Wall Control Blasts*

The gas pressures measured in empty sealed boreholes near the blasts followed the trend of other researchers in that no explosive gas penetration was observed from the production blast or the wall control blast. The wall control blast resulted in an under-pressure of 70kPa below gauge pressure (Figure 11) and the production blast resulted in an under-pressure of 67kPa.

The time of the greatest pressure drop in the wall control blast corresponds to the detonation of the second last row and final row of blastholes. These detonations generated a PPV of 850mm/s and 1300mm/s, 5m behind the pressure monitoring hole The second last row of blastholes was 8m from the instrument array. The rock mass likely dilated along a combination of pre-existing discontinuities that opened as the stress wave passed as well as new fractures. There was also likely to have been some heaving from the blast that would also cause dilation.

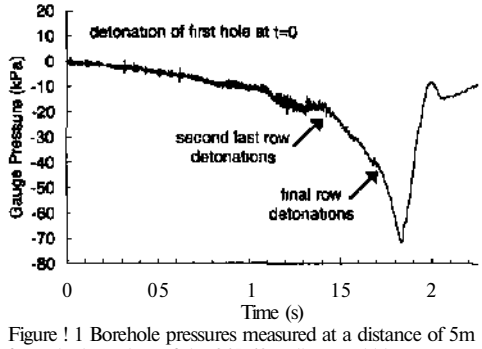

Figure ! 1 Borehole pressures measured at a distance of 5m from the boundary of the 345-40 wall control blast

The production blast had a similar trace to the wall-control blast. The pressure drop was slightly larger (70kPa) than the production shot. By comparing vibration signatures from individual holes on the vibration trace to die pressure trace, it is clear that the pressure drop did not occur until the second last row was detonating. The blast was choked on the free face closest to the pressure sensor (Figure 10). As a result, the PPV values at that monitoring location were double the values at the second location.

Penetration of explosive gases was not observed for the production or wall control blasts because the gases appear to preferentially vent towards the free face where the resistance to flow is the smallest.

4.4 *Borehole Pressures During the Pre-Shear Blast*

Borehole pressure monitoring was also carried out on the 330-45PS pre-shear blast. For this blast, explosive gas penetration was observed as indicated by an increase in borehole pressure in the monitoring hole that was 5m from the nearest blastholes. The pressure trace is shown in Figure 12. The pre-shear holes were all detonated at the same time (at t=0s on the trace).

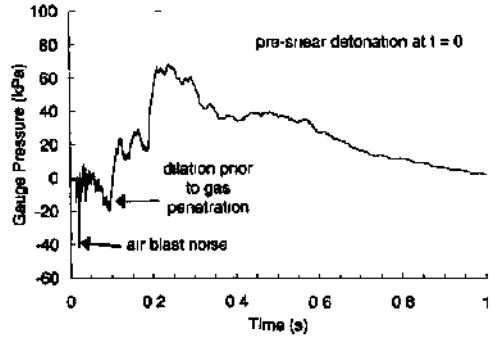

Figure 12. Borehole pressures measured at a distance of 5m from the 330-45PS pre-shear blast

The PPV recorded from the pre-shear blast was 685mm/s. There was no change in borehole pressure as the stress wave passed the monitoring hole. There is some high frequency noise at the beginning of the trace that is likely caused by an air blast from the unstemmed pre-shear holes. The air blast traveled at a velocity of =330m/s arriving at the monitoring hole 15ms after detonation.

Following the air blast noise and prior to the increase in borehole pressure there is a pressure drop of 18kPa. This phenomenon has been observed by others and according to McKenzie et al. (1992), it results from rock mass dilation occurring prior the inflow of gases. It İs assumed that the penetrating gases act like a wedge driven into the rock mass causing tensile stresses and fracturing ahead of the gas front. The rock dilation manifests itself as a pressure drop immediately preceding the arrival of the gases themselves in the borehole.

By comparing the vibration and pressure traces it is possible to calculate the average velocity for the explosive gases from the blastholes to the pressure monitoring hole. The gases took 100ms to travel a distance of 5m, giving an average velocity of 50m/s.

LeJuge et al. (1994) published a similar trace to Figure 12 recorded behind a pre-shear blast. This study also monitored pressures at greater distances from a pre-shear. While all holes showed an initial dilation, it was only the closest hole that recorded an overpressure. They concluded that bench swell can extend significantly further than gas penetration. This also appears to be the case at Ekati Mine.

5 CONCLUSIONS

Ekati Mine has implemented a number of modifications to their blast designs to improve fragmentation and diggability as well as to minimize blast damage to the final bench walls. Blast monitoring showed that explosive gases from the wall control blast do not penetrate past the row of previously fired presplit holes. Blast vibrations measured in the final pit wall from production or wall control blasts are also reduced because of the presence of the holes and fractures from the pre-split blast. The use of 30m long pre-split holes allowed creation of stable double lift benches without any lips.

It appears that there are two main blast damage mechanisms. The first is from the penetration of explosive gases from the pre-shear blasts. The second mechanism, heaving, results from the production and wall control blasts. This is caused by the vertical movement from the blast, and can extend tens of metres from die blast perimeter. This mechanism causes the greatest damage to the final wall.

While the pre-shear appears to cause some damage to the wall, it also helps to reduce the subsequent damage occurring from heaving. Reducing the damage to the final wall would best be accomplished by minimizing the confinement of the last two or three rows of the wall control blasts, and therefore reducing the resulting heave. Reducing or eliminating the stemming in these rows could achieve this. LeJuge et al. (1994) saw improved results after eliminating decking and stemming of buffer holes in wall control blasts.

ACKNOWLEDGEMENTS

The authors wish to thank BHP Diamonds Inc. Ekati™ Mine and Polar Explosives Ltd. for financial support for this project. The intent of project was to develop a better understanding of the blast damage mechanisms at the Ekati™ Mine.

REFERENCES

Brent G.F. & Smith G.E. 1996. Borehole pressure measurements behind blast limits as an aid to determining the extent of rock damage. *Fragblast 5, Proc. 5th In/. Symp. on Rock Fragmentation bv Blasting,* Montreal, Balkema, 103-112.

Brent G.F. & Smith G.E. 1999. The detection of blast damage by borehole pressure measurement. *Fragblast 6, Proc 6th Int. Symp. on Rock Fragmentation by Blasting,* Johannesburg, Balkema.

Bulow B.M. & Chapman J. 1994. Limit blast design at Argylle Mine. *Proc. Open Pit Blasting Workshop,* Curtin University, Perth, 104- 109.

Dowding C.H., 1985, *Blast Vibration Monitoring and Control,* Prentice Hall, Inc., Englewood Cliffs, New Jersey, 297p.

Forsyth W.W., Connors C.& Clark L. 1997. Blast damage assessment al the Trout Lake Mine. *Proc. 99th CIM Annual General Meeting,* Vancouver, on CD, 9p.

Holmberg R. & Persson P.A. 1979. Design of tunnel perimeter blasthole patterns to prevent rock damage. *Proc. /MM Tunnelling '79 Conference,* London, 280-283

LeJuge G.E., Jubber L., Sandy D.A. & McKenzie C.K. 1994. Blast damage mechanisms in open cut mining, *Proc. Open Pit Blasting Workshop,* Curtin University. Perth, 96-103.

Lilly J.D. 1987. Achieving pit wall integrity with large diameter blast holes. *Proc. 2" International Symposium on Rock Fragmentation Bv Blasting,* Keystone, Balkema, 634-645

McKenzie C.K.. Holley K.G. & LeJuge G.E. 1992. Rock damage from blasting. *Proc. Asia Pacific Con/. - Quarrying the Rim,* Hong Kong.

Ouchterlony F.. Nie S., Nyberg U. & Deng J. 1996. Monitoring of large open cut rounds by VOD, PPV and gas pressure measurements. *Fragblast 5, Proc. 5th Int. Symp. on Rock Fragmentation bv Blasting,* Montreal, Balkema. 167-176.

Peterson J. 1998. Fragmentation Analysis - BHP Diamonds Inc. Ekati Mine. Polar Explosives Ltd., Report to BHP Diamonds, 9p.

Preston C.J. & Teinkamp N.J. 1984. New techniques in blast monitoring and optimization, *CIM Bulletin,* 77(867), 43-48,

Williamson S.R. & Armstrong M.E. 1986. The measurement of explosive product gas penetration. *Proc. '.arge Open-pit Mining Conference,* AuslMM, 147-151.

17* International Mining Congress and Exhibition of Turkey- IMCET2001, ©2001, ISBN 975-395-417-4

Evaluation and Analysis of Blasting Procedures for Removing Hard Formations at the South Field Lignite Mine, Ptolemais, Greece

Z.Agioutantis
Department of Mineral Resources Engineering, Technical University of Crete, Hania, Greece

S.Bozinis
LCP-A, Public Power Corporation, Greece

G.Panagiotou
Department of Mining Engineering and Metallurgy, National Technical University of Athens. Greece

C.Kavouridis
Assistant General Director, Public Power Corporation, Greece

ABSTRACT: Drilling and blasting procedures are utilized for removing various types of hard overburden formations at the South Field Lignite Mine, at the Lignite Center of Ptolemais-Amydeon, operated by the Greek Public Power Corporation. This paper presents a statistical analysis of blasting performance parameters for a number of years as well as an evaluation of blasting results as recorded by mining personnel at the site. Appropriate blasting and overburden removal indices are also presented.

1 INTRODUCTION

Greece is the fifth largest producer of soft brown coal in the world and the second largest in the European Community, producing about 63Mt of lignite per annum. The Lignite Center of Ptolemais-Amydeon (LCP-A), operated by the Greek Public Power Corporation (PPC), is located in northern Greece, about 110km west of the city of Thessaloniki. The lignite deposits under exploitation cover an area of 120km^2. This area includes approximately 4000Mt of proven geological reserves and about 2500Mt of exploitable lignite under current economic and technological criteria. Today (January 2001), the LCP-A operates four large lignite fields, which produce lignite used to cover 60% of power generation in Greece. At the present rate of extraction, 51Mt of lignite is produced annually (comprising over 80% of total lignite extraction in Greece), by moving a total volume of 250Mm^3 (waste and lignite).

The South Field Mine (SFM) is the largest of the four operational surface mines at the Lignite Center of Ptolemais-Amydeon, covering an area of 24km^2 (Figure 1). The original lignite deposit in the area was estimated at 1.2 billion tons of lignite. Mining operations commenced in August 1979 and the mine currently operates on ten benches, mainly using the continuous mining method, which employs bucket wheel excavators (BWEs), conveyors and stackers. For operational purposes, die field İs divided into 10 sectors (Galetakis & Agioutantis, 2000). Currently, sector #2 is being mined, while preparatory work is under way for sector #3. In addition to the continuous mining method, conventional mining equipment, including off-highway trucks, front-end loaders, electric rope and hydraulic shovels, dozers and mobile crushers, are utilized for mining the hard rock formations which are encountered in the overburden strata.

The South Field Mine can be considered unique regarding the mining conditions and the methods used to exploit the lignite deposit. More specifically, İn sector #2, benches la, lb, 2a, 2b and 3 are designed to excavate overburden, while benches 4, 5, 6a, 6b and 7 are set in the lignite seams. Sixty-five

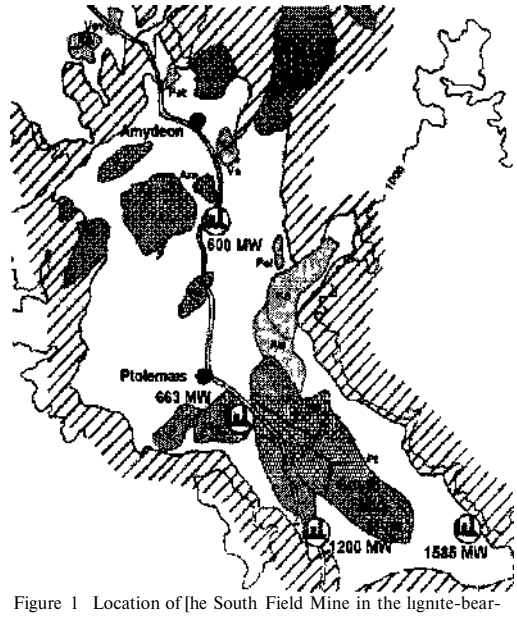

Figure 1 Location of [he South Field Mine in the lignite-bearing Ptolemais-Amydeon valley

conveyor belts with a total length in excess of 100km are installed in the SFM. The mining depth İs expected to reach 200m. The scheduled annual lignite production at the SFM ranges from I8-21Mt (covering about 33% of the total lignite production in Greece for the year 2000), while overburden removal operations produce 47-53Mm^3 of bank material annually. The volume of total annual excavations amounts to 90Mm^3 (Table 1). From the beginning of mining operations up to the end of 2000, 1005Mm^3 of total earth material was removed and 221Mt of lignite was produced with an average exploitation ratio of 3.75:1 (nvVt).

Table 1. Material handling at LCP-A.

Location	Lignite production (Mt/year)	Total excavations (MnvVyear)
South Field Mine	18-21	90
Other LCP-A Mines	30-32	160
Total LCP-A	51.5	250

2 OVERBURDEN REMOVAL OPERATIONS

Overburden strata in the SFM consist of fine and coarse clastic sediments such as clays, marls, gravel, conglomerates with embedded hard layers of sandstones, cemented conglomerates and mudstones. The average specific weight of the overburden is 19.62kN/m (2ton/m^3) and the average bulking factor ranges from 1.4 to 1.5. The average thickness of the overburden material is 90m. Table 2 summarizes the range of the mechanical and physical properties of the hard rock formations, while Table 3 presents the approximate extent of each formation at the SFM.

Table *2.* Range of mechanical and physical properties of the hard rock fo nn a tions.

Parameter	Range
Uniaxial compressive strength (MPa)	15-143
Tensile strength (MPa)	2.4- 11.2
Density (kN/m^3)	23.5 - 26.5
Density (ton/m^3)	2.4 - 2.7
Bulking factor	1.4- 1.5

Approximately 25-30% of the overburden consists of hard and semi-hard formations, which are removed using conventional mining methods, while the remainder is excavated by BWEs. As early as 1981, there was a decision to apply large-scale drilling-and-blasting operations to loosen the hard rock formations and to use mobile load-haul equipment to move the blasted material. The semi-hard formations within the overburden strata that cannot be excavated by BWEs are loaded by shovels without any blasting. It should be noted that one of the unique features of the overburden removal operations is that drilling-and-blasting and shovel-truck operations are considered supporting mining operations that should accommodate the needs and priorities of the primary excavation operations, which are carried out by BWEs.

Currently, five blasthole rigs (Tamrock C50 K.3L) are deployed, drilling over 1000 m of blastholes per day at 7^{7} and 9in diameter in 4x5m or 6x6m blasthole grids. In recent years, about 1250-1650 tons of explosives were consumed annually (Figure 2) by detonating about 700 shots. That corresponds to 2-3 blasts per day, with the explosives' load ranging from 1 to 8 tons per blast. The drillheads are air-cooled tricones (IADC 622) with embedded carbide bids.

Originally, blasting was accomplished by utilizing ANFO mixes with either ammonia dynamite (extra dynamite) products or gelatin dynamite (30% weight strength) for boosters. Wet holes were loaded with 30% weight strength gelatin dynamite (Agioutantis, et al., 2000).

For the first time, in 1995, SFM engineers used a special mixture of ANFO and an emulsion called Heavy ANFO (H-ANFO), which was prepared in situ by mixing the emulsion (nitrate salts dispersed as small droplets in a continuous oil base) and porous ammonium nitrate. Several mixing ratios were evaluated for application in the SFM before selecting the optimum one (Agioutantis & Kavouridis, 1998). This mixture has relatively high bulk strength, a higher critical diameter (over 150mm), but good blasting characteristics in wet blastholes. Hence, ANFO is currently used in dry holes and H-ANFO İs used in wet holes. Ammonia dynamite is used as a booster to ANFO and gelatin dynamite as a booster to H-ANFO- or ANFO-loaded blastholes. The use of water resistant explosives has increased in recent years (Figure 3).

Table 3. Estent and dimensions of each overburden formation group (Papageorgiou & Pakas, 1997).

Rock type	Rock description	Area (km')	Average thickness (m)	Volume (Mm^3)	Percent (%)
Hard material	conglomerates, sandstone	24	11	264	13
	conglomerates, breccia	10.5	10	105	5.2
Semi-hard material	clay, sandstone, gravel	10.5	10	105	5.2
Loose material	clay	24	61	1464	72.3
	sand, gravel	22	4	88	4.3
Total		24		2026	100

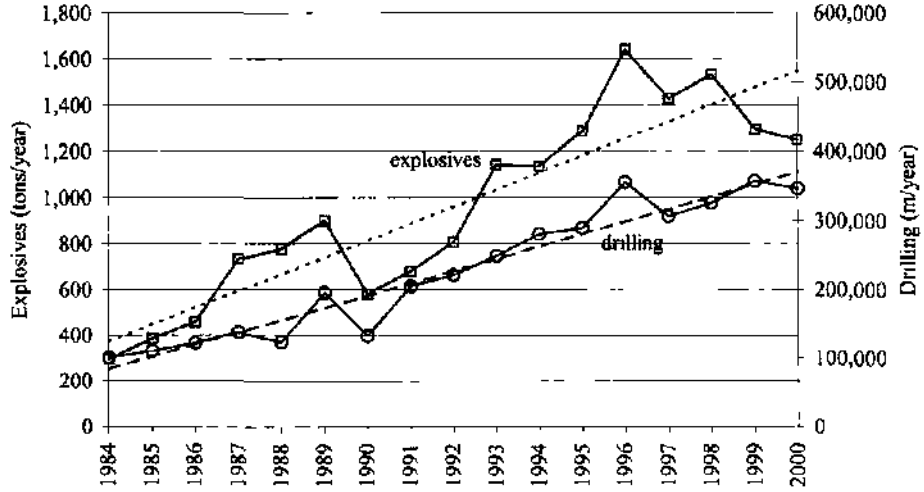

Figure 2 Total explosives consumption and total drilling at the South Field Mine.

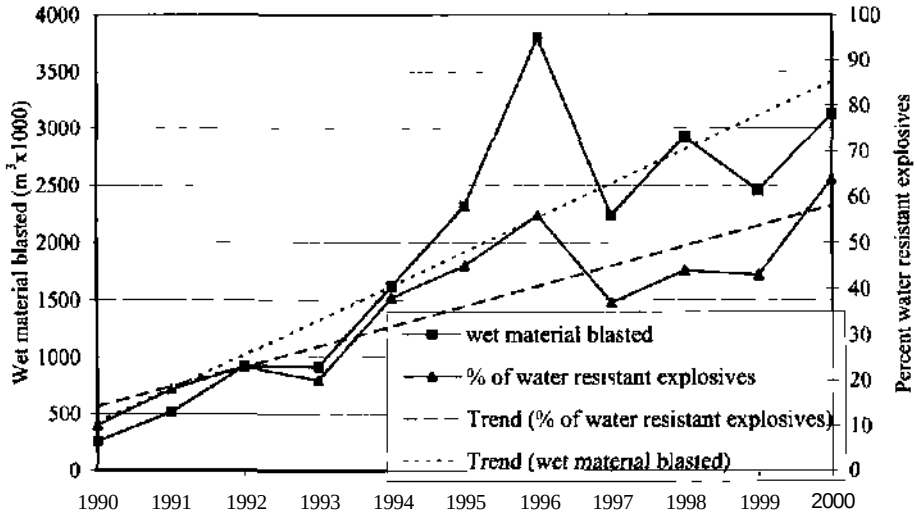

Figure 3. Wet blasted material and percent of water-resistant explosives used at the South Field Mine

The hard formation mining operations at the SFM employ about 240 people in 3 shifts moving approximately 13Mm of overburden material annually. However, in order to carry out mining plans for the preparation of sector #3, external contractors using conventional equipment excavate an additional 5Mm^3 of overburden material. In summary, the PPC currently handles all of sector #2 mming (hard and soft rock formation removal) while contractors handle all of sector #3. In past years (1996, 1997), contractors were involved in sector #2 operations as well.

3 BLASTING PERFORMANCE STATISTICS

Figure 2 presents the total explosives consumption per annum and the corresponding total drilling effort in the SFM for the last 16 years. As is shown by the corresponding trend lines, both explosives consumption and drilling is steadily increasing. It should be noted that since the hard formation lenses are not uniformly distributed within the overburden, drilling and blasting statistics may experience fluctuations over a given time period.

Figure 3 presents the volume of the wet material mat was blasted and the corresponding percentage of water-resistant explosives used for these operations (e.g., H-ANFO) from the total amount of explosives used per annum for the last 10 years. Currently, the specific consumption is approximately 250g/m^3 of overburden.

Table 4 presents the distribution of me production of the hard and semi-hard overburden materials for benches lb, 2a and 2b (sector #2), The total production handled by conventional equipment ranged from 10 to 12Mm^3 per year for the period 1996-2000. BWEs removed volumes ranging from 10 to 15.6Mm^3/year, while contractors excavated smaller volumes (in 1996 and 1997 only). During the last five years, an average of 45% of the overburden volumes handled by the PPC were removed using drilling-and-blasting and shovel-truck operations.

Table 5 presents the total overburden excavations handled in the SFM, (using conventional equipment) between 1996-2000. This data includes excavations in sector #3 as well as in benches la and 3 (not included in Table 4), which account for only 10% of the total excavations. From the data presented in Table 5, the blasted/moved ratio of the hard and semi-hard waste material is calculated, showing that 44% of the excavated volume requires blasting. In practice, all hard rocks are blasted while semi-hard rocks are excavated directly. In this respect, drilling and blasting operations need to negotiate all aspects of hard formations, includmg thin hard lenses embedded in soft or semi-hard benches. In these cases, all soft and semi-hard material is directly removed, the hard lenses are blasted, and operations resume for the remainder of the bench. Therefore, it is not unusual to blast 2m thick ledges using 9in holes in 5x5 grids. Evaluation of the bench-specific data presented in Table 5 highlights the variability of the overburden material. For example, the need to blast overburden in bench lb decreased to 13%, compared to 96% in 1996, while the blasting requirement remained constant for bench 2a over the same time period.

Figure 4 shows the density distributions (histograms) of the drill hole depth using data collected during 1996 and 2000 (Bozinis, 2000). It should be noted that such data have been available through daily logs since operations started. It can be observed that the trend in 2000 is for shallower drill holes, which corresponds to thinner lenses. Figure 5 presents the corresponding cumulative distribution function for the same data.

Table 4. Distribution of production of hard and semi-hard overburden materials (m^3 x 1000) between BWEs and conventional excavation equipment (shovels) for benches 1 b-2a-2b (sector 2. oenod 1996-2000).

	1996				1997				1998			
	BWEs (1)	Shovels* (2)	Total (3)	Ratio U>/(3)	BWEs (1)	Shovels (2)	Total (3)	Ratio (2)/(3)	BWEs (1)	Shovels (2)	Total (3)	Ratio (2)/(3)
bench-lb	3915	630'	4545	0.14	5058	2331"	7389	0.32	6642	916	7558	0 12
bench-2a	2894	4586*	7480	061	4186	4993*	9174	0 54	3737	5978	9715	0 62
bench-2 b	3649	5510'	9159	0 60	4381	5642*	10023	0 56	5358	4566	10124	0.45
Total	10458	10726*	21184	0.51	13625	12966'	26586	0 49	15737	11460	27397	0.42

	1999				2000				Totai \ 996-2000			
	BWEs (1)	Shovels (2)	Total (3)	Ratio (2)/(3).	BWEs (1)	Shovels (2)	Total (3)	Ratio (2)/(3)	BWEs (1)	Shovels (2)	Total (3}	Ratio (2)/(3)
bench-lb	6908	1417	8325	017	4235	2415	6650	0 36	26758	7709	34467	0 22
bench-2a	2933	7294	10227	0.71	3972	7011	10983	0 64	17722	29862	47579	0 63
bench-2b	5799	2277	8076	0 28	5359	1197	6556	0 18	24546	19192	43938	044
Total	15640	10988	26628	041	13566	10623	24189	0.44	69026	56763	125984	0 45

partial contractor production is included

Table 5 Comparison of moved and blasted hard and semi-hard material (m^1 x 1000) al the South Field mine (period 1996-2000)

	1996			1997			1998		
	blasted(l)	moved (2)	ratio (1V(2)	blasted (1)	moved (2)	ratio (11/(2)	blasted (!)	moved(2)	ratio (l)/(2)
sector-3	301	330	0.91	546	677	081	1470	1550	0 95
bench-la*	15	20	0 75	0	1	0 00	52	60	0 87
bench-lb*	607	630	0.96	1595	2331	0.68	294	916	0 32
bench-2a*	2040	4230	0.48	1703	4812	0 35	2899	5978	0 48
bench-2b*	1445	3546	0.41	830	3870	0.21	1470	4566	0 32
bench-3*	0	236	0 00	0	343	0.00	0	86	0.00
Total	4408	8992	0 49	4674	12034	0.39	6185	13156	0.47

	1999			2000			totals 1996-2000		
	biasted(l)	moved(2)	ratio(l)/(2)	blasted(l)	moved (2)	ratio(l)/(2)	blasted(1)	moved(2)	ratio (l)/(2)
sector-3"	998	1172	0 85	610	620	0.98	3925	4349	0.90
bench-1 a*	0	1	000	505	582	0.87	572	664	0.86
bench-lb*	594	1417	0.42	323	2415	0.13	3413	7709	0.44
bench-2a*	3168	7294	0 43	3517	7011	0 50	13327	29325	0 45
bench-2b*	536	2277	0 24	180	1197	0 15	4461	15456	0 29
bench-3*	0	199	0 00	0	209	0 00	0	1073	0 00
Total	5296	12360	0.43	5135	12034	0 43	25698	58576	044

* benches belong to sector 2
currently a single bench operation using conventional equipment only.

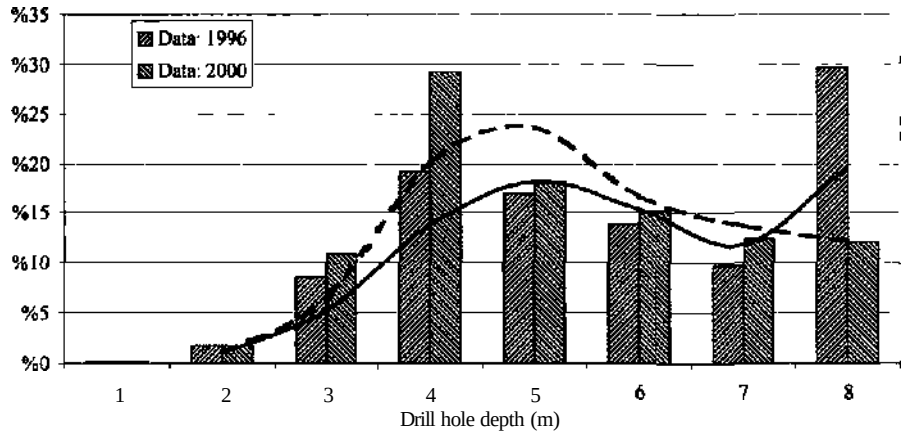

Figure 4. Distribution of drill hole depths

Figure 6 shows the density distributions (histograms) of the total weight of explosives per blast (tons), using data from the same time period. The data indicate that most of the time the blast load ranges from 1 to 4 tons of explosives, although local peaks may be observed in particular months. Again the distribution for the 2000 data is smoother, which results in better predictions and thus better mine planning. Figure 7 presents the corresponding cumulative distribution function for the same data. The results presented in Figures 4 and 6 are interrelated since the decreasing thickness of blasted benches resulted in lower drill depths and lower explosives consumption per blast.

Figure 8 presents an analysis of monthly explosives consumption for the year 2000. It should be noted that although the total consumption is below that of previous years (Figure 2), the trend in the last quarter of 2000 may lead to the conclusion that increased consumption should be expected in 2001.

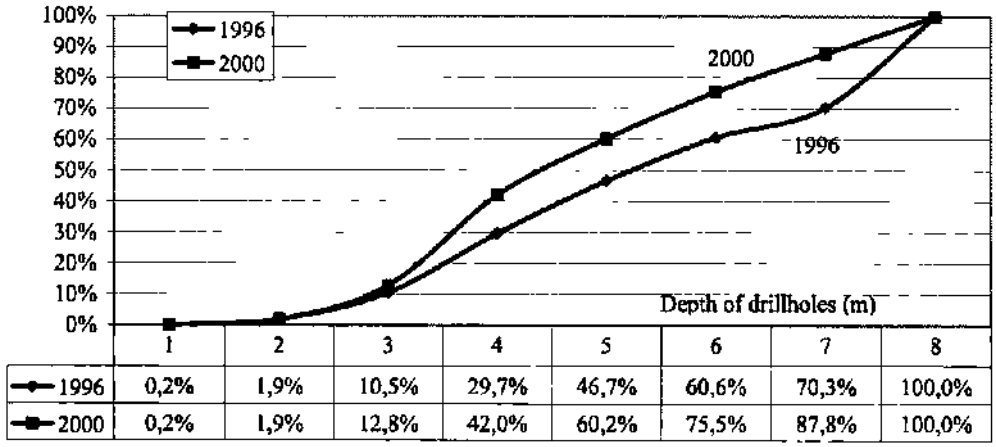

	1	2	3	4	5	6	7	8
1996	0,2%	1,9%	10,5%	29,7%	46,7%	60,6%	70,3%	100,0%
2000	0,2%	1,9%	12,8%	42,0%	60,2%	75,5%	87,8%	100,0%

Figure 5. Cumulative distribution of drill hole depths.

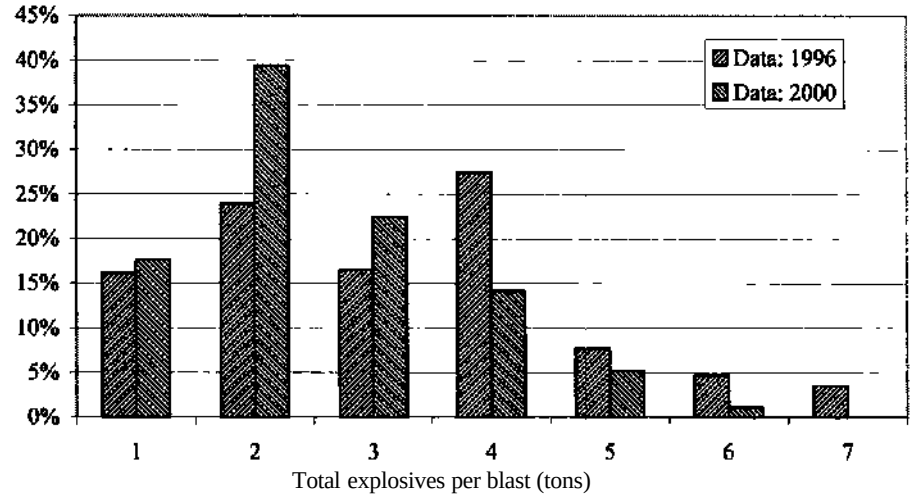

Figure 6. Distribution of total explosives per blast.

This is in accordance with the occurrence of thicker and stronger formations in the currently mined benches. In addition, increased use of water-resistant explosives is evident due to the presence of water in the deeper permeable hard rocks (Figures 8 and 9).

4 SUMMARY AND CONCLUSIONS

Overburden removal operations at the South Field Mine at the Lignite Center of Ptolemais-Amydeon utilize both conventional and continuous excavation techniques. Continuous mining is carried out entirely by the PPC, while conventional mining is carried out by both the PPC and contractors. This paper presented data pertaining to conventional overburden removal operations that require the use of explosives to break up the hard rock formations that occur sporadically within the overburden strata.

It should be noted that blasting conditions are unique due to me variability of the hard rock formations and the fact that hard rock removal has to ac-

commodate the needs and advance rates of the continuous systems that handle the majority of the overburden material. It should also be noted that it is preferable (and more economical) to remove the soft cover of a bench and then blast the hard lenses directly rather than blast the full height of the bench using complicated blast hole loading techmques such as decking

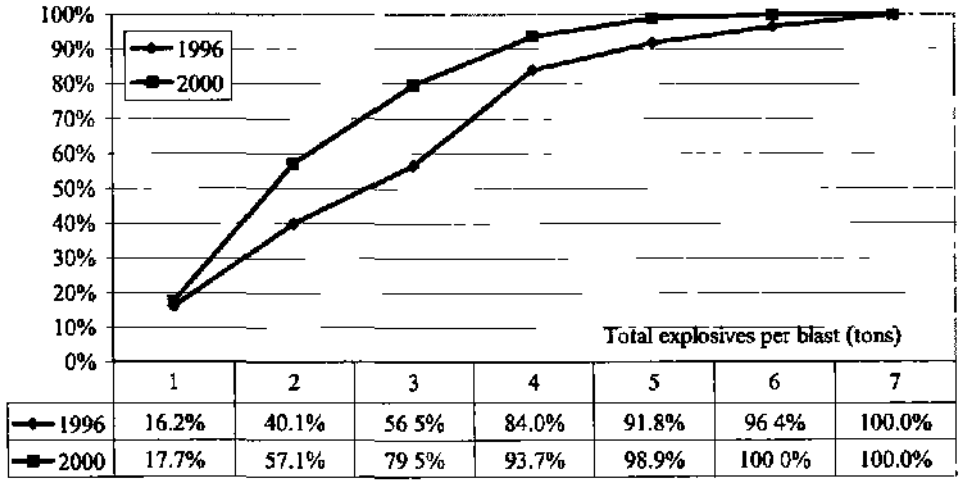

	1	2	3	4	5	6	7
1996	16.2%	40.1%	56 5%	84.0%	91.8%	96 4%	100.0%
2000	17.7%	57.1%	79 5%	93.7%	98.9%	100 0%	100.0%

Figure 7 Cumulative distribution of total explosives per blast

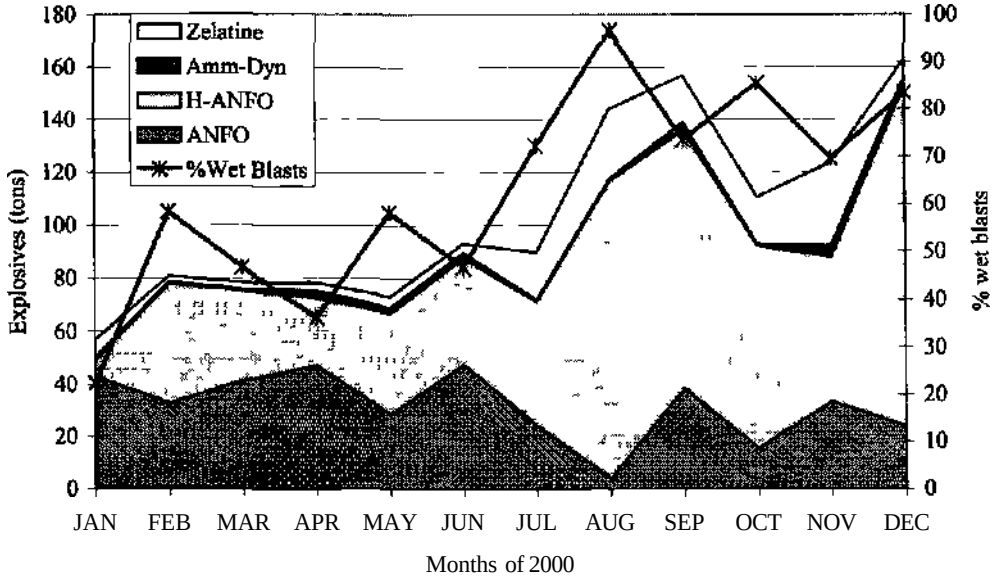

Figure 8 Explosives consumption for year 2000 at the SFM Note that ammonium dynamite is used spanngly

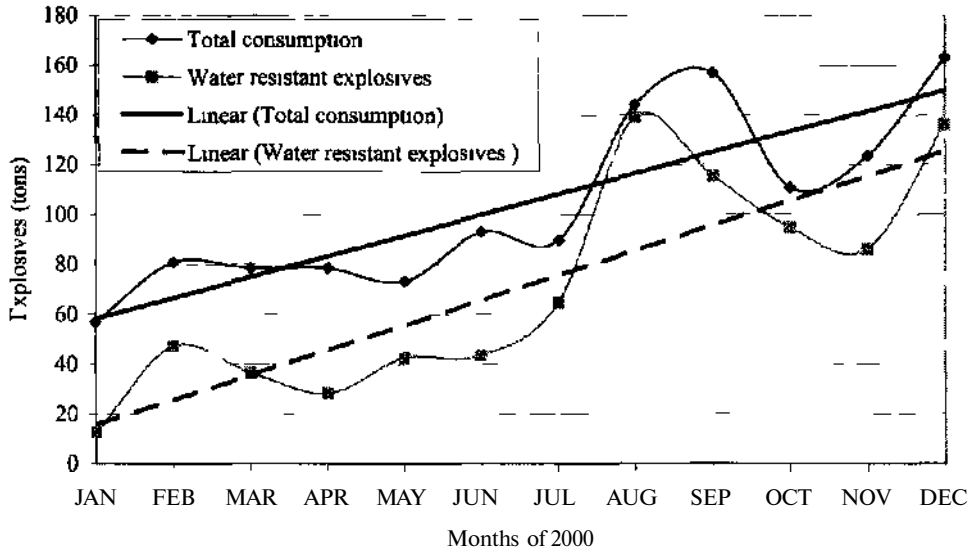

Figure 9 Total explosives consumption and percent of water resistant explosives for year 2000 at the SFM

More specifically, the following statistics were observed

- The annual total explosives consumption ranged from 1650 to 1250 for the last 5 years The projected consumption for the following year{s) is to exceed 1700 tons annually, based on the increased explosives consumption dunng the last quarters of the year 2000
- The total length of blastholes drilled per year is currently m the order of 350km
- In recent years, there has been an increasing need to blast overburden material under wet conditions Currently, the explosive of choice is Heavy ANFO, which is a mixture of ANFO and emulsion explosives, and is produced in situ by special ANFO Mix trucks
- The percentage of water-resistant explosives has also increased m recent years
- The linear trends (projections) for explosives consumption and wet blasts show similar rates (2000 data)
- Forty-four percent (44%) of the material moved by conventional methods needs to be loosened by blasting The remainder is excavated directly from die face using heavy-duty shovels
- In the benches where both the continuous and conventional excavation methods are used (1b, 2a, 2b), forty-five percent (45%) of the overburden material is excavated using conventional methods
- The variability of the overburden material can be established by the variability of the blasted/moved ratios presented for each bench

Statistical distributions of blast load per blast show that currently, the most common configuration is a 2-ton blast

Statistical distributions of drill depth per blast show that currently, the most common depth is 4m, which is rather shallow considering that drill diameters are either $7^{7/8}$ or 9 inches and the blasting grid is usually 5x5m

REFERENCES

Agioutantis Z, C Kavourıdıs, S Bozınıs&K. Tsampis, 2000 Assessment of vibration measurements due to blasting of the hard formations at the South Field lignite mine, Ptoiemais, Greece *Proceedings,* 9th International Symposium on Mme Planning & Equipment Selection, Athens, Greece - November 6-9

Agioutantis, Z & C Kavoundis, 1998 Technological enhancements in the drilling and blasting procedures for removing hard formations at the South Field Lignite Mine, Ptoiemais, Greece *Proceedings,* 7th International Symposium on Mine Planning & Equipment Selection, 1998, Calgary, Alberta, pp 173-177

Bozinis S , 2000 Computenzed South Field Mine Blasting Re cords *Unpublished Data* Public Power Corporation

Galetakis, M & Agıoutantıs Z, 2000 The influence of strategic development options on the long term quality variation of mined lignite the case of the South Field Mine in Ptoiemais, Greece *Proceedings,* 9th International Symposium on Mme Planning & Equipment Selection, Athens, Greece November 6-9

Papageorgiou, C *& Z* Pakas, 1997 The hard rock removal in the overburden of South Field Lignite Mine of Ptoiemais, Greece *Proceedings,* 2 Konferenz zur Mobilen Gerate techmk, Leipzig, September 17 19

17* International Mining Congress and Exhibition of Turkey- IMCET 2001, ©2001, ISBN 975-395-417-4

Increasing the Effectiveness of Blasting in Underground Mines

B.U.Raskildinov
"Underground Developing of Minerals " Department ofK Satpayev Kazakh National Technical University

ABSTRACT: This article describes a new alternative technology of blasting using ampoule technology of column charge dispersion. This technology ensures the quality of blasting of a rock mass and an increase in the effectiveness of blasting in development and slope operations in ore deposits.

1 INTRODUCTION

The main technological process in underground ore body development is the blasting process. During development and sloping processes, drilling and blasting operations take up 50-70% of all the process and volume. The quality and the cost of development depend on the effectiveness of the drilling and blasting operation. The duration and laboriousness of drilling-blasting operations mainly depends on the physio-mechanical properties of the blasted rock, the cross-section of the development, the blasting parameters and also the blast hole and hole charge construction.

2 INCREASING THE EFFECTIVENESS OF BLASTING

One of the ways to increase the effectiveness of drilling and blasting operations is the improvement of blast hole design and column charges in hard rock blasting operations.

Analysis of the existing design of explosive charges used the blasting of rock masses in mining enterprises provides an opportunity to see that along with widespread solid cylinder columns of explosives, there are various more effective designs for a better control of the heat of explosion under rock mass destruction. The basis of this design is the application of a wide range of factors, such as decreasing of the initial pressure of the explosion product, increasing of the time of influence upon the rock mass, the creation of several groups of detonation waves in a charge. However, in spite of the advantages of dispersed charges İn comparison with solid charges; they are not so widely used because of their cost and the time necessary for the charging of blast holes.

With a solid, full column charge of explosives, the greatest part of the heat of explosion is spent in excessively strong fragmentation and grinding of the rock, while much of the heat is absorbed because of the viscosity of the rock and its heating. The remainder of the heat of explosion energy is utilized for displacement of the pieces of rock over a significant distance. As a result of such heat or energy losses in the explosion, the efficiency of the process sharply decreases.

An essential increase in the efficiency of the explosion and decrease in the plastic deformation zone, over grinding of the rock and increasing the area of harder influence of the explosion to the rock can be achieved by increasing the time of the explosion influence for the file, decreasing the "peak" of the pressure and strengthening the interaction of the Shockwaves and gas flows due to the air intervals remaining in the cavity of the column charge.

At synchronous blasting of the parts of dispersed charge from the thread of the detonating cord or from additional initiators, intense collision of gas flow and shock waves occurs İn each part of the charge several times increasing the pressure İn the air gap limit. This sharply increases the seismic influence upon the roof and walls of stopes and m developing negatively influences the stability of the massive rocks found m the contour. Therefore, during initiation of the dispersed charge, based on the transmission of detonation inside the blast hole from one part of the charge to another through an air gap without initiation system supply, which does not involve the collision of gas flows and shock tubes, the seismic influence of the blast upon the massive

rocks in the contour is decreased and its stability increases. Moreover, the influence time of the blast gasses is increased and this raises the heat of the explosion use ratio.

In respect of the statement above, the creation of air intervals by using ampoule technology of the dispersion was designed (Bitimbayev, Bekbayev, Raskildinov, 1987; Raskildinov, 1991; Raskildinov, Alzamarova, 1995; Raskildinov, 1995; Raskildinov, 1994). Compared to other methods, it İs more practical; it simplifies the technology of blasting operations because it does not need any additional time for charging. Ampoules are filled with air and are placed between the parts of the dispersed charge of explosive. This method completely avoids the installation of detonating cord in the blast hole charge because air is an ideal sphere for transmission of detonation by influencing between separate parts of dispersed charges. The proposed construction provides the opportunity to decrease the seismic influence of the explosion upon the roof and walls of development and slopes, and to minimize with this sticking of rocks of out contour massif and to obtain quality fragmentation of the rock mass, reducing the yield of over-fragmented ore fines.

Detonation from the active part of the dispersed column charge to the passive part is transmitted by shock-wave influence. The main factors influencing the transmission of detonation through such influence are: impulse (J), pressure of the detonation product (P), velocity of the shock wave (U), and the temperature of detonation formed by initiation of the active part of the column charge.

The parameters of the factors above mainly depend on weight, the type of explosives, the VOD of the active charge, the physicochemical properties of the passive part of the charge and its density, and also the sphere where the dispersed column charges are placed. For the passive part of me charge of the explosives with no clear period of burning, the detonation occurs toward the zone where the parameters of the detonation products (J, P, U) of its active part will be big enough. If a shock wave of lower value comes to the passive part of the dispersed charge, the burning period precedes the detonation. The stimulating ability of the passive part of the dispersed column charge to detonation through the influence is determined by the weight and construction of its active part.

Expérimenta! blasts for determination of the distance transmission of detonation between the active and passive parts of the dispersed column charges were held in underground mines in the Irtysh, Belousov and Mirgalimsaisc fields. The blasts took place in a breakage face with two outcrop planes with a strut of room boards. The distance from the column charge to the free surface was 400-600 mm. Blast hole charges with a diameter of 40 mm and depth of 4 m were dispersed between the active and passive parts of polyethylene ampoules filled with air. The research was carried out with different types of explosives, with the active part of the dispersed column charge placed in the collar of the blast hole (direct initiation).

There were three blasts for each type of weight of active charge and exact distance. The results for transmission of detonation through influence were considered positive only if stimulation of detonation in the passive part of the charge through the air gap occurred in all three attempts. Experimental blasts were carried out with the weight of the active part ranging from 0.050 kg to 0.500 kg and the size of the passive charge being no less man 1.00 kg.

The results of the experimental blasts determined the critical distance between the active and passive parts of the dispersed column charge through influence. However, when forming the dispersed column charge without using additional initiators or detonating cord (DC), it is necessary to know the distance of stable transmission of detonation through the influence of die active part to the passive. If the passive part of the charge is not subject to enough shock-wave influence, the size of which depends on the detonation parameters of the active part of the charge and the distance between them, the explosive in the passive part will not detonate or will detonate with a very low velocity, causing burning-out of the explosive. This will affect the quality of explosive, which is not desirable during blasting operations, deadlock excavation and breakage. Thus, İn order to set the distance of stable detonation in the passive part of the charge, we carried out these blasts in the underground mines mentioned above.

During the experimental blasts for determination of the VOD of the explosives, the active and passive parts of the charge were placed in steel tubes with diameters of 36-100 mm and with walls of 10-20 mm thick.

Mathematical treatment of die data from the experimental blasts for determination of the distance of transmission of stable detonation in the passive part of the charge through influence led to empiric dependence as follows:

$$L^{S}_{SD} = \left(-0.15 + 4.05 Q^{2}_{AC}\right) \sqrt{\frac{D_{ST}}{D_{EX}}}, (\text{m}) \qquad (1)$$

at $0.050 \le Q_{AC} \le 0.500$ kg,

where $L^{S}SD$ - the distance of the transmission of detonation in the passive part of the charge, m; $Q_{A}c$ - weight of active charge, kg; and $D_{S}T$, DEX - velocity of detonation of standard {Ammonite 6 GV) and used explosives, m/s.

During the experimental blasts, detonation in the passive part of the dispersed column charge was

considered stable if its velocity was not less than 0.8-0.9 of the VOD of the active part of the charge.

The experimental blasts showed that the distance of transmission of stable detonation through influence depends on the weight of the active part of the charge, but it is considerably less than critical. For example, when the weight of the active charge is 0.200 kg, the stable distance is 0.600 m.

The dependence (1) makes it possible to set the possible distance of transmission of the detonation through influence inside the blast hole which will give a stable VOD in the passive part of the dispersed column charge.

Therefore, the results of the experimental blasts, by definition of the distance of transmission of detonation and velocity of detonation in the passive part of the charge with stimulation through influence due to the shock-wave effect, confirm that when forming the column charge dispersed by air gaps of polyethylene ampoules filled with air, additional initiators or DC installation, which make the blasting process complicated and expensive, are not necessary in either deadlock excavation or breaking.

The physical essence of charges separated into lengths by cylinder ampoules filled with air without DC installation between the parts lies in the fact that after initiation of the active charge inside the column charge, the shock wave occurs with certain parameters, typical for a given mass of the charge and type of explosives. It was determined Úiat air is a favorable sphere for transmitting detonation over a distance, which is why the effect of the shock wave stimulates detonation in passive charges. In addition to this, explosion products, expanding relatively fluently during an artificial interval created beforehand, initially decrease the peak pressure of detonation products and increase the time of influence upon the blasted rock mass. Part of the heat of the explosion is retained, and is used in plastic deformation and regrinding of the rock. Next, the retained part of the heat of the explosion is usefully spent in destruction of the sphere in great volume, which finally increases the general ratio of the heat of explosion application.

On the basis of the research, the construction of dispersed column charges and blasting technology as a whole, both for preparatory development and breaking in underground ore deposits, was designed.

The blasting technology and its rational parameters of blast hole blasting in preparatory development operations using the recommended ampoule technology of dispersed column charge were tried in different mining geological conditions in the Irtysh, Belousov, Mirgalimsay, Aksay and Shalkiin fields. The number of blast holes during the commercial trials with dispersed charges was equal to the number of blast holes blasted during solid charge construction as any reduction in the number of blast holes under the dispersion led to a sharp decrease in heading advance per round to shot hole length ratio. The results of the experimental blasts were evaluated in accordance with this ratio, the deviation of the rock mass contour and the powder factor of the explosives. The rational parameters were those parameters which allowed minimum deviation of the rock mass contour and the minimum powder factor of the explosives and heading advance per round to shot hole length ratio not less than that used with solid charge construction.

During the blasting of development and breaking faces with dispersed charge, active and passive parts of the charge with interchange of explosives and ampoules filled with air were formed inside the blast hole. The size of die air gap (la) in one stage of dispersion consisted of l-2 ampoules. The air gap between separate parts of the dispersed column charge did not exceed the permissible stable distance of transmission of detonation through influence.

The experimental blasts showed that the ampoule technology for creating and blasting the dispersion charges during the preparation works decreased the additional quantity of rock from behind the contour from 16.0-18.0 to 0.5-1.0% and decreased the specific charge of the explosives up to 15-20% at breakage and up to 35-40% at contour boreholes. Using the results of the trials and obtained dependence, ways of forming the blast hole charges and methods of rock blasting for deadlock excavation and breaking operations were examined (Raskildinov, Alzamarova, 1995; Raskildinov, 1995).

The application of the designed technology of the blasting and breaking of ore deposits underground enabled (Raskildinov 1995; Raskildinov, Usupov 1992; Raskildinov, Usupov, 1996):

- qualitative rock mass fragmentation with the minimum yield of small ore (15-18% instead of 50-60%) working with overhand stopes with two and three exposure levels, decreases of 3-4 times in operational losses and dilution, and a 35-40% decrease in the powder factor of the explosives;
- decreases in the yield of non-standard quality ore from 8-10% to 2-3%, the yield of small ore from 48-50% to 18-20% and operational dilution from 8-10% to 2-3%, and a decrease of 15-20% in the specific charge of the explosives in room mining with hole ore breakage.

3 CONCLUSIONS

The recommended technology for blasting operation in development and face-entry operations and breaking of ore deposits using the ampoule technology of formation of dispersed blast hole charges, compared to current methods, decreases the

seismic influence of the explosion to the rock of the out contour file. The explosives become harder and more resistant and the effectiveness of contour blasting increases, allowing qualitative fragmentation of the rock mass and reduction in the yield of small ore.

REFERENCES

Bitimbayev, M., Bekbayev S., Raskildinov B. 1987. Choice of rational parameters of blast hole blasting at excavation of flat seams. *Mining Journal.* 7.

Raskildinov B- 1991. Determination of distance of transmission of detonation between the parts of the column charge dispersed by the air gaps. *Gas-dynamic of Blast and Shock Waves of Detonation and Supersonic Burning: All-union Symposium Thesis.*

Raskildinov B., Alzamarova E. 1995. *Method of Blasting the Ore Massif (Patent 2298 PK)* 3.

Raskildinov B. 1995. *Method of Blasting the Ore Massif (Patent 2298PK)* 3.

Raskildinov B. 1994. Perfection of the Construction of Dispersed Column Charges. *Actual Problems of Modern Science and Technique.*

Raskildinov B-, Usupov H. 1992. Way of Blasting of Steeply Falling Thin Veins.

Raskildinov B., Usupov H. 1996. Way of Blasting of Steeply Falling Thin Veins.

17* International Mining Congress and Exhibition of Turkey- IMCET2001, ©2001, ISBN 975-395-417-4

Timing Simulation for the Selection of Optimum Delay Time

G.G.U.Aldaş
Barutsan A.Ş., Elmadağ, Ankara, Turkey
H.A.Bilgin
Department of Mining Engineering, Middle East Technical University, Ankara, Turkey
S.Esen
Julius Krüllschnitt Mineral Research Centre. The University of Queensland, Brisbane, Qld, Australia

ABSTRACT: This paper presents the use of the blast monitoring system to determine the optunum delay time for blasts in stripping work at Demir Export Kangal/Sivas Surface Coal Mine in Turkey. The blasting procedures and blast monitoring program followed are explained. Eight signature blasts were conducted at (he mine. A high-speed video camera system was used to determine the delay time interval resulting in an adequate relief. A timing simulation of the ground vibration record of one of these shots is carried out. The effect of the delay time on the amplitude of peak particle velocity and frequency İs shown. It was determined that the delay time for this mine was 120 ms, considering both timing simulation and high-speed video camera system output.

1 INTRODUCTION

With the recent advances in blasting technology, it is now possible to avoid many assumptions in blasting. Thus, optimum blast results are achieved considerably faster than with the trial and error approach of relying on the experience factor alone.

This study illustrates an experimental methodology to determine delay time using a blast monitoring system. Ground vibrations from the signature blast, which is defined as the detonation of a single hole at one time, were monitored by seismographs and evaluated by the software of die seismograph. The timing simulation approach to an event in the signature blast may help to determine the optimum delay time that results in lower peak particle velocity (PPV) amplitudes and higher frequencies. Combining the results with a high-speed video camera system, the optimum delay time may be determined. Adequate relief, low PPV amplitudes and high frequency are essential aims of these analyses. Thus, it is necessary to consider the outputs of both the blast vibration monitoring and high-speed video camera system.

One of the most important and constantly growing uses of seismographs is in recording and analysing single hole signature shot waveforms. This is the basis of investigating how delay times and detonator (conventional) scatter can affect ground vibration amplitudes and frequencies from time shifts and the resulting constructive or destructive interference patterns. Without proper simulations, a blaster could unknowingly create intense vibration levels by selecting improper delays (Chıappetta, I998).

This paper is part of a project carried out jointly by the Middle East Technical University and the BARUTSAN Co. (Bilgin et al., 2000). Fieldwork was conducted in November 1999 at Demir Export Kangal/Sivas Surface Coal Mine in Turkey (Esen et al., unpubl.).

2 OVERBURDEN LITHOLOGY

Discontinuity surveys and seismic refraction technique are employed to characterize the rock mass at Kangal Surface Coal Mine. The rock type and properties of rock (intact and mass) are given in Table 1. The upper part of the current bench, consisting of weak and clayey limestone damaged by the previous blast, has a thickness of 1.0-1.5 m. The insitu p-wave velocity of this layer is 650 m/s. The clayey marl formation which is below this layer has an in-situ p-wave velocity of 1500 m/s. A thin and unexploitable coal layer İs occasionally present in this layer.

3 BLASTING OPERATIONS AND BLAST MONITORING

Blasting operations for stripping work at Kangal/Sivas Open Cast Coal Mine in Turkey are carried out to loosen the rock formations for efficient

Table 1. Rock type and properties of rock (intact and mass).

Bench No	310
Rock Type	Clayey-Marl
Weathering	Low-medium
Discontinuity Spacing	1 m
Number of Joints	3
Joint Spacing	0.9 m
Joint Aperture	-
Joint Persistence	Continuous
Insitu p-wave Velocity	1500 m/s
Lab. p-wave Velocity	2902 m/s
Fracture Index	0.64
ROD (calculated)	35.1%
Uniaxial Compressive	8.5 MPa
Tensile Strength	1.23 MPa
Density	1.96 g/cm^3

loading and hauling operations. A shovel / truck combination is utilised for the removal of the upper horizons of overburden, whereas dragline removes the lower parts above the coal seam. This study was conducted at one of the upper benches where the shovel/truck system is used. The bit diameter of the drilling machine was 241 mm. The principal blasting agent was ANFO. Table 2 and Table 3 list the surface blast design parameters of the signature and production blasts, respectively.

The authors did not interfere with the surface blast design parameters of the production blasts. The complete sets of delay detonators were not available in the mine. Therefore, during vibration monitoring, instantaneous (0 ms), 30 ms *and* 330 ms delay caps were used in blasting operations. The authors simply monitored the blasts and obtained the records.

All blasts were monitored by continuous velocity of detonation recorder for assessment of explosive performance and detection of incomplete detonation, if any. A high-speed video camera system was used for determining dynamic response time, delay time and face velocity, and seismographs were used for measuring ground vibration and airblast. The evaluation of the records is discussed in the next section.

4 EVALUATION OF THE RECORDS OF THE BLAST MONITORING SYSTEM

Field velocity of detonation (VOD) measurements were performed with a continuous VOD recorder (VODR-1) developed by EG&G and BAL They were carried out to assess the performance of the blasting agent (ANFO) and primer. It was found that the average VOD of ANFO was 3955 m/s. The tetonation performance of ANFO and the primer has been shown to be sufficient, yielding good blast results (Esen et al., unpubl.).

In order to determine the delay time for this bench which will provide an adequate relief, a KineView 1256p high-speed video camera system was used (Figure 1). Images were obtained at 250 frames per second. MOTION TRACKER - 2D software was used to carry out motion analysis. Markers on the bench were tracked to compute the face velocity and delay time.

Table 2. Blast design parameters for signature blasts.

Bench height	13m
Hole length	12 m
Burden (B)	7m
Stemming length	7m
Weight of Explosive	150 kg
Blasthole inclination	Vertical
Charging configuration	Bottom priming, continu-
Initiation system used	Electric detonator

Table 3. Blast design parameters for production blasts.

Bench height	13 m
Hole length	8.2-11.7 m
Burden (B)	9.8-12.3 m
Spacing (S)	8.0-12.3 m
Stemming length	4.9-6.6 m
Weight of Explosive	150-250 kg
Average Specific Charge	0.181 kg/m^3
Blasthole inclination	Vertical
Charging configuration	Bottom priming, continu-
Blasthole partem	Rectangular
Initiation system used	Electric detonator
Delay between rows	0, 30, 330 ms

The delay time between rows was found to be in the range of 120-140 ms by the high-speed video camera system. However, the best delay time between rows should be determined by considering the outputs of both a high-speed video camera system and ground vibration analysis.

Eight signature blasts were conducted at bench no. 310. The ground vibration monitoring line was parallel to the bench face (N84E). Blast vibration measurements were carried out using two 4-channel seismographs and one 8-channel seismograph. The PPV in transverse (T), vertical (V) and longitudinal (L) components, the distance from the measurement point to the blast site (R) and the maximum weight of explosives per delay (Q) are shown in Table 4.

When the records from all eight signature blasts are analysed, it can be seen that body waves dominate due to the short scaled and absolute distances. It was also observed that in six of the eight records from single shots, the longitudinal (L) component of vibration dominates. Therefore, in the evaluation of the timing simulation, this component İn particular was taken into account.

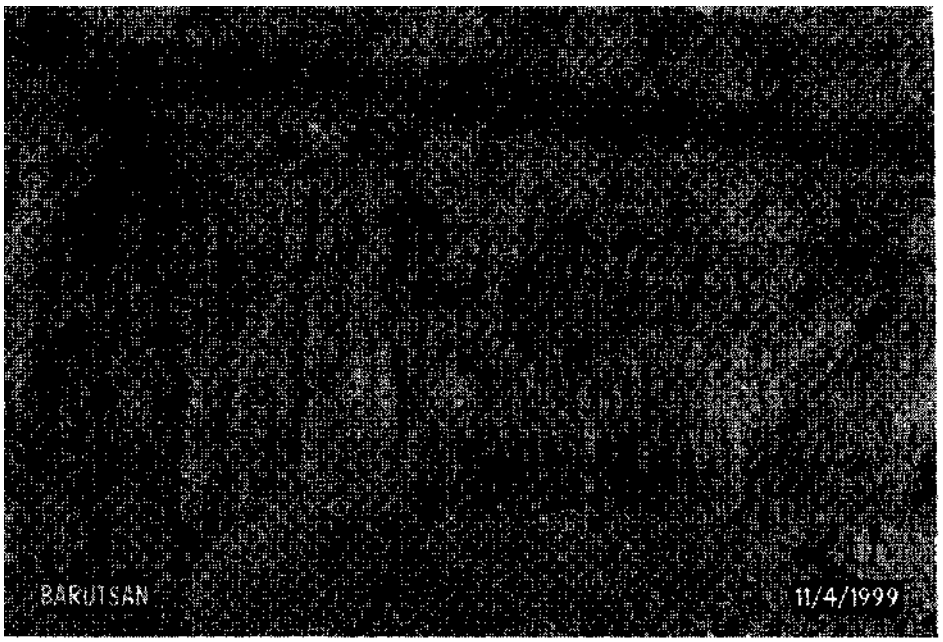

(a)

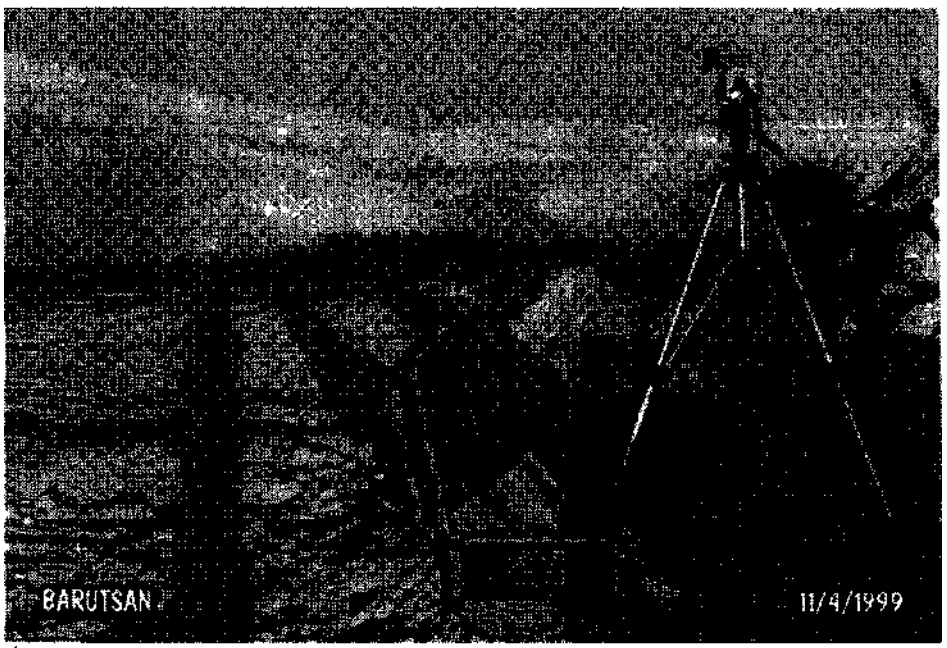

(b)

Figure I {a) Bench face ı!tuvtı<ıltng maiker* (.b) High - speed video camera system

Table 4. Ground vibration levels for signature blasts

Shot No	*Date*	***R, m***	*Q.kg*	*\m/kg^{ni}*	*T, mm/s*	*V, mm/s*	*L, mm/s*
İ	03.11.1999	20.3	150	1,66	128.0	247.0	178.0
2	03.11.1999	30.3	150	2.47	104 0	208.0	136.0
3	03.11.1999	62 1	150	5.07	125.0	53-7	140.0
4	03.11.1999	50.3	150	4.11	84.5	116.0	123.0
S	03.11.1999	36.0	150	2.94	83.6	85.7	119.0
6	03.11.1999	46.0	150	3.76	87.9	63.8	113.0
7	03.11.1999	77.8	150	6.35	47.4	35-3	58.5
8	03.11.1999	66.0	150	5.39	34.8	35.8	71.1

*SD: Scaled distance

It is well known that pyrotechnic detonators have a certain scatter İn their nominal detonation time. In other words, blastholes in a production blast may detonate at a time different than their nominal detonation time. Furthermore, blast design parameters certainly affect vibration levels. Therefore, it is not possible to use a ground vibration record obtained from a production blast in timing analysis. Ground vibration records from signature blasts should be used in these analyses. Different delay times may be simulated to determine the optimum delay time by using the timing analysis. The optimum delay time is selected considering the PPV amplitudes and frequency spectrum.

The timing simulation of the 7th shot shown in Table 4 was performed. The delay times used in time simulation were 30, 60 90, 120, 150 and 330 ms. the effect of the delay time on the amplitudes of PPV and frequency is shown in Table 5.

It is shown that minimum PPV and suitable frequency values were attained when the delay time was 120 ms. Higher frequency is preferred as there is less risk of damage than with lower frequencies. Figure 2 and Figure 3 illustrate waveforms and frequencies, respectively, for the signature blast and simulated blast with a delay time of 120 ms. Tran, Vert and Long refer to the PPV components in transverse, vertical and longitudinal directions, respectively. SSM1, SSM2 and SSM3 are the PPV components in transverse, vertical and longitudinal directions, respectively, for the new waveform obtained with a delay time of 120 ms.

By considering both the timing simulation of the signature blast vibration and high-speed video camera system analysis, the best delay time between the rows was selected as 120 ms. While determining the optimum delay time for the blasting operations in stripping work, the following criteria are taken into account: good looseness for subsequent loading and hauling operations, minimum PPV values and greater frequencies (above resonant frequencies) that are as high as possible so as not to cause environmental damage.

The site factors determined for signature and production blasts are given in Table 6. Twenty-two ground vibration records were obtained for production blasts. When all of the 22 vibration records from production blasts were analysed in terras of PPVs for the L-component, it was observed that the blasts with instantaneous and 30-ms detonators produced higher vibrations than those blasts with a 330-ms delay penod (Bilgin et al., 2000). This experimental result is also supported by the evidence derived from the timing simulation given in Table 5. Another finding from vibration monitoring of the production blasts was that surface waves (especially Rayleigh waves) dominate in most of the waveforms (Bilgin et al., 2000).

The scaled distance (SD) and monitoring distance (R) ranges of signature and production blasts were 1.66-6.35 m/kg^{0}*, 20.3-77.8 m; 10.25-29 70 nVkg^{05}, 290-630 m, respectively. Unfortunately, due to physical limitations arising from the bench dimensions, the monitoring distances for the signature blasts could not be kept the same as those of the production blasts.

Due to the differences in waveforms, scaled distances and absolute distances, any comparison (and prediction) between signature and production blasts would not be meaningful and reliable. Therefore, in the future, new signature blasts should be conducted at similar distances so that the predicted ground vibrations using timing simulation of the new signature blasts can be meaningfully compared with the ground vibrations resulting from production blasts.

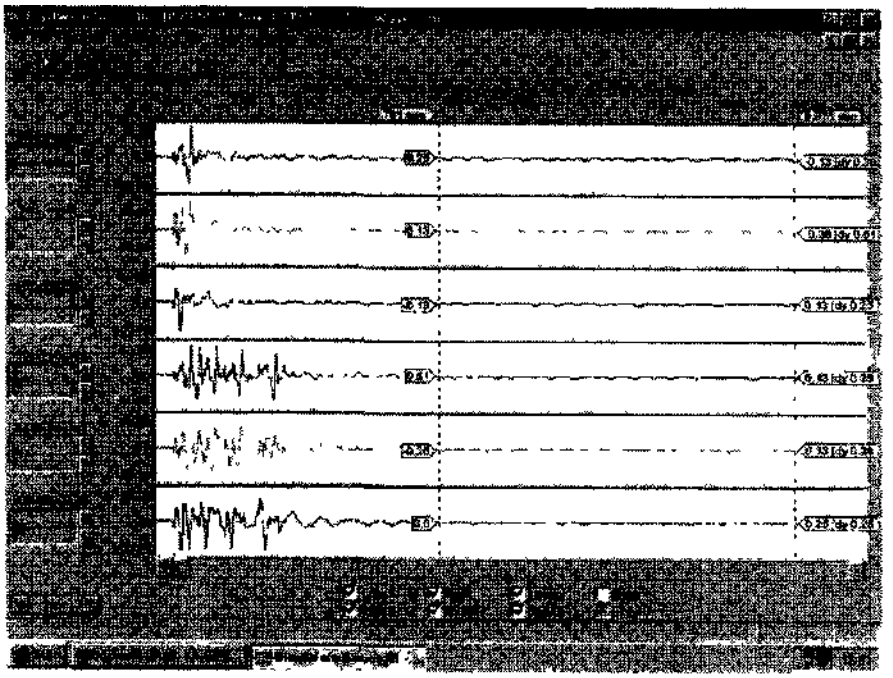

Figure 2 Waveform» *of signature* blast and *simukicd blast* with detay (ime of f 20 *ms.*

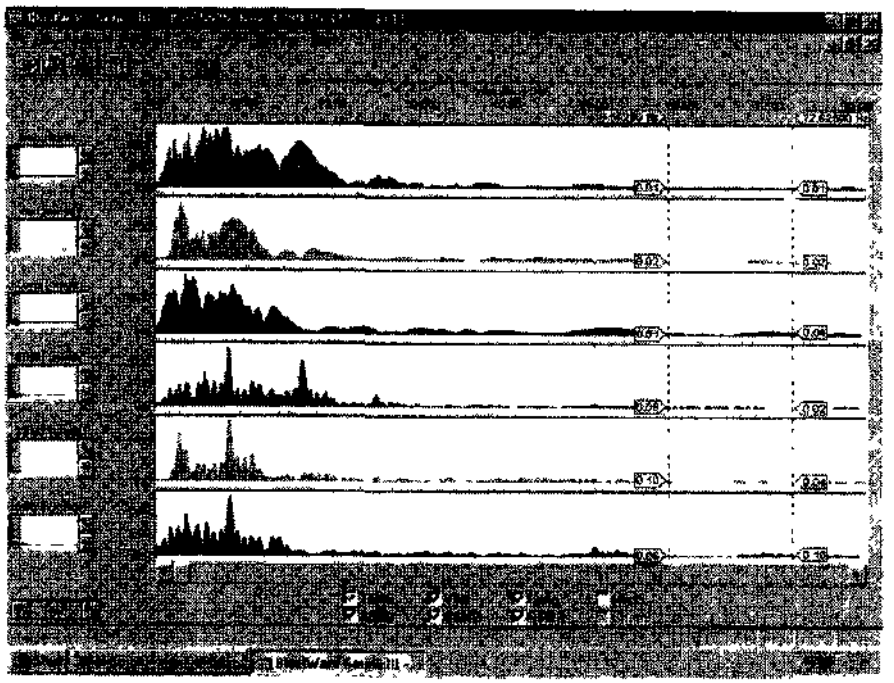

Figure 3. Frequencies of signature bla« and Minulaied blast with delay time of İ20 *m%.*

Table 5. Delay timing simulation results with 30, 60,90,120, 150 and 330 ms delays in ternis of predicted ground vibration amplitudes and frequencies.

	Peak Simulated Amplitudes			*Dominant Frequencies*		
	T,	*V.*	*L.*	*T Hz*	*KHz*	*L.Hz*
Signature	47.4	35.3	58.5	8.0	3.0	4.0
30 ms delay	62.2	74.8	79.6	6.9	3.1	1.5
60 ms delay	68.1	60.8	60.2	16.5	3.1	3.5
90 ms delay	59.9	48.1	65.5	11.1	11.0	3.5
120 ms delay	63.0	58.5	58.4	8.3	8.4	8.4
150 ms delay	59.7	43.1	67.2	6.6	2.9	6.9
330 ms delay	53.3	41.8	65.5	6.1	3.0	9.1

Table 6. Site factors determined at 50% confidence interval for signature blast and production blasts.

	Signature Blast			*Production Blast*		
	k	**ß**	***R'***	***k***	**ß**	***R²***
T	191.96	-0.6754	0.4400	843.87	-1.5846	0.4057
V	608.89	-1.5561	0.8476	3797.5	-2.048	0.5144
L	253.18	-0.6152	0.5765	1370.9	-1.6878	0.3784

5 CONCLUSIONS

The main conclusions derived from this study are given below:

1. Blast monitoring is a very valuable, indispensable and quaJ'tative tool which eliminates the trial and error approach and most of the guess work.

2. Blast monitoring which enables the quantitative evaluation of blasting results helps to optimize blasting and minimize the environmental effects.

3. The primer and ANFO perform very well, as indicated by the VOD measurements.

4. Motion analysis of high-speed camera records indicated that the best delay period varied in the range 120-140 ms.

5. The best delay time obtained by timing simulation was 120 ms. Thus, the optimum delay time for this mine was found tu be 120 ms considering both timing simulation and high-speed video camera system output.

6. Timing simulation of the ground vibration record from signature blasts enables manipulation of the PPVs and frequencies and helps to determine the best delay period so as to minimize the risk of structural damage.

7. In order to be able to carry out meaningful and reliable one-to-one comparison of predicted values from timing simulation of signature blast records and values from production blasts, new signature blasts should be conducted at similar scaled and absolute distances as the production blasts.

ACKNOWLEDGEMENTS

The authors would like to acknowledge the support in this research project given by the Demir Export Company. We greatly acknowledge the help of Mr. Aykut Ünal during the research study. Many thanks go to Mr. Muharrem Kılıç for his assistance in the blast monitoring stage.

REFERENCES

Bilgin, H.A., Aidas, G.G.U., Esen, S., & Kılıç, M., 2000. Effects of rock mass properties on the wave propagation mechanics of blast induced ground vibrations, *Research Fund Project (AFP) Final Report,* Project No: AFP-99-03-05-02. ODTÜ, Ankara, Turkey, 35 pages (in Turkish).

Chiappetta, R.F. 1998. Blast monitoring instrumentation and analysis techniques, with an emphasis on field applications. *FRAGBLAST-International Journal of Blasting and Fragmentation. VoL2. No. I:* 79-122. Rotterdam: Baikema.

Esen, S., Aidaş, G.G.U., & Kılıç M., 1999. Report on experimental blasting studies at Demir Export Kangal /S i vas Surface Coal Mine. *Internal Report.* Barutsan Co., Ankara, Turkey, 8 pages (unpublished report in Turkish).

17* International Mining Congress and Exhibition of Turkey- IMCET 2001, ©2001, ISBN 975-395-417-4

An Approach for Selection and Design of Rock Bolting Systems

N.Nikolaev
Antech TFA ltd, Sofia, Bulgaria
V.Parushev
University of Mining and Geology, Sofia, Bulgaria
S.Nikolaev
Antech TFA Ltd. Sofia, Bulgaria

ABSTRACT: This paper considers rock bolting characteristics resulting from different roof bolting principles and their influence on rock mass stability in underground excavations. The effectiveness of each bolting principle in regard to geotechnical data is analyzed. An approach is developed for designing frictional rock bolting systems, taking into account the rock mass properties.

! INTRODUCTION

In the present paper, an attempt is made, on the basis of the differences between the characteristics of conventional and frictional rock bolts, to identify an appropriate method for designing a rock bolt system with frictional pipe anchors. Different design methods are known for conventional rock bolts, whereas for frictional rock bolts, rational methods expressing the characteristics of this new class of anchors have not yet been developed. Current practice in this area is based mainly on known schemata for designing rock bolting systems with conventional anchors. Therefore, the authors focused mainly on rock masses susceptible to developing plastic zones, where frictional pipe anchors, in contrast to conventional ones, also perform well.

2 ROCK BOLT CHARACTERISTICS

Resistance, which exercises certain anchor types to the rock displacement, can be defined best by means of its working characteristics. Most scientists have replaced the working characteristic of the rock bolt with the initial pull test characteristic obtained immediately after rock bolt installation. This type of characteristic usually occurs with increased stiffness and because of this it is called the initial pull test characteristic. For the purpose of defining the characteristics of several types of expansion rock bolts in different mines and geological conditions in Bulgaria, numerous long-term studies have feeen carried out, both to determine the reaction of the anchor in time with magnetostriction dynamometers and to measure the displacement of me anchor end.

The type of the characteristic is defined only after statistical processing of a large quantity of data.
In investigations carried out by Nikolaev (1964, 1989), a relation was sought between the initial pull test and working characteristics of expansion rock bolts with retensioning. The results processed show that for most cases, the curve of these rock bolts is a square parabola, but this is according to observations started after the initial anchor tension, which is linear. The parabola begins from one certain value $P_0 = C_0$. In Figure 1 two example curves of pull test characteristics are illustrated as follows:

$$P, = a_0u + b,,u+ c_0 \quad (1)$$

where Pi = the tension force of the anchor; u = displacement of the anchor end during tensioning; a_o, b_o, C_o = coefficients of the pull test characteristic, differing for the individual expansion types of rock bolts.

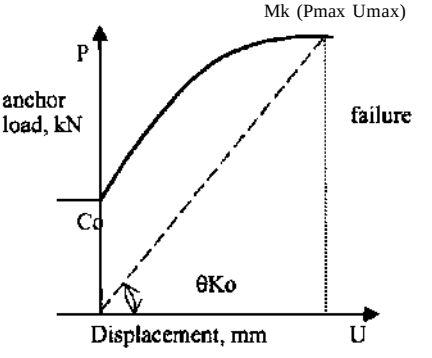

Figure 1. Initial pull test charac(eristic of expansion shell rock bolt.

In Figure 1, a typical pull test characteristic of an expansion rock bolt is given, ending with anchor rod failure or with slipping.

The observations show that in rock bolts with a wedge expansion device, the initial anchor tension is not maintained for a long time. After a relatively short time (from 2 to 10 h), the force P, begins to decrease to a certain value. After this, by appropriate density and length of the rock bolts for each individual case, an increase İn the rock bolt reaction can be observed, followed by another decrease in the tension force and another increase until a certain value of anchor reaction is reached. In this case, the rock mass displacement is stopped and force P_t remains almost constant if the mine and geological conditions are not changed. After translation of the beginning of the coordinate system P- U in point Co, the equation of the working characteristic is simplified as follows:

$$P_k = a_k u_k^2 + b_k u_k^2 \qquad (2)$$

This is illustrated graphically in Figure 2. The pull test characteristic of the rock bolt İs shown by Pk, and a broken line, while P_{pi} and a continuous line show the working characteristic.

We must emphasise that the decrease from the pull test characteristic to the working characteristic of the rock bolts with the wedge expansion device in each step is in the same proportion, namely:

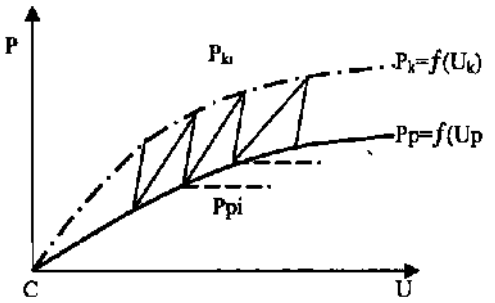

Figure 2 Relationship between initial pull test and working characteristics of expansion shell rock bolts.

$$(P_{ki} - P_{pi})/P_{ki} = \Delta_h \qquad (3)$$

With some approximation we assume that the decrease from Pt, to P_p, is at right angles with abscise u. The maximum derivation of 100 observations carried out was 8%.

With some margin of safety, we can assume for the working characteristic that the parabola passes through the down points of the steps (curve P_{pi}). From Equation 3, we can express the working characteristic by multiplying the pull test characteristic by the constant q:

$$P_p = q\,P_k = q\,a_k u_k^2 + b_k u_k^2 = a_p u_p^2 + b_p u_p^2 \qquad (4)$$

where q depends on the ratio between the plastic and Theological components in the strength characteristic of the rock masses.

The characteristic of the ordinary wedge anchor is that it has great stiffness and it exhibits almost a straight line. The initial expansion force of the wedge head is constant and cannot be increased during its lifespan. In Figure 3, the characteristic of this type of rock bolt is illustrated graphically. The stiffness of this bolt is exceptionally high, and the values of Pk and P_p are two to four times lower than those for the expansion anchors, with increasing expansion of the anchor head. The value of P^ma* increased in the range of 60 to 80% only in the massive with uni-axial compressive strength of about 30 to 40 MPa, but with substantial increase in the stiffness.

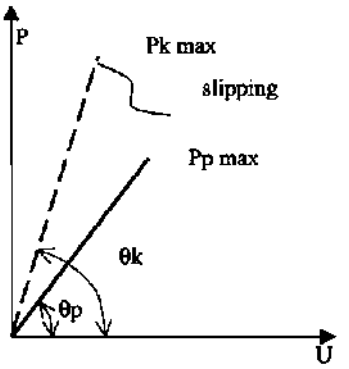

Figure 3. Pull test and working characteristics of expansion wedge rock boh

The characteristic of the cement-grouted rock bolt is that it has infinitely high stiffness, i.e., with an angle of inclination of almost 90°. In this case, the pull test characteristic differs from the working characteristic in that tension acts directly on the anchor rod. With good design and implementation, P_p mx has a high value.

For the frictional pipe anchor TFA, the pull test characteristic consisted of two lines connected by a small curvilinear section. This section expresses the relation between the first part with increasing resistance and the second part with constant resistance. The stiffness is lower than in the other types of anchor (Fig. 4), which ensures a certain amount of yield without decreasing the initial resistance. The upper branch of the curve illustrates the working characteristic of TFA. The increase of the installing

load-bearing capacity of the anchor marked by AP_p depends on physicomechanical and structural characteristics. The greater the necessity of rock mass anchoring is, the bigger the force is that clamps and presses the rock bolt, i.e. the bigger AP_p is.

In Figure 5, a characteristic curve of interaction for anchor support-rock mass is shown. The stiffness and the time of anchor installation are of particular importance in competent rock structures in the high-stress conditions existing in deep mines and tunnels. The installation of bolt support with rigid characteristics before the relaxation of stresses and passing of the initial deformations might be dangerous because of the risk of overloading this type of anchor.

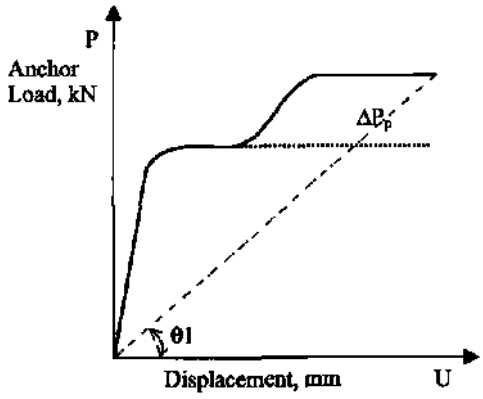

Figure 4. Initial pull test and wn<V-»» characteristics of factional pipe anchor TFA.

3 THEORETICAL MODEL FOR INCREASING THE BEARING CAPACITY OF TFA

During installation of TFA in an anchor hole with a diameter smaller than its elliptical cross section, the elastic deformation causes normal stresses toward the hole wall. The friction strength T induced determines the initial bearing capacity of the rock bolt Po as follows:

$$P_0 = T_0 = N_0 \mu \quad (5)$$

where μ = coefficient of the friction rock-metal; and No = normal stresses caused by elastic deformation.

Immediately after installation or after a short rime, the pull test shows identical results for Po, while for a longer period it is increased, which in any case can reach values which are twice as high as the initial installing stress. This increase can be explained by the process of deformation in the rock mass caused by plasticity or plastic flow. This effect can be described approximately by assuming that the rock mass is an elasto-plastic medium.

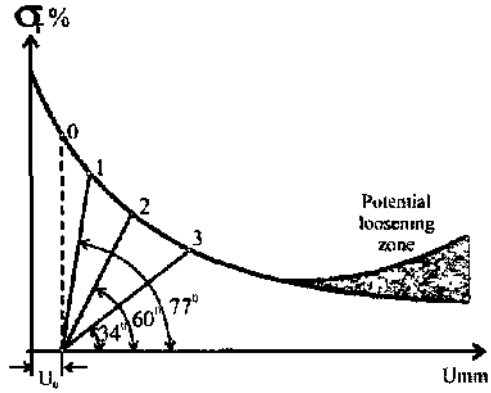

Figure.5. Interaction curve: anchor support-rock mass, where 1 = stiffness of expansion wedge rock bolt; 2 = stiffness of expansion shell bolt, 3 = stiffness of fractional anchor TFA.

A circular mining excavation driven to a certain depth is considered, ensuring the development of a plastic ring around the excavation. The plastic area causes additional stresses around the rock bolt and it is assumed that the compressive stresses have a positive sign.

The increased bearing capacity can be approximately described by Equation 6:

$$P_в = P_0 + \sigma_{\theta p} \mu S_k K_p \quad (6)$$

where $P_в$ = increased bearing capacity; $\sigma_{\theta p}$ = tangential stress in the plastic area around the mining excavation; Sjt = contact zone of the anchor with the rock on 1 meter length; μ = coefficient of the friction rock-metal; Kp = Lp/ Ro - relative thickness of the plastic area; and Lp, Ro = thickness of the plastic area and radius of the excavation.

The tangential stress $\sigma_{\theta p}$ can be expressed as shown in Equation 7.

$$y = \sigma_{\theta p} / p = (1 + K_p)^{\alpha} \beta + W_k \operatorname{ctg}\varphi \left[(1 + K_p)^{\alpha} \beta - 1\right] \quad (7)$$

$$W_k = C_{kp}/p; \ \alpha = 2\sin\varphi/1-\sin\varphi \ ; \ \beta = 1+\sin\varphi/1-\sin\varphi$$

where Ctp = cohesion in the plastic area.

Equation 7 İs worked out for the stresses in the plastic area with cohesion and angle of internal friction. Using a solution proposed by Bulichev (1994), which takes into account the influence of the support resistance p, the resistance of the support on the contour of the excavation can be expressed by the equation:

$$p = \delta n_a \ ; \ p_0 = 0.4 b a n_a p_0 / Ro \quad (8)$$

where n_a = the number of rock bolts per square meter; S = coefficient of correction, which expresses the irregular loading of the anchors; and b_a = dimension of die square anchor plate;

If we substitute CTap = y p İn Equation 6 and Equation 8, after the transformations we obtain die expression for increasing the bearing capacity as a percentage:

$$C\% = 100\ (P_a / P_o - 1) = 2.55\ 10^{-2}\ n_a\ y\ K_p \qquad (9)$$

Using die conditions for plasticity, we can express the relations between die radius of die plastic area, hydrostatic stress, cohesion and die angle of internal friction. In a manner appropriate to our task, we transform dial Equation 9 as follows:

$$\gamma H / C_{kp} = [(1+K_p)^{\alpha} - (1-\sin\varphi)] / [tg\varphi(1-\sin\varphi)] \qquad (10)$$

4 DESIGN OF ROCK BOLTING SYSTEM WITH TFA

The interaction of the frictional pipe anchor (TFA) with the rock mass is fundamentally different from mat of other anchor types.

The strength elastic contact, which occurs along die whole length of die rock mass, allows influence on the deformation processes in the rock mass.

Over twenty years' experience with TFA shows that it plays a successful part not only in the deformation processes along the axis, but also in those at die cross-section of the axis, sometimes even with increased bearing capacity. These advantages of TFA even allow rocks to be reinforced in mining excavations driven İn mining and geological conditions susceptible to developing well-formed plastic areas.

This advantage of TFA allows the replacement of other types of support with anchor supports in old mining excavations subject to great deformations, or it allows the support to be reinforced by anchoring of the area between the usual standing supports.

It is well known that conventional rock bolts are used for suspending the plastic area to the solid rock.

The metfiod suggested here for designing the rock bolting system is based on die idea of taking into account the increase in die cohesion value in the plastic area; first, from the direct action of die side strength contact, and second, from the component acting İn the cross-section of the axis (between four rock bolts).

The increased cohesion in the plastic area Cj^ is expressed as follows:

$$C^{*}_{kp} = (l_p / l_a)\ C_{kp}\ K_{1p} + (l_e / l_a)\ C_{kp}\ K_{2p} \qquad (11)$$

where l_a, l_p and I_e are the total (active) length of the anchor, the length of the anchor İn the plastic area, and the length of the anchor in the elastic area respectively. All these lengths are relative because they are expressed in the ratio to radius of the excavation. Ckp = cohesion in the plastic area; $K|_P$, $K2_P$ = coefficients of reinforcement resulting from die direct action of the cross-section contact stresses (from the mounting of the anchor and deformation process in the rock mass), and the reinforcement coefficient from the action of the side component of a pyramidal body weight, and also the coefficient taking into account the reaction of the anchoring forces.

The investigations carried out by Parushev (1986) with TFA frictional rock bolts İn a non-fractured medium by modeling in an equivalent material defined the coefficient $K|_P$ by the equation:

$$K_{1p} = [(n_a+6,3)^2 /24] - 0,87 \qquad (12)$$

The coefficient K_{2p} by S.Nikolaev (1994) is expressed by the formula:

$$K_{2p} = [(1+\sin\varphi)\ p_m\ n_a]/(1-\sin\varphi)\gamma \qquad (13)$$

where p_m is the reaction of the rock bolt for the linear meter length, MN/m.

After replacing l_p and l_e with l_p= Kp and l_e= I_a- K_p and dividing the expression to Ckp, we obtain the coefficient of the reinforcement n, which after transformations is:

$$n = \delta\ K_{1p} + l_a\ (1-\delta)\ K_{2p} \qquad (14)$$

where $\delta = K_p / l_a$

As we know, the strength indices of the rocks at a certain point of the massive have the character of random values with a definite law of distribution. The great experimental experience of both Bulgarian and other researchers show that with enough accuracy for practical use, we can assume the normal Gauss distribution.

With this precondition, the probability of failure can be described by a function of Laplace as follows:

$$V = 0.5 - 1/\sqrt{2\pi} \int_0^z e^{-x^2/2} dx \qquad (15)$$

The upper limit of the integral is:

$$z = (1-1/n)/v \qquad (16)$$

where v is the coefficient of variation, which in most cases exhibits the values: $20\% \leq v \leq 30\%$.

Assuming an upper limit of v = 30%, for z we obtain: z = 3.33(l-l/n)

The coefficient of failure probability in mining excavations must not exceed V<0.02

Replacing these requirements in (15), we found the nearest solution for z = 2.06

For this value, V = 0.0197 < 0.02

For the found z, the requested value of n = 2.618

Replacing n with this value İn (14), and finding the solution of the equation for l_a we obtain:

$$U=(2.618-\delta K_{lp})/(1-\delta) K_{2p} \quad (17)$$

where practical values for S and 1 a are:

0<S«1 i.e. 5>1

RoU >1 and l_a<1.3

The calculation data for design are obtained by laboratory-strength indices transformed by methods taking into account structural disturbances.

Using the method of Hoek-Brown described by Hoek (1996) for compressive strength, we obtain the following:

$$\sigma_{CM} = \sigma_{ci} S^{a} \quad (18)$$

and using the strength theory of Mohr-Coloumb, the analogical equation for cohesion İs

$$C_{kM} = C_{ki} S^{a} \quad (19)$$

where *a^* and Ck_M = transformed compressive strength and cohesion in rock mass respectively; and Gci and Citi = laboratory compressive strength and cohesion respectively.

Example: circular mining excavation at depth H =350m; radius Ro= 2m; density of rock *y* = 0,022MN/m^3; laboratory strength indices: uniaxial compression strength a_ci - 48Mpa; cohesion C^ = 16.8 Mpa; angle of internal friction (p = 20°.

By Hoek (1996) we obtain S = 0.015 and a = 0.5. From Equations (18) and (19) we can calculate the strength indices in the rock mass c_{CM} = 5.88 MPa and Cii_M = 2.06 MPa. Using relation (10) expressed toward Kp and replacing the indices above, it İs calculated that Kp= 0.53. The distance between the rock bolts is determined by the Equation 20:

$$a = 2hf + 2.5b_a = 2h\cos\varphi / (1-\sin\varphi) + 2.5b_a = 2.856h + 0.375 \quad 20$$

where h = the height of the equilibrium volume between the anchors. For the mining excavations we can assume h = 0.2m; f = coefficient of hardness by Protodiakonov. For masses with f < 6, the coefficient can be calculated by the trigonometric expression f = costp / (l-sinif>); b_a = dimension of the square anchor plate. In this case, b_a= 0.15m

Then we calculate a = 0.946m = 1.00m.

From the illustrations in Figure 6, we can read the value of l_a. If Kp= 0.53 and n_a= 1 piece/m^2 then l_a= 1.025 or for the active length of the rock bolt we have L„= 1.025, Ro = 2 05m, and the total length of the rock bolt is: L_{l01a}i= L_a+ 0.10 = 2.15m

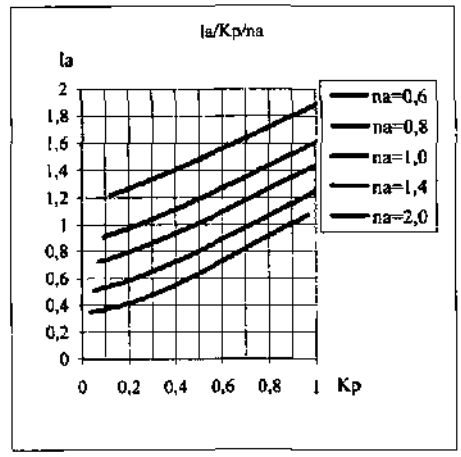

Figure 6 Relationships between thickness of the plastic zone Kp, anchor length 1. and density of anchor distribution *n,*.

5 CONCLUSION

The theoretical, laboratory and in-situ investigations, as well as the analyses of the results found allow us to draw the following conclusions:

1. The working - long-lasting characteristic of a relevant type of rock bolt should be taken into account when a rock bolnng system is designed.
2. The real increase in the load-beanng capacity of TFA is proved both by pull tests and theoretically.
3. Frictional pipe anchors including TFA are also effective in mining excavations surrounded by plastic zones.
4. An approach developed allows frictional rock bolting systems to be designed by taking into account the specific properties of this class of anchors by the availability of plastic zones

REFERENCES

Bulıchev, N 1994 Mechanics of underground excavations Moskva, Nedra

Hoek, E 1996 Strength of rock and rock masses *News Journal* V 2,2,4-15

Nikolaev, N 1964. Investigation of the characteristics of mechanical rock bolts *Reports of Mining Research Institute 2*

Nikolaev, N. 1989. Development of the theory and practice of rock bolting in underground excavations. *Dissertation*. Sofia, UMG.

Nikolaev, N. & Habenicht, H. 1995. Operational and technical performance of the tube-anchor in die staring chamber of a longwall in a Bulgarian coal mine. *Proceedings of the InternationalSymposium on Anchors in Theory and Practice*. Rotterdam. BaUcema.

Nikolaev, S 1994. Selection of a method for supporting and design of support in expérimenta] section of a tunnel. *Diploma project*.

Parushev, V. 1986. Study of the combined action of frictional pipe anchors in a rock massif before and after its destruction. *Proceedings of the 9-th Scientific Session of IBSM* Rotterdam. Balkema.

if International Mining Congress and Exhibition of Turkey- İMCET 2001, ©2001, ISBN 975-395-417-4

Temporary (Short-Term) Mining Workings Stability

H.Sauku, A.Bakiu & V.Jorgji
Faculty of Geology and Mining, Tirana, Albania

ABSTRACT: Rational coal and metal underground mining methods are used and there are correlations between the mining spaces, characteristics of surrounding rocks and the mining depths. In a generalized representation, the temporary mining workings in Albanian coal mining together with the respective RLI (Rock Loading Index) values are presented. An analogue analysis of different mining workings used İn metal mines (Cr, Cu, Fe-Ni) is introduced.

Albanian mining activity over the last half century has mostly concentrated on underground metals (Cr, Cu, Fe-Ni) and coal mining. The respective mining situations and the consideration of their RLI (Rock Loading Index) in time are illustrated in Figure 1.

Such a correlation has been shown frequently (Sauku, 1992, 1994) as a more representative form for the relative stability of mining workings used as layout, development and extraction. Meanwhile, the expression of RLI is:

$$RLI = \frac{k_n \gamma H}{\sigma_c} \qquad (1)$$

where:

k_n - probable stress concentration coefficient around the working;

Y - rock mass density, kN/m3

H - mining depth, m;

a_c - uniaxial compression strength of rocks, kN/m^2.

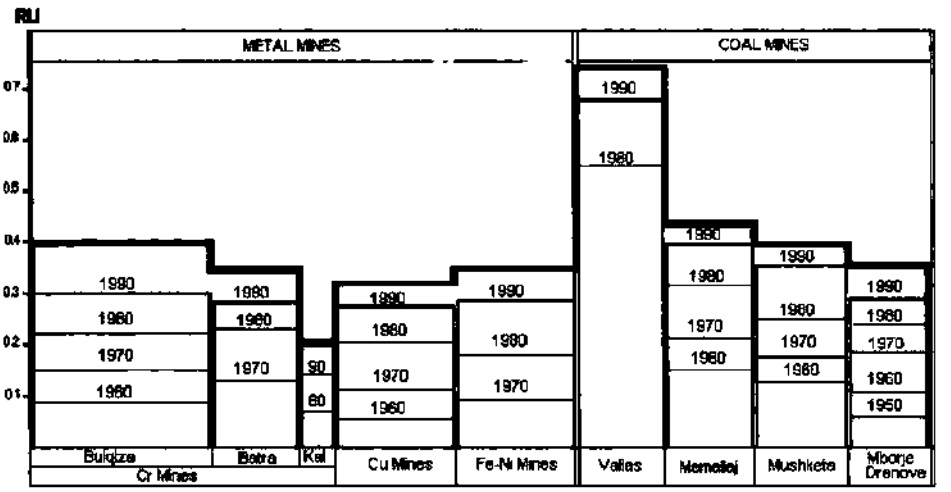

Figure I. RLI changes accordingto exploitation time in metal and coal mines (width is related to quantity of workings in each mme or mine group İn %).

For each mine, after the studied and projected exploitation methods (A.A.C.M.M., 1985), three mining methods are proposed or applied by time, in different mining conditions, determined particularly by the increase in exploitation depth.

A generalized representation of coal seam mining by coal extraction in slabs of different widths (B) shows that slabs become gradually narrower by their application at deeper levels and by their RLI growth.

As can be seen in Figure 2, using mining data for graphical expression slab width - RLI, a mathematical correlation is observed, analogue at a compression low:

$$B \times RLI = cons. = c \quad (2)$$

Actually it is a belt of data, included in two curved delimiting Unes of two constants, ci = 1.2 and C2 = 1.5.

Such a phenomenon is also observed İn ore exploitation mines, where similar working methods by slabs are used. In each case, the slab width is reduced in higher RLI conditions.

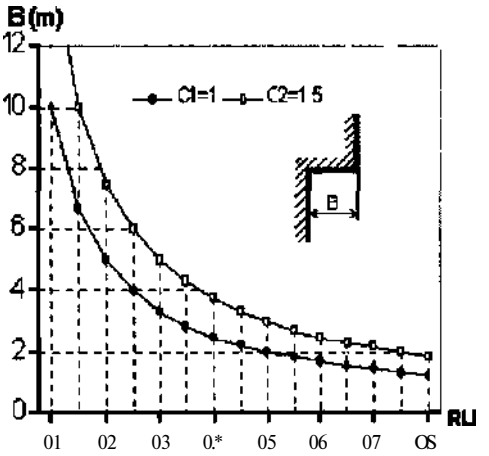

Figure 2. Adiabatic correlation B - RLI in coal mining

Meanwhile, it is observed mat for higher values of RLI (usually for RLI > 0.3), the rock mass deformability in time around the working space clearly increases.

The mechanization of coal or ore breaking and transport at the working space diminishes the time of the extraction. Hence, the same activity of the respective extraction working, or the temporary existence of the working diminishes. Such operations are indispensable for better control of the working space and of all the temporary exploitation workings used.

In support design calculations (C. Biron & E. Arioglu, 1983) (J. Lat&A. Iliev, 1993), the possible time calculation of the worked space fillings in a parallel line (in coal and metal mines) is presented. A calculation method for the probable pressures and rock mass deformations İn time is applied. The aim is to determine the reaction force and the deformations of the powered supports used.

In an advancing longwall support system for extraction with a given speed a temporary stability of all me respective workings must be ensured. Thus, it is possible to use the calculation method of the rock mass pressures and deformations developed in time (H. Sauku, 1994).

Considering the problem calculable İn an analogue way as the calculation of the "self support time" of rock masses around a working deformable in time (TS), the time of the temporary stability for the given reactive conditions may also be evaluated, as force and deformation by the support systems used (Sauku, 1995).

Commencing with the condition:

$$q_{max} > q_i > q_0 \quad (3)$$

where:

qi - applied reaction force by time of the support system used;

qo - contact rock structural block action from roof rocks ($q_0 = y$ bo, y - rock density, bo - rock block thickness;

maximal possible reaction for a higher arch raising (b_{max}) on an exploitation working.

Table 1 Some mining characteristics İn coal mining

Coal	Mining depth, m	Slab width, m	Slab length, m	$RLI=YH/O_c$
Mborje D rénove	200	8	50^H)	0 15-0.16
Mborje Drenove	500	6	50-40	0 33-0 36
Memaliaj	200-400	6-4	60-50	0.13-0 36
Krrabe-Mushqeta	150-350	6-4	60-50m	0.14-0 30
V alias	120-160	Working space 4-2.6m	Longwall face !00-70-50m	0 6-0.8

In the case of q_i = qo, the maximal self support time of the surrounding rocks is calculated by:

$$t_z = \ln\left[(1 - r_0)^{-1}\right] z^{-1} \quad (4)$$

where:

$$r_0 = \frac{q_0}{q_{max}} = \frac{b_0}{b_{max}} \quad (5)$$

Such a method of calculation was first presented in "Calculation Method of Critical Depths" with their evolution in time (Sauku, 1992, 1994, 1999), where:

$$z = k_{pl}\, k_n \frac{\gamma H}{\sigma_c} \quad (6)$$

for time in months.

kp] - rock mass plasticity.

An example of Ts calculation for an evaluation of the probable dispersion of the temporary stability of workings in coal and metal mines (Cr, Cu, Fe-Ni mines) by Albanian mine practice, represented by more evolved workings in depth can be given as follows:

a) calculation of representative data from different mines and workings;

b) selection and systematization of the results for r, z values and Ts calculation of different levels and workings in them;

c) calculation of the support systems useable at each temporary working;

d) a representative graph may be used for a generalized view of the mining situation in all relevant mines and another graph may by used for the workings opened at deeper levels of individual mines.

In Albanian metal and coal mines, we have the situation generalized in Table 2.

The representative graph for the situations observed and described İn Table 2 is given in Figure 3.

There are three different conditions of temporary workings in activity: low stability (Ts = 0.1 - 0.3), normal stability (Ts = 0.3 - 0.6) and high stability (Ts > 0.6 months), which indicates the low stability of temporary workings.

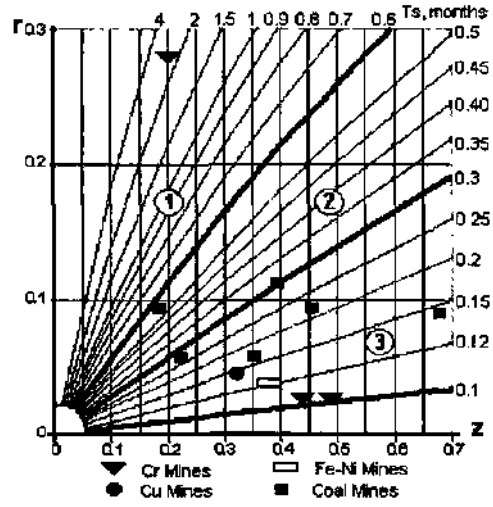

Figure 3. Temporary mining working stability: I. high stability, 2. normal stability, 3. low stability.

Table 2. General data on temporary workings.

	MINES		Mining depth	RLI	Space elements, m			Parameters		T, values months
					B^x.n,	B, m	bo, m	r	z	
METAL MINES	Cr Mine	Bulqiza	800	0.37	31.7	25	1.0	0.05	0.44	0.116
		Batra	800	0.35	12.5	12	0.6	0.044	0.40	0.120
		Rragam	300	0.188	3.47	25	1.0	0.289	0.128	2.74
	Cu	Gjegjan Kurhnesh	300	0.25	5.35	5	0.25	0.047	0.33	0.14
	Fe-Ni	Prrenjas Guri i kuq	300	0.35	12.57	12	0.6	0.048	0.40	0.12
COAL MINES	Mborje-		200	0.18	8.4	12	0.5	0.059	0.216	0.15
			500	031	8.72	8	0 5	0 057	0.35	0 18
	Kiraba-Mushoeta		200	0.167	4.03	6	0.4	0.099	0.20	0.50
			350	0.292	3.61	4	0.4	0.110	0.40	0.28
			400	0.384	4Sft	4	0.4	0 0%	0 4ft	0 71
	Vali as		160	0.74	2.72	2.6	0.4	0.147	0.85	0.173

REFERENCES

Albanian Album of Coal Mining Methods (AACMM) 1985 Mining & Processing Technology Institute, Tirana, Alba ma

Bırön, C & Anoglu, E 1983 *Design of Support Systems m Mines* Wiley Interscience Publications

Lat,J & Ihev, I A 1993 *Manual of Underground Coal Mm ing Methods* Ostrava, Czech Republic

Sauku, H 1992 Drift Support Estimated by "Critical Depths Method *Proceedings of the 8th Coal Congres? of Turkev 291 306*

Sauku, H 1994 *Mme Workings Stability and Rock Masses Support Interaction* Adapted dissertation work

Sauku, H 1995 *On the Self Support time of Underground Cavities in Squeezing Rocks* Int Scientific Conference TU Ostava, Czech Republic

Sauku H 1999 *Mine Working Stability and Rock Masses Peformabtlity* 16-thMiningCongressofTurkey Ankara

17* International Mining Congress and Exhibition of Turkey- IMCET2001, © 2001. ISBN 975-395-417-4

Backfill Practices at Çayeli Mine

M.Yumlu
Çayeli Bahr İşletmeleri AŞ (CBl), Rize. Turkey

ABSTRACT: Backfill is an integral part of the mining operations at Çayeli Bakır İşletmeleri AŞ (CBl). The mining operations at CBI currently create an annual void of around 250,000 m\ Since 1994, more than 1 million cubic meters of backfill have been placed. There are three types of backfill İn use at CBI, namely, cemented rock fill (CRF), unconsolidated waste fill (WF) and cemented paste fill (PF). The use of backfill at CBI serves four main functions: *(i)* to stabilize the ground to permit the extraction of adjacent ore, *(ii)* to fill voids to provide regional support, *(Hi)* as a working floor for the next lift of stopes and *(iv)* for disposal of development waste. This paper describes current backfill practices at CBI with emphasis on different types of fill systems in use, transport and placement of backfill, and backfill quality-control practices.

1 INTRODUCTION

Çayeli Bakır işletmeleri A.Ş. (CBI) operates a mechanized underground Cu-Zn mine İn northeastern Turkey in the province of Rize. The mine is located approximately 8 km from the coastal town of Çayeli, about 25 km east of Rize and about 100 km west of the border with Georgia (Fig. 1). The mine is a joint venture, with Inmet Mining of Canada owning 49%, Eti Holding owning 45%, and Gama owning 6%. The mine uses a long hole stoping method with delayed backfill to produce 2,800 tonnes of ore per day from the Çayeli volcanogenic massive sulfide (VMS) deposit.

Backfill is an integral component of the mining operations at CBI. Backfill İs used at CBI; *(i)* for stabilizing ground to permit the extraction of adjacent ore, *(ii)* for filling voids to provide regional support, *(Hi)* as a working floor for the next lift of stopes, and *(iv)* for disposal of development waste. The mining operations at CBI create an annual void of about one quarter million cubic meters. Table 1 below details the types of backfill placed during the year 2000.

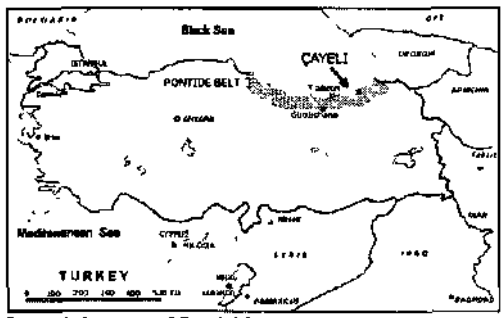

Figure 1. Location of Çayeli Mine.

Backfill is an indispensable component of the mining method. A brief review of the mining method employed and current backfilling practices at CBI is described.

2 MINING METHOD

The mining method employed at CBI is designed for 100% extraction with complete pillar recovery while allowing no perceptible surface subsidence. The mining method is transverse and/or longitudinal long hole stoping with delayed backfill. This is a common low-cost mining method, integrating mining and backfilling systems.

The ore body is accessed from a ramp system located in the hangingwall (HW) and a production shaft located İn the footwall (FW) of the ore body. The main levels are at 80-100-m vertical intervals with sublevels at 20-m intervals.

Table I Backfill placed during 2000.

Type	m^3	%
CRf	93,620	42
PF	74,291	33
WF	55,020	25
Total	222,931	100

The ore is developed by driving stake access drifts with a cross-section of 25 m^2 along the hangingwalJ or footwall or in the center of the ore body to the boundaries. Stope preparation is carried out by driving sill drifts across the strike to the hangingwall or footwall, or in the case of low-grade areas, to the boundary of the economic cut-off grade. The sill drifts are 7 m wide by 5 m high. The length of the sill drifts depends on the thickness of the ore body and the location of the strike access drifts. The average length of the sill drifts/stopes is presently 35 m.

Stope production comprises the extraction of the 15-m-high bench between two sill drifts. A drop raise is driven between sublevels at the end of the sill drifts. The raise is widened out to a slot to create a free breaking surface. The remainder of the bench is blasted towards the open slot. The ore is mucked from the lower sill drift using remote-controlled LHDs. The open stope İs then backfilled to the floor level of the upper sill drift. The backfilled floor becomes the mucking floor for the next lift. Once two adjacent primary stopes are completely backfilled, the intermediate primary pillar can be mined as a secondary stope. The primary stopes then become backfill pillars. The secondary stopes are also backfilled. The uppermost sill drifts in each main level are tightly backfilled to the back to support the back. The sequencing of the mining method is as follows:

1. Retreat from the boundary of the ore body to the central pillar.
2. Retreat up-dip from main levels.
3. Alternating primary and secondary transverse stopes.
4. Secondary stopes are mined between primary stopes after consolidation of the cemented backfill.
5. Completion of a mining area (main levels) by mining tertiary stopes (longitudinal stoping) in the strike direction between strike access drifts.

Figure 2 depicts a partial longitudinal projection of the current state of mine development.

3 TYPES OF BACKFILL

Several types of fill are used at CBI for backfilling mined-out stopes, are summarized in Table 2. These are: cemented rock fill (CRF), cemented paste fill (PF), and uncemented waste fill (WF).

Table 2 Types *af backfill in* use at CBI

Type	Description	Application
Cemented Rock Fill. CRF	Graded river aggregate plus cement	Primary and ternary stopes and partially in secondary stopes at ac cess side
Paste Fill. PF	Total mill tailings filtered lo 82% solids by weight plus cem em	Primary, secondary and tertiary slopes
Waste Fill, WF	Waste rock from surface or underground	Secondary slopes

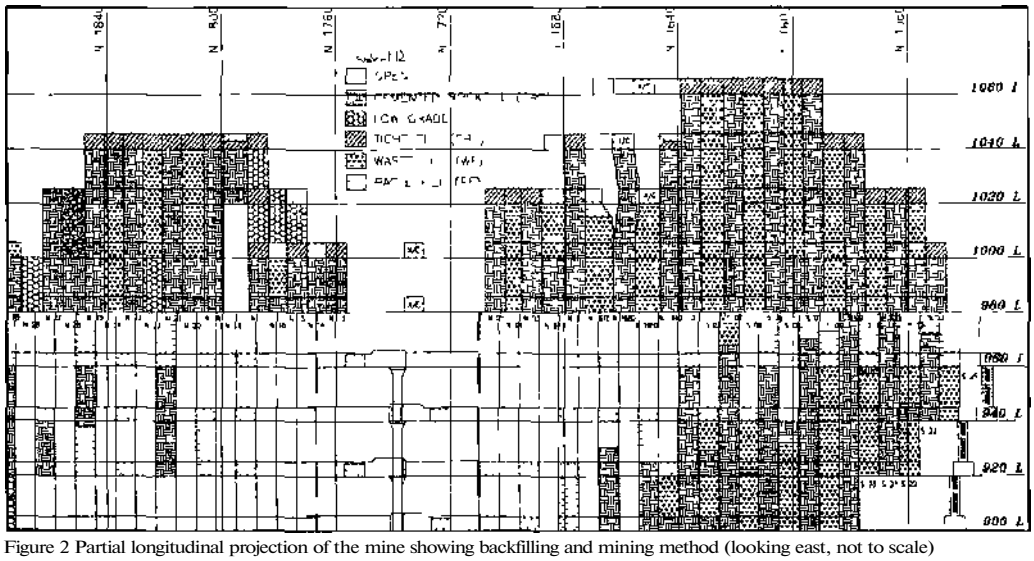

Figure 2 Partial longitudinal projection of the mine showing backfilling and mining method (looking east, not to scale)

Backfill İs used to fulfill the following roles. For primary stopes, CRP and/or PF are used. The primary requirement here is to stabilize the ground to permit the extraction of the adjacent ore. The fill is exposed by the subsequent ore extraction, and hence must have sufficient strength to support itself when the constraining ore walls are removed. The primary stopes are filled with cemented rock or paste fill with 5% cement depending on the availability and stope requirements.

Secondary stopes, except for the brow section, which will be exposed during tertiary extraction, are backfilled with uncemented development waste material or 2% cemented paste fill. Here, the voids generated after secondary extraction are filled to provide regional support. Use of WF for the most part facilitates disposal of waste from development mining, eliminating the need to truck or skip the material to surface waste stockpiles. A portion of secondary stope fill will be exposed during extraction of tertiary stopes. In order to minimize dilution, secondary stopes, on the access drift side, are filled with CRF or PF (with 5% cement).

Tertiary and longitudinal stopes are backfilled with cemented rock fill and/or paste fill with 5% cement.

The uppermost sill drifts on main levels usually require the backfill to be tight against the back to minimize spans and to improve regional stability.

Generally, the cement content for CRF and PF is 5% by weight. However, the stope geometry and the prevailing mining conditions usually dictate the final dosage of cement in the backfill.

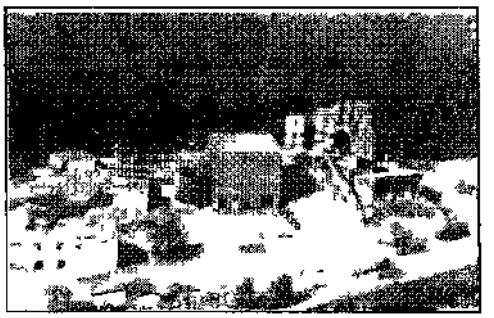

Figure 4 Phoiograph showing CRF and PF plants

There are two backfill systems in use at CB1 *(i)* the CRF system and *(it)* the PF system (Figs. 3-4) A bnef description of the two systems is presented in the following sections.

4 CEMENTED ROCK FILL SYSTEM

During the early years of the mine's life, the mine was shallow; hence, trucks moved backfill underground from a temporary surface mixing station. In mid-1996, a new surface slurry plant and two underground mixing stations were commissioned.

CBI's cemented rock fill (CRF) system comprises a surface slurry plant, a slurry pump, dual 1.5-inch slurry delivery pipe lines, aggregate backfill raises, and two underground mixing stations A bnef review of the backfill system is described here (Figs. 3-4).

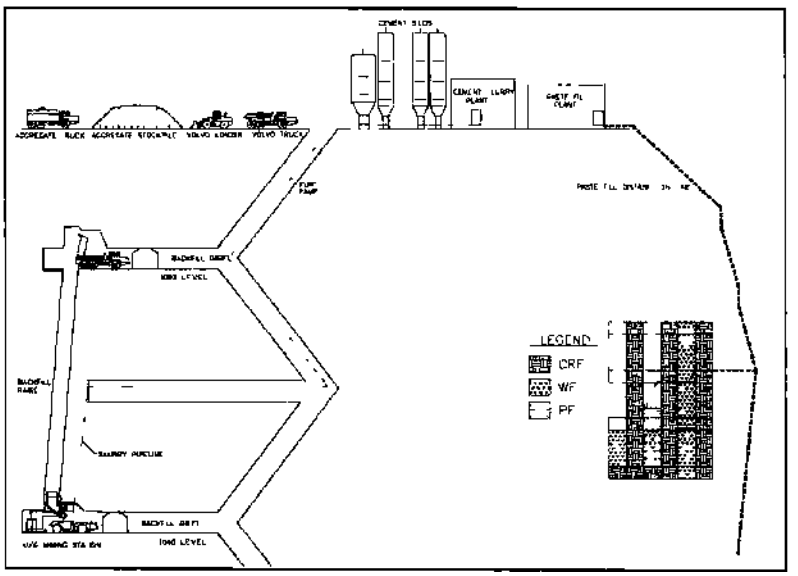

Figure 3 Schematic diagram showing the cemented-roclrfill and paste backfill system at CBI (not to scale).

4.1 *Surface Cement Slurry Preparation Plant*

Figure 3 depicts the backfill preparation system in use at the mine. The cement slurry plant, located near the Kurt portal, comprises a programmable logic controller (PLC) system that is totally automated. Basically, the components of the slurry batch plant include two 75-tonne-capacity silos for holding cement, a mixing tank, and the necessary controls for the PLC. The bulk cement is brought to the site by truck, and is unloaded pneumatically into the storage silos. The bottom of each silo İs equipped with a rotary valve that feeds into a screw auger. The PLC system delivers the proper amount of water and cement into the mixing tank. The mixing tank has been sized to provide 4 $m^{'}$ of cemented slurry, enough for 5.5 truckloads of CRF. Once adequate mixing has been achieved, the entire batch is pumped underground using a Schwing KSP25 poppet valve pump via a 1.5-inch reticulation pipeline to the mixing station, where it is stored in a 4-m^3-capacity agitating tank for discharge. A single batch of cement slurry consists of 1,200 kg of cement and 720 kg of water. This yields a water-cement ratio of 0.6 and a slurry pulp density of 62.5%.

When the trucks are loaded at the underground mixing station, the cement slurry is sprayed on top of the aggregate via a spray bar mounted on the lip of the chute. Additional mixing is achieved during subsequent transportation. The mixture is then transported by truck and dumped into the stope from the upper sill drift. The mixture of cement, water and fines coats the coarser aggregate and creates a strong bond at contact points. The result is a cemented rock fill of sufficient static strength to be self-supporting, and of enough dynamic strength to resist blast vibrations from adjacent secondary stopes.

4.2 *Underground mixing stations*

There are two underground mixing stations, one on the 1040 level and one on the 1020 level.

At the 1040 backfill station, the slurry is pumped to the spraybars which are arranged around the lip of the chute. The aggregate and cement mix as they fall together into the truck box and undergo additional agitation and percolation during truck haulage to the filling stope.

The 1020 backfill station utilizes the same surface slurry plant and pipeline. At the mixing station on the 1020 level, an agitator and pump identical to those at the 1040 station are used. The backfill is prepared in batches and the mixing is by a 3.5-$m^{'}$ twin-shaft paddle-type concrete mixer. This was chosen to ensure complete distribution of cement throughout the aggregate. The 1020 station is more complex and modern, but is currently used as a standby station.

Both stations have aggregate supplied to them by means of dedicated backfill raises regulated by a standard chute arrangement. The slurry İs kept İn agitation in an intermediate holding tank.

4.3 *Aggregate*

Surface rocks in the vicinity of the mine are highly weathered and are therefore regarded as unsuitable for backfilling. For CRF, a well-graded river aggregate is used. The aggregate consists of a fine fraction and a coarse fraction. The fine fraction is 0-9 mm and approximately 30% by weight, while the coarse fraction is +9-100 mm and approximately 70% by weight.

On the surface, close to the Kurt portal next to the slurry batch plant, there is a temporary aggregate stockpile with an estimated capacity of 5,000 rrr\ The aggregate is loaded using a Volvo LI 50 loader and transported to one of the two underground backfill raises, located on the 1080 level, using a Volvo A35 truck (Fig. 3).

4.4 *Transport and Placement*

For transporting and placing the backfill, Wagner MT 400 series trucks are used. Backfill is dumped into stopes from the top sill drift (Figs. 5-6). Gravity fall is used when the truck initially dumps from the upper drift. The brow is therefore filled by gravity free fall, resulting in compaction of fill at the brow and barricade. Some of the fines are initially washed away due to the impact. Once the backfill reaches the upper level floor elevation, then trucks will dump backfill gently over the tip of previously placed backfill. The angle of repose for cemented backfill is about 35 degrees. Whether filling CRF or WF, the last 1m of stopes is usually filled with CRF using LHDs to finish off the surface for tramming. The low water content of the fill allows the trucks and LHDs to drive on freshly placed backfill.

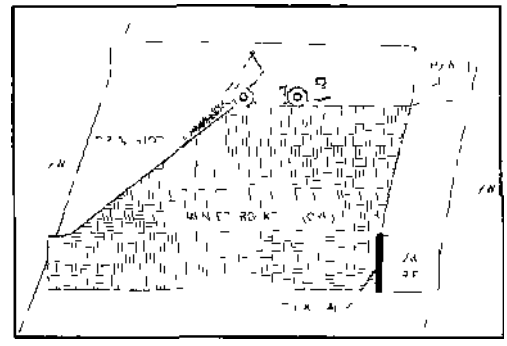

Figure 5. Method of truck-placed backfill at CBI (not to scale).

ıgopenstop——#——

CRF.

The stopes are mined up-dip until the top of the ore or sill pillar is reached, as seen in Figure 2. The uppermost sill drifts, such as those on the 1060 and 960 level are tightly backfilled against the back (locally known as rightful) İn order to minimize subsidence and to maintain the structural integrity of the back when the adjacent stopes are mined.

Based on 2800 tonnes production per day, the average CRF rate İs 700 m or 70 trucks per day. To date, the record is 1000 m^3 per day.

4.5 *Bulkhead*

Bulkheads are used at the base of open stopes to retain backfill in open stopes. Bulkhead design at CBI is such that bolts are drilled and installed around the perimeter, and then cables are woven vertically and horizontally, tied to the perimeter bolts. Wire mesh is then laid out to contain die backfill. Two horizontal and vertical U beams and two pipe poles are used to carry the deadweight. A portion of fhe pipes, cables and U beams are usually recycled for use elsewhere after the stope is filled and backfill set. The bulkheads are monitored by visual inspection.

4.6 *Quality Control*

The need for a comprehensive quality-control program for CRF is recognized. However, CBI does not have an on-site laboratory, as it is prohibitively expensive and impractical. For this reason, a more hands-on approach is taken for quality control of cemented rock fill. Proper filling and slurry preparation procedures have been set up to produce a high-quality fill product and these practices are monitored on a regular basis.

Slurry quality is a fundamental component for a high-quality fill product. The objective is to strike a balance so that there is enough water added to the slurry for the mix to coat the rock adequately, but not so much water that the strength of the final product is compromised. Below a pulp density of 50% solids by weight, the slurry will be too thin, there will be excess free slurry in the fill, and the final product will be well below the design. If the slurry density is too high (above, say, 80%) difficulties with slurry coating and transport result. The design target pulp density at CBI is 62.5% solids by weight. In order to maintain this density, spot checks are made through routine follow-ups and regular calibration of cement and water metering load cells. At underground mixing stations, the operator controls the quality of the final CRF mix to be delivered to the stope.

Spot checks are made to control cement consumption. As a rough measure, approximately 1.0 tonne of cement is used for one backfill truck. At the end of each shift, the U/G backfill operator and the surface slurry plant operator will report the number of trucks placed and the total tonnes of cement consumed for the shift. Furthermore, month-end total aggregate consumption is used to cross-check bulk cement consumption for backfill.

In addition, the slurry plant supervisor regularly checks the quality of aggregate delivered by the supplier. If the product is substandard, it is sent back to the supplier.

Figure? Good exposure of high quality cemented rockfitl in adjacent stopes

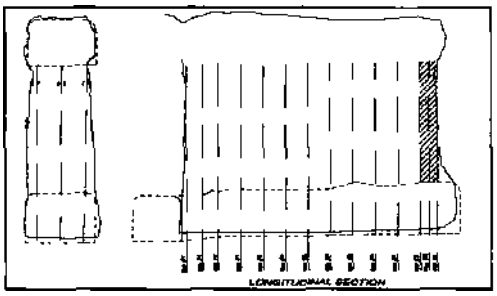

Figure 8. Planned stope versus actual stope extraction as captured by CMS survey.

The two notable properties of cemented rock fill at CBI are its free-standing ability and low contribution to dilution (Fig. 7). Dilution from backfill is around 4% and is due primarily to damage caused by close-proximity production blasting. The backfill mix provides an unconfined compressive strength in excess of 1.5 MPa at 28 days.

Procedures for correct drilling and blasting practices and the use of light explosives at stope ribs minimize dilution in secondary stopes. CBI purchased a cavity monitoring system (CMS) instrument in 1999 and since then has been monitoring the performance of stope blasts with CMS surveys. This instrument has made it possible to delineate and identify stope overbreaks/underbreaks. Figure 8 compares an actual stope cross-section with the planned stope blast layout.

5 PASTE BACKFILL SYSTEM

CBI commissioned a paste backfill system in 1999 to allow backfilling of underground voids using dewatered full plant tailings. The benefits of the paste fill method include: *(i)* low operating costs, *(ii)* ease of operation, *(Hi)* environmental friendliness, *(iv)* homogenous and consistent quality, and *(v)* allowance for tight filling of stopes and uppermost sill drifts on main levels.

A full description of the paste backfill system is beyond the scope of this paper. Only a brief description of the main components of the system follows.

The design capacity of the plant is 90 dry t/h of tailings or 42 m /h of paste containing about 82% solids. The plant receives total mill tailings through a 4-inch pipeline at a solids concentration of 65%. The tailings are then thickened in a I6-m-diameter thickener, agitated in a storage tank and then fed onto two vacuum disc filters. The filtrate is reversed to the tailing thickener and together with the overflow sent to the discharge head tank.

The filter cake is discharged on a reversible conveyor belt. The solids content of the filter cake is around 86%. The filter cake is fed to a conditioning surge hopper where the solids concentration is adjusted by adding make-up water. In a second mixer, cement is added at a predetermined rate of 2-9%. From the mixer, the paste is extruded to the feed hopper of a pumping and pipeline system. There are two interchangeable positive displacement pumps with s-swing tubes and two underground distribution systems, of which only one will operate at any one time. The fully automated paste plant produces a 7-inch slump paste and pumps it underground through a steel 5-inch-diameter surface and underground distribution line.

The paste plant is currently operating at about 25% of its design capacity due to restrictions in the tailings disposal system. A project is currently underway to address restrictions in the tailings disposal system and allow the paste plant to operate at full capacity.

5.1 *Transport and placement*

Paste is distributed and discharged through a DN 125-mm surface and underground pipeline system. The discharge piping runs on the surface horizontally for approximately 20m and then down a ramp at a 17% gradient for 220m. Thereafter, the pipeline runs down through a series of boreholes at 60 to 70 degrees to various levels. There are take-offs at active levels. The last 100m of the flat runs on the levels consist of 5-inch HDPE piping. The stope is filled from the upper sill drift by gravity. Real-time CCTV is installed and signals are sent through the underground leaky feeder system to the paste plant control room. This helps the operator to monitor the flow through the pipeline.

The last one meter of the paste-filled stope İs also usually filled with CRF in order to provide a base for the next lift.

5.2 *Bulkhead*

Bulkheads are used for retaining paste fill İn stopes. The simplest form of paste fill barricade at CBI is constructed from a pile of waste rock dumped in the draw point with a small wire-mesh-reinforced shotcrete fence sealing off the top of the rock pile. The other commonly used design consists of two layers of cable slings woven vertically and horizontally, wire mesh, and 20-cm-thick shotcrete.

5.3 *Strength and Quality Control*

For paste fill, there is a strict quality-control program in place. Paste fill samples are taken during operation for laboratory UCS strength testing. The typical strength of paste fill with 5% cement after 28 days is in excess of 1.0 MPa, about twice the strength required for the self-supporting of paste fill when exposed. Slump is also measured on a regular basis throughout each shift.

6 CONCLUSIONS

Backfilling is an important component of underground mining operations at CBI. Backfilling costs account for 15-20 percent of the total mining costs.

CBI has successfully integrated backfilling into the mining cycle, and since start-up, more than 1.0 million m of backfill has been successfully placed. Cemented primary stope pillars have proven to be stable and allow 100% extraction of secondary slopes without any major failures. Paste fill has recently been introduced to recycle mill tailings for backfilling mined-out areas underground. The use of combinations of PF, CRF and WF optimizes costs.

ACKNOWLEDGEMENT

The author wishes to thank the management of CBI for their permission and encouragement to present this work

Thanks are also due to the engineering staff who contributed lo this work

17 International Mining Congress and Exhibition of Turkey-IMCET 2001 ,©2001, ISBN 975-395-417-4*

Critical Dimension Concept in Pillar Stability

T.Ünlü
Department of Mining Engineering, Zonguldak Karaelmas University, Zonguldak, Turkey

ABSTRACT: This paper is based on a study carried out to investigate the stability and dimensioning of coal pillars at various depths. Critical dimensions for coal pillars are discussed. The results of the study show that the minimum width for small and/or yielding coal pillars should not be less than 10 metres. In the case of soft roof and/or especially soft floor strata conditions, special attention should be given to pillars with width-to-height ratios (W/H) between 4 and 10. Pillar strength increases as the pillar width is increased, depending on the geomechanical characteristics of the coal seam. However, after a certain W/H value, th^trength of a coal pillar increases rapidly and it is almost impossible to yield the pillar completely.

1 INTRODUCTION

Pillar design and stability are two of the most complicated and extensive problems in rock mechanics and strata control. Although these problems have been investigated for a long time, to date only a limited understanding of the subject has been gained. Empirical pillar strength formulas together with the tributary area concept have been used to design pillars for room-and-pillar mining systems at relatively shallow depths (< 300 m). Although these pillar formulas do not give accurate results, they have often been found to be satisfactory for general design at shallow depths. At shallower depths (i.e., 100 - 300 m), pillars are subjected to considerably lower stresses, which make it easier to apply various mining methods. Despite the generation of horizontal stresses, which could assist in confining pillars in some situations, in general, the major constraint to pillar design at great depth is the high vertical stresses due to overburden depth. This is particularly relevant to deep coal mining because of the weak nature of the coal and coal-bearing strata. As the mining activities go deeper (> 300 m), these pillar equations suggest very large pillars since they consider only a limited number of factors related to the strength of coal pillars (i.e., size and shape effects). However, there are some other important factors related to the strength of coal pillars. These factors are depicted in Figure 1.

What are the critical dimensions for coal pillars? In order to comprehend the problem and therefore to seek a solution, the following questions must be addressed and reasonable answers should be sought concerning pillar loading and stability.

- How much load is imposed on a pillar and how is it distributed over a single pillar or row of coal pillars?
- What are the most important factors involved in the strength of the coal pillars under scrutiny?
- What İs the role of pillar confinement offered by the roof and floor strata in pillar stability?
- The final question: what type of formula or design criterion is the most appropriate for designing pillars in coal mining applications?

Before seeking answers to these questions, in order to understand the mechanical behaviour of coal pillars, İt İs important to classify them according to their stability.

2 CLASSIFICATION OF PILLARS

Pillars may be classified according to their functions underground, for example, as support pillars, protective pillars and control pillars. These descriptions, however, do not give any useful information about the stability of these pillars. Therefore, it becomes necessary to establish an alternative pillar classification system to distinguish pillars according to their stability and according to the possible failure zones İnside pillars (Figure 2). These are as follows:

- Abutment pillar (stiff pillar).
- Critical pillar (semi-stiff pillar).
- Yielding pillar.

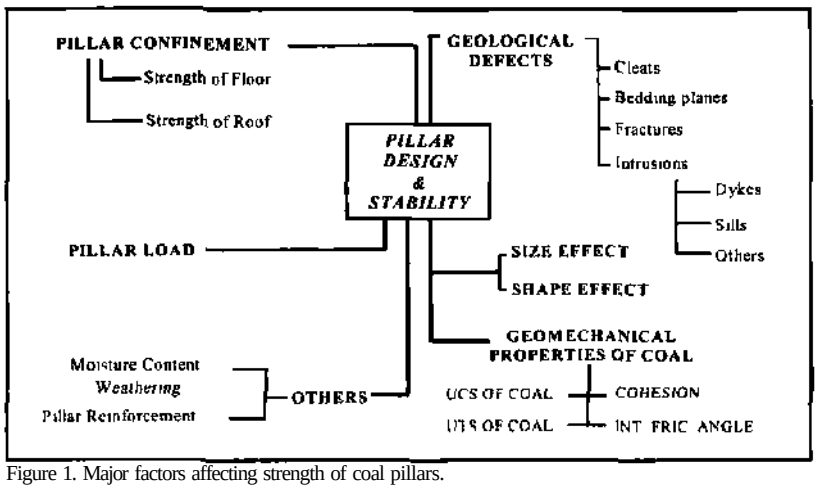

Figure 1. Major factors affecting strength of coal pillars.

2.1 *Abutment pillar*

This type of pillar is capable of supporting development loads and additional transferred loads during the service life of working areas without yielding or transferring any significant part of the load. They need a sufficient width of unyielded core so that stresses are smoothly dissipated into the floor without creating any adverse effects (i.e., preventing floor failure). These types of pillars are the essential backbones of the entire mine support system.

2.2 *Critical pillar*

This type of pillar is characterised by a failure mode which occurs where roof and particularly floor conditions are unfavourable. The mechanism is as follows: an insufficient width of elastic core remains during pillar loading, and this elastic core transfers highly concentrated stresses into floor strata, causing them to yield. As a result, yielding of the floor initiates beneath the pillar and gradually develops towards the roadway, which suffers from a considerable amount of floor heave and convergence. Similar observations have been made during mining practices (Carr et al., 1984, 1985; Koehler et al., 1996). The critical pillar size should be avoided at all costs by either widening or narrowing the pillar. This case is similar to the footing problem in soil mechanics.

2.3 *Yielding pillar*

A stable yielding pillar can be defined as a pillar which can sustain some part of the load being imposed on it and transfer any excess load without losing its overall integrity and residual load-bearing capacity. It is not necessary that these pillars should always have small dimensions, but they are generally designed to be narrow to maximise coal recovery. *Any* yielding pillar may lose its integrity during loading and/or by spalling from the ribs, thus gradually reducing its original dimensions. Under such conditions, a stable yielding pillar can become an unstable yielding pillar and can rapidly and completely collapse. To avoid this, side meshing in conjunction with nb or cable bolting should be considered.

3 PILLAR DESIGN EQUATIONS

Many formulas of average ultimate pillar strength that have been proposed take into account two important factors. Most of these formulas can be grouped into two categories:

$$\sigma_p = \sigma_c \left[a + b\left(\frac{W}{H}\right)\right] \rightarrow \text{The linear form} \qquad (1)$$

$$\sigma_p = K\frac{W^{\alpha}}{H^{\beta}} \rightarrow \text{The power forai} \qquad (2)$$

where-

Cp = pillar strength,

o_c = uniaxial compressive strength of a cubic coal sample of the critical specimen size,

a, b = dimensionless constants usually chosen so that a+b=l,(Table2)

K = represents numerically the strength of coal, (Table 1),

a, ß = dimensionless constants expressing the shape effect (Table 2), and

W, H = pillar width and height, respectively.

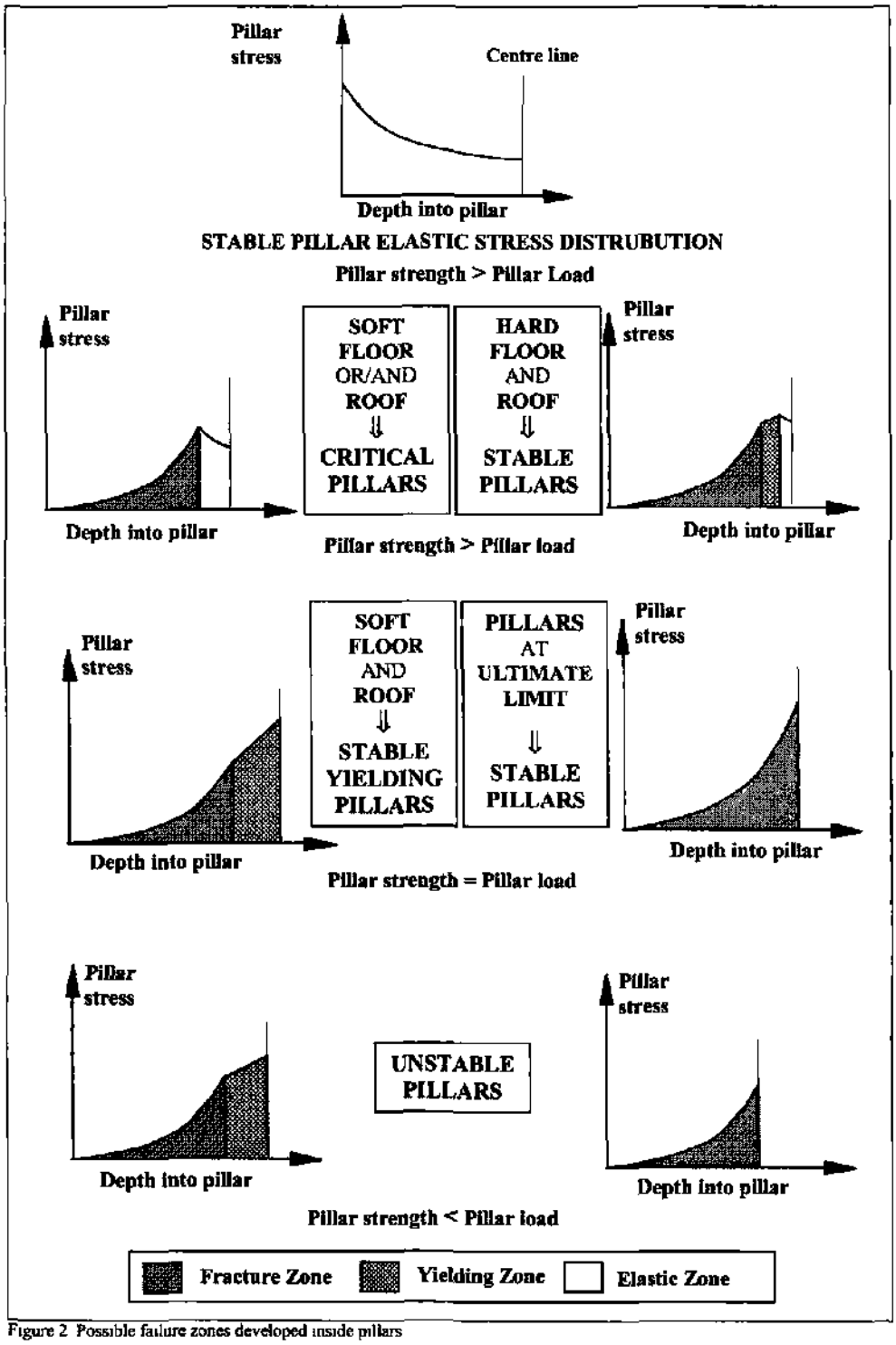

Figure 2 Possible failure zones developed inside pillars

Table 1. Values of K used inequation 2 (Farmer, 1985).

Researchers)	K. (MPa)	Comments
Greenwatd et al. (1939)	19.3	Orig. in psi for W, H values in inches (ABD)
Salamon - Munro (1967)	9.1	Orig. in psi for W, H values in feel (S.Africa)
Bieniawski (1968)	6.9	Orig. in psi for W, H values in feet (S.Africa)
Jenkins - Szeki (1964)	12.4	Originally in psi for W, H values in feet (S.Africa)
Wagner (1974)	11.0	W, H values in metres. In-situ tests (S.Africa)

Table 2. Constants used in equations 1 and 2 (Farmer, 1985).

Researcher(s)	a	b	α	β	Comments
Bunting (1911)	0.7	0.3	-	-	Laboratory
Obert, Windles and Duvall (1946)	0.78	0.22	-	-	Laboratory
Bieniawski (1968)	0.64	0.36	-	-	In-situ, S. Africa
Van Heerden (1974)	0.70	0.30	-	-	In-situ, S. Africa
Wang, Skelley and Wolgamott (1977)	0.78	0.22	-	-	In-situ, USA
Sorensen and Pariseau (1978)	0.69	0.31	-	-	Statistical, USA
Greenwald, Howarth and Hartman (1939)	-	-	0.5	0.83	Statistical, USA
Streat (1954)	-	-	0.5	1	Statistical, S. Africa
Hotland (1964)	-	-	0.5	1	Statistical, USA
Salamon - Munro (1967)	-	-	0.46	0.66	Statistical, S. Africa
Bieniawski (1968)	-	-	0.16	0.55	Statistical, S. Africa
Morrison, Corlett and Rice (1975)	-	-	0.5	0.5	In-situ, Canada

Aldiough rectangular pillars as well as square pillars have been widely used in underground coal mining, there are only a few formulas available for designing rectangular pillars (Salamon & Oravecz, 1976; Wagner, 1980; Peng, 1986; Mark, 1996).

All of the empirical pillar strength formulas were developed particularly for room-and-pillar mining at relatively shallow depths. Hence, they are most suitable for pillars in a particular coal region and for small W/H ratios (i.e., up to 4). However, weak roof or floor conditions and/or weak bands in coal seams are particularly important because they may cause the pillar to yield in tension radier than compression. Babcock (1981, 1985) conducted a series of experiments on model pillars, using concrete, coal and rock, and he concluded that the end constraint, not width-to-height ratio, is a significant variable in determining the pillar strength. Moreover, the failure mechanism of a large (squat) coal pillar is different from that of a coal sample tested in the laboratory. This is because the constraint offered by the yielded region to intact core will not build in small coal samples and small coal pillars. As a result, empirical pillar strength formulas are not recommended for coal pillars wiüi width-to-height ratios (W/H) of ten or more as they underestimate pillar strength due to the fact that most of them were derived from laboratory and/or in-situ tests conducted on prismatic coal samples up to 2 m in width.

Mark & Barton (1996) state that the size effect is related to the coal structure. Significant strength reduction due to increased specimen size is only valid for blocky coals. Tests conducted on small-size friable coal samples can be used to predict the uniaxial compressive strength of the coal mass itself.

3 INVESTIGATIONS OF CRITICAL PILLAR DIMENSIONS

3.1 *General*

The first step in pillar design is to calculate the pillar stress due to overburden load and transfer loads as a result of roadway development and coal extraction operations in longwall panels. The second step İs to calculate the pillar strength, which is more difficult than calculating pillar loads. The strength of slender pillars (W/H<4) can be predicted more easily than those of intermediate (4<W/H<10) and large coal pillars (W/H>10), because die failure mechanism of these pillars is roughly similar to laboratory-scale pillar specimens (up to 2 m) and the uniaxial compressive strength of slender pillars can be predicted more accurately. Therefore, pillar strength equations derived from the results of these investigations may be used for slender pillars at shallow depths with a reasonable degree of accuracy. The strength of large pillars, however, cannot be determined easily. This is because of the confinement built up through the centre of the pillar, depending upon the intensity of vertical stress and the geomechanical characteristics of the coal pillar.

3.2 *Critical dimensions of pillars in room-and-pillar mining*

Two main pillar design approaches have been suggested and widely accepted for designing pillars in room-and-pillar and/or longwall mining. The first one is Wilson's Confined Coal Concept (Wilson, 1980) and the second one is Barron's approach (Barron, 1982, 1992). Both of these approaches

consider some of the important parameters affecting pillar stability, such as confinement developing from the sidewalls to the centre of coal pillars. Although these two approaches seem to have similar features, there are significant differences regarding the post failure characteristics assumed for the coal seam.

In order to determine the strength of coal pillars with various geomechanical properties, a Windows-based computer program which was developed to design pillars in underground mining systems was used to estimate pillar strength taking into account various parameters related to the strength of coal. The program mainly uses Barron's approach, but with several modifications. Some of the input parameters used in Pil-Sta are shown in Figure 3 (Ünlü, 1994).

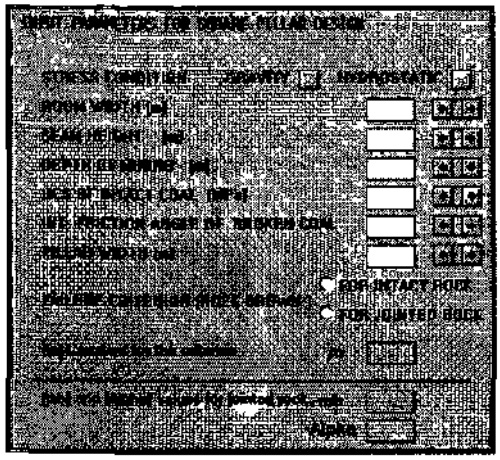

Figure 3 Input parameters used in Pil-Sta

The critical dimension is the minimum width of a pillar that can maintain stability without transferring loads by losing its integrity and load-carrying capacity at a certain depth. This dimension is affected by not only the vertical stress intensity increasing with depth, but also the geometric and geomechanical characteristics of coal pillars and the roof and floor strata.

The results show that the most important factors in pillar strength are the pillar width and the geomechanical characteristics of the coal seam. Width-to-height ratio also plays an important role (Figure 4). After a certain pillar width, there is a small change in required pillar width since the strength of the coal pillar increases dramatically (Figure 5).

Figure 5 and Figure 6 also show that after a certain pillar width, the pillar strength develops rapidly and tends to go to infinity. However, the geomechanical characteristics of roof and floor strata and the magnitude of secondary stress distribution around roadways surrounding coal pillars are more important in terms of the stability of underground openings. Physical and numerical modelling studies conducted on gateroad stability in deep mining conditions have shown that while squat pillars remain stable, gateroads suffer from a considerable degree of side spalling and convergence (Figure 7a). Moreover, intermediate-size pillars (W/H=7.5) designed in relatively soft floor conditions show a considerable degree of floor heave and buckling-type strata failure (Figure 7b) (Whittaker, 1993; Ünlü, 1994).

3.2 *Critical dimensions of pillars in longwall mining*

As previously mentioned, at shallower depths, pillars are subjected to considerably lower stresses. This makes it easier to apply various mining methods. Despite the generation of horizontal stresses which could assist İn confining pillars in some situations, in general, the major constraint to pillar design at great depth is the high vertical stresses due to overburden thickness. This is particularly relevant to deep coal mining because of the weak nature of the coal and coal-bearing strata. Transfer loads from neighbouring faces should also be taken into account.

Some design approaches and/or pillar strength equations suggest very large pillars (e.g., 100 m or more). This is irrelevant because the author believes that total disintegration of a pillar is not expected if the pillar width-to-height ratio is 10 or more. If only this condition is satisfied, i.e., the pillar width-to-height ratio is 10 or more but the ultimate load limit is exceeded, catastrophic pillar failure would not be expected. However, because of the high stresses due to depth, instability problems in gateroads such as roof and/or floor failure may be encountered.

In order to examine pillars in longwall mining and to determine reasonable pillar dimensions for longwall pillars wim various gateroad layouts, the Pillar Stability (Pil-Sta) program was used. The results show that pillars less than 50 metres in width are satisfactory in all cases without transferring loads to neighbouring panels (Figure 8). If pillars are designed with less than this dimension, they can still resist loads without losing their integrity. However, additional support should be introduced to gateroads to maintain the stability of these openings.

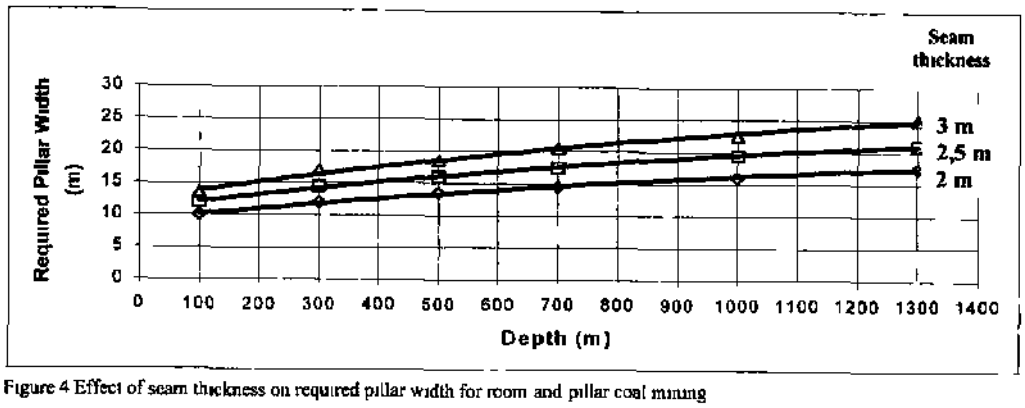

Figure 4 Effect of seam thickness on required pillar width for room and pillar coal mining

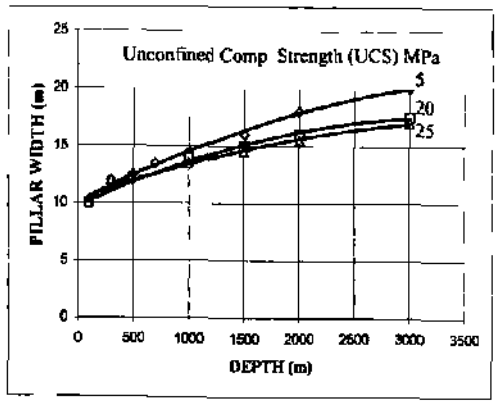

Figure 5 Effect of UCS of coal on pillar width

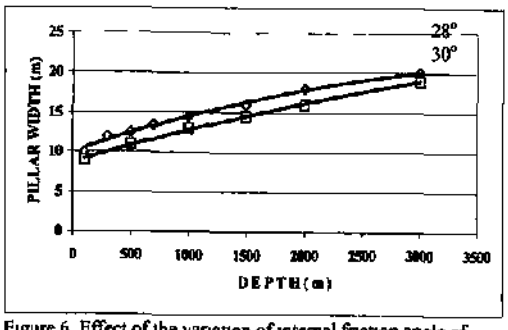

Figure 6 Effect of the variation of internal friction angle of coal on pillar width

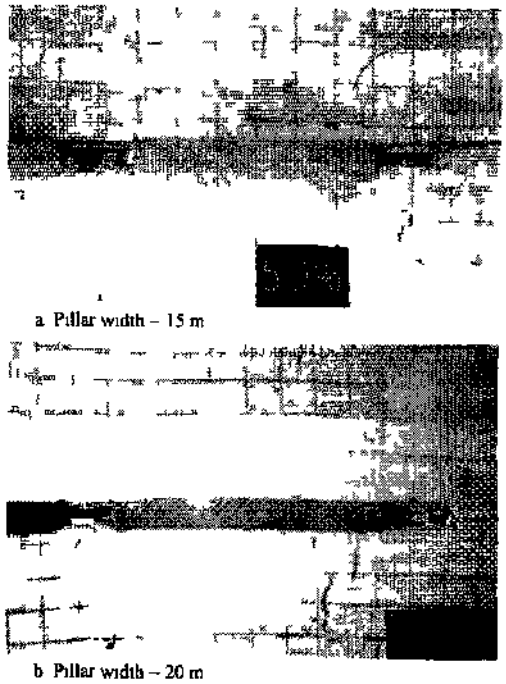

a Pillar width – 15 m

b Pillar width – 20 m

Figure 7 Physical modelling results

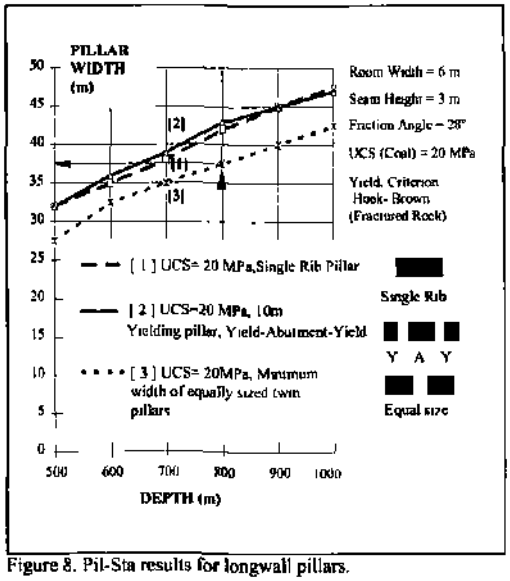

Figure 8. Pil-Sta results for longwall pillars.

As can be seen in Figure 9, increasing the width of small pillar (Y) from 10 to 15 m results in only a small change in terms of required abutment pillar (A) width for the same depth. It is also important that the design engineer be careful not to design critical pillars. Therefore, designing "one yielding + one squat" pillars is better than designing "two equal pillars" or "one intermediate + one squat" pillars.

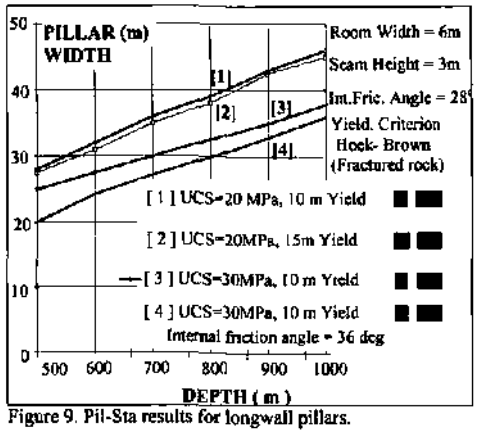

Figure 9. Pil-Sta results for longwall pillars.

4 CONCLUSIONS

The minimum width for small and/or yielding coal pillars should not be less than 10 metres. Any stable smalî pillar may lose its integrity and residual load-carrying capacity, depending upon the other environmental factors.

Special attention should be given to pillars with width-to-height ratios between 4 and 10, if soft roof and/or especially floor strata conditions exist. These pillars may lead to excessive roof sagging and floor heave.

After a certain pillar width, which is affected by the geomechanical characteristics of the coal seam and coal-bearing strata, the strength of coal pillars increases rapidly, and it is almost impossible to yield pillars completely. However, the stability of roadways and surrounding openings becomes much more important than the stability of the pillars themselves. Some of the pillar strength equations or design approaches suggesting very large pillars (more than 40-50 m) for deep coal mines should not be used.

REFERENCES

Babcock, C. O. et al. 1981. Review of pillar design equations including the effect of end constraint. *Ftr\t Conference on Ground Control in Mining July:* 35-43

Babcock, C. O 1985. Constraint is Ihe prime variable in pillar strength. *Proc. 4h Conference an Ground Control in Mining:* 105-116

Barron, K. İ984. An analytical approach to the design of coal pillars, *CIM Bitllelin.Aug.* Fo/. 77:37-44

Barron, K. *&* Pen, Y. 1992. A revised model for coal *pMais.USBM Information Circular. IC* 95/5:144-157

Carr, F. et al. 1984. How to eliminate roof and floor failures with yielding pillars. *Coal Mmtng.Dec.:62-70*

Carr, F. et al. 1985. How to eliminate roof and floor failures with yield pillars. *Coal Mining.* Jan.:44-51

Farmer, I. 1985. *Coal Mine Structures.* Chapman and Hall310 P

Koehler, J. R. et al. 1996. Critical pillar concept in yield-pillar-based longwall gate-road design. *Mining Engineering Vol. 48. No.8. August:* 73-78

Mark, C. 1996. Empirical methods for coal pillar design. *Proc. Of the Second International Workshop on Coal pillar Mechanics and Design. NIOSH IC 9448:* 145-154

Mark, C. & Barton, T. M. 1996. A new look at the uniaxial compressive strength of coal. *Rock Mechanics. Aubertin, Hassam & Mitri (eds). Balkema Rotterdam:* 405-412

Salamon, M. D. G. & Oravecz, K. L. 1976. *Rock Mechanics m coal mining.* Chamber of Mines of South Africa. PRD Series 198:59-65

Ünlü, T. 1994. *Stability and reinforcement of pillar workings with particular reference to deep coal mining.* Ph.D. Thesis. University of Nottingham. UK:302 p.

Ünlü, T. 1994. Multiple entry pillar stability assessment using the limit equilibrium method. *Int. J Of Rock Mech. Min. Sei & Geomech. Abstr. Vol. 31. No. 5:* 429-438

Wagner, H. 1980. Pillar design in coal mines. *J. of South African Institute of Min. Metall. Jan.* :37-45

Wilson, A H. 1980. *The stability of underground workings in soft rocks of the coal measures.* Ph.D. Thesis. University of Nottingham. UK, April.

Whittaker. B. N. et al. 1993. Pillar design aspects for stability in deep coal mines. *Assessment and Prevention of Failure Phenomena in Rock engineering. Pasamehmetoglu el al. (eds.). Balkema/Rotterdam:* 375-3RÖ.

17* International Mining Congress and Exhibition of Turkey- IMCET2001, ©2001, ISBN 975-395-417-4

Analytical Investigation of Overburden Rock Strata Movement During Monitoring of Rock Massif at Stage of Finishing of Ore Deposit Mining

Sh.M.Aitaliyev & T.M.Yermekov
National Academy of Sciences of Kazakhstan, Almaty, Republic of Kazakhstan
A.B.Yun & MZh.Satov
"Kazakhmys "Corporation, Zhezkazgan, Republic of Kazakhstan

ABSTRACT: In this paper, new results are presented. They were obtained jointly by scientists - both theorists and practical workers. It is noted that rheology has an effect on die development of deformations of rocks in time and also on mine workings destruction in terms of achieving long-term strength. Creepage of a rock massif is studied on the basis of the hereditary theory of Boltsman-Volterr. Analytical expressions are given, both of subsidence of the clay surface and the rate of subsidence. The possibility of taking account of irregular increasing of working excavation space dimensions at a moment of stability loss (destruction) in support pillars is shown.

1 INTRODUCTION

The Zhezkazgan polymetal deposit (Kazakhstan), the largest in Eurasia, at one time produced up to 45% of all copper output in the world. It has been exploited for more than 70 years, since the end of the 1930s. Now the deposit İs in the final stage of mining. The finish of mining of the deposit İs characterized by complications of the stressed-deformed condition of the rock massif as a result of long-term technical-in-genesis activity. The depth of mining operations increased and ore reserves which remained in pillars were extracted. These processes caused disturbance of the steady-state balance, deterioration of geomechanical conditions, and activated processes of movement and destruction of the rock massif. The large volume of rock movement due to the creation of worked-out space had such negative consequences as caving of the overlying strata up to the clay surface. It can cause great physical and economic damage through destruction of industrial developments and housing, quite often endangering human life. All this necessitates the monitoring of the current condition of the undermined rock massif with a broad analytical information system.

2 ANALYTICAL EVALUATION OF CLAY SURFACE SUBSIDENCE

To determine the current condition of an area of clay surface above worked-out space, we can represent it as extended in horizontal direction ellipse in the vertical plane of cross-section. Then elastic deflection - strata subsidence - at a moment of worked-out space forming may be represented by Muskhelishvili's formula (Muskhelishvili, İ954):

$$\eta = \gamma H_b l_e \frac{1-\nu^2}{E}; \ m \qquad (1)$$

where $r\backslash$ - deflection value, m; y - specific gravity of rock, kg/m^3; Hb - depth of rock-bridge bedding, m; U - equivalent span, m; v and E - Poisson's coefficient and modulus of elasticity of rock.

Practice shows that deformation of the overlying strata is a process in time. The deformation has two factors. First, properties of creepage of the rock massif take place. Secondly, in the course of time, the effect of long-term strength of roofs and pillars occurs. As a result, the span of worked-out space changes.

In accordance with Volterr's principle, which was formulated by Rabotnov (Rabotnov, 1966), subsidence in time may be obtained from elastic solution (1) by way of replacing the elastic parameters v, E with elastic operator functions v_t, E_t. Taking into account the elastic solid deforming of TOcks and the small variation of Poisson's coefficient in time, subsidence in time takes the form:

$$\eta_t = \gamma H_b l_e \frac{1-\nu_t^2}{E_t}; \ m \qquad (2)$$

where $E_t = E\left[1 - \beta \Im_\alpha^*(-\beta)\right]$

Here $3_0\{-ß)$ - special operator of Rabotnov.

In accordance with the hereditary theory of rock

creepage of Yerzhanov (Yerzhanov, İ964), for simpler two-parameter (a. 6) core of Abel with parameters approximation operator function of modulus of elasticity, we may write:

$$E_t = Ee^{-\omega t\beta^{1-\alpha}} \quad (3)$$

Then, expression (2) may be written in the form

$$\eta_t = \gamma H_b l_e \frac{1-\nu_t^2}{E} e^{\omega\beta t^{1-\alpha}} \quad (4)$$

or, more simply,

$$\eta_t = \eta_{t=0}^{y} e^{\omega\beta t^{1-\alpha}} \quad (5)$$

where: $\omega = (1-\alpha)^{1-\alpha}$; $\beta = \delta\Gamma(1-\alpha)$; $0<\alpha<1$.

Here $\eta_{t=0}^{y}$ - elastic subsidence (1) corresponding to the initial moment of time f=0. As is clear, if $\omega>0$, $\beta>0$ with time increase $t\to\infty$ $e^{\omega\beta t^{1-\alpha}} \to \infty$ and $\eta_t\to\infty$, then subsidence increases in the course of time.

For Zhezkazgan rocks İn laboratory conditions, parameters of elasticity and creepage ($\alpha \approx 0.7$, $\delta \approx 10^{n3}$) were established. As shown by Aitaliyev (Aitaliyev et al., 1966), in natural conditions near isolated mine workings natural values of parameter So are by an order of magnitude greater than laboratory value 5/, that is S/r=108j. Near extracting mine workings this effect is built up, that is $\delta_H \approx 10^n \delta_l$, n=2-3.

3 EVALUATION OF RATE OF SUBSIDENCE OF CLAY SURFACE

The main source of information about processes of rock and clay surface deformation as the result of underground mining operations are instrumental observations. Important parameters of the process of movement of the rock massif are the maximum values of subsidence η_{max} and rate of subsidence $\dot{\eta}_{max}$.

In analytical terms, determination of the rate of subsidence is a more difficult problem. The point is that subsidence is a complex function of time, depending both on creepage and on irregular changing span of extracting mine workings. Limiting of constant span l_e = const may be obtained from (5):

$$\dot{\eta}_t = \frac{d}{dt}\eta_t = \eta_{t=0}^{y} \frac{d}{dt}\left(e^{\omega\beta t^{1-\alpha}}\right) = \eta_{t=0}^{y}\omega\beta \frac{e^{\omega\beta t^{1-\alpha}}}{t^{\alpha}} \quad (6)$$

İt is clear that when $t\to\infty$ and $e^{\omega\beta t^{1-\alpha}} \to \infty$ and $t^{\alpha}\to\infty$, thore *is* uncertainly in the form ∞/∞. This uncertainty is evaluated by the Lapital rule:

$$\frac{\left(e^{\omega\beta t^{1-\alpha}}\right)'}{\left(t^{\alpha}\right)'} = \frac{\omega\beta}{\alpha} \frac{e^{\omega\beta t^{1-\alpha}}}{t^{2\alpha-1}} \quad (7)$$

At the n step, this will be:

$$\frac{\left(e^{\omega\beta t^{1-\alpha}}\right)^{n}}{\left(t^{\alpha}\right)^{n}} = \left(\frac{\omega\beta}{\alpha}\right)^{n} \frac{1}{(2\alpha-1)\ldots(n\alpha-n+1)} \frac{e^{\omega\beta t^{1-\alpha}}}{t^{n\alpha-n+1}} \quad (8)$$

When

$$n\alpha - n + 1 < 0,\ n > 1/(1-\alpha) \quad (9)$$

Uncertainty occurs, showing the growth of the rate of subsidence in time.

Thus, for determination of the extreme value of time t_{ext}, after which increase in the rate of subsidence is unlimited, İt is necessary to take:

$$\frac{d}{dt}(\dot{\eta}_t) = 0 \quad (10)$$

Then, from (6) can be obtained:

$$ln\, t_{ext} = \frac{1}{1-\alpha} ln \frac{\alpha}{\omega\beta} \quad (11)$$

However, the formulae above should be used with great care. Their accuracy depends on the accuracy of approximation (3). It may not work absolutely accurately much of the time. More reliable results may be obtained with due account of the ability to injure and use of the approach of Aitaliyev and Iskakbayev (Aitaliyev et al., 1990).

4 EFFECT OF WORKED-OUT SPACE SPAN CHANGE ON CLAY SURFACE SUBSIDENCE

The geomechanics of change of the worked-out space span in time and its effect on the process of subsidence of overlying strata may be represented as an approximation as follows.

In spite of the fact that the long-term strength of pillars, and roofs takes place continuously, the worked-out space span changes irregularly in a moment of pillars and roofs destruction. Write these moments of time as $t_1, t_2, \ldots_y U$ and the corresponding

increments of span as Δl_{e1}, Δl_{e2}, ... Δl_{ei}. The value of the total span may be written in the form:

$$l_e = l_{e0} + \Delta l_{e1} + \Delta l_{e2} + \ldots + \Delta l_{ei} + \qquad (12)$$

Here lco is an initial equivalent span.

Increment of the span takes place in conditions of creepage of the massif. It is very difficult to describe analytically the combination of such processes, but we may show one possible procedure.

Up to moment ti subsidence in time is determined by formulae (4) and (5), and in a moment of time *t*\ it is equal to:

$$\eta^{\Pi}_{t=t_1} = \gamma H_b l_{e0} \frac{1-\nu^2}{E} e^{\omega\beta\, t_1^{1-\alpha}} \qquad (13)$$

At this moment, because of increment of span /eo by Δl_{e1}, there is an immediate growth in subsidence by the value:

$$\eta^{y}_{t=t_1} = \gamma H_b \frac{1-\nu^2}{E}(l_{e0} + \Delta l_{e1}) \qquad (H)$$

Then, total subsidence at time moment *h* will be:

$$\eta^{\text{общ}}_{t=t_1} = \eta^{\Pi}_{t=\eta} + \eta^{'}_{t=\eta} = \\ = \gamma H_b \frac{1-\nu^2}{E}\left[l_{e0} e^{\omega\beta\, t_1^{1-\alpha}} + (l_{e0} + \Delta l_{e1}) \right] \qquad (15)$$

Following this, subsidence is described by the following expression in comparison with formulae (4) and (5):

$$\eta^{\Pi}_{t>\eta} = \eta^{\text{общ}}_{t=\eta} e^{\omega\beta\,(t-t_1)^{1-\alpha}} = \\ \left\{ \gamma H_b \frac{1-\nu^2}{E}\left[l_{e0} e^{\omega\beta\, t_1^{1-\alpha}} + (l_{e0} + \Delta l_{e1}) \right] \right\} e^{\omega\beta\,(t-t_1)^{1-\alpha}} \qquad (16)$$

At time moment fc, at the expense of rock creepage, subsidence will be:

$$\eta^{\Pi}_{t=t_2} = \left\{ \gamma H_b \frac{1-\nu^2}{E}\left[l_{e0} e^{\omega\beta\, t_1^{1-\alpha}} + (l_{e0} + \Delta l_{e1}) \right] \right\} e^{\omega\beta\,(t_2-t_1)^{1-\alpha}} \qquad (17)$$

Subsidence at this moment because of the increase of span $(l_{e0} + \Delta l_{e1})$ by Δl_{e1} instantaneously increases by value:

$$\eta^{y}_{t=t_2} = \gamma H_b \frac{1-\nu^2}{E}(l_{e0} + \Delta l_{e1} + \Delta l_{e2}) \qquad (18)$$

Total subsidence at a time moment *h* will be:

$$\eta^{\text{общ}}_{t=t_2} = \eta^{\Pi}_{t=t_2} + \eta^{'}_{t=t_2} = \\ = \left\{ \gamma H_b \frac{1-\nu^2}{E}\left[l_{e0} e^{\omega\beta\, t_1^{1-\alpha}} + (l_{e0} + \Delta l_{e1}) \right] \right\} \\ * e^{\omega\beta\,(t_2-t_1)^{1-\alpha}} + \gamma H_b \frac{1-\nu^2}{E}(l_{e0} + \Delta l_{e1} + \Delta l_{e2}) \qquad (19)$$

Hereafter, subsidence in time, in contrast to (4), (5) and (16), is described by the expression:

$$\eta^{\Pi}_{t>t_2} = \eta^{\text{общ}}_{t=t_2} e^{\omega\beta\,(t-t_2)^{1-\alpha}} = \\ = \left[\left\{ \gamma H_m \frac{1-\nu^2}{E}\left[l_{e0} e^{\omega\beta\, t_1^{1-\alpha}} + (l_{e0} + \Delta l_{e1}) \right] \right\} * \right. \\ \left. * e^{\omega\beta\,(t_2-t_1)^{1-\alpha}} + \gamma H_m \frac{1-\nu^2}{E}(l_{e0} + \Delta l_{e1} + \Delta l_{e2}) \right] \qquad (20)$$

Continuing the procedure above, we may write the most general formula of subsidence in time, when *f>t,* in the form-

$$\eta^{\Pi}_{t>t_i} = \eta^{\text{общ}}_{t=t_i} e^{\omega\beta\,(t-t_i)^{1-\alpha}} \qquad (21)$$

5 CONCLUSIONS

In the limits of the hereditary mechanics of rocks, an attempt was made to describe analytically the clay surface subsidence above worked-out space. Imposition of the development of creepage and long-term strength of rock massif in first approximation was studied. Evaluation of the rate of subsidence of the clay surface was developed analytically to the end; however, ite accuracy depends on the approximation of operator functions. Other approaches of one of the authors are offered with due account of the ability to injure of the rock massif and the immediate fractional-exponential function of Rabotnov. The reliability of the analytical expressions proposed must be established by means of carrying out observations of rock movement and clay surface subsidence.

REFERENCES

Muskhelishvili, N.I. 1954 *Some mathematical problems of plane theory of elasticity* Moscow, "Science".

Rabotnov, Yu.N 1966. *Creepage of Elements of Constructions.* "Science"

Yerzhanov, Zh.S. 1964 *Theory of rocks creepage and its application.* Almaty. Science.

Aıtalıyev, Sh.M., Yerzhanov, Zh.S., Tsai, T N., Urofeyev, L M. 1966 Complex investigation of non-fixed rock pressure in main horizontal mine workings. *Problems of rock mechanics,* Alma-Ata,

Aitaliyev, Sh.M, Iskakbayev, A. I 1990 Approximate calculation of parameters of rocks creepage and long-duraıion strength with due account of ability to injure, *Actual problems of mechanics of deforming solid body,* Alma-Ata, "Gylym", v.1.

1 f International Mining Congress and Exhibition of Turkey- IMCET2001, © 2001. ISBN 975-395-417-4

Estimation of Current Condition of Undermined Rock Massif by Deflection of the Earth's Surface

T.M.Yermekov, M.Zh.Bitimbayev
Kunaev Institute of Mining, Almaty, Republic of Kazakhstan
M.K.Alipbergenov, M.Zh.Satov
Kazakhmys Corporation, Zhezkazgan, Republic of Kazakhstan

ABSTRACT: Analytical estimation of the current condition of undermined districts by subsidence of the earth's surface was carried out with due account of creepage of the rock massif, and an increase in subsidence in time was determined. The processing of experimental data by actual subsidence of the earth's surface by the method of extrapolation made it possible to describe qualitatively and quantitatively the behaviour of the propagation of caving in space and in time. On the basis of theoretical and experimental investigations, the current condition of studied districts of the undermined massif was estimated by deflection of the earth's surface.

1 INTRODUCTION

When catastrophic technical-in-genesis cavings take place, the unavoidable condition of cones forming on the ground surface is the destruction of supporting pillars, and then propagation of the process of deformation and destruction of enclosing rocks up to the surface. The current condition of worked-out space may be estimated by the results of experimental observations of ground surface movement.

For the purpose of analytical estimation of the current condition of mining districts by deflections of the ground surface, we take Muskhelishvili's formula:

$$\eta = \gamma H_b l_c (1 - \nu^2)/E_e, \text{ m} \qquad (1)$$

where n - deflection value, m; *y* -specific gravity of rock, kg/m^3; H_m - depth of rock-bridge bedding, ra; l_c - equivalent span, m; v and Ee - elastic properties of stratified fissured rock strata.

In accordance with the hereditary theory of rock creepage of Yerzhanov (1964) the value of subsidence in time may be obtained from this expression by means of replacing the elastic modulus Ee with the elastic operator-function İn time Et:

$$\eta_t = \gamma H_b l_e (1 - \nu^2)/E_t, \text{ m} \qquad (2)$$

where $E_t = E(1-E^*) = E[1 - \beta \Im^*_\alpha(-\beta)]$,
$\beta = \delta\Gamma(1-\alpha)$;
$3_Q(-ß)$ - special operator of Rabotnov;
a and ß - parameters of creepage;
l_e - span of worked-out space.

The special operator of Rabotnov $3_a(-ß)$ has a number of remarkable properties, assisting problem solving in the theory of creepage. For the simpler two-parameter core of creepage of Abel with parameters a and 5 and with approximation of function $\Im^*_\alpha(-\beta)$, we may obtain:

$$E_t = Ee^{-\omega\beta t^{1-\alpha}} \qquad (3)$$

where $\omega = (1-\alpha)^{1-\alpha}$.
Then subsidence with due account of massif creepage is determined by the expression:

$$\eta_t = \gamma H_b l_e \frac{1-\nu^2}{E} e^{\omega\beta t^{1-\alpha}} \qquad (4)$$

As is clear, with time increase $t \to \infty$ with due account of $\omega>0$, $\beta>0$, $e^{\omega\beta t} \to \infty$, $\eta_t \to \infty$, that is , subsidence increases in the course of time.

The final algorithm for determination of subsidence for a moment of any tj and time t>t, may be written as:

$$\eta_{t>t_1} = \eta_{t-t_1} e^{\omega\beta (t-t_1)^{1-\alpha}} \qquad (5)$$

Considering subsidence as a factor of geomechamical inhomogeneity, it should be noted

that it is taken into account most reliably by means of instrumental observations in natural conditions

The main source of information about prolonged processes of deforming and movement of ground surface from the effect of underground mining operations are instrumental observations. An important parameter of the process of movement is the maximum subsidence n. As far as we could judge on the basis of the results of instrumental observations, the geometrical dimensions of worked-out space (thickness and depth of mining), the presence of overlapping ledges and other factors have a substantial effect on the process of movement value.

Instrumental observations and processing of the results were carried out by standard methods (temporary regulations, 1986), which made it possible to determine the pattern of ground surface movement in the limits of the zone of effect of underground mining operations, in order to determine the principal behaviour and parameters of the process of movement by lines of observation.

However, such methods, in spite of their ability to provide information, do not make it possible to generalize data from measurements by the area of a deposit or to present a visual representation of the process of ground surface movement in time and space. They do not allow evaluation and long-term forecasting of damaging dynamic occurrences, such as caving. As a result, it was necessary to carry out expert evaluation, based on the opinions of specialists.

Practical instrumental observations of ground surface movement and visual observations in mines suggest the existence of a direct connection between increases in the parameters of flexure of movement and the condition of voids formed by underground winning operations. Thus, İt would be a great omission to disregard this connection. Voids in the rock massif in the first stage are filled by rocks bedding immediately above. As a result of these rocks caving, pores are formed in the caved massif, the compactness of rocks of all strata decreases, and this causes rock stress re-distribution (Satov, Alipbergenov, 1999).

The flexure of subsidence forming point to a fact that the process of movement of elementary volumes of massif to a side of worked-out space reached the ground surface. Today, the total area of undermining of the ground surface of the Zhezkazgan deposit by contour of flexures, with 5mm subsidence of points, has reached 8 km^2. Consequently, hundreds of different protecting objects are now m zones suffering dangerous effects of mining operations. The measures taken to avoid ground surface deformations, in spite of the use of data from instrumental observations, have not been effective enough in the field of forecasting cavings. For this reason, the results of these observations were the subject of further analysis and interpretation.

The processing of a large subsidence database of by standard methods (temporary regulations, 1986) did not give positive results when evaluating the actual discrete deformation process taking place in the undermined rock massif.

Therefore, the "method of determination of boundaries of zones of dangerous rock movements at a deposit" (Satov, Alipbergenov, 1999) was worked out for more reliable evaluation of the deformation process. This is based on taking account of the prognostic properties of the criterion n. The main advantage of this simple but effective method is that it enables determination in a volume of deposit anomalous zones of deformation, which are attributed to local breaks of undermined strata in time and space.

Subsidence data from a large number of registration points may be represented in the form of a map with isohypses describing difficult patterns of undermined rock massif deformation. Such patterns are the most suitable for characterizing the space location of the flexure of subsidence. Using this plan, it is possible to solve the following problems:

- to evaluate the quantitative pattern of the deformation processes taking place in the rock massif;
- to determine the development of the process of destruction practically İn all directions;
- to evaluate the location and space dimensions of cones;
- to forecast possible cavings in the long term.

The presence of a large number of subsidence values by different oriented profile lines indicates the effective use of the method of extrapolation with the purposes of evaluation of forecasting, extending a large number of selected subsidence data of remarkable points in zones of the ground surface, which were not studied at once. The worked-out method (Satov, Alipbergenov, 1999) makes it possible to: carry out in-depth statistical analysis of obtained values of subsidence; exclude random errors when measuring deformations; and obtain a substantial quantity of results conforming to different combinations of zones of profile Unes.

For this method, the procedure used is given below.

1. A coordinate grid (X,Y) İs drawn on the plan and all profile lines with points of observations (remarkable points) are drawn.
2. Subsidence values for a moment of observation, taken from logs or albums, are put down on every point of observation. The deflection of flexure of movement (vertical component Z) is determined at the same time.
3. Extrapolation İs carried out after detailed analysis of numerical subsidence values at separate points and for the zone as a whole.

4. Isolines are obtained by joining points of equal subsidence value.
5. The plan of subsidence isolines is superimposed onto a plan of the mining operations and a plan of the ground surface, and then corresponding conclusions are made.

The worked-out method of determining boundaries of zones of dangerous movement (Satov, Alipbergenov, 1999) has the following advantages in comparison with other common methods:

- it İs based on subsidence values obtained from data from long-term natural observations, in contrast to type curves and analytical methods;
- extrapolation is carried out from known conditions to be determined with due account of factors affecting the process of movement;
- it characterizes the development of the process of deformation in time;
- it locates the place and geometrical dimensions of flexure of movements;
- it allows reliable long-term forecasting of cavings reaching the ground surface.

Thus, the study of deformations and movements of rocks by this method makes it possible to obtain relatively simple and effective mathematical apparatus for the determination of places of possible caving in space and time, running down the development of deformation processes in overlying strata.

The worked-out method makes it possible to carry out long-term forecasting of cavings, and also to choose such parameters of extraction mine workings and a relative position which will ensure that deformations of the ground surface do not exceed allowable deformation values for undermined objects. In the case of impossibility of change in the parameters of worked-out space, this method allows an increase in the worked-out space stable condition and the taking of protective measures.

Use of the new method to control deformation processes based on actual behaviour of rock movements also allows a substantially increased coefficient of recovery of useful minerals under built-up areas and natural objects trouble-free in operation, and a decrease in environmental danger in administrative and industrial regions.

Now a forecasting map of the Zhezkazgan deposit has been drawn using the maximum subsidence data of the ground surface (Fig. 1).

Practical use of the method ensures safe mining conditions and prevents damage from possible cavings, especially İn conditions where there is a high concentration of protected buildings and structures.

The worked-out investigations made it possible to carry out diagnostics of the undermined rock massif and long-term forecasting of cavings. When carrying out investigations, methods were proposed for evaluation of the current condition of the rock massif by a complex of criteria, distinguished from common methods in that the value of an area of destruction in the rock massif with expected negative consequences is evaluated by space-time changes in the deflection values of the ground surface.

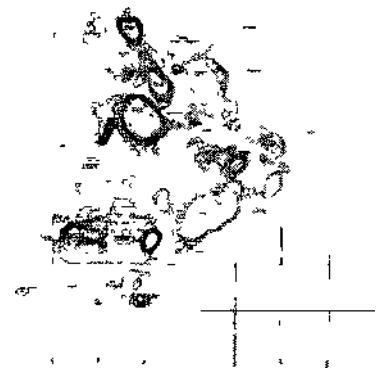

- - ısolmes of maximum subsidence,
- boundary of weakened area;
- cone of caving at ground surface

Figure 1 Information plan of subsidence of ground surface

As a result of evaluation of the current condition of areas by deflection of the ground surface, the geomechanical conditions at Zhezkazgan deposit were determined, and areas that are dangerous due to caving were established.

2 CONCLUSIONS

The principal scientific and practical results of this study are as follows:

- a method was worked out for determination of the boundaries of zones of dangerous rock *movement* at ore deposits, which allows determination and long-term forecasting of possible cavings and an increased coefficient of useful mineral extraction;
- a long-term forecasting map for the Zhezkazgan deposit was worked out, and on the basis of data, zones dangerous due to caving were determined.

REFERENCES

Yerzhanov, Zh.S. 1964 Theory of rocks creepage and ils application. Almaty. Science.

Temporary regulations of protection of structures and natural objects against negative effect of underground mining operations of deposits ores of non-ferrous metals with non-studied process of rock movement 1986 VNIMI Leningrad 76 p

Satov, M.Zh, Alipbergenov MK 1999 Forecasting of condition of worked-out space by data of instrumental observations Proceedings of Scientific-Research Conference devoted to centenary of Academician ICSatpayev Zhezkazgan. Pp 584-588

Satov, M'Zh, Alipbergenov MK 1999 Method of determination of boundaries of zones of dangerous rock movements at a deposit Pre-patent of the Republic of Kazakhstan No 6891 Solution of Russian patent issue on inventor's application No 99109641 /03(010213)

if International Mining Congress and Exhibition of Turkey- IMCET 2001, ©2001, ISBN 975-395-417-4

The Geometrical and Geomechanical Characteristics of Sublevel Caving

V.Arad&S.Arad
Petrosani University, Petrosani, Romania
G.Cioara & G.Clipici
Livezeni Colliery, The National Bituminous Coal Company, Petrosani, Romania

ABSTRACT: During recent years, great attention has been given to high-productivity methods such as sublevel caving. This method accounts for 25 % of the coal mined in the Jiu Valley. This paper deals with the geometrical elements of the mining method depending on the geomechanical characteristics of the coal. A comparison is also made between the high-productivity method and other mining methods, which shows that productivity is ten times higher with the high-productivity method than with the classical methods.

1 INTRODUCTION

The Jiu Valley is the greatest coal basin in Romania, and is a tectonic depression 50 km long with an area of 137 km^2. The mining technologies used in this area are very different because of the very hard conditions and a great depth of working.

Researchers have focused their attention on designing and implementing high-productivity mining methods in the coal industry such as coal and surrounding rocks caving and sublevel caving.

The efficiency of mining activity is a problem which should preoccupy the specialists in the field. The market economy enables competition mechanism and requests low prices and high quality raw-material production.

Taking into account the opportunity of mining the deep coal-deposits in the Jiu Valley effectively, it is necessary to choose and use high-productivity mining-methods. This can be achieved by considering the specific geological and mining conditions and by geomchanical characterization based on a profound study of the coal and surrounding rocks.

The use of the above-mentioned methods has been increasing steadily, accounting for 25 per cent of all Üie mining methods applied in the Jiu Valley Basin. In the future, coal mining will operate in certain competitive conditions, reducing production costs.

The sublevel mining method was first applied in its classical variant without complex mechanization at the Barbateni, Lupeni, Vulcan, Paroseni and Livezeni collieries.

Since 1997, the collieries have progressed to the mechanization of the method. Thus, prop and beam support has been replaced by powered supports consisting of:

SMA-2 powered supports (modified for sublevel caving);
KS-3M cutter-loader;
TR-7A conveyor.

2 THE GEOMETRIC AND GEOMECHANICAL CHARACTERISTICS OF THE MINING METHOD

The sublevel caving-method can be applied with good results in coal seams with a horizontal thickness greater than 4 m and a dip greater than 45°. It has been determined experimentally that the optimum lower limit of the dip of the seams is about 50°-55°; under such conditions, coal losses are at a minimum.

The method can also be applied in lenticular zones, lodes, and pillars where classical methods are not profitable.

The geological-mining conditions as well as the geomechanics of coal and surrounding rocks are influenced by the application of this method.

The accuracy of design as well as optimization of the support parameters depend on the interaction model between the rock massive and the supporting system for all mining methods (Goldan, 1999).

The mining method ensures a considerable reduction in the amount of first mining and coal face work as well as higher labor productivity and output.

The significant parameters related to geometric and geomechanical features of the method are the roof coal height and caving step.

The roof coal height is calculated according to the type of coal face support.

When the face support is rigid, then the height of the roof coal is computed with the Equation I.

$$H_b = 2.12 l_a \sqrt{0.75 - ctg\xi} \quad (1)$$

where: l_a = face width ; ξ = coal caving angle in the roof coal.

In cases where the support has a subsiding bearing, the computation Equation 2 is used for the height of the roof coal.

$$H_b = 1{,}73 l_a \sqrt{0{,}75\left[\frac{1}{1 - \frac{3E_c * I}{K l_a^3}}\right] - ctg\xi} \quad (2)$$

where K - support rigidity; E_c - coal elasticity module; and I - inertia moment of the roof coal.

If the support constitutes an active bearing, then the roof coal height can be determined by Equation 3.

$$H_b = l_a \sqrt{x * ctg\xi - ctg^2\xi} \quad (3)$$

The value of the caving step, x, of the roof coal can be calculated using Equation 4.

$$x = l_a ctg\xi \quad (4)$$

3 THE PARAMETERS OF THE MINING METHOD

The main parameters of the method are:

- the seam thickness: h = 20-60 m;
- seam dip on the strike: a = 4°-7°;
- face height: h^ = 3 m;
- roof coal height: H_b = 15-20m;
- working face length: L_{ab} = 40-60 m;
- mining panel length: Lp= 100-300 m;
- face advancing-step (web width): x = 0.63 m;
- face width: !„ = 5.8-6.5 m;
- coal dislocation from the roof coal is carried by natural caving, drilling blasting, or by water jet under pressure;
- roof control is achieved by complete caving of the roof rocks.

In order to help coal mining, it is necessary to achieve a certain plane of rupture and sliding of coal, all along the face. This plane is achieved artificially, by drilling and blasting.

The working face technology phases, after the caving plane achievement, present the following succession:

- cutting off the coal from the face, using explosives;
- hoisting the cantilever bars and roof lagging;
- evacuating the mined coal and installing the roof bars with hydraulic props;
- moving (advancing or flitting) the conveyor and controlling the roof along the working face. The roof control is achieved by pulling the last row of props and roof so that roof blocks of about one bar length are allowed to cave;
- evacuation of coal from the roof coal. This is made through the eyes of die lagging steel mesh. The spacing of the evacuating eyes is one meter along the and about 0.5 meter lower then the working face roof.

When compared to other frequently used mining methods, the technical economic indicators obtained are clearly superior, as shown in Table 1.

Table I. Frequently used mining methods and their technical characteristics.

No.	Indicator		Mining method				
			Room	Shortwall	Longwall	Subleve caving	
						With mechanization	Without mechanization
1.	Wood consumption	mVlOOO t	45-50	8-17	17	2	1.5
2.	Timber consumption	m^3/1000t	12-18	2-7	3^t	3	2.5
3.	Explosives	kg/10001	160-220	280-350	200-250	50-100	20-50
4.	Blasting caps	pieces/ lOOOt	580-800	750-850	700-1000	100-300	50-150
5	Wire metallic	kg/1000 t	500-1200	1550-2600	1500-3000	800-1000	500-700
6.	Slice output	t/day	70	90-100	150-200	i 50-200	250-300
7.	Coal roof output	t/day	-	-	-	600	800
8.	Overall output	t/day	70	90-İ00	150-200	750-800	1050-1100
9.	Number of workers		[6	18	18	25	25
10	Productivity	(/man	4.37	5	8.3-11	30-32	42-44

4 MEASURES AND CONCLUSIONS

In conclusion, the results obtained during the testing period at the mining plants justify the general use of the mining method.

- It is noted that with sublevel caving methods, labour productivity is 3 to 10 times greater than with classical methods. Wood and timber consumption decreases 4 to 25 times with direct bearing on the first cost.
- The volume of first mining is 50 % lower with the proposed mining methods than with the classical methods, while the prime cost per ton of mined-out coal ton is three times lower.
- It should be noted that if the coal face technology is not maintained adequately, coal losses may increase and there is a greater danger of fires occurring.

In order to reduce the danger of fires breaking out, the following measures should be taken:

- the worked-out space should be treated with thermo-power station ashes in a mixture with antipyrogenic substances or chemical foam;
- sealing dams should be built to seal off fires in the access working to the face;
- fire prevention by local inertization with nitrogen;
- gas samples should be taken from the mined-out area for the purpose of monitoring the content of the following gases: carbon monoxide, carbon dioxide, methane, etc.;
- correlation of the technological parameters of the mining method: face length, coal roof height, advance rate.

REFERENCES

Goldan, T. 1999 *Optimizarea paramelnhr metodelor de exploatare a stratelor groase cu inclinare mare tn vederea reJucern perwohdui de autoaprtndere a cärbunelw.* Doctoral Thesis. Pelroşam University

Jurca, T, ş a. 1995 - High productivity methods for coal mining applied in Jiu Valley region *Mining Review* No.3/1995

Moroz, S , ş a. 1995 Practical contnbutions at the viable exploilation of the coal in Jiu Valley. *Mining Review,* No.4/1995.

17* International Mining Congress and Exhibition of Turkey- IMCET2001, ©2001, ISBN 975-395-417-4

Going Underground in Quarrying: Technical Perspectives for Marble in Portugal

M Fomaro, C.Oggeri, P.Oreste & D.Valentino
Department of Georesources and Land, Polytechnic of Turin. Italy

ABSTRACT: This paper examines the application of the criteria for the alternative choice of underground quarrying in ornamental stone. In these quarries, the rock mass quality is usually good, and in most cases exploitation is carried out by means of open pit methods. Underground quarrying in ornamental stones is possible when certain prerequisites are satisfied: geostructural features, stability contraints, land planning, and when the recovery and safety goals are achievable. After a general discussion of these items, the paper analyzes the case of the pink marble of the Alentejo basin in Portugal, in which a first tentative design method and monitoring approach has been proposed. The development of open pit exploitation İn Alentejo has determined the creation of very deep pits from the flat ground surface: in some cases, a depth of one hundred meters has been reached with vertical lateral surfaces

1 GENERAL FEATURES

The production of ornamental stones takes on noticeable importance in the sector of natural building materials, both from the economic and technological point of view.

The quarries are exploited by open pit methods, but there are several cases in which exploitation is actually carried out underground: Italy, Croatia, Portugal, Greece, and France are example of countries where these methods are applied.

Underground exploitation of dimension stones will be proposed increasingly as production methods, not only in cases where the underground option İs imposed by the features of the rock mass as in the past, but also for a number of reasons that have gained weight in recent years, make underground exploitation preferable in terms of economy and in cases where surface operations are technically feasible.

The underground option can be necessary or preferable when: 1) the surface is very dipping and irregular (mountain areas); 2) me external surface is regular but the overburden is thick; 3) land costs and reclamation taxes are too high; 4) the selected rock mass is confined in a well-defined ore body; and 5) safety requirements and stability features are no longer suited to open pit methods.

Five elements should be evaluated when the underground choice has to be considered: 1) good structural conditions of the rock mass (in ornamental stone quarries this aspect is generally satisfied, even though there are very particular rock mass conditions, such as the case of stratified rocks with very thin clay filling); 2) technology of the excavation (mainly mechanical cutting to separate the blocks from the mass); 3) commercial features (some properties, for example colour and grain size, are not always the same, due to the limited homogeneity of the rock mass, where change of colour, and stains and inclusions can be encountered); 4) economic profitability compared to the costs of open pit exploitation, taking into account the probable lower recovery due to underground support structures such as pillars, but also the savings on overburden removal and muck disposal; and 5) safety and environmental reclamation.

The stability features in this particular type of void should be ensured on a long-term basis, without significant contribution from artificial supports.

The geostructural conditions determine both the design of the excavations and the methods that should be used to separate the blocks from the faces. The availability of structural data for rock masses where some underground quarries have been developed and technical results after some years of exploitation can allow one to consider the above-mentioned elements in a critical way, with an emphasis on the first two elements in particular. The collection of statistical data on rock mass

structure and block recovery should become a regular procedure in ornamental quarries.

2 THE MARBLE QUARRIES IN ALENTEJO

The pit quarries in the Alentejo region have two types of problems. The first is a geomechanical problem, and it is linked to the redistribution of stresses under the new geometrical configuration, where a lateral confinement is no longer applied and therefore the instability of lateral walls is possible when discontinuities occur in unfavourable orientation.

The second is a technical and economic problem when changing the excavation method to go underground. In this case, the underground adits are excavated directly in the productive and massive rocks, avoiding the removal of ovreburden. It is necessary to maintain stable structures İn the rock (rib pillars and eventually thick horizontal beams) without excessive loss in block recovery .

This study, on the basis of geostructural surveys and geomechanical tests, describes the modelling of the rock excavations, as the first answer to support the industrial decisions for the development of the exploitation, taking into account the particular conditions of the area. The study has the purpose of suggesting a possible formulation of a tunnel site for the feasibility of successive underground mining.

The Estremoz-Borba-Vila Viçosa basin is situated about 100 km East of Lisbon. The anticline in general presents a northwest/southeast immersion direction, with inclinations that vary from 15° to 75° on the southeast side to vertical on the northwest side.

The lithologies involved İn the mining are different-coloured marbles: blue marble, cream marble, pink marble, etc., but also primary dolomites which are locally called Cascalva rock.

The area appears, from me orographic point of view, to be made up of slight and gradual land reliefs which are frequently sub-level. The quarries are practically all located in plain areas and are exploited by means of a pit whose vertical walls reach an elevation of several tens of metres. The mining involves rock mass portons with altered coverings of soil and rock of variable thickness, but which are of the order of 5-15 m. The transition between covering and rock in some places is not complete because of the presence of karst voids later filled with soil material that goes deep into me substratum.

The examined quarry takes up an area of about 21,250 m^2, and 5,000 m^2 of this is subject to mining.

The quarry has been mined down to eight levels; the base yard at the moment reaches a depth of 35 m. The presence of joints and karst, sometimes even at a depth, creates a rather important static and mining problem to which block recovery is connected. Furthermore, the destressing phenomenon due to excavation and the final removal of the blocks from their position further increases the negative effect of the joint systems.

Block recovery, which has so far been carried out through open pit mining, is, however, satisfactory. The rock overall appears to be quite compact and in particular at least one homogeneous and accessible area can be recognised, so that the formulation of underground quarrying can be considered.

In the northeast area of the quarry, at about 58 m in depth, tiie exploitation intercepts the primary dolomite layer. As this layer is not encountered in the southwest area, it is assumed that it runs at a deeper level, perhaps at 70 m or even more. As the pink marble is above the primary dolomite, the southwest area would seem more suitable for the experimentation of underground mining, also because the stone presents better characteristics for ornamental use: reduced jointing and probably greater cubature.

2.1 *Geomechanical features*

The geomechanical characterisation of the studied material was performed at the I.S.T. laboratories in Lisbon. Different tests were carried out on the numerous samples that were collected (85) and then a statistical elaboration was performed and me geomechanical parameters of the rock were defined on the basis of these results.

The tests were performed on four denominated lithological classes: azure marble (MA), clear marble without veins (MSV) and dolomite (D), obtaining the results given in Table 1.

The characterisation of me rock also involved İn-situ tests that were carried out to establish the acting stress state.

This was determined through die reset of the deformations using a flat jack technique.

This involves the measurement of a cortical stress state which is influenced by tiie condition of the walls in which the measurements are performed, which can limit the significance of the measurements. For this reason, a back analysis was performed in order to make the results of the measurements congruent due to external factors, with the optimal configuration of the model, and to evaluate the geomechanical parameters that best represent me problem under examination.

In order to obtain a complete characterisation of the rock mass, it was necessary to evaluate the mass parameters, after having determined me parameters

referring to the test scale, to insert into the modelling.

At this point, it was possible to approach the design stage of the work, imposing the stability analysis for different mining levels.

Table 1. Main mechanical properties of rock materials: in columns 6 and 7 C and cp are the shear strength parameters; in columns 8 and 9 c and ip are the discontinuity parameters.

Rock type	σc [MPa]	E [Gpa]	ν [-]	σt [MPa]	C [MPa]	φ [°]	c [MPa]	φ [°]
D	46	43	0.31	3.6	15	37	0.77	38
MA	64	59	0.38	4.0	10.0	47	0.54	40
MSV	94	66	0.22	5.2	14.5	47	2.15	32
MCV	61	57	0.40	4.5	8.7	48	0.08	40

3 DESIGN GUIDELINES

The excavation of ornamental carbonate rock is today carried out almost exclusively with mechanical cutting techniques. Diamond wire saws and chain saws are used above all; they have reached such high levels of performance that it is actually disadvantageous not to use them in an efficient production process.

The importance of using such equipment during mining is so great that it conditions the geometry of the underground chambers. In other words, efforts are made to "adapt" the geometry of the chamber for optimal performance of the chain cutters in order to optimise the yield of the cutters, which, during the production stage, can affect the costs of extraction remarkably. In the case under examination, it was considered appropriate to visualise chamber and diaphragm mining on a single level, which could then be converted into a classical room and pillar scheme, with the width of the room being equal to that of the diaphragm (9 m), and a height of 13.5 m. This precautionary choice was adopted to compensate for a certain margin of uncertainty in the results obtained from the design, which is inevitable in work of this kind. Once the mining has been started, the objective is to integrate the classification of the rock mass with new data so as to be able to take best advantage of the whole of the useful deposit.

The geometry of the underground rooms is also naturally influenced by the static state of the work one wishes to perform. In rock masses similar to that under study, the geomechanical behaviour would allow the continuation of mining in chambers similar to those just described on two superimposed levels. In this case, however, it would be necessary to precisely respect the geometry imposed at the upper level in order to avoid dangerous stresses outside the axis. This could influence the yield of the blocks, this being of great importance as this is a commercial activity which tries to obtain the greatest possible profit.

The planning of a work of mis kind can be approached in different ways: analytical methods based on theoretical simplifications are easy to apply, but supply results that, in this case, do not reach a good level of reliability; graphical methods are still quite simple to apply, but, like the previous methods, do not satisfy some indispensable planning criteria for a work similar to that dealt with here; numerical methods, though articulated and complex in their calculation procedures, can supply more precise values with a good margin of reliability. Numerical methods can be distinguished according to how one considers the rock mass. Finite element calculation codes (FEM) and finite difference codes (FDM) consider the rock body as a continuous body. Another procedure, expressed by distinct elements (DEM), considers the rock mass as a discontinuous body.

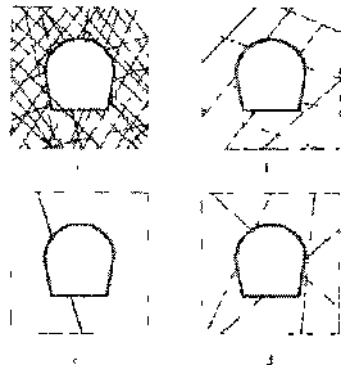

Figure 1 Geometrical schemes for modelling a) Pseudo-continuum using continuum approach (FEM, FDM); b) discontinuum approach (DEM, wedge analysis), c) continuum approach (FEM, BEM), d) intermediate case, continuum with few joints (DEM, stereograms)

From Figure 1 it is evident how difficult it is to identify the model that faithfully reproduces the behaviour of the rock mass in question. For this reason, the analysis was carried out using two different models.

The first one was that of finite differences FDM (FLAC code - Itasca Consulting Group). This model consists of 35070 quadrilateral elements with dimensions of 0.5 x 0.5 m^2 İn its central part, where the mining chambers were simulated. This model allows one to analyse the rock mass around the chamber for a total width of 225 m and a height of 140 m, in such a way as to position the artificial borders of the model so that the stress and strain disturbance produced by the presence of the

Chambers is not felt (that is, at a distance in which the equitensional lines in the rock appear horizontal in correspondence to the artificial borders of the model). The upper border of the model is real and corresponds to the surface of the soil.

In order to optimise the process, the dimensions of the elements were made to increase as they became distant from the chamber, in relation to the lowering of the stress gradient, so as to limit the total number of elements and to reduce the computational burden.

Three contiguous 9-m-wide and 13.5-m-high rooms are visualised, and excavated on one single level.

At the same time, a second model of the distinct elements DEM (UDEC code - Itasca Consulting Group) was set up.

The second model takes an area 130 m wide with a depth of 90 m from ground level into consideration. This is necessary to get around tbe border effects, which can reflect on the conditions of the chamber under examination. The rock mass is divided into three areas, with different jointing levels, in order to better represent reality and avoid excessive calculation volumes that would need to be processed, which could lead to overflow errors. The first area, the most jointed, starts from the ground level and descends to a depth of 12 m; the second, subject to the excavation of the chamber, starts from a depth of 12 m and reaches a depth of 65 m; the last starts from a depth of 65 m and continues to a depth of 90 m.

The discontinuities inserted into the model are: Ki = 292/90 and K_2 « 255/64, while the attitude remains constant, as anticipated, and the values of the length of the discontinuity and spacing vary; in particular, both increase when passing from the surface area to a depth.

The attitude data refer to the central values of the frequency distribution; both the length and the spacing refer to the in-situ geostructural analysis. The mechanical characteristics of the rock, also identified from İn-situ and laboratory geomechanical analysis, are applied to all the model. However, the geomechanical parameters of the discontinuity change according to the area. The boundary conditions foresee a horizontal pressure that varies according to the depth, from the left side of the model, the other is blocked by a series of horizontal constraints (simple supports). Another series of simple vertical supports is placed on the lower border of the model.

When the results of the models are compared, the optimal correspondence between the two models of the stress analysis is first shown; however, as far as the deformations are concerned, the distinct element model has resulted in being more sensitive to the presence of the blocks, which are relatively small in comparison to the size of the chamber, that is, it influenced the result in correspondence to the walls of the chamber.

At this point, having positively evaluated the compatibility of the stress state induced by the excavation with the resistance of the rock, it was necessary to evaluate the stability of the portions of rock isolated by the mining operations on the roof and walls of future chambers. In practice, an analysis was performed according to the K-Block theory developed by Goodman and Shi (1985).

This analysis, performed with the attitude data of the discontinuities found on the external walls, only provides results indicative of the reality. This analysis showed in particular the high probability of the formation of blocks, both on the walls and on the roof, that can in some cases be considered unstable, both due to the geomechanical characteristics and the attitude of the discontinuities. In this case, it is necessary to intervene with local stabilising, that is, bolting of sufficient length to pass the destressing area with the anchorage.

4 OPERATIVE PROCEDURES

Underground mining occurs in two distinct stages: the opening, with the excavation and enlargement of the tunnel, and lowering, with the mining of the chambers through gradual lowering.

The extraction techniques used in the second stage, that İs, from the development at the top to the squaring of the blocks, are the same as those used for open pit mining; on the other hand, the excavation of top tunnels anticipates specific techniques.

The advancement operations can be performed with two different cutting configurations; one with only the use of a chain saw, as in the classical type of tunnel, while in the other this type of machine is used together with a diamond wire cutter.

Vertical and horizontal cuts are performed with the first type of technique in order to isolate a portion of the rock that corresponds to the chamber face. The cut at the back is performed using hydraulic cushions which, through vertical direction pressure, break the rock by bending.

With the second technique, a smaller portion of the rock is detached using a hydraulic jack and then the cut is performed behind using a four-pulley return frame. A noteworthy advantage of this method is the ability to control the direction of the cut.

At present, specific frames have appeared İn some sites, with chain cutting machines mounted on self-propelled tracked vehicles.

This could simplify the overall cutting operations, leading to a time reduction of 20% with a saving of manpower of at least 30%. This innovation, which is potentially important in underg-ound marble excavations, could thus improve feasibility in cases like the one under examination.

In both cases, the excavation anticipates the removal of a wedge of variable dimensions that are dictated both by the characteristics of the machine and by the space required to carry out subsequent work correctly.

5 NUMERICAL MODELLING

The numerical modelling led to the detailed evaluation of the stress state induced in the rock following excavation operations. The creation of the anticipated mining rooms was simulated in stages. Two different hypotheses were formulated concerning the geometric shape of the rooms: first rooms with dimensions of 10.5 m in height and 9 m in width on two levels (case 1), then rooms with dimensions of 13.5 m in height and 9 m in width on one single level (case 2).

The stresses calculated in the pillars and in the horizontal beam are of particular interest. These are necessary for evaluating the project thicknesses of these natural support elements and for suggesting the level and modality of any possible partial recuperation of the diaphragms in a second successive stage.

The vertical stresses in the rock at the end of construction of the six chambers for case 1 are shown in Figure 4. It should be noted how the roof of the lower chambers is subjected to traction stresses in the vertical direction and that these involve almost the entire thickness of the beam (6 m). From Figure 4 it is also possible to see a stress state inside the lower pillars that is slightly higher than that which develops in the higher pillars. The maximum values, however, do not exceed 2.5 MPa. The calculation allows one to show how the horizontal stresses in the pillars do not exceed 0.25 MPa and a localised presence of horizontal traction stresses is registered in the higher pillars at half of the borders. Horizontal stresses are noted in the beam that are always higher than 1.5 MPa, while in the central part they are always higher than 1.75 MPa. They never, however, exceed the limit of 1.85 MPa.

A more detailed examination of the stress state in the pillars can be made from Figure 5, which refers to the pillars of the column on the left.

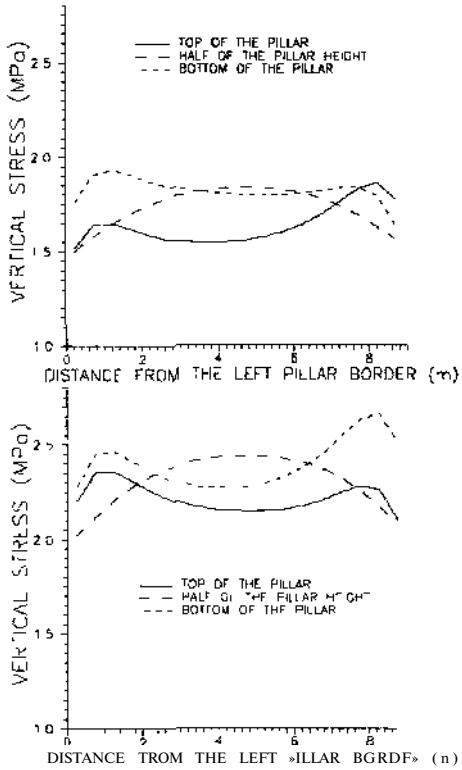

Figure 3. Vertical stresses in the upper left pillar (upper) and lower left pillar (lower) (case I).

In Figure 3 it is possible to see how in the upper part and in the lower part the vertical stress state of the pillar suffers the effect of the corner, and therefore the maximum values are concentrated towards the edges. In the central part, the maximum values are instead in the centre of the pillar, where the lateral confinement is greater. It is possible to determine an increase in the mean vertical stresses of about 0.6 MPa passing from the higher to the lower pillars. From the calculation, a certain symmetry is furthermore evident between the stress conditions in the pillars on the left and those of the right of the hypothesised mining scheme.

The studied mining scheme is adequate for the stress state that is present and for the geomechanical characteristics of the rock mass. The stresses induced in the pillars and in the horizontal pillars are, in the configuration of case 1, very much lower than the maximum permitted values. The chambers turn out to be stable on a large scale, except for the necessity of intervening with precise reinforcement elements to eliminate any possible danger of movement of unstable rock blocks. Given the low values of the vertical stresses induced İn the diaphragms, it has been possible to examine the possibility of dividing them, attacking tiansversally, so as to create chamber and pillar mining on various levels.

The results for case 2, referring to the situation that occurs at the end of the excavation of the three chambers, are shown in Figure 3.

The vertical stress state in the pillars does not change substantially in comparison to the previous scheme. The width of the diaphragm increases slightly (from 3.23 to 4.15), remaining, however, at very low values.

As far as the horizontal stresses are concerned, a horizontal strip of limited height can be seen at the middle of the pillar (3.7 m at the borders and 50 cm at the centre) that is subject to traction stresses. This strip was not present in the scheme that had chambers 10.5 m in height (case 1).
The mean vertical stress inside the pillar is, in this case, a little lower than 2 MPa.

From the results of the numerical calculation obtained for the two different hypothesised geometrical configurations, the following can be stated:

- the stresses induced at the borders of the mining chambers and inside the pillars and the beam are compatible with the resistance characteristics of the rock mass, so much so that no areas were revealed in which the elastic limit was exceeded (plastic areas);
- even heights of the chambers of 13.5 m can be considered permissible;
- there are limited portions of the rock that show traction stresses in die vertical direction, horizontal direction or in both directions, which require careful observation of the conditions of the rock mass in order to verify the possibility of unstable blocks breaking off;
- the lateral thrust coefficient KB results in influencing the distribution of the stresses inside the mining voids;
- it is possible to consider a second mining stage that can attack the diaphragms, thus increasing the recuperation coefficient of the deposit; an initial quick analysis of the stress state of the diaphragms led to the belief that a further 50% recuperation of the diaphragm would be possible, which would mean leaving 9 m x 9 m pillars in situ;
- the displacements relative to the borders of the mining voids are very limited, being less than millimetric.

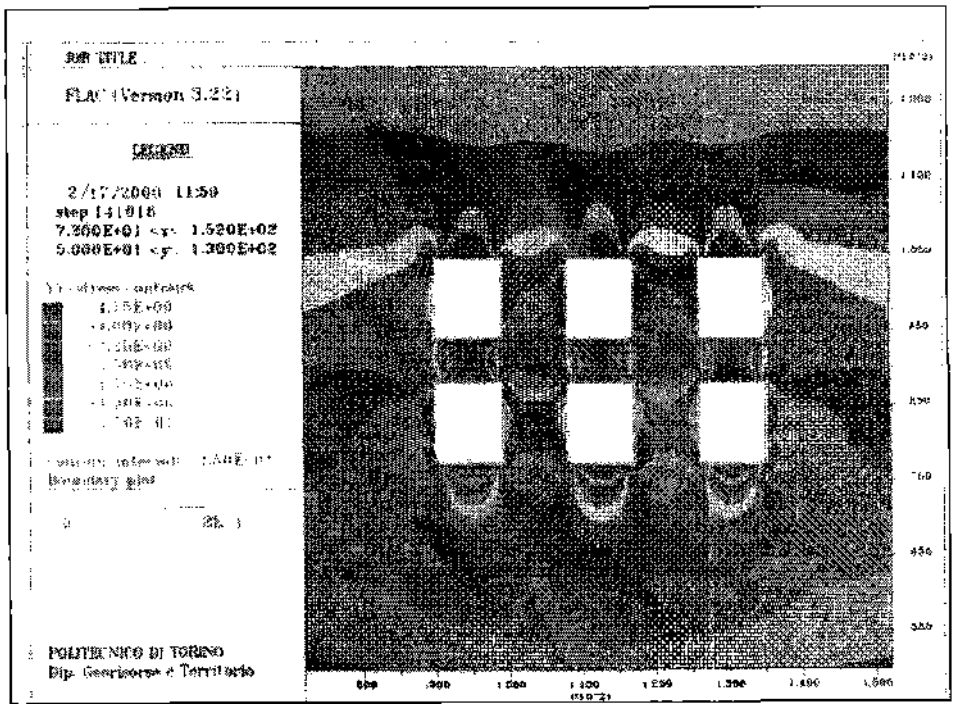

Figure 4. Vertical stresses in **the** numerical **model at the end** of **the** excavation of the six mining chambers (case I).

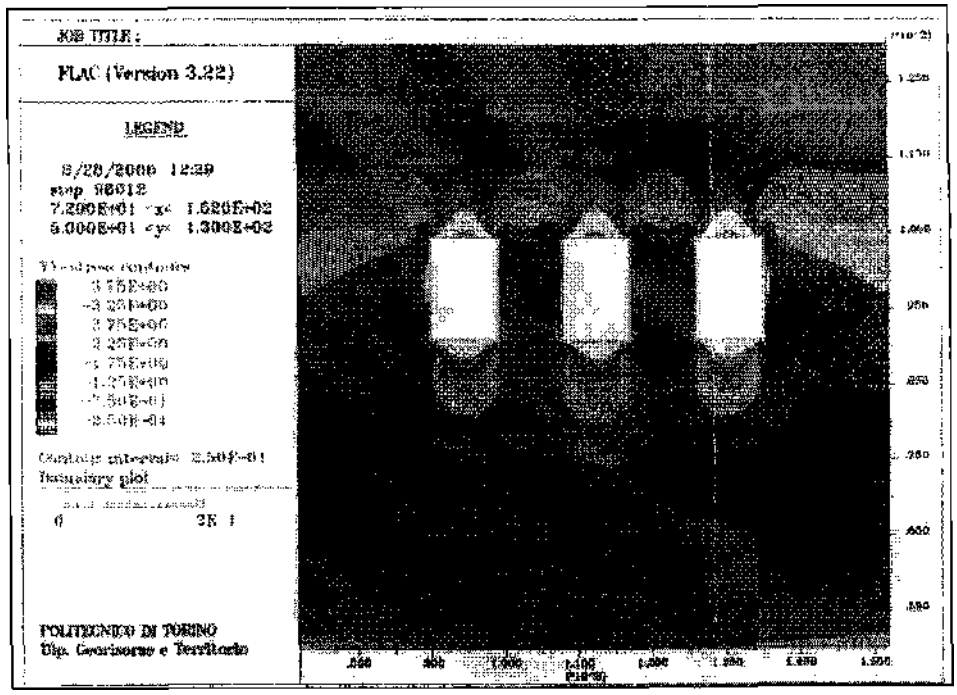

Figure 5. **Vertical stresses** in **the numerical model** at **the end** of excavation of **the** three **mining chambers** (case 2).

6 MONITORING

There are basically three aims of monitoring underground excavations for ornamental stone quarries: a) validation of die hypothesis of die numerical modelling by means of in-situ measurements (back analysis); b) control of the behaviour of natural and artificial structures; and c) updating of the stress state and geostructural conditions.

The directly measured parameters are usually displacements, stresses and loads, whilst the use of indirect methods allows one to define the fracturing state of the rock or the related physical properties (mechanical wave velocity and other geophysical parameters).

The convergence measurements can be performed next to the portals and across transverse sections of the rooms, using long-base extensometers equipped with undeformable wire and Potentiometrie transducers. In the same way, crack meters with Potentiometrie transducers can measure the movements across die walls of the discontinuities. One or two monitoring sections can be quipped with rod extensometers, also passing dirough the entire pillar, eventually equipped with vibrating wire transducers.

Induced stress measurements in the pillars can be performed using flat jack equipment, but the measurement points must be repeated adequately because of die gradient of the stress near the corners.

Alternatively, some measures can adopt the surface overcoring technique with a large diameter of the overcoring, or the overcoring in the borehole with the doorstopper method.

7 CONCLUSIONS

An initial study concerning the technical and economic feasibility of underground mining of a marble rock mass has been developed in this work. The results of significant geomechanical and structural investigations and geognostic measurements, which can be further investigated, were already available for the studied case thanks to the presence of extensive functioning sites on the surface. This led to the field of hypotheses being cut down, so that operative proposals could be developed, both as far as any further investigations and the experimental starting-up of the tunnels are concerned. This stage is fundamental in compensating for the inherent difficulty of extrapolating reliable data relative to the parameters of the rock mass directly from the geomechanical classification, whose applicability seems to be problematic for rock masses of good to optimal quality.

Two different numerical models of the stress and strain analysis of the rock mass were set up for prediction of the development of the underground production sites. The first, based on the concept of "continuous equivalent", led to an evaluation of the static situation on a large scale, with particular attention being paid to the work conditions of the pillars in abandoned rock. The second, which was instead based on *the* distinct element method, was able to analyse the stability of the underground chambers in more detail, evaluating the behaviour of the potentially unstable rock blocks at the borders of the voids. These latter results were compared with those obtained from more traditional calculation approaches, which refer to the well consolidated "block theory" and "limit equilibrium theory".

The results that have been obtained, apart from guiding technical and operative choices in the development of the underground caverns, also supply an overall view of the static situation, in terms of both production and safety, and constitute operative support for planning and updating, even during the work process. Adequate monitoring and control programmes should allow timely decisions of an operative nature. In particular, given the small nature of the expected displacements, it was decided to cany out measurements of the stress state, even though they were limited to the edges of the mining voids. The continuous comparison, through back-analysis procedures, of the measured data and those obtained from the numerical calculation with the models that were set up, will allow an improvement İn me reliability of the results and make it possible to optimise the project through the increase of the recovery percentage of the rock mass.

ACKNOWLEDGEMENTS

The authors thank Cevalor (Pt) for the opportunity given to study the case. This paper has been financially supported by the MURST project

The authors have contributed equally to this work.

REFERENCES

Del Greco, O., Fornaro, M. and Oggeri, C. 1999 Underground dimension stone quarrying, rock mass structure and stability. *Proc. Int Symp on Mining Science and Technology,* Beijing, Balkema, pp.385-390.

Oggeri C. 2000. Design methods and monitoring in ornamental stone underground quarrying *Proc Int. Conf. GeoEng2000,* Melbourne.

17 International Mining Congress and Exhibition of Turkey- IMCET2001, ©2001, ISBN 975-395-417-4*

Mining and Technical Monitoring at Coal Mines

B.V.Vlasenko, V.P.Potapov & V.A.Fedorin
Institute of Coal and Coal Chemistry. Siberian Branch of Russian Academy of Sciences, Russia

ABSTRACT: The most important element of the physico-technical process of coal deposit mining processes is information about both physical processes in the rock mass (most of all, changes in gas-geomechanical, hydro-geological and ecological states) and mining processes in mines (technological, economic, social, etc.)- It is necessary to create a rather general geoinformation model of physico-technical processes because of the all-round character of the data, and the various methods of data collection, storage and analysis. The approach proposed in the building of a geoinformation system is rather general and allows the construction of various subsystems of mining monitoring on a combined methodical and program basis simple enough to unite them together.

V INTRODUCTION

The reorganization of the economy, transition to market practices and restructuring of the coal industry today require new methods of analysis for all processes in mine control. For appreciation of the dynamics of the changes in the coal industry, the reengineering questions of systems in mine control are gaining in importance. It is with the restoring of information, communication and engineering software of systems and processes that mining will change to modern control methods of technological mine systems. Decision making in this field must be preceded by analysis of data. The data should be regularly updated and should be varied to reflect the state of processes and systems of mining, both in individual mines and m regions as a whole. In these cases, systems of active monitoring of various information sources are being developed. They include modern models of mining data analysis with the capacity for conversion into maps, graphs, animation sequences, object-oriented databases, etc.

2 INFORMATION MODELS OF SYSTEMS OF MINE TECHNICAL MONITORING

For the last few years, there has been a quantitative and qualitative body of streams of information connected to the operation of various sorts of mining monitoring systems. This has resulted in the need to develop by their new paradigm in view of those changes, which today occur in mining computer science.

In the first stage of monitoring system development, for example, in the geomechanical system and monitoring of gas and dynamics in mines, most attention was given to technologies of information collection (sensors for determining changes in various parameters of physical and geomechanical conditions, controllers, transmission data lines, models of primary data processing). In the second phase, elementary databases were developed, models of which were not for the most part practically formalized in any way. This eventually resulted in various monitoring systems that were either simply disjointed or had a complex enough interface. As for methods of primary data processing, it should be noted that in connection with the large variety of methods of monitoring data processing, the construction of a common enough model could not be achieved, such as systems of cartridges DBMS Oracle, pcniiitting floppy change of algorithms of processing for concrete databases and collection of them into a uniform hardware-software complex.

The changes that have taken place over the last few years m the field of information technology and the geocomputer sciences in particular have shown that the presence of huge streams of geoinformation force us today to see it as one of the major factors necessary for solvmg problems in mining and handling by geosystems. Unfortunately, that which is known to be true all over the world, that he who controls information controls the world, is only today receiving recognition in the world of mining.

The huge quantity of geoinformation today appears to be simply lost and, practically, not restored. This is because in the creation of various sorts of automized systems, the conceptual model was incorrectly selected, and information was structured and transformed according to this into appropriate databases. In a number of cases, even with the presence of conceptual data models, they were either lost, or remained without appropriate support, so that they eventually disappeared from the information subspace.

We propose an approach to the creation of modern information models of geomechanical monitoring based on the change in the common scheme of information processing, as shown in Table 1. The table shows that the appearance of new methods of processing and data models is characteristic for modem monitoring. Such methods are:

- intellectual data processing (extraction of knowledge - data mining);
- models of data warehouses oriented with OLAP technology.

Instead of traditional imitative and network models, the transition to object-oriented models proposed is more universal from the point of view of the creation of models of these or other geomechanical and geotechnological processes.

A very general view of the scheme of geotechnical monitoring is represented in Figure 1.

Table I. Methods and models of monitoring systems.

CLASSICAL MONITORING	MODERN MONITORING
Statistical analysis of the data	Methods of intellectual data processing, Datamining
The numerical methods (MFE, BBH and etc.)	The numerical methods (MFE, BIE and etc.)
Analytical Methods	Model of data warehouse
Imitation and network models	Object-oriented models (UML.CASE)
Making decision	Decision making an risk estimation

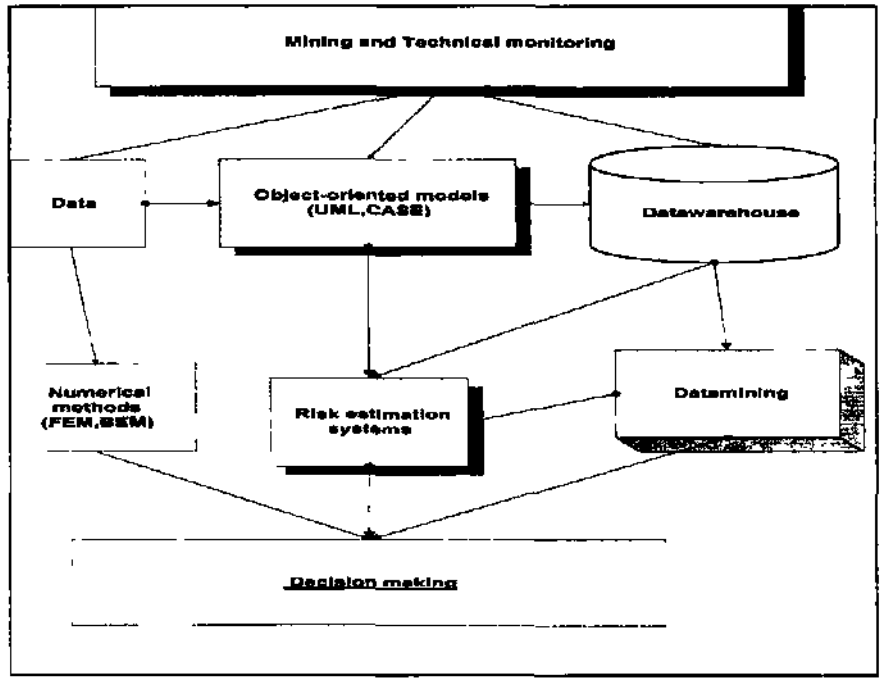

Figure I. New schema of the mining and technical monitoring.

%

3 TECHNOLOGICAL MONITORING OF COAL-MINES IN KUZBASS

Technological monitoring is carried out in the Institute of Coal and Coal Chemistry. It contains the basic work indicators of mechanized longwalls in the coal mines of Kuzbass. Computing facilities of database generation and of processing incoming information by methods of classification are developed in order to determine the tendency of the change in the mine technological structure of coal mines (^»efiOpHH, 2000). About 120 Kuzbass longwalls are processed İn terms of mme technological, technical and economic indicators (HJieBCKHfi, OCfiOpHH, 1998).

Each longwall is characterized by:

- a set of X factors-determinants describing the mine geological conditions of longwall work (angle of dip and seam thickness, thickness of main roof and immediate one, bottom thickness, coal hardness, and enclosing rock hardness, seam gas content, water intrusion of seam and constructive parameters of a panel, specific volume of driving and roadway maintenance of a development, main workings and panel);
- a set of Y function parameters ("variables of behaviour"), reflecting indicators of work (average monthly output of a longwall and underground output per man-shift, cost, specifications of longwall sets, transport ways, etc.).

It has been stated (<É>e/topHH, 2000) that the evolution of a mine's technological structure towards increasing the efficiency of longwall work can be considered as follows:

TM—M»M—• MP-+-NMD-*MS

where TM stands for traditional mines without division into panels. Traditional mines are widespread in the Russian coal industry. PM stands for panel mines or mines with division of the mining area into panels. A typical representative of this type is the great Raspadskaya mine in Kuzbass. MP stands for mines-panels. A representative of this type is the Zyryanovnskaya mine in Kuzbass. MMD stands for modular mine districts, with one highly productive longwall.

Each stage of the development of the mining technological mine structure is characterized by a decrease in the number of structural units and simplification. Thus, in mines with one stope, in comparison with traditional mines, the number of units of underground structure is considerably reduced (from 8 to 3). The quantitative estimation of the complexity of the mining-technological mine structure is carried out by a metric of entropy Ho, which characterises the complexity of the transport network of mine workings in the mine (see Figure 2). The quantitative estimation Ho of the structural complexity of the network of mine workings is reduced from 3 to 0.5. The more metric Ho, the more complex is the structure of the mine.

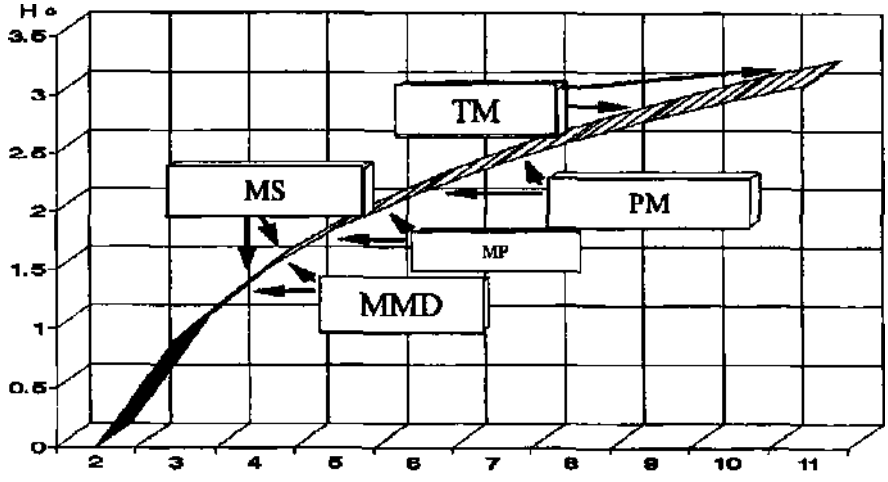

Figure 2 A summary quantitative estimation of entropy H_0, depending on number of units of mining-technological structure of coal mines.

With technical progress, the evolution of the mining-technological mine structure provides conditions for intensive engineering operations, and thus, is a large factor in the efficiency of coal mining underground.

Investigations (OeAOptm, 2000) show that the economic metrics of coal mines at the fiat bedding of seams immediately depend on the productivity of the mechanized slope, which, in turn, depends, except for active factors (technological level of equipment, professional preparation of staff, etc.), on the type and parameters of the mining technological structure of coal enterprises.

For years, districts with autonomous coal winding to the surface were mined in the Kuzbass collieries. Nowadays, mine districts are in the mines: Raspadskaya (panel 5a), Vahrushev (West Taldinsky), Alarda, Kyrgaiskaya, etc. Most of the mining districts are privately owned and highly productive (juieBCKirif, <&e,nopHH ,1998).

The study of work in mines with only one highly productive longwall led to the creation of modular mine technological structure for mines being designed and reconstructed in Kuzbass. Mining systems (MS) appeared not so long ago and at present they are employed in the USA, Australia and South Africa. Since 1995, there have been technical and economic justifications for investment in building MSs in the opening of new coal deposits in eastern Kuzbass (Russia).

The mine technological structure of MSs presents a set of MMDs together with a corridor of communication İn an integrated technological system on the surface. The Kotinskaya mine, having been designed with a modular mine technological structure in terms of main indicators, is classified as a mine with a world-class technical and economic level.

Modular systems of mining in Kuzbass are provided with sufficient coal reserves to a depth of 300 m with an angle of dip of up to 18 degrees. An electronic directory of geological districts has been made. It includes districts with more favourable mine geological conditions in terms of seam bedding, thickness and structure so that highly productive mining systems and new technological schemes can be used, as patented in the Russian Federation. It has been determined that there are 150 geological districts with deposits of more than 3 billion tons.

In the generation process of the electronic directory, two schemes of program realization were developed:

- local - on the basis of hypertext technologies;
- distributed - on the basis of the intranet of the Institute of Coal and Coal Chemistry.

The division of the directory is performed by means of a standard server method and allows the generation of complex forms of inquiry through tables specially developed for these purposes, providing a connection with the database of the directory.

In the working process, various DBMSs were investigated, such as MS ACCESS through the ODBC interface and MS SQL in the Windows NT server environment. The Linux system with DBMS Postgres was chosen because of its high database access speed. When tested as to its capability, it displayed speed of access to the directory's elements 4-6 faster than the Microsoft environment.

The electronic directory is designed not only for workers in the coal industry but also for businessmen intending to invest in coal mining in Kuzbass by forming small (modular) highly productive mines (Internet: www.Kemsc.ru in the interface of the Kemerovo Research Centre of the Siberian Branch of me Russian Academy of Sciences).

4 GEOMECHANICAL MONITORING SYSTEM

The rock mass of coal deposits represents a complex natural environment based on a solid component, saturated by gas and liquid, containing inclusions. Research into geomechanicai processes in rock masses as a result of technological factors (mining of mineral resources) is best achieved by monitoring.

The information geomechanicai monitoring system (Gm MS), which is used in computerized mine planning and mining operations control, is a technical means of geomechanicai monitoring (GmM). It is a complex system of regulated observations, estimation and prediction of changes in the geomechanicai (Gm) state of the rock mass and workings during underground mining of coal deposits. Geomechanicai monitoring at coal mines and the automated system perform data collection, analysis and calculations of geomechanicai (Gm) conditions in the panel during planning, development and execution of mining operations for ensuring the geotechnical stability of underground mining.

These concepts were formulated and published at the end of the 1980s (Bnacemco, 1990), obtained concrete appendices for estimation tasks of rock mass Gm - state İn me locality of coal faces with mechanized support setting (BUTIHHCKH H *op.,* 1991) and were generalized İn the work (Bjiacemco, 1993).

Formulated determinations, composition and structure of monitoring and monitoring systems have been developed (BnaceHxo H up., 1994; Vlasenko et al., 1994), extended to changes in rock mass gas geomechanicai state (GGm) and published (Vlasenko et al., 1993; Gritsko, Vlasenko & Fedorin, 1995; Gritsko et al., 1995), including the materials of the Second and Third International Symposiums on Mine Mechanization and Automation (Vlasenko etal., 1993; Gritsko et al., 1995).

5 CONCLUSION

1. An approach to building a geoinformation .ystem for mine engineering monitoring was developed. Some system elements were realized by a complex program of technological and geomechanical monitoring.

2. Mine technological monitoring of main indicators of mechanized longwall work at coal mines showed that modular mine technological structures are more effective in the mining of flat coal seams.

3. The rational region of geological resources was found to be modular mine districts in the coal deposits of Kuzbass. A database (150 geological districts) and electronic directory of technological solutions for modular structures of mine district opening and development were created.

REFERENCES

(iritsko, Ü.I.. Vlasenko, B. V.& Fedorin.V.A. 1995. Prediction of gas-geomechanic situation of coal gas deposit dining underground mining in panel. *Proceedings of the Fourth International Symposium on Mine Planning and Equipment Selection, 31.10. -03.11.1995'.* 71-76. Calgary, Canada.

Gritsko.G.I., Vlascnko3V., Polevshikov.CJ. & Presler, V.T.I995. Computer control and prediction of gas-geomechanic situation during monitoring at coal mines. *Proc. of the 3-rd International Symposium on Mine Mechanization and Automation. 12-14.06.1995:* Vol. I: 4.1-4.12. Golden, USA.

Vlasenko,B.V, Kozlov.V.I, Risovcr.V.N, Nekrasov, V.V. & Magdytch, V.J. 1994. Geomechanic Monitoring System for Coal Mines - A Means of Providing Efficiency and Safety of Mining. *Proceeding of the 3-rd Internationalen Mine planning and equipment selectiort, 10-20.10.1994.* 823-828.

EiuHHCKH A.,BjiacefDco E.B.XPHIIKO IMf, K>HCBH>I CT., Hepooiiui A. 1991. reoMexamreecKHft MOHHTOPHHT O'IHCTHUX MexamnnpoBaHHux 3a6oea npn oTpafonce yrojibtiux iwacTOB (Geomechanic monitoring of mechanized longwalls during coal seams writing) *UnauKomemuHvcKue npoôneMbt pcapaöomxu naaeintux in-KonaeMbtx (5):* 94 - 101. HOBOCWOHpCK: Hayxa, CO.

BjiaceHKo B.B. 1990. PeoMexajnnecKidt MOHHTOPHHT yrOiibHbix maxT Kyioacca (Geomechanic monitoring of coal mines in Kuzbass). *HanpXKennoe cocmonuue Miiccusoa <'opHux nopod u ynpasnenue êopHtiM ùtmettueM. IX KontpepeinfuH noniexanuKe zopuux nopod. 3-5-10.1989:* 170-178. Emmêle.

ßjiaceHKO. E.B. 1993. PajpaßoTKa MCTOAOB npornOTHpoBaMH» nposaneHHfi ropHoro aasaem« *ma* reOMexanmecKoro MoiiHTopuiira Ha yrojmaix utaXTax (Working out of predicted methods of rock pressure manifestation for geomechanic monitoring at coal mines). *Aemope<pepom Ouccepmaifuu na coucnanue yienoü cmenenu donmopa tnexiiuieCKux uayie.* KeMeposo: HY CO PAH.

BjiaceHKO B.B.. KOIIIOB B.H., PHCosep B.H.. IUHK B.M. 1994. TenneHUH» coiaasvw reoMcxaHiwccKoro Monnrapwnra ua tiiaxTax H pa3pa6oTxa cpejicTB aBTOMaTmaiuut KOHTpoJia ^^eKTHBHOCTH ynpaBJiemw ropHtiM aamjieHncM (Tendency of geomechanic monitoring engineering in coal mines and automation facility design for effective rock pressure control). *16-btü BceMupnuü sopnuù nompecc - Cadnut'94. 'Topuaa npoMtaumennocmh »a nopoie XXI aeica". 12-16. 08. 1994. TOM 5. flpo&ieMt* MCXOHUKUeop-HUX nopod: ffomaà I-30, 265-274.* CoıptuL Eojirapiu.

rioTanoB, B.n. 1999. MaTeManpiecKoe B itHipopMauHOHRoe MoaompoBaHHe reocHcreM yrojibHbix npejuipHimfft. (Mathematical and information simulation of geosystems of coal factories), KemepoBo, Hm-so CO PAH, 178 c.

floranoa, B.n. 1999. Paapaoonca MareManmecKHx H KHtpopManHOBHUx Moaejieti Ha OCHOBC pBCnpeaejiemrofi *BU-*•wcJnrrcjibHofi cpeou ana aBrouaTmaOHH ttccjieaaBatuin reocHCTeM ropnoro npomeoflCTBa. (To devised the mathematical and information models on the basis of distributed computing environment for automation of studies of geosystems). *Aemopeipepam duccepmayuu* NO *coucKOHue ynenoü cmenenu donmopa mexnuwecKUx nayx* KewepoBo: HW CO PAH. 42c.

OejiopHR, B.A. 2000. Pa3paöOTKa MOayntHHX ropHorexHojioniMecKHX crpynrryp BCKPUTHH H JIOATOTOBKH njaxrtibix nonefi Kyraensoro oacceftna (Mining of modular mining and technological structures of opening and preparation of Kuznetsk basin mine fields. *Aentapeipepam duccepmauitu na caucKanue yvenoä cmenenu doxmopa mexnutecKux Hoyit.* KewepoBo: HW CO PAH.

OeztopHH B.A., TIoTatiOB B.n. 1999. 3jieiapOHHtifi cnpaflo'i-HHK reonorHHecKHX yqacTKOB ans BUcoKos^etrmBHoK flo6uiK janacoB yrjis MOjiryjiöttHMH CHcreMaMH paipaSoncH B Ky-j6acce (Electronic directory of geological districts for highly effective coal mining with modular systems of mining in Kuzbass) *Tpydbt naymio-npaKmutecKOù Kond>epeıtuuu TeomexnoJiowu na pyßexce XXleeKa":* 80-83. HoBOCHÖMpCK: HT/l CO PAH.

Äneacratft B.p,., QeaopHK B.A. 1998. Knaccw^HKatisu! H KOjimecTHeHHax ouetnea paJBirrmi ropHO-TexHOJiorniecKoö crpyicTypbl yrojitHMX uiaxr (Classification and quantitative estimation of development of mine technological structure of coal mines) *CoBepiuencmaoeanue mexnowsuveacux npoifeccoe npu paspaGonixe MeçmopoJtCdenuù nojiejHbix ucxonaeMbix: CôopHux naytHbix mpydoe (13)* • 3-17. KeMepoBo.

17* International Mining Congress and Exhibition of Turkey- IMCET2001, ©2001, ISBN 975-395-417-4

Impact of Blast Fragmentation on Truck Shovel Fleet Performance

M.Doktan
Julius Kruttschnitt Mineral Research Centre, The University of Queensland. Brisbane, Qld, Australia

ABSTRACT: This paper presents an outline of the work conducted to date at the Julius Kruttschnitt Mineral Research Center (JKMRC), Brisbane, Australia on the effect of blast fragmentation on truck shovel fleet performance. The project is an important component of the ongoing " Mine To Mill " project which looks at the optimisation of downstream processes after blasting. The results of numerical modelling studies and site work are presented.

I INTRODUCTION

"Mine to Mill" is a comprehensive project initiated and developed at the Julius Krutschnitt Mineral Research Center of the University of Queensland, Brisbane, Australia. The project aims to optimise down stream processes in relation to blast fragmenattion. One of trie important component of the project is to determine the impact of blast fragmentation on truck shovel fleet performance. This paper summarises the work done to date on this issue.

In order to achieve the project objectives three large scale field trials were conducted. Three different blast designs were tested in the same rock domain. Performance of truck shovel fleet was monitored after each blast. The key performance indicators of the truck shovel performance were assessed in the light of fragmentation achieved.

2 DISPATCH DATA

Raw dispatch data were supplied by the sponsor mine site. The data included truck arrival times to the shovel and primary crusher, as well as the start and end of loading times over the period of testing. The data were sorted and analysed for individual loading times, full and empty return times and waiting times. Only the trucks with the Cat Weightometers installed have been assigned to the nominated shovel.

Breakdown of the dispatch data of the October trial is shown İn Figure 1.

Empty haul (10.9 minutes), full haul (11.5 minutes) and dump time (7 minutes) take the biggest proportion of time.

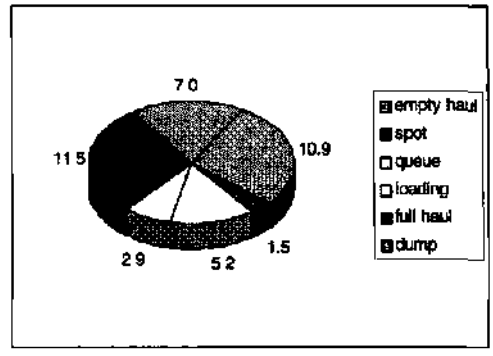

Figure 1 Break down of average cycle time in minutes (Dispatch records over 98 cycles, October 2000 data).

3 LOADING PERFORMANCE MEASUREMENTS

The individual dig times for each pass were measured from the recorded video tapes of the operation. The measured dig time distribution is shown in Figure 2. The average dig time is 12.2 seconds with a standard deviation of 1.75 seconds. Measured values ranged from 7.6 to 21 seconds. The May trial value was 18.8 seconds. This represents a 35 % improvement over the May trial average. The difference is statistically significant at 95 % confidence level.

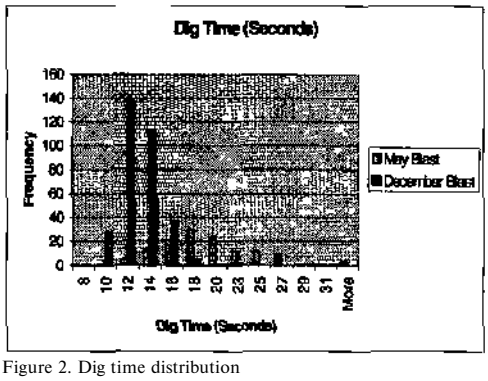

Figure 2. Dig time distribution

Video count of the loading operation in the December trial shows that 40 % of the total passes were 5 pass, the rest being 6 pass loading (total of 61 passes recorded). However, m the May trial some 77 % of loading passes were 5 pass (total of 75 passes).

Average individual truck loading time in December trials was 2:39 minutes with a standard deviation of 0:33 seconds. The May trial vlaue was 3:24 minutes with a standard deviation of 0:31 seconds. This represents 22% improvement over the May trial loading time.

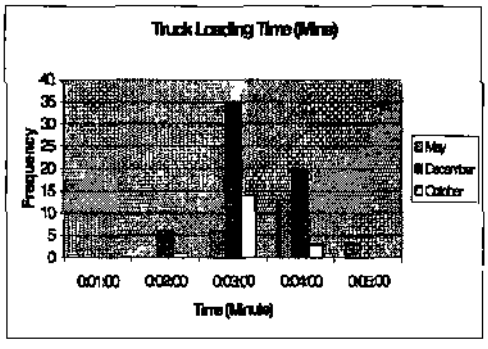

Figure 3 Loading time distribution.

The mean payload in the December trials was 192 tonne with a standard deviation of 20 tonne (Figure 4). This is only marginally greater than the May value of 186 tonne with a SD of 21 tonne. The increase in the average truck payload (approximately %3) is not statistically significant at 95 % confidence levels.

The average loading productivity (measured) is 4,213 tonne/hr with a standard deviation of 626 tonne/hr. This represents a 23 % improvement compared to the May trial result of 3,261 tonne/hr (Figure 5).

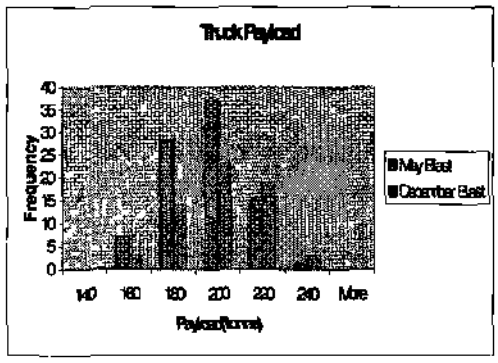

Figure 4 Payload distribution

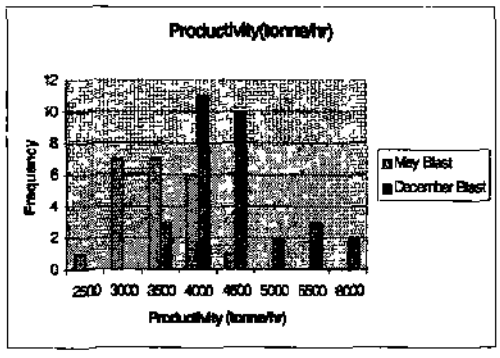

Figure 5 Loading productivity distribution.

A T-test was conducted to determine if the difference in December and May productivities is significant. The results clearly show that the difference between the May and December mean productivity is statistically significant at 95 % confidence level.

4 LOAD AND HAUL SIMULATIONS

Load and haul simulations have been performed to understand the impact of various mining parameters İn the economics of the operation at the trial mine. As was the case in this study, the Dispatch was reporting abnormally high empty return times. This was discovered when the results of haulage simulations were compared with the Dispatch values.

Simulations are carried out using an in-house developed load and haul simulator. The simulator İs an Excel based workbook with a small database of commonly used mining equipment. There are three major components of the simulator:

- Haulage;
- Loading;
- Costing.

Haulage is simulated using the haulroad and truck fleet characteristics. Each segment of the haulroad characterised by length, gradient, rolling resistance and speed restrictions are entered to the spreadsheet. In the loaded segments the simulator assumes that trucks are nominally loaded to their gross vehicle weights. The maximum acceleration is assumed to be 4 km/hr/s. Haulage simulations produce outputs such as speed, distance curves along the profile and times taken to complete each segment and the total haulage time. These outputs are then used in the loading spreadsheet to determine the loading productivity. User defined costs and annual operating hours are used in the cost calculations to estimate the cost of loading and hauling per tonne of material from the face to the dumping point.

The haul profile based on updated information obtained during tfie site visit is shown in Figure 6. The profile features multiple uphill segments designed at 10% to reach the crusher level from the face area. There is a junction on the return route where trucks *must stop.* The rolling resistances will vary from location to location in the pit. The high traffic areas such as the loading face and crusher area have been assigned higher rolling resistances. The downhill segments have a maximum speed limit of 40 km/hr.

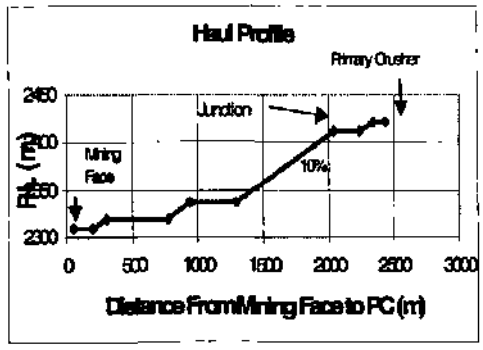

Figure 6. Haulage profile.

The average loaded haul time is estimated to be 593 seconds (from edited Dispatch records). The average empty return time is 270 seconds (from edited Dispatch data). These are in line with the measured values at the site during the experiments (Figure 7).

Assuming all other conditions are the same and no hold ups at the crusher, and with the improved fragmentation, the loading productivity increases from 3,262 tonne/hr to 4,213 tonne/hr. This gives a unit cost of $1.62 and $ 1.76 per bcm for the December and May trials respectively. This represents a saving of 9% or $0.14 per bcm. It must be pointed out that this analysis is based on the assumption that the dump time at the crusher is 30 seconds (ie no waiting time at the PC). If the waiting and dump time at the crusher is taken as 420 seconds (7 minutes) as is with the current set up, then the unit costs in May and December are $2.07per bcm and $2.21per bcm respectively. In this case only a saving of %7 ($0.14 per bcm) can be achieved with better fragmentation.

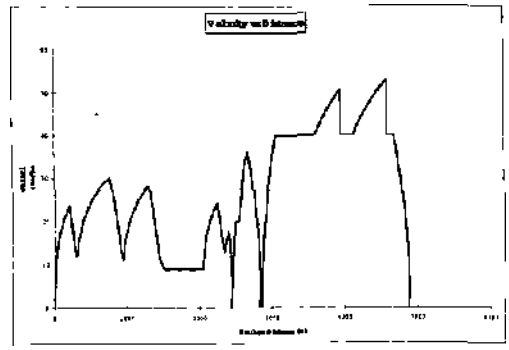
Figure 7. Speed/time graph.

The cost savings come from faster truck loading time and better fill factors only. Other cost savings such as less tear and wear of the equipment and others are not accounted for.

5 FRAGMENTATION AND FILL FACTORS

Blast fragmentation has two major impacts on loac ing and hauling performance of a truck shovel fleet:

- Digability (dig time)
- Bucket payload (void ratio and fill factor)

Bucket payload is a function of void ratio and fill factor. The fill factor is defined as the ratio between the nominal volumetric capacity and the volume of material in the bucket. It is predominantly an operational variable (loading strategy, operator experience and willingness to fill the bucket and the angle of repose of the material on top of bucket). Furthermore a high fill factor does not necessarily mean higher payload. If the material is not well fragmented and loosely packed inside the dipper with lots of voids between the rock fragments, the actual payload may be lower than in the case of a low fill factor but adequately fragmented and densely packed load.

The void ratio is more directly related to the fragmentation level and indicates how well the available room in the bucket is used. In other words, it is an index that indicates the effectiveness of the use of a given volume in relation to fragmentation. It is a direct indication of bulk solid density in the

bucket. If the bulk density of the material inside the bucket is increased with optimised fragmentation and packing men the payload İs increased. In general, as a first step to maximise the bulk density of the material in the bucket, it is advantageous to optimise the particle size distribution of the material involved.

Numerical models or physical models can be used to study the optimum size distribution for dense packing. The three dimensional particle flow code (PFC3D) package was successfully used in understanding the packing problem at the initial stages of the project. The results had been presented in die previous reports (May and October trial reports). Also a limited number of scale model experiments had been conducted to complement the PFC results (refer to the May Blast report). However the PFC models using spherical fragments may not represent the actual rocks faithfully as real materials are not perfectly spherical.

The linear-mixture packing model as developed and used in the powder technology area offers an alternative approach. The linear Mixture Packing Model as an algorithm was first proposed by Westman and Hugill (1930). Standish and Yu (1987) further enhanced die model algorithm to predict the porosity of particulate mixtures of multicomponent materials. The model is based on the analytical arguments of the packing structure of particles. Depending on the size ratio (small/large) involved, two packing mechanisms may be observed in random packing of particle mixtures:

- Filling mechanism (unmixing)
- Occupation mechanism (mixing)

Other the studies show that mere is a critical ratio of entrance, which is determined from simple geometrical considerations between the binary mixtures (Cumberland and Crawford, 1987). The above packing mechanisms have been evaluated on the basis of the following considerations. If the size ratio is smaller than the critical ratio of entrance, the packing of particles is formed by the filling mechanism. If the size ratio is larger than the critical ratio of entrance, the packing is then formed by occupation mechanism.

The payload model based on the linear mixture packing model has been developed as an VBA model. The model requires a number of input parameters including relative quantities of size fractions, effective size for each fraction and specific packing density of each fraction. The specific packing density values are especially important as it provides information on the geometrical characteristics of the bucket and material packing in the bucket. The model has been successfully used İn the estimate of void's ratio of mixtures especially for small diameter particulate media. The validation of the model needs to be done for large sized mixtures with controlled experiments.

Truck by truck size distributions characterised with the X50 and n are determined using the Split image analysis software. These are used in die Payload model to estimate void ratio for each dipper load. The model estimates are based on increasing initial specific packing density from 0.4 to 0.49.

The average dipper payload is estimated by dividing the truck payload by the number of respective loading passes. Each dipper load is then derated by an historical bucket fill factor supplied by the mine site (0.84). Then the void ratio is estimated by the nominal dipper capacity and the calculated dipper load. It is assumed that the dipper is full at each loading pass.

The model estimates and the measured void ratios are shown İn Figure 8. The first 30 data is related to the December trial and the last 10 points represent the data from the May trial.

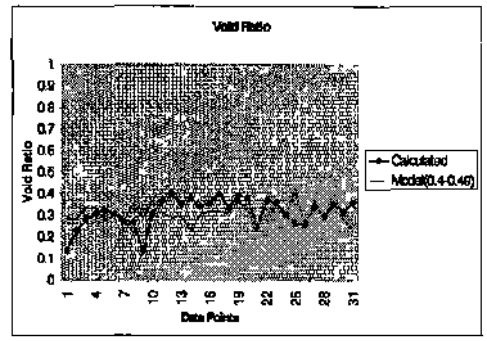

Figure 8. Void ratio and model estimates.

The variations in me measured void ratio are expected due to probable variations in the individual dipper payloads. Especially the last loading pass may not always have a full bucket load. The Payload model shows an increase in me void ratio based on the increased mean fragment size. This is in line with the previous PFC and scale model results.

The mean void ratio as estimated from the modelling studies for December trials was 0.30 with an SD of 0.035. Similarly the mean value for the May trials was 0-31 with an SD of 0.066 distribution.

Another important factor in the load haul performance in relation to fragmentation is the digability of the muckpile. The digability is simply defined here as the digging time of the loader. If the dig time is low, the muck pile is considered to have high digability, if the digging time is big then the muckpile is considered to have low digability.

The dig times as determined from the measurements done at the trial mine site have been correlated with the Rosin Rambler parameters X50 and n.

The best fit relationship (Figure 9) to the available data İs:

Dig Time = a-b*X50*Un where;
a=8.9942
b=-6.8706e-2
X50 = 50 % passing size
Un= Uniformity coeffient

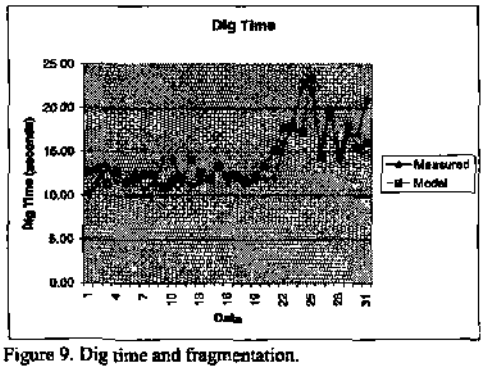

Figure 9. Dig time and fragmentation.

6 RESULTS

Due to better fragmentation, shovel dig times in the December trial were reduced by 35 % compared to the May trial from 18.8 seconds to 12.2 seconds. This is related to easy loading conditions with finer fragmentation. The number of 6 pass loading on the other hand has increased in proportion from 23 % to 60 %.

Despite the increase in the number of loading passes, the overall individual truck loading times have decreased by 22 % to 2:39 minutes in December from 3:24 minutes in May.

The loading productivity in December has increased by 22% compared to the May results from 3,261 to 4,213 tonne/br.

The increase in loading performance is a result of faster dig and swing times of the dipper and higher truck payload. This is a direct outcome of the finer fragmentation generated in the December blast.

Despite substantial improvement in' the loading performance, due to high waiting times associated with dumping at the primary crusher and time losses during haulage, this improvement may not be transferred fully into overall load and haul productivity. It is imperative that necessary upgrades of the primary crusher are made if the benefits of finer fragmentation is to be accomplished in the load and haul performance.

Cost comparison of loading and hauling has been done using the spreadsheet model on the basis of some cost assumptions. The results show that approximately a 9 % saving in loading and hauling costs {from $1.76 to $1.62 perbcm)is achievable if the haulage at the pit is optimised and also waiting time at the PC is eliminated. With the current waiting times at the crusher (420 seconds), the unit costs have decreased from $2.21 in May to $2.07 per bcm in December.

The Payload model is still under construction and validation. The model's principle is based on the Linear Mixing Model developed for fine particulate materials. However, there is a significant potential in the prediction of void ratio of mixed size rock materials.

REFERENCES

Cumberland, D.J., Crawford, R.J.,1987. The packing of particles, *1st Ed, Elsevier Science,* Amsterdam, The Netherlands.

Westman, A.E.R., and Hugill, H.R.J.,1930, *The Packing of particles,* J.Am. Ceram. Soc., 13,767

Yu, A.B., Standish, N., 1987, *Powder Technology,* 52,233

Internal Report, *Mine to Milt May 2000 trials progress report,* The JKMRC3risbane,Australia.

Internal Report, *Mine to Mill October 2000 trials progress report, The* JKMRC,Brisbane,Australia.

Internal Report, *Mine to Mill December 2000 trials progress report,* The JKMRC,Brisbane Australia.

1 7* International Mining Congress and Exhibition of Turkey- IMCET2001, © 2001, ISBN 975-395-417-4

Estimation of Current Condition of Undermined Rock Massif with Regard to Thickness of Mining

T.M.Yermekov, M.Zh.Bitimbayev
The Kunaev Institute of Mining, Almaty, Republic of Kazakhstan
R.B. Yun, M.Zh.Satov
Kazakhmys Corporation, Zhezkazgan, Republic of Kazakhstan

ABSTRACT: In this paper, analytical estimation of the condition of constructive elements of worked-out space in terms of thickness of mining is presented on the basis of forecasting attributes (elasticity modulus E and compliance 1/E). These attributes make it possible to determine the relationship of the current condition of the undermined rock massif with the working order by depth, during detailed estimation of surface subsidence on a plan of a studied district, with due account of the mechanical properties of the enclosing rock and the thickness of worked-out ledges. On the basis of actual data of geometrical dimensions of overlapping worked-out spaces at the Zhezkazgan deposit, an informational plan was created with regard to the thickness of mining, the anomalous zones of which are in agreement with the calculated data for geomechanical estimation carried out at the districts studied.

1 INTRODUCTION

In the stage of finishing of ore deposits in market conditions, the running thin of reserves of ores of non-ferrous metals and the general tendency of the decreasing content of useful components in raw ore create more difficult requirements as to the quality and quantity of the mineral raw materials. The increase in volumes of mineral raw material extraction necessitates the mining of ore reserves retained in the undermined rock massif, including supporting pillars.

However, the forming of large working spaces in the rock massif causes an increase in their potential risk. This is related to the fact that the increasing of the worked-out space height causes a decrease in the carrying ability of pillars and also destruction of them. The greater the thickness of mining is, the greater the volume of worked-out space and the scale of cavings. Geomechanical processes take place, complicating mining and causing threats to mine safety.

Therefore, in order to ensure mine safety and increase the effectiveness of mining practice, first of all, it is necessary to know the locations of possible caving and to select mining technology appropriate for the situation. This may be done by preliminary diagnostics of the rock massif containing deposits of useful minerals, and by following systematic liquidation of worked-out space by caving during repeat mining (Yun, 1999). The results of such diagnostics make it possible to determine the priority of liquidation of the worked-out space and increase substantiation of technical decisions when mining retained mineral reserves. At locations of possible caving as revealed by diagnostics, it is necessary to arrange observations by means of monitoring with the purpose of predicting cavings.

The parameters of caving and the time of its development mainly depend on the height of the worked-out areas and the overlying rocks from the boundary of the worked-out space up to the ground surface with due account of the coefficient of loosening. The caving of overlying rocks and fall-through cone depends on me ratio of the volume of overlying rocks and worked-out space.

The geomechanical basis for evaluating the condition of worked-out spaces of deposit areas in terms of the thickness of mining and ratio of undermining is dependent on the deformation of strata in respect of stress and mechanical properties, which in an elemental case for an elastic medium is defined by Hooke's law:

$$\varepsilon = \sigma/E \quad (1)$$

where e - deformation; a - stress; and E - elasticity modulus.

For inhomogeneous strata of enclosing rocks and ores, an equivalent modulus of elasticity may be presented in the form:

$$E_e = \left(\sum_{i=1}^{N} E_i h_i\right) \Big/ \sum_{i=1}^{N} h_i \; ; \qquad (2)$$

where E_c - equivalent modulus of elasticity; E, - modulus of elasticity of enclosed rocks or ores; and h, - thickness of enclosing rocks or ores.

For overlapping enclosing rocks and ores, the formula (2) may be presented as:

$$E_e = \left(\sum_{i=1}^{N_{rock}} E_i H_i + \sum_{i=1}^{N_{ore}} E_i H_i\right) \Big/ \left(\sum_{i=1}^{N_{rock}} H_i + \sum_{i=1}^{N_{ore}} m_i\right) \qquad (3)$$

where E_e - equivalent modulus of elasticity; H, - thickness of enclosing rocks; and n^ - thickness of ore ledges.

Quantity, which is reciprocal to the modulus of elasticity İ/E, is compliance, characterizing medium ability for deformation, and it eventually causes subsidence of the ground surface: the smaller E the more deformation or subsidence. When ledge mining with m, thickness, Ei = 0 is given for the corresponding ledge. And E as a whole decreases in proportion to the number of mined ledges with great thickness. Therefore, subsidence above the mined area İs more than that above the non-mined area. Above destroyed roof $\sum_{i=1}^{n} h_i = H_m$, and the equivalent modulus E_e above the roof will be less than its value above pillars. This means that the deformation ability of the rock massif above worked-out space will be more than that above pillars.

The forecasting attributes E or l/E are used for detailed determination of the subsidence of the ground surface on a plan of the district studied with due account of the mechanical properties of the enclosing rocks and ore ledges, the thickness of mined ledges and the presence of overlapping. It makes it possible to determine the relationship of the current condition of the rock massif and the order of ore mining by depth. Thus, the deformation of inhomogeneous (lumpy-homogeneous) strata takes the form of the following expression:

$$\varepsilon = \sigma_1/E_1 + \sigma_2/E_2 + \ldots + \sigma_n/E_n, \qquad (4)$$

where e - deformation of strata; σ_i - stress; and E, - modulus of elasticity.

To express stresses in the form of the product of solid weight and depth of bedding of the rock layers, calculations can immediately be performed by the formula:

$$\varepsilon = \gamma_1 H_1/E_1 + (\gamma_1 H_1 + \gamma_2 H_2)/E_2 + \ldots + (\gamma_1 H_1 + \gamma_2 H_2 + \gamma_N H_N)/E_N, \qquad (5)$$

where γ_i - solid weight of the i^rock layer; Hj - depth of the i layer bedding; and E! - modulus of elasticity of the i^{th} rock layer.

For a mined ore ledge it is necessary to take *y,* = 0, preserving H, and E,. It is not difficult to see that the different values of deformation e may be obtained depending on different sequences of ore ledge mining by depth.

On the basis of these behaviours of space changes in the mechanical properties of rocks and stresses, informational plans were drawn up with regard to the thickness of mining and ratio of undermining.

In order to show the effect of this factor on the process of cone forming at the ground surface, data from mine surveys, mining and geological forms and records were studied. Using these data, a plan was drawn showing isolines of the total thickness of the Zhezkazgan deposit, as shown in Figure 1.

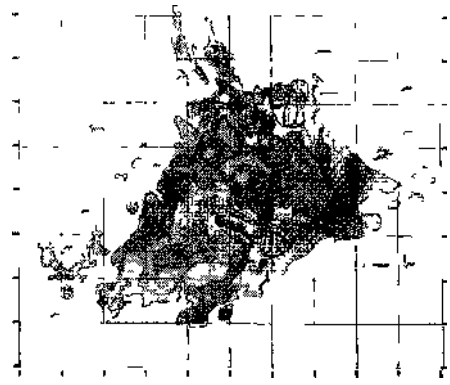

- potential dangerous zones by criterion of total thickness of mining;
- pillar;
- cone of caving on ground surface

Figure *I* Informational plan with regard to thickness of mining.

As can be seen in Figure 1, zones where earlier cavings took place correspond to districts with the maximum values of total thickness.

The presence of tight massifs (pillars) creates particular interest, because knowledge of them is necessary for solving problems in future mining of the deposit From the point of view of prediction, a tight massif is a barrier to the development of large cavings.

The zones of the deposit drawn with regard to the thickness of mining are convincing evidence of the effect of this factor on the parameters of caving.

The drawing of such plans has an influence on the scale studying of the effect of different voids if the worked-out space has different multi-level geometrical structure and section areas at different

heights differing substantially from each other. It is necessary to know this information in order to take account of the full volumes of overlying rocks and worked-out space.

Generalization of the large volume of materials of natural investigations made it possible to identify that the important characteristic of the process of movement in space and time is the value H/m.

Thus, caving of the overlying rocks and cone of fall-through depend on the ratio of the volume of the overlying rocks and the worked-out space. When determining the ratio H/m in a space of the deposit on the plan of the ground surface, we obtain contours of the possible forming of cones.

It has been established (Makarov & et al., 1999) that with due account of the empirical criteria of equivalent span l_e and coefficient of loosening Ki, on the basis of an analysis of cavings carried out at die Zhezkazgan deposit, the conditions of fall-through forming are established by the ratio H/m < 10.

The condition of full caving of overlying strata up to the ground surface is determined by experimental dependence:

$$L = -9 + 1.2H, \text{ m} \qquad (6)$$

where L - equivalent span of worked-out space; and H - depth of mining, m.

Study of the causes and effects of previous caving made it possible to connect the limiting-permissible value of subsidence Tji by a correlation relationship to the ratio of undermining H/m:

$$\eta_{ji} = 3.95(H/m)^2 - 21.28(H/m) + 55.17, \text{ mm} \qquad (7)$$

where rii - limiting-permissible value of subsidence, mm; and H/m - ratio of undermining.The correlation relationship describing the parameters of worked-out space and ground surface movement is presented in Figure 2.

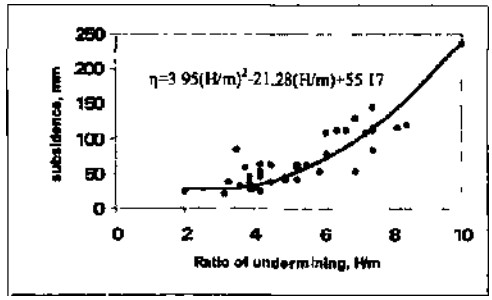

Figure 2. Graph of ground surface subsidence as a function of ratio of undermining.

The criterion H/m < 10 under a conventional assumption of pillars supporting worked-out space that have lost their carrying ability makes it possible to perform diagnostics of the final condition of the undermined rock massif.

Physical simulation of the final condition of the worked-out space with artificial extraction of supporting pillars will allow: evaluation of the consequences of deposit mining on the ground surface; preparation of preventive measures of protection; an opportunity to finish remaining reserves, including supporting pillars; the selection of technology for carrying out mining operations; and mine planning.

The open-stop system is widely used in the mining of underground ore deposits. The use of self-propelled machines of high capacity for drilling, loading and transport of ore ensures a high production capacity. At the same time, significant losses of useful minerals in inter-chamber pillars, which increase constantly together with the depth of mining, are its major disadvantage.

It has been noted (Airuni et al., 1985) that an increase in the intensity of mining useful minerals causes the deposit to run thin, rises in price to occur and mining to decrease. In such conditions, the preservation of pillars is not acceptable because of the high level of ore losses in pillars, inasmuch as both dimensions of pillars and non-covered expenses for the opening-up and development of reserves increase when the depth of mining increases (Airuni et al., 1985).

Use of the results of preliminary diagnostics helps solve this problem, which İs important in the industry.

Use of the obtained relationship makes it possible to take account of such factors as the extracting thickness m and depth of mining H, and permissible rate of subsidence q, and these factors determine the conditions and location of cones forming on the ground surface. The reliability of the results was confirmed by the fact that all cavings which took place at the deposit were located in zones determined by the criteria mentioned above.

The obtained correlation relationship makes it possible to predict limiting-permissible deformation of the ground surface as a function of the depth of mining H/m. It also solves opposite problems, that is, the choice of parameters of voids, ensuring that deformations of the ground surface not will be greater than the limiting-permissible deformation for undermined objects. It will enable a substantial increase in the coefficient of recovery of useful minerals under built-up areas.

When H/m>10, catastrophes are prevented and caving may appear on the ground surface in the form of terraces, smooth deflections, secant fractures, and negligible movements. In these conditions, it is possible to fill in such caving and to use constructive measures of protection for surface constructions.

For practical use of the identified behaviour of the changing of the effect of undermining depending on the geometrical parameters of the worked-out space, a method was developed to determine zones on the ground surface which are potentially dangerous due to caving during underground mining of ore deposits (Satov, 1999).

The solid anomalies of total thickness are superimposed on the plan of mining operations of the deposit. The most dangerous zones are those with maximum values of the total thickness of deposit mining. Then, using the values of total thickness and depth, the ratio of total depth H to total thickness m is determined. With these results, isolines of the ratio of undermining H/m are drawn by extrapolation. The value H/m <10 is taken as a criterion of the prediction of cavings. The solid anomalies revealed by the criterion above, the ratio of undermining, are presented in Figure 3. Dangerous districts are zones where isolines show H/m<10.

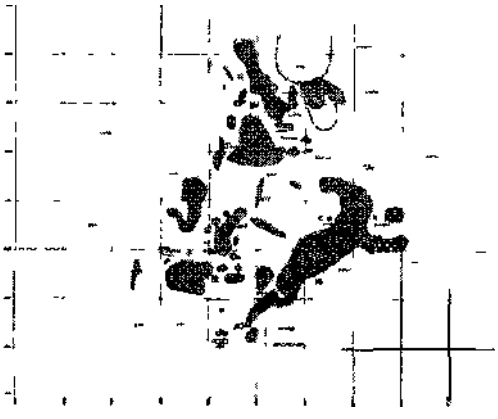

- potential dangerous zones by criterion of ration of undermining;

- cone of caving at ground surface.

Figure 3. Informational plan of deposit on ratio of undermining

By superimposing drawn plans with isolines of tbe criteria on the plan of mining operations, anomalous zones which are potentially dangerous due to caving are determined. Dangerous zones are taken as those where the isolines of values by criteria m and H/m fall in the same interval. These districts have the greatest risk of caving İn comparison with other parts of the deposit, and this is confirmed by previous cavings which occurred at the deposit

When further mining operations are carried out, the mining and geomechanical situation changes, and the values of m and H/m also change. In such districts, for every cycle of winning operations changes are introduced in corresponding plans, and the identification of potential caving zones on the ground surface is carried out again. Zones on the ground surface determined by this method, are fenced off, and protective measures are taken: depending on economic expediency, dangerous volumes of voids are filled in, engineering constructions are moved from the ground surface, or voids are liquidated by controlled caving of overlying rocks. Therefore, knowledge of such zones allows protective measures to be taken İn good time, preventing possible catastrophes which have taken place at the Zhezkazgan deposit.

The introduction of new methods of evaluation of the current condition of districts of the deposit in terms of the thickness of mining enables preliminary diagnostics of the rock massif to be carried out by established criteria, and the locations of possible catastrophic occurrences such as caving up to the ground surface to be predicted long in advance. The introduction of these methods also allows protective measures to be taken in good time, and effective and safe mining operations to be carried out in hard geological conditions.

Diagnostics of the final condition of worked-out space facilitates ore extraction at mines and the methods and order of liquidation of potentially dangerous voids, and shows the necessity of moving surface constructions.

Practical use of this method ensures safe conditions of mining operations and prevents damage due to possible cavings, especially in conditions where there is,a high concentration of protecting buildings and constructions.

The result of this investigation is: the current evaluation of districts of the Zhezkazgan deposit was carried out in terms of the thickness of mining, and the geomechanical situation at this deposit and dangerous caving zones were determined.

Owing to the methods developed, the locations of possible cavings were identified in good time, and the long-term forecast ensured that corresponding protecting measures were taken.

Current evaluation of the districts with regard to the thickness of mining helps solve an important problem - liquidation of worked-out space - or liquidation of volumes of voids which were formed over previous decades. In the future, with successful liquidation of the existing volumes of voids, such dynamic occurrences of rock pressure as sudden caving will be practically non-existent.

For this purpose, schemes of districts for immediate liquidation of worked-out space by means of rock caving have been established at some ore mines. For districts which contain dangerous caving zones as revealed by diagnostics, designs for

worked-out space liquidation have been prepared, and operations for the liquidation of existing dangerous volumes of voids have been begun.

As a result of these investigations, data of geomechanical forms and records were generalized and current evaluation of districts of the deposit in terms of thickness was carried out.

2 CONCLUSIONS

The mam scientific and practical results are the following:

1. The volume of worked-out space is a cause of the process of caving, and the volume of undermining of the ground surface İs an outcome. The conditions, dimensions and location of cones formed are determined at the end *of* mining by the geometrical dimensions of the worked-out space.

2. A correlation relationship was obtained for the limiting-permissible value of subsidence of the ground surface as a function of the ratio of undermining, which may be used for evaluation of the value of the zone of destruction in the undermined massif.

3. Methods were developed for identifying anomalous zones which are potentially dangerous due to caving during underground mining of ore deposits. These methods allow current evaluation of the condition of districts.

4. The diagnostics of the undermined massif enable locations of possible caving to be determined at the stage of design and planning of mining operations so that measures can be taken to prevent caving, enabling ore extraction and determination of the order of liquidation of dangerous volumes of voids.

REFERENCES

Yun, R B. Kazakhmys Corporation today. *Mining Journal,* 1999,No.3,pp.8-ll.

Makarov, A.B., Satov, M.Zh, Yun, A.B. 1999 Condition of forming of fall-through at ground surface when repeal mining of Zhezkazgan deposit by caving system *Proceedings ofJnlemaaonat Conference on "Geodvtiamics and stressed condition of interior of earth".* Novosibirsk.

Airuni, A.T., lofis, M.A. 1985 Deformation of rocks when underground mining of deposits of useful minerais *Mining Science in USSR.* Moscow, IPKON, pp 41-64

Satov, M.Zh. 1999 Metiiod of determination of zones on ground surface, which are potentially dangerous for caving when underground mining of ore deposits Pre-patent of the Republic of Kazakhstan No 8159. Solution of Russianpatent issue on inventor's application No 99109642/03(010216).

17* International Mining Congress and Exhibition of Turkey- IMCET2001, © 2001, ISBN 975-395-417-4

Drilling for Underground Excavation and Support in Sedimentary Rock

G.Nord
Senior Construction Advisor, Atlas Copco Rock Drills AB

ABSTRACT: It is a well-known fact that the drilling is carried out differently depending on the rock soil conditions. This paper will deal with drilling for blast holes, bolt holes, grout holes and use of support measures like bolting and spiling that are depending on well performed drilling. As there from drilling point of view does not exist a well-defined border between igneous rock and sedimentary rock discussions on the mechanical behaviour of the drilling equipment as well as the response of the rock can be performed in the same way for the two types. This discussion will be held in general terms without any deeper mathematical analysis, and will end up in some general conclusions. A couple of cases on support ahead of the tunnel face will also be given showing the possibility to achieve longer excavation rounds which hopefully will end up in safer cheaper and faster tunnel excavation.

1 DRILLING IN VARIOUS TYPES OF ROCK

1.1 *Drilling technology*

It is well known that there exist two methods of drilling namely percussion drilling and rotary drilling. Rotary drilling is almost 100% used for larger and longer holes in all types of rock and most well known is the oil drilling where the hole-diameters are in the range of 12 to 25 inch (300 to 600 mm). The roller bits are rarely smaller than 3 inches (75 mm) and that means that they are almost never used in under ground construction and mining. In specific mining applications and in some construction in very soft ground so called rotary drag bits are being used. To be able to use the dragbits it İs necessary to ensure that the soft rock does not host any layers or seems of hard rock, as they will most probably stop the dragbit drilling. A good example is mining of salt from the underground. The salt formations normally have a massive character without any intrusions of other rocks.

The percussion drilling is widely used as it can cope with all kinds of rock though less successful with very weak rock like soft sediments. Percussion drilling is however not one of a kind and there is a number of factors to consider when designing percussion drilling tools and few words will be spent on these. The most important parameters to consider are related to the piston, the bit, the rod and the loads that are applied. Concerning the piston it is the mass, the geometry, the frequency of blows and the velocity at which it strikes the rod, for the bit it is the type, the diameter, the rotational speed and the kind of flushing and finally for the rod the geometry and the thrust force. To make this factor operate at an optimum in every situation is very difficult and somebody would say impossible, as rock is very variable. How is the variation in rock relevantly characterised with respect to percussion drilling and also rotary drilling? Two parameters have been found to have a very good capacity to fulfil this target and those are the so-called stamp strength and the brittleness value. These rock parameters are retrieved from the stamp test, which is shown in the figure 1 below. In the test a circular indentor with a defined radius is pressed into a flat surface of the actual rock. At first the rock surface deforms elastically but as the indentor is forced deeper into the rock the tensile stress at the surface exceeds the strength and tensile cracks arises around the indentor and the rock just under the indentor itself is crushed as it has lost its side support. In connection with the collaps of the under and around the mdentor debris of finer and coarser İs scattered around and a crater in the flat rock surface has been created. This indentation resembles very much of what İs happening under the buttons in a bit in the bottom of a bore hole irrespective of it is rotary or percussion drilling and will inform what loads are required to be able to penetrate the rock. There are two more parameters to be extracted from this test that is correlated to the drilling rate and they are the penetration depth corresponding to the maximum fracture force and the volume of the crater.

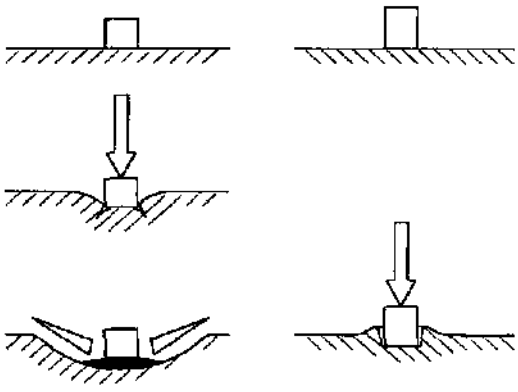

Figure 1. Indentation in brittle (left) and very ductile rock material (right)

Stamp test on brittle rock results in fairly deep and wide craters see figure 1 (left). For a very ductile rock the crater volume is only slightly larger than the indented volume (indentor area times indentation depth). The rock has flowed up around the indentor without fracturing. The material acts almost like a chewing gum that after a bite shows the groves of the teeth. In figure 1 (right) is this schematically demonstrated. Conclusively it can be said that in brittle rock only percussion is required for effective fragmentation in bottom of the borehole why very ductile rock is favoured by both percussion and drag.

2.1 *Sedimentary rock versus igneous*

Igneous rocks are considered brittle and they are to a certain extent. Sedimentary rocks are often believed to be ductile and they are in some cases but in many cases they may be just as brittle as the igneous rocks. In Atlas Copco throughout the years some extensive rocktesting has been carried out with respect to Brittleness, Abrasivity, Strength and Density. Density is only of importance for the flushing. The results from a number of these tests are shown in the figures 2- 4 below and there are also some igneous rocks for comparison.

As can be seen it is not that obvious difference between sedimentary and igneous rock in general. There are sediments mat are ductile and has typically low strength like shales of various kinds not shown here. Sedimentary rocks are estimated to cover some ^{3}A of the continents of the earth and not less than 70% of them are considered to be shale still the number of test results from shales normally are far less than those from limestone and sandstone in any reference library. Man seems, in his construction activity, to avoid shales and this might be explained by the fact mat shale is frequently highly weathered and can easily be excavated by regular backhoes without any blasting operation.

2.2 *Performance in sedimentary rocks*

What drilling results can be achieved in sedimentary rocks when comparing with igneous rocks. To give an answer to that five typical rocks have been defined namely a shale, a limestone, a sandstone and for reference a granite and a basalt. In order to illustrate how not just Atlas Copco drill machines cope with this kind of rock machines from other suppliers have been tested in the simulation model created by Atlas Copco named Diarot. This computer model is based on a number of algorithms derived from theoretical considerations and later confirmed in laborotary and field tests.

Input values are for the rocks those described above namely stamp strength, brittleness and abrasivity. For the drill machines the machine's characteristics like the geometry of the hammer its velocity and frequents are stored in the program files. The same applies for rods and bits where geometry and design features are entered. The drill string İs a limiting factor when transmitting the blow generated by the drill machine in one end to be used by the drill bit in the other end. When comparing the various drill machines having roughly the same energy output the criteria for running them is that the relative steel stress in the rod should not exceed 100 % of practical fatigue limit from experience. The results are shown in figure 5 and 6 below where the accumulated drilling rate is very variable due to the fact that the suppliers of the machines have different opinion on what is the optimum design. The variation in bit life is though far less affected.

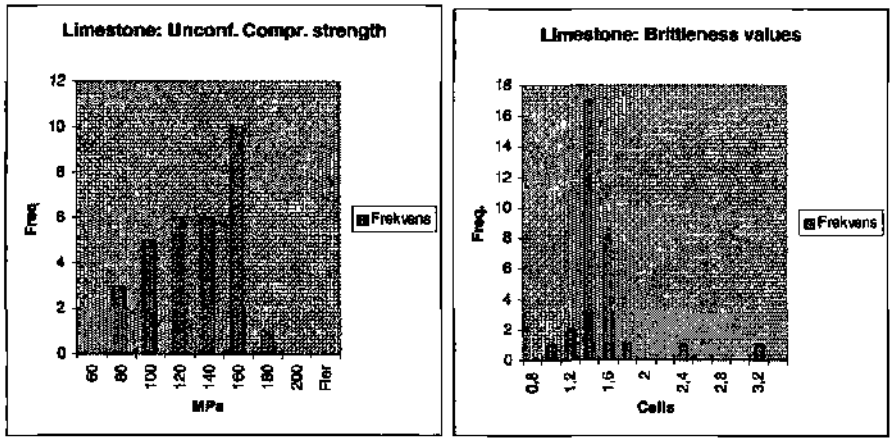

(a) (b)

Figure 2. UCS and brittleness test results performed on limestone samples

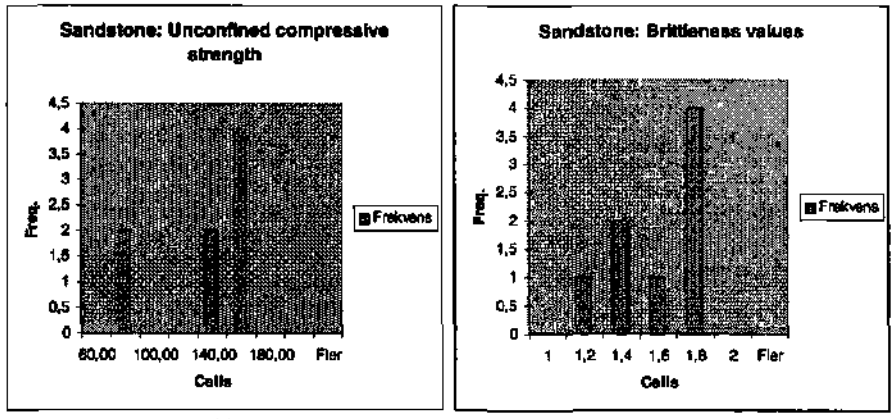

(a) (b)

Figure 3. UCS and brittleness test results performed on sandstone samples.

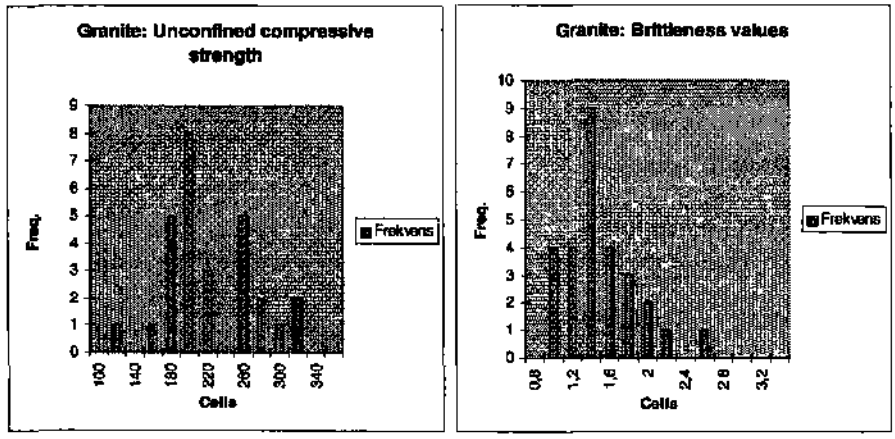

Figure 4 UCS and bnttleness test results performed on grämte samples

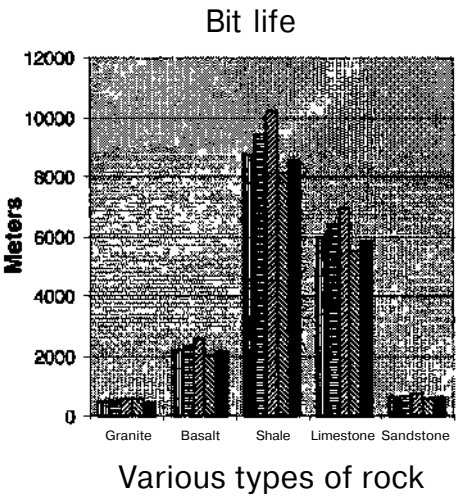

Figure 5. Bit lives within various type of rocks

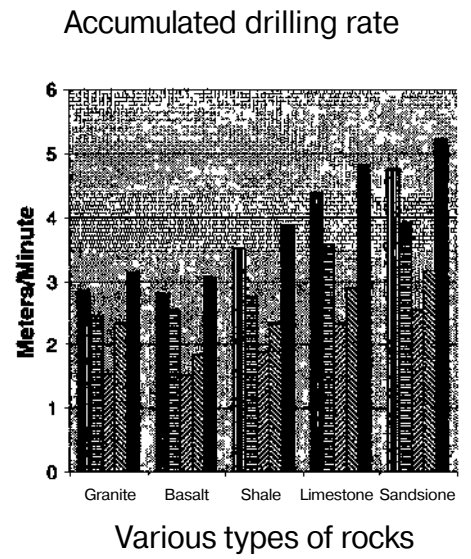

Figure 6. Accumulated drilling rates within various type of rocks.

2.3 *Adjustments of drill machine setting with respect to rock condition*

As the rock may vary from one round to another as well in one hole it is an advantage if the machine settings can be adjusted as the rock conditions vary. Atlas Copco has solved this on their 1838 and 1440 by introducing a rotation pressure controlled feed force and impact force. They are given the abbreviations RPCF & RPCI this means that both the hydraulic pressures for the feed as well as the percussion is ruled by torque that is required to turn bit and rod. A too high torque is interpreted as a too high feed force which will result in too tight threads of the drill string and the feed pressure is then reduced which will hopefully result in a reduced torque. If torque still is too high the RPCF will reduce the impact pressure. If still not sufficient, the drill string will be retracted and a new drill start is initiated. A too low torque will result in too loose threads which eventually will lead to pitting and a too fast wear of the rods.

2.4 *Drillbits*

The design and selection of drill bits is a science İn itself and can only be touched upon. In weak and ductile rock typically a shale there are problems to achieve torque large enough to maintain tight joints. There is obviously a need for a bit that penetrates deeper into the rock in the bottom of the hole. At the same time there is a demand for a bit that has some of drag bit characteristics. As the ballistic button bits are longer than the sperical ones they simply stay longer in the hole during a longer transversal movement, which tn fact is the drag.

Drilling in sedimentary rocks often means higher drilling rates and this means a demand for increased flushing. Some designers have sorted that problem by giving the bit larger or more openings and by creating flow routes on the outside. The front flush of the bit is often omitted as it has a tendency get clogged. Another mean is to increase the flushing pressure, which also will result in an increased flow.

Increasing the pressure and flow is not a problem as long as the bore hole is stable but in weak sedimentary rock this is not always the case. Air flushing has a far less eroding effect on the bore hole wall than water and is therefore a viable alternative in unstable conditions. As air flushing is unhealthy in underground drilling some minor quantities of water has to be added in order to trap the dust. This is normally called water mist drilling. The water bearing compressed air that enters the flushing channels shall have a pressure of not less than 0.7 MPa.

3 STABILISATION AHEAD OF THE TUNNEL-FACE A MEAN TO DEAL POOR GROUND-CONDITIONS

Drilling ahead of the tunnel-face and install bolts or grout is a common way of improving the rock-quality before the actual excavation takes place. Atlas Copco has as a supplier been involved in a number such projects both in mining and construction and few cases will be presented below. The first two cases is a reprint from a paper

presented by Mr F. Charette Atlas Copco North America and J.F. Lessard Louvicourt Mine Canada on use of Swellex as spiling and a third case is support of a tunnel portal for a highway project in Japan where so called Odex drilling by use of a regular Boomer was applied.

3.1 *Use of Swellex in support ahead of the tunnelface*

Pre-reinforcement is a different way of approaching ground control. Instead of relying on supporting the ground following excavation, pre-reinforcement increases rock strength prior to excavation. There are several benefits to this. First, a pre-reinforced rock mass will be less damaged and influenced by the excavation process, namely the blasting and the elastic and non- elastic stress redistribution. Second, the rock mass is never without support, even at the split second following blasting of the round. Third, the support can be more active when installed early, rather than passive when installed later. Fourth, pre-reinforced ground will not deteriorate or collapse as rapidly as a totally unsupported excavation, allowing a safe working period for installation of regular support.

Figure 7 shows a well-known relationship between the unsupported stand-up time of an excavation in relationship with its rock mass quality. Empirical observations have shown that, for a given excavation size, a linear reduction in Rock Mass Rating (Bieniawski, 1974) will lead to a logarithmic reduction in unsupported stand-up time. Hence, a linear increase in excavation span results in a logarithmic increase in instability potential. For large span drifts the time period available to install roof support is significantly lower than for small drifts. In the case of a 4,3-meter span tunnel driven through poor to very poor quality rock, it may be logistically impossible to support the roof before it collapses. Obviously, the operational and safety implications of such cases are tremendous.

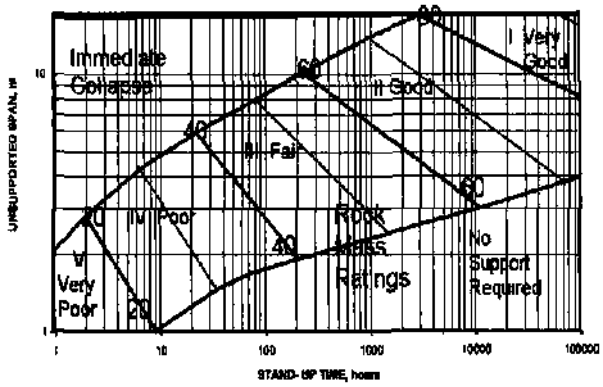

Figure 7. Unsupported Stand-up Time and Support Requirements (After Bieniawski, 1984)

Field observations show that cable bolts installed in slopes before the first blocks are blasted are more effective than cable bolts installed after the slot or cut has been excavated. Firstly, for cable bolts installed prior to stope exploitation, the grout curing period is generally respected. This is not always the case for cable bolts installed during stope exploitation, when production concerns may over-ride ground support design concerns. Secondly, the cohesive effect of the cable is greater when added to undisturbed ground than when added to weakened and disturbed ground.

In tunneling, a pre-reinforcement method called "umbrella grouting" exists. The method consists of pre-supporting the planned roof area with steel rods. Large holes are drilled in the future roof perimeter, and high-pressure-grouted with high strength/small particle size cement grout. Through each cemented hole a smaller hole is then drilled, İn which a high-strength reinforcement bar is cement-grouted. Although highly effective for shallow tunnel's driven in very adverse ground conditions, it is easy to see that such a work-intensive operation would be deemed neither practical nor economic for mining applications, although the underlying concept could definitely be useful.

3.2 *The Mine Doyon Experience*

A variation of the umbrella method was attempted at Mine Doyon, located near Rouyn- Noranda in

northwestern Quebec. The Mine Doyon property is one of the most important gold-bearing orebodies in production in Canada. The mine is located 40 km east of Rouyn-Noranda. At least 4 major ore zones are found on the Doyon property. Economic mineralization is found on a corridor that extends at least 2 km E-W, and from surface reaches a depth of over 1000 m.

The ore zone which will be discussed here, the No.1 Zone, is defined by a major quartz and sulphide vein system, oriented east-west. The orebody is also oriented E-W, dips steeply south and has an average width of 8 meters at depth. It is surrounded by sericitic schist corresponding to the sub-unit 4b of the Blake River Group (Savoie et al, 1991). Mining method is long hole stoping with cemented rock fill. Mill production is around 3500 tons per day.

Several tectonic events have been identified, among them a N-S compression followed by a N-S extension; an inverse shearing caused by a NW-SE compression; and a polyphased fracturing caused by an as-yet undetermined stress gradient.

The footwall of the No. 1 Zone İs located İn very poor quality sericitic schist, with RMR values between 0 and 30. This alteration zone runs for about one hundred meters up to the ore body, located itself in very weak chloritic schists (Fig. 8). Stope development in this ore zone was delayed due to repetitive caving in access drifts.

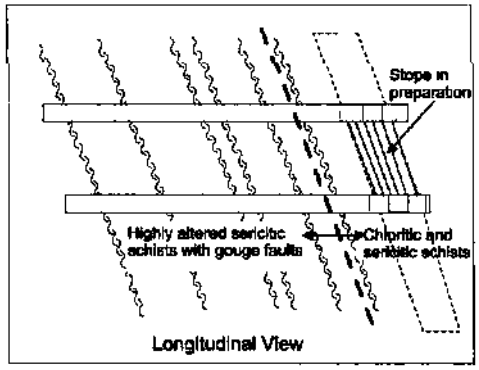

Figure 8. Structural geology setting of the Zone 1 at Mine Doyon

The author, employed at the time as Rock Mechanics Engineer at Mine Doyon, designed a pre-reinforcement method using cable bolts installed over the future roof of the access drifts. An array of nine 50-foot cable bolts was used to pre-support the roof during drift development (Fig. 9). The method wag, successful from a rock mechanics point of view, allowing three to four rounds to be taken before installing heavy support consisting of vertical cable bolts and shotcrete. Primary support could be installed during the normal cycle without safety problems.

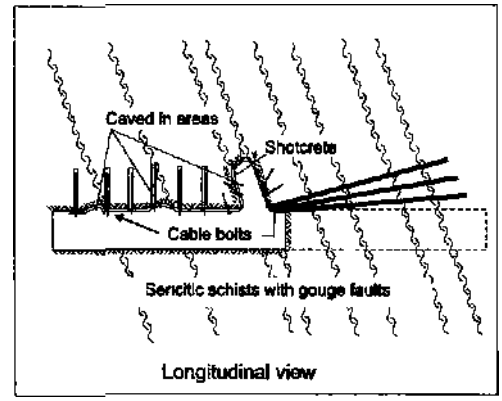

Figure 9. Failure patteras and pre-reinforcement with long cable bolts.

Although stability was achieved, however, high productivity was compromised, since the bolter was tied up in stope preparation and rehabilitation work. Also, since several levels were being developed concurrently, travel time for the equipment and cable grouting crew was significant. A better solution was needed. Requirements were: 1) easy integratioP in the normal development cycle; 2) installation before the next drift advance; 3) effective support; and 4) reasonable cost.

In order to increase productivity and regain some flexibility, it was decided to try pre-reinforcement using Super Swellex bolts instead of cables, and to slightly reduce drifting length to about 3 meters. Five to sbt Super Swellex, parallel and spaced 60 to 75 cm apart, are installed subhorizontally over the perimeter holes. Holes are drilled using the development Jumbo drifter. Pre-reinforcement holes are 50 to 60 cm longer than drifting length, to accomodate the 3,6-meter long bolts. Inflation pressure is 240 bars. Figure 10 illustrates the principal components of the method. Several variations of the method were used to secure pillars and cuts in stopes (Charette, 1996).

With the Super Swellex bolts, productivity actually increased to the same level as for ramp and drift development in fair to good quality rock.

Since the few extra holes required for the spiling bolts are drilled at the same time as the blasting holes, and the bolts are installed in the short period between drilling and loading, this pre-reinforcement method adds no additional time to the excavation cycle. The experience was a total success, and the method became a standard at Mine Doyon for bad ground conditions. Presently, around 300 meters of access drift and stope have been developed using this method. Close cooperation between the engineering and production departments made this success possible.

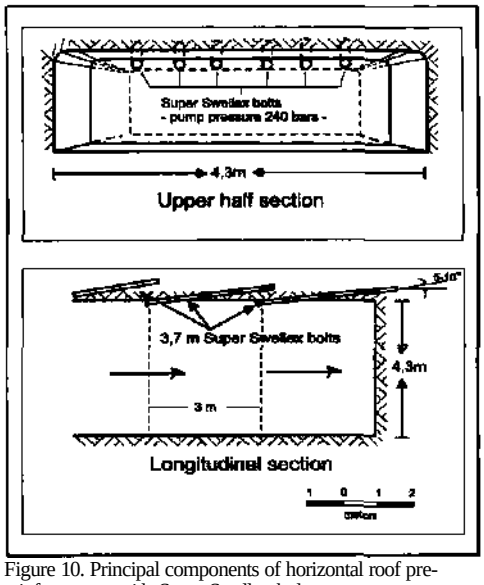

Figure 10. Principal components of horizontal roof pre-reinforcement with Super Swellex bolt.

3.3 *The Louvicourt Experience*

The Louvicourt Mine is a polymetallic orebody of copper, zinc, silver and gold, 25 km east of Val d'Or in northwestern Quebec. It is a volcanogenic massive sulphide deposit starting 47,5 m below ground surface. It is part of the Abitibi Greenstone Belt within the Precambrian Shield of eastern Canada. The orebody dips 70° North and strikes E-N-E with a plunge to the east. Dimensions of the orebody are 300 m along strike and 500 m along dip. Thickness varies from 20 to 100 m. The mining method is long hole stoping with paste backfilling.

Systematic stability problems are encountered while drifting through fault zones disseminated in the orebody. The gouge associated with the faults, the unfavourable dip of the two main joint sets, and the intense black chlorite alteration of the joints, contribute to the formation of high roof and unstable ground conditions (Fig. 11). Gouge thickness can reach up to 90 cm.

An efficient solution to this problem has been to use Super Swellex bolts as a pre-reinforcement method (see Fig. 12). Three to four rings of 3,6-meter long Super Swellex, on a 1,5 X 1,5 m to 2,0 X 2,0 m pattern, are installed on tie roof of the drift before the next advance in the fault zone. The holes are drilled 50° upward, using a Jumbo drifter, and the bolts are inflated to 300 bars using a pneumatic Swellex pump. Steel straps are sometimes used to increase support capacity and cohesion. The immediate support effect, and simplicity of the operation, with minimum handling, are definite advantages to using Swellex instead of cable bolts in this case.

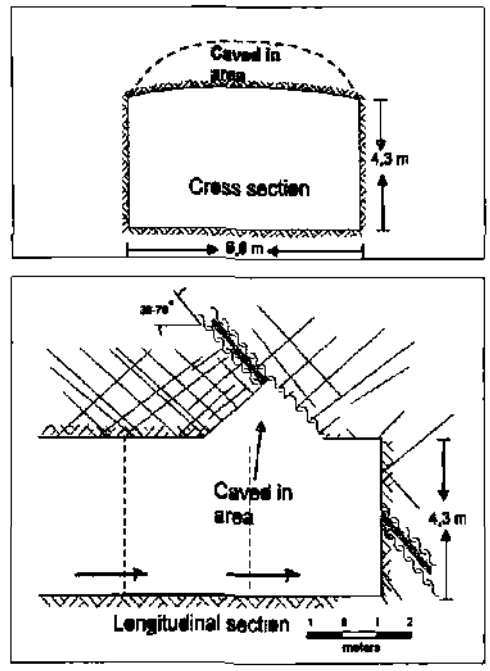

Figure 11. Unstable ground conditions at Louvicourt Mine

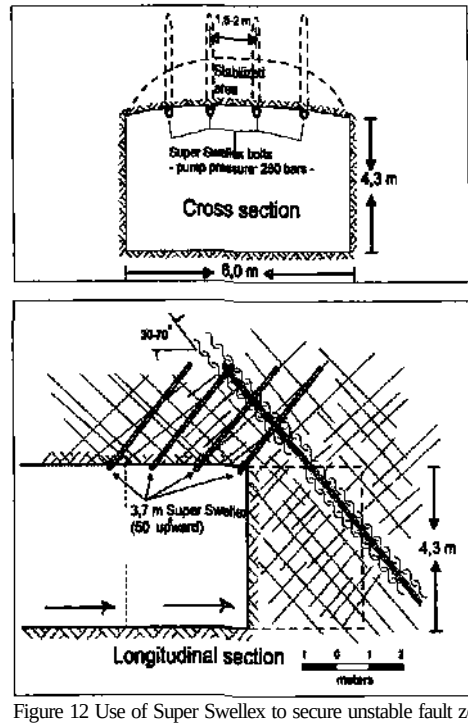

Figure 12 Use of Super Swellex to secure unstable fault zone

The method creates a small increase İn normal cycle time, but the drilling and installation time are more than justified by the cost, risk and lost time associated with rehabilitating a caved roof. The collaboration of the production department was crucial to developing the method.

3.4 *Support ahead of the tunnel-face by use of long grouted tubes so called Boodex.*

So called Odex drilling is a well known drilling method in suface drilling irrespective of the type of rock. In fact Odex stands for overburden drilling using excentric drillbit. The method is used for drilling through soil thus leaving a casing tube and then continue İn rock with or without casing. This drilling tool has turned out to work very well in horisontal drilling using a regular large Boomer like 352 and 353 for tunnelling as drilling machine. Long holes in the range of 10-40 meters are drilled just outside the periphery of the tunnel with a moderate look out angle of some 5 degrees giving enough head room for another set of holes to be drilled. The drill-holes are placed at a spacing of 1 meter down to 0.3 meters depending on the ground conditions. The casing tubes that are functioning as lining of the hole has an outer diameter of 115 mm. In underground application 1,5 meter long sections of the tube is used due to the weight and bulkiness of the rod-tube assembly.

When applying Boodex in the portals 3 meter long sections can be used as it is possible to use a small crane for the handling.

When the drilling has reached the the requested depth the excentric drill bit and the rod is retracted.. The pipe will then be used for grouting of the ground around it by either use of a probe that is sent into the tube bringing the grout to the valves in the tube or by individual hoses. This grouting has a lot in common with die tube a manchette method.

There are not many cases where this method has been used but one site will be described briefly. The first site where the Boodex was used was in the Tsuda tunnel in Japan where it was necessary to improve the quality of the ground before the excavation could start, see figure 13, In this case it was decided that not less than 28 nos of 36 meter Boodex pipes should be installed in the crown of the 60 m^3 large tunnel and grout the whole crown by use of individual grout-lines to every valve of the Boodex-pipe. To complete the drilling of one pipe the time was cut to 7 to 8 hrs. The Boodex - installation took 20 days working on dayshift only. The deviation of the pipes did not exceed 2 %. The result of the ground-improvements fulfilled the expectations. The road that is located only 3 to 5 meters above the crown had a settlement after excavation of only 1 mm in some places.

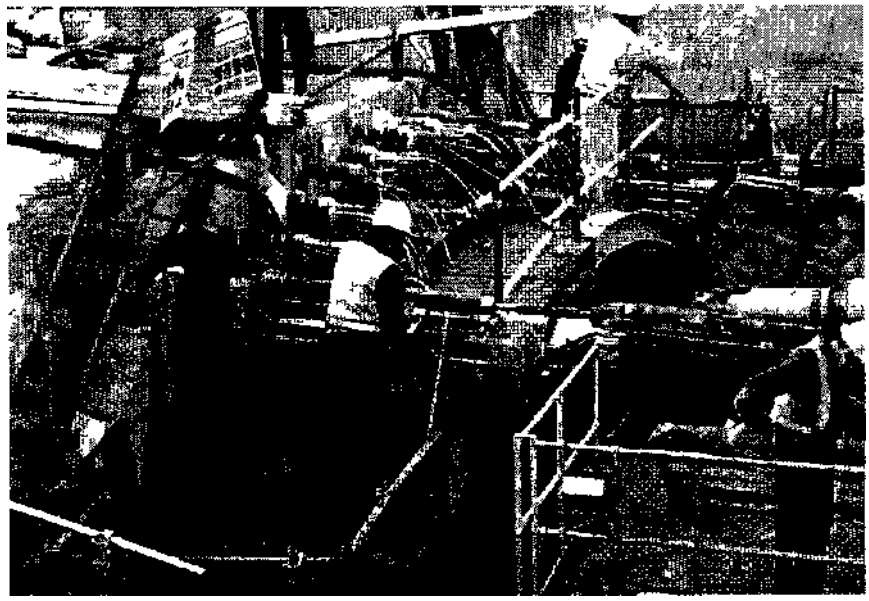

Figure 13. Drilling and grouting with Boodex-pipes, Tsuda-tunnel portal, Japan

4 DISCUSSION

Experience with Swellex bolts as a pre-reinforcement method shows that it can be a valuable improvement to current excavation methods. Faster support action, smaller effect on excavation cycle time, and active roof arch building are some of the obvious results achieved.

However, there is still a lot to learn about the optimum application of the technique. The installation angle in relation to joint orientation and dip, the inflation pressure in relation to rock strength and fabric, and the optimal distance between bolts have yet to be defined, in order to obtain a quantifiable approach to Swellex pre-reinforcement.

Although some experiences were not totally succesful, they have taught us a better way to use the bolts. Because the Swellex is not a passive reinforcement dowel, the way it works must be well understood in order to achieve the expected results, and avoid local detrimental effects on roof stability.

5 CONCLUSION

The two examples presented here show that Swellex bolts can be efficiently used as a pre-reinforcement system in order to improve productivity and safety while excavating mining tunnels in incompetent rock. The method can be applied to systematically support roof, or to prevent caving from a nearby fault zone. The method is fast, improves safety, and can be easily integrated *into* development operations. Cooperation of the underground department İs paramount to the success of the technique, as the experience of the miners and supervisors is a valuable asset in improving excavation techniques.

It is often claimed that drilling sedimentary rock is completely different from drilling in crystalline rocks. This may be the case but rarely in sandstone and limestone may be just as brittle as igneous rocks By fully understanding the mechanics of the failure of the rock when exposed to percussion drilling the design of the drill machines can be optimised. In this optimisation the drill machine, the rod bit and rock is treated as one unit. This means that just the nominal figures on a drill like power and frequency etc. will never tell the performance characteristics in its full range. The Atlas Copco computer based program, Diarot, certainly improves the opportunities to advice an optimized drilling result.

Sedimentary rocks are in many cases also weak rock and as such requires improved strength and deformation capacity ahead of excavation. In these cases the Atlas Copco Swellex bolts and Boodex system offers opportunities to perform this pre-strengthening of the ground beyond the tunnelfase in what many consider a cost efficient way. The savings are manually on the time side but use of longer rounds means also cost reductions.

REFERENCES

Btcmawskt, Z T (1974) *Geomechanıcs* classification of rock masses and its application in tunnelling Proc Third International Congress on Rock Mechanics, ISRM, Denver, Volume HA,p 27-32

Biemawski, ZT (1984) Rock Mechanics Design in Mining and Tunnelling Balkema, Rotterdam

Savoie, A, Trade!, P , Sauve. P, Hoy, L and Lao, K (1991) Géologie de la mine Doyon Ministère de l'Énergie et des Ressources du Québec, ET 90-05, 80p

Charette, F, (1995) Utilisation du pré-soutènement pour le fonçage de galènes en terrains très incompetents Compte Rendu du Colloque en Contrôle de Terrain de l'AMQ, Val d'Or

Wijk, G, (1989) The Stamp Tool for Rock Dnllability Classification Int J Rock Mech Min Sei and Geomech Abstr. Vol 26 No 1 pp 37-44

Charette, F and Lessard JF (1997) Rock pre-reinforcement with Super Swellex bolts for excavation in very poor ground conditions

17 International Mining* Congress and *Exhibition* of Turkey- *MCET 2001, ©2001, ISBN 975-395-417-4*

Yielding Pillar Concept and its Design

H.Yavuz
Department of Mining Engineering, Süleyman Demire! University, İsparta, Turkey

ABSTRACT: Yielding pillar theory and the comparative performance of yield-pillar-protected roadways to critical and stable pillar systems are described. The applicability of empirical methods, the mine stiffness concept, enhanced confined core concept and numerical modelling in designing a yield pillar during the development stage of mining in two-entry systems was investigated and the drawbacks of each method are outlined. These methods were compared by evaluating published data from field measurements. Finite difference models were arranged for estimation of strata stiffness at the pillar location for comparison with the post-failure slopes of pillars of 5, 7.5 and 10 m İn width, which are the intended preliminary design for a UK coal mine. The estimated pillar width ranges of the methods for this example were compared. The findings are verified by those from previous investigations.

1 INTRODUCTION

The safety and productivity of the longwall mining method depend on the maintainence of ground control in the gate entries. The stability of a development roadway serving a new panel is ensured by leaving a stable pillar of such a width that the stresses induced by the nearby excavation do not significantly influence the level of original virgin vertical stress over the working region of a new panel. As longwall mining progresses to greater depths, conventional stable pillar designs require greater and greater pillar width. Widths in excess of 60 m are necessary to provide ground control under 600 m depth of cover. The narrow pillar, designed to yield during longwall mining operations, has been popular especially in the US and recently in the UK. It is used to increase productivity and to minimise problems associated with mining at greater depths. The pillar between the gate entries is designed such that the width/height ratio provides a destressed zone over the supply gate of the new panel by gradual yielding and transfer of the potentially dangerous stress concentrations to the adjacent pillar.

This work arose from the necessity of leaving a pillar between the gate entries of extraction and development panels in Bilsthorpe coal mine. This was the case after an extensive fall of the supply gate of a development panel driven immediately adjacent to the loader gate of an excavation panel had occurred. First, the theoretical basis for yielding pillars is explained. Then, a preliminary design for such a pillar with a view to safer supply gate location (Figure 1) is sought by evaluating various design methods and previous measurements of different field site applications. A finite-difference-method-based two-dimensional code, FLAC, was also used to determine the local mine stiffness by applying force to the roof for various pillar width configurations. Numerical analysis was also performed for the same configurations in order to investigate the magnitude of vertical stresses over the pillar after yielding.

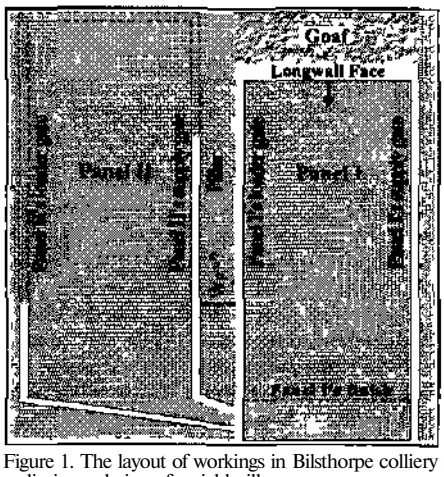

Figure 1. The layout of workings in Bilsthorpe colliery for preliminary design of a yield pillar

2 YIELDING PILLAR THEORY

The yielding pillar concept was first developed for room and pillar mining to create a destressed zone in the working area. The size of the pillars is determined so that yielding of the pillars is ensured and loads are transferred from the working area to the adjacent barrier pillars. The yield pillar system has proven more stable and more economic than abutment pillars at mining depths greater than 450 m. However, there have been documented cases of yield pillar successes at mining depths of less then 450 m (Kripakov et al., 1994). A conceptualised relationship between yield, critical and stable pillars in terms of gate road performance is illustrated in Figure 2. The horizontal axis represents the minimum performance standard differentiating stable gate road configurations from unstable configurations. A pillar design whose performance falls above the horizontal axis is considered successful, while a design whose performance falls below the horizontal axis is considered unsuccessful. The deterioration of ground conditions is generally more gradual for abutment pillars as pillar size decreases. Changes in performance are witnessed by the onset of minor floor heave, an increase in audible coal popping and an increase in the frequency of roof-related problems (Koehler et al., 1996).

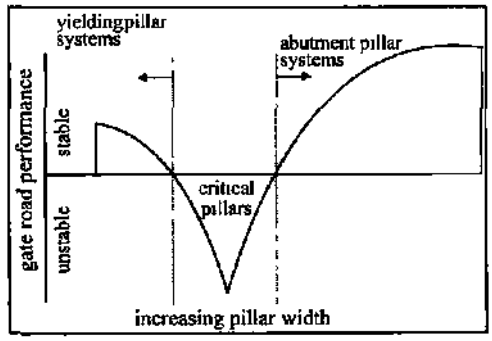

Figure 2. Conceptualisation of the yield pillar concept

Incorrect sizing of yield pillars can result in worsened entry conditions. Mark (1990) stated that between yield and abutment pillar sizes, there are intermediate pillar sizes that are too stiff to yield but also too small to redistribute stresses effectively within themselves. Such pillars, called "critical pillars", maximise disturbance of the surrounding ground. Field observation and stress measurements in a US coal mine showed that a 16.8-m pillar width at a depth of 800 m is a critical pillar design. Pillar sizes of 12.2 m and 10.6 m were found to be yielding pillars (Koehler et al., 1996). Studies İn British coal mines have shown that narrow pillars with widths in the range of 10-30 m result in a high degree of gate roadway closure, producing a 70% change in cross-sectional area (Whittaker & Singh, 1979). Figure 3 shows that when very large conventional pillars were used, better conditions were common. However, yield pillars exhibit better performance than critical-size pillars.

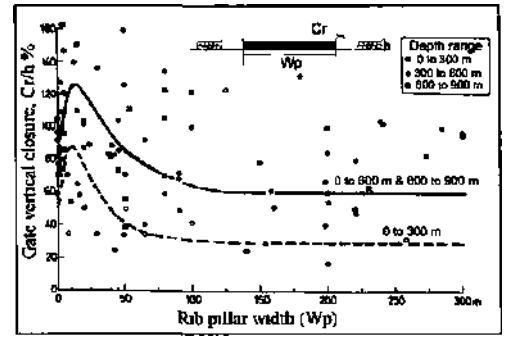

Figure 3 Statistical analysis of roadway closure for various pillar widths (Whittaker & Singh, 1979)

Holland (1973) studied the pressure arch concept for board and pillar mining and suggested that a pressure arch develops between the two barrier pillars in a panel when the pillars are designed to yield. İn this approach, the yield pillars are expected to redirect the overburden stresses to the solid abutments, thereby allowing greater extraction ratios within the panels. In the development stage of longwall mining, the pillar will be loaded by the tributary area theory. Where yield pillars are left under an intact pressure arch, the effective upper boundary of the tributary area is the bed separation limit. The pillar can be designed to yield either at the development stage or at the longwalhng stage. Figure 4a shows that the pillar is too wide to yield and yielding occurs at the ribs; the load carried by the yielded section is probably transferred to the inner pillar elastic core and to the abutment sides. In the second case (Figure 4b), the pillar is not proportioned so that it will retain sufficient flexibility and not pick up the full overburden load. The pillar load increases when die size of the entries is increased. However, tensile failure probability at the mid-span of the entry restricts the size of the entry. Failure of the pillar should occur İn a non-violent manner and it must maintain enough residual strength to support the weight of the rock within the pressure arch.

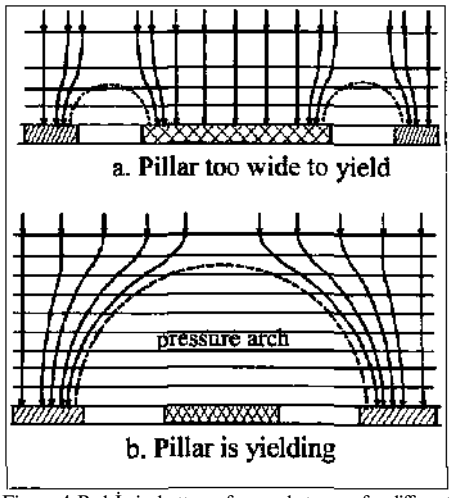

Figure 4 Red İ sin button of ground stresses for different pillar widths due to entry development

In the longwalling stage, cantilevered beds above the caved zone load the rib of the coal seam. These loads can cause excessive damage to the roadway depending on pillar behaviour. A theory was developed in the UK which states that a destressed zone develops inside an ellipsoid, while outside the ellipsoid the stress is high (Alder et al., 1951). The width of the ellipsoid 'b' shown in Figure 5 depends upon the cover depth. The vertical width of the ellipsoid is twice the horizontal width.

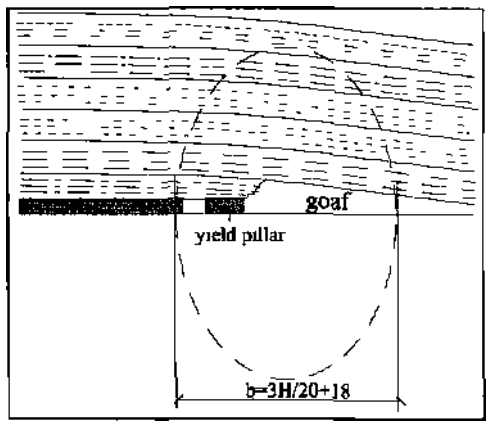

Figure 5 Pressure arch concept for longwalling stage of mining.

3 DESIGN OF A YIELDING PILLAR

A pillar design method should simply take into consideration that the width of a pillar should be adjusted so that yielding is ensured and that the width-height ratio should be adjusted so that it has high residual strength, maintaining the stability of the roadway. The failure and load-carrying capacity of a pillar depends on the intact and broken strength properties of the coal, the width-height ratio of the pillar, the rock properties and the properties of the rock-coal interfaces for a site-specific investigation. Current methods do not consider all of these factors. However, they can be applied to specific cases with the necessary experience in die field.

3.1 *Empirical methods*

In a two-entry system, the design of a yield pillar may be accomplished using empirical formulae and by determining a mine-specific safety factor through field experience. All empirically derived equations can be written in two types of expression.

$$S_p = S_i[\ A + B(w_p/h_p)\ ] \quad (1)$$

$$S_p = S_i(w_p^a/h_p^b) \quad (2)$$

where S_p is die pillar strength in MPa, Si is the in-situ strength of coal in MPa, w_p is the width of the pillar in m, h_p is the pillar height m m and A, B, a and b are constants expressing the shape effect (Table 1).

Table I. Details of pillar strength equations.

Author	A	B	a	b
Obert& Duval! (1967)	0.778	0.222		
Holland (1973)	-	-	0.5	0 5
Bieniawski (1984)	0 64	0.36		
Salamon & Munro (1967)	-	-	0.46	0 66

The empirically derived equations given above can predict the overall strength of squat pillars. The strength of infinitely long and rectangular pillars can be significantly greater than that of square pillars due to the greater confinement generated within them. The strength of large rectangular specimens may be expected to be the same as that of large square specimens with a side length equal to the effective width of rectangular specimens. Wagner (1974) suggested the following equation for estimating the effective width of long pillars:

$$W_{eff} = \frac{4.A_{pp}}{U_{pp}} \quad (3)$$

where App is the area of the pillar and Upp is the pillar circumference. According to equation 3, the

effective width of an infinitely long barrier pillar is twice the actual width.

The load coming over the pillar İs calculated using the tributary area method, which is commonly used in room and pillar mining. This load is called the development load and İs calculated as follows:

$$A_d = \gamma H \left(\frac{w_p + w_e}{w_p} \right) \quad (4)$$

where w_p is the pillar width (m), w_e is the entry width (m), H is the-depth (m) and y is the unit weight of the overburden (MN/m^3).

Empirical methods can be successful provided that correct selection of the safety factor, which is the ratio of pillar strength to stress imposed on the pillar, is made through field experience for each specific formula. A comparison was made for a depth of 600 m and a 2-m-thick seam. The strength equations give varying safety factors for the same pillar width as illustrated İn Figure 6. This difference İs more significant when the width of the pillar increases. Carr (1992) reported that safety factors in the range of between 0.52 and 0.73 were successful. The width of the pillar to yield ranges between 6 and 11.5 m. This range of widths İs in agreement with successful field applications, as shown below.

Although the empirical design of pillars gives an idea of the width-height ratio of the pillar where yielding is expected, it does not estimate the failure behaviour of a pillar that exhibits either gradual or sudden failure.

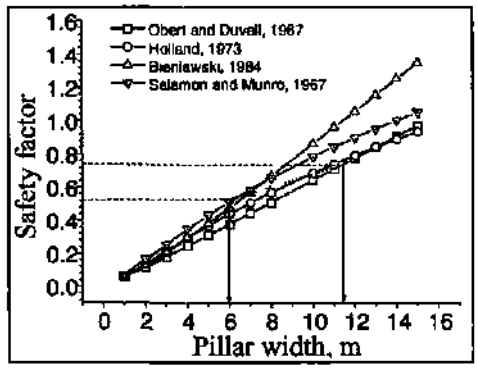

Figure 6. Yield pillar width ranges for 2-m pillar height.

3.2 *Mine stiffness concept*

In-situ tests performed by Wagner (1974) clearly showed that the failure of a pillar is a gradual process as shown in Figure 7. The distribution of the load across *the* cross-section of the pillar varies as the loading proceeds. Yield at the pillar edges and an increase in the load bome by the pillar core can be seen clearly. Wagner's tests proved conclusively that a pillar has a significant load-bearing capacity even when its maximum resistance, which is traditionally regarded as the strength of the pillar, has been overcome. This is the main area of interest in the design of yield pillars.

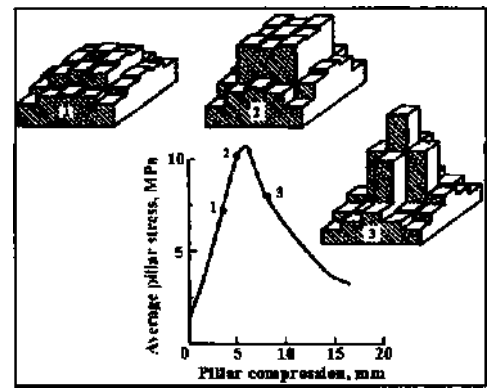

Figure 7. In-situ complete stress deformation curve and stress distribution of pillar with width/height ratio of I (Wagner, 1974).

The deformation characteristics of coal pillars were investigated by means of underground tests on large coal specimens which were carried out by Van Heerden (1975) in South African coal mines. The results of these tests indicated that the deformation characteristics, in particular the post-peak behaviour, of coal pillars are not only a function of die coal itself, but most importantly of the pillar geometry (Figure 8). These tests can be used for the estimation of stiffness estimation in pillars with width/height ratios of up to 3.5.

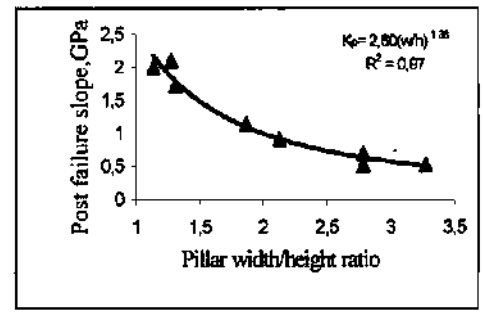

Figure 8. Effect of width/height ratio on the post-tailure slope of coal pillars (Van Heerden, 1975).

Bearing in mind the yielding mechanism of pillars, Salamon (1970) showed that equilibrium

between the loading of a pillar and post peak pillar resistance is stable, regardless of the convergence experienced by the pillar if;

$$K_{LMS} - K_P < 0 \quad (5)$$

where $K^{\wedge}$ is the stiffness of the loading strata and K_P is the minimum slope of the post-peak load-deformation relation for the pillar (both $K^{\wedge}$ and K_P have negative values). These cases are illustrated in Figure 9, showing that the relation between the stiffness of the strata and post-peak load deformation determines the stability condition of the pillar.

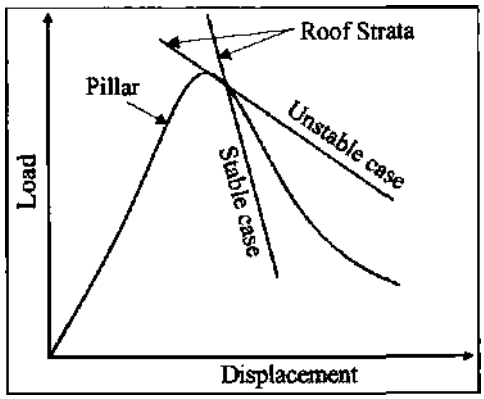

Figure 9 Stable and unstable cases for a pillar depending on stiffness of loading strata.

In assessing the stability of a mine structure, the required information consists of the post-peak stiffness of the pillar and die mine local stiffness at various pillar positions. The stiffness of the strata at an individual pillar location, local stiffness, is described as the load deformation between the hanging wall and footwall. The finite difference method was utilised to find the stiffness of strata at a pillar location at Bilsthorpe coal mine. The model conditions are illustrated in Figure 10. The average depth is 600 m. The deformation modulus of the rock mass is 14 GPa. The detailed input data for the Mohr-Coulomb plasticity model was described by Yavuz (1999).

The pillar was replaced by stresses for pillar widths of 5, 7.5 and 10 m as illustrated in Figure 10. The strains between the hanging wall and footwall at the pillar location are plotted against the stress applied on the roof (Figure 11). The post-failure slopes of the 5, 7.5 and 10-m pillars were found to be 0.73, 0.42 and 0.28 respectively from the equation given in Figure 8. If the slope values of the strata given in Figure 11 and the post-failure slope values are put into equation 5, an unstable condition will be expected for 5 and 7.5-m. pillar widths. This finding is questionable in terms of the predicted post-failure slopes for pillars with width/height ratios of 3.75 and 5 due to the unavailability of data.

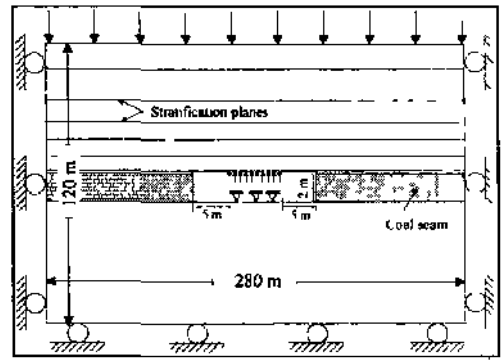

Figure 10. Modei conditions for mine stiffness estimation

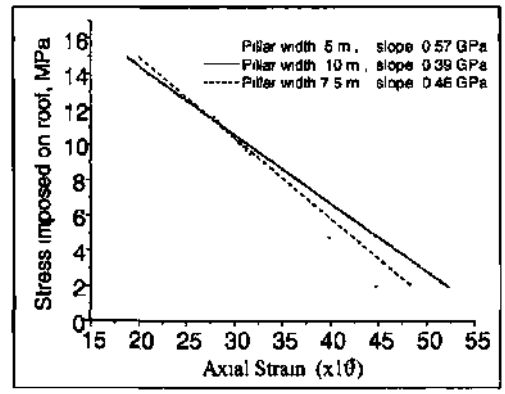

Figure 11 Stress & strain relation from roof to floor for 5, 7 5 and 10-m pillar widths

3.3 *Enhanced confined core method*

The friction between the loading platens and the specimen significantly affects the strength of the specimen under uniaxial loading conditions This will be a primary factor in the generation of confining pressure and increase in strength. The Wilson confined core concept considers confinement of the pillar; how ever, this method İs based on an assumed horizont.il restraint and does not consider the level of confinement for varying properties of the coal-rock interfaces. It is a known fact that if the friction angle is reduced due to filling material, the strength of the coal is reduced.

Salamon (1992) developed an enhanced confined core concept which takes the coal-rock interface properties into account Failure at pillar edges depends upon the following criterion:

$$\sigma_{max} \geq kp + S_1 \quad (6)$$

where k= $(1+\sin\phi)/(1-\sin\phi)$, ϕ is the friction angle of the coal, p İs the pillar side restraint, S, is the in-situ compressive strength of the coal, and σ_{max} is the maximum stress at the edge of the fully elastic pillar, found by the following equation:

$$\sigma_{max} = q\left[1 + \frac{w_e'}{\theta h \tanh(w_p'/\theta h)}\right] \quad (7)$$

where q is the vertical virgin stress, $w_e = w_e / 2$, w_e is the entry width, $w_p = w_p/2$, w_p is the pillar width (Figure 12), h is the seam thickness, and the constant 6 İs given by the following relation:

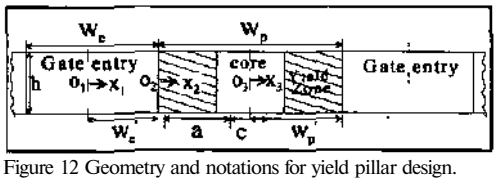

Figure 12 Geometry and notations for yield pillar design.

$$\theta = \left[\frac{(1-\upsilon_s-2\upsilon_s^2)\lambda E}{2(1-\upsilon_s)hE_s}\right]^{1/2} \quad (8)$$

where E, andt), are the Young's modulus and Poisson's ratio of the seam. E is the Young's modulus of the rock. X is a constant related to the deformation of the surrounding strata found from $X= H / 2(\hat{u}^2$, (0 is a constant related to surface subsidence. Salamon suggested values for to of 5-7 for coal mining. If equation 6 satisfies the condition, the pillar edges will yield and the load-bearing capacity of the pillar is found as follows:

$$S_{max} = \frac{p}{\mu R_p}(e^{\eta R_p/2} - 1) \quad (9)$$

where R_p is the width/height ratio of the pillar, p. is the interface coefficient of friction(ti = tan(p), <p is the interface friction angle and

$$\eta = 2\tan\phi\left[\frac{\sin\varepsilon_m}{1-\sin\phi\cos\varepsilon_m} + 2\tan\phi\tan^{-1}\left(\frac{1+\sin\phi}{\cos\phi}\tan\frac{\varepsilon_m}{2}\right)\right] \quad (10)$$

$$\varepsilon_m = \sin^{-1}(\mu/\tan\phi) \quad (11)$$

The load on the pillar is estimated by using the tributary area method in the following way:

$$q_m = \frac{w_p + w_e}{w_p} q \quad (12)$$

If the load q_m exceeds the load-bearing capacity of die pillar S_{max}, then the pillar fails. If it does not exceed the load-bearing capacity, then the pillar edges will yield, but the pillars will be able to sustain the load.

The changes in the width of die pillar for failure were investigated for a depth of 600 ra, wheic S, is 5 MPa, γ is 0.025 MN/m^3, E is 10 GPa, E_s is 2.5 GPa, υ_s is 0.3, ω is 7, h is 2 m and w_e is 5 m. The width of the pillar was calculated. This width is given in Table 2 for different friction angles of coal and interface and for different side restraints.

Table 2. The width of the pillar for complete yield for various friction angles for (ϕ), bedding friction a n g (φ) n d edge restraints (p).

ϕ (deereet	φ (degree)	p(MPa)	Wp(m)
35	25	0.1	8.4
30	25	0.)	10.9
35	20	0.1	9.9
35	25	0.02	10.9

3.4 *Numerical method*

As mentioned above, a yielding pillar provides a destressed zone around the entries by transferring the stresses from over the pillar to over abutment sides. The numerical modelling technique, when compared to the other design methods, is a powerful method for demonstrating the yielding situation of a pillar and stress state over the working area provided that enough in-situ data are available to construct the models. Although most design methods ignore the stress distribution within the pillar and interaction between the roof, pillar and floor, these data can be taken into consideration in numerical models. Parametric studies and field applications showed the importance of these factors in the design of yielding pillars. Numerical models using a two-dimensional finite difference code, FLAC, were arranged for investigation of the stress magnitudes over the pillar

under the influence of depth stress and front abutment stresses. The boundary conditions of the models are the same as those given in Figure 10. A strain-softening model constituted the post-failure behaviour with widths of 6, 7.5 and 10 m for the model pillars. By applying back analysis to the data available from the large-scale tests of Van Heerden (1975), the friction angle and cohesion of the yielded coal were found to be 23° and 0.35 MPa. The in-situ compressive strength and deformation modulus of the coal mass are 4.78 MPa and 2.5 GPa. The rock mass surrounding the working area is quite strong. Bedding planes, illustrated in Figure 10, were also modelled and the friction angle between the coal-rock interface is 27 degrees.

The distribution of vertical stresses immediately above the pillar, gate entry and abutment are illustrated in Figure 13. In this model, it is assumed that the Iongwall face is far enough for building up front abutment stress over the modelled section. The stresses are illustrated for just a half side of the pillar due to its symmetry. The findings from these models are that a 6-m pillar yields and retains a small amount of stress, about 10 MPa, at the centre of the pillar, while 7.5 and 10-m pillar rib sides yield. However, the pillar core retains a significant quantity of stresses.

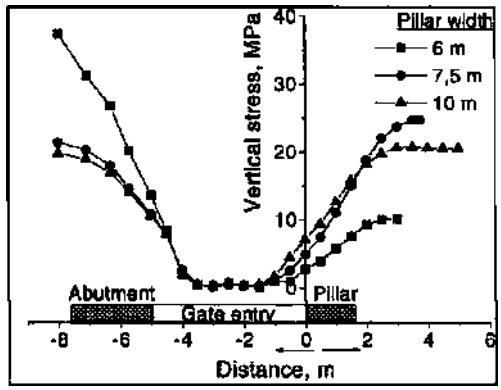

Figure 13. The stress state over the wotting region and pillar at a depth of 600 m with no front abutment stress.

The vertical stress was gradually increased over the vertical upper boundary of the models in order to represent the front abutment stresses over the modelled section. The stress distribution over the modelled section illustrated in Figure 14 is just for a 25-MPa boundary stress condition. In this case, no increment occurred over the 6-m pillar; excess stresses were transferred to the abutment side. It is interesting to note that the 7.5-m pillar failed gradually with the increment of front abutment stresses and the stress at the centre of the pillar decreased from 25 MPa to 19 MPa. The 10-m pillar width can be regarded a critical width for the properties assigned to the model.

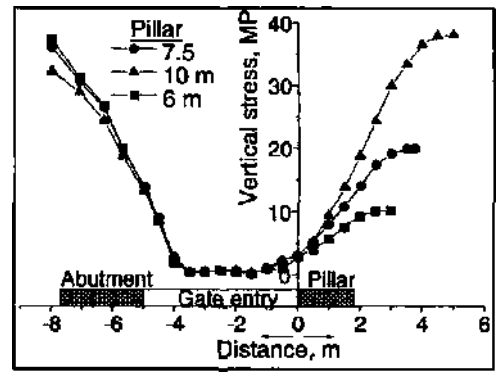

Figure 14. The stress state over the working region and pillar at 600 m depth with front abutment stress

Parametric studies showed that the properties of the pillar-rock interface, as well as the softening properties of die coal material, significantly influence the yielding state of a pillar and stresses over the pillar and working area.

3.5 *Field experience and stress measurements*

The difficulty in stress measurement is the reliability of the obtained values. However, the evaluation of stress measurements and observation of roadway stability is a practical method of site-specific design, especially for yield pillars. The width of the pillar to yield during the development loading or the side abutment loading stage ensures improved ground conditions for pillars between 6 and 10 m wide, depending on the coal mass strength, seam height, roof and floor constraint and mining depth. The application of these sizes is generally successful in deep mines (Table 3). However, a 9-m-wide pillar failed to yield properly under 365 m of cover load, and at some mines, the changing of a proven successful design to slightly larger 12-15-m yield pillars under deeper cover seems to have resulted in renewed ground control problems, both in the roof and floor (Demarco et al., 1988).

4 CONCLUSIONS

For a pillar to be called a yielding pillar, it must display gradual yielding, not sudden failure, and maintain enough residual strength to support the weight of the rock within the pressure arch during

Table 3. Yield and critically sized pillar widths at various depths in the field.

Pillar width (m)	Depth (m)	Yield condition	Pillar core stress (MPa)	Face position (m)	Reference
16.8	795	critical	65	0	Ko*leraaL1996
12.2	580	yield	20	-24	KœhkyetaU996
10.6	855	yield	-	-	KœhfcxetaU996
9	460	yield	12	0	Demacoaall988
9	460	yield	14	0	Danacoetall988
6.1	610	yield	7	76	Newiml989
10	840	yield	10.5	25	HadnetaL1997

*(0 longwall race is approaching measurement point

the development and side abutment loading stages of mining. The current design methods introduced in this study are not unique themselves to explain the yielding mechanism of these pillars. All the methods used for the preliminary estimation of long yielding pillar width ranges for Bilsthorpe Colliery estimated a reasonable width range when compared to the previous applications. The main conclusions of this study can be summarised as follows:

1. Empirical equations with regard to the tributary area method predicted a width range for a yielding pillar of between 6 and 11.5 metres for Bilsthorpe colliery by considering safety factors between 0.5 and 0.73. The ultimate strength concept, of course, does not consider the residual strength of the pillar, interaction between die roof, pillar and floor, and the stress distribution within the pillar. However, diese factors can be taken into account by determining a site-specific safety factor. This means that generally the predicted width ranges of the empirical equations are acceptable based on field experience.

2. The mine stiffness concept has two weaknesses in predicting the stability of a yielding pillar. Firstly, there are not enough data available for the post-failure slopes of large-scale pillars. Secondly, it does not take the pillar-roof interface properties into consideration. The predicted post-failure slopes and calculated stiffness values from the numerical models suggested that a 10-m pillar could be regarded as a yielding pillar, while the 5 and 7.5-m pillar widths were found to be unstable in a two-entry system. This finding is true for the 10-m pillar; however, the 7.5-m pillar width in the two-entry system is a yielding pillar in some mines.

3. The confined core concept is a valuable analytical method in comparison to the other analytical methods in which no account is paid to the properties of coal-rock interfaces. However, pillar side restraint is based on an assumed value which strongly affects prediction of the yielding width of a pillar. There İs no attention paid İn this method to the post-failure properties of the pillar.

4. Numerical modelling has certain advantages when compared to the other methods since it takes the main factors into account in the yielding process of the pillar. However, the prediction and reliability of results in mis method depend on the availability of in-situ data. For a pillar height of 2 m, the predicted width of the yielding pillar for the properties assigned to the models is 6 m, without considering the front abutment stress. The 7.5-m pillar can also be regarded as a yield pillar. The 10-m pillar, which was determined for this example mine as a critical width, could be successfully applied in other mines, depending on the shear strength properties of rock-coal interfaces as well as the softening properties of the coal material.

REFERENCES

Alder, H., Potts, E. L. J. & Walker, A. 1951. Research on strata control in the northern coalfield of Great Britain. *A8, International Conference About Rock Pressure and Support in the Workings.* : 106-134.

Bieniawski, Z. T. 1984. *Rock Mechanics Design in Mining and Tunnelling. A. A. Balkema.*

Carr, F. 1992. Ten years' experience of the Wilson/Carr pillar sizing method at Jim Walter Resources, inc. *Workshop on Coal Pillar Mechanics and Design. :* 166-179.

Demarco, M. J., Koehler J. R. & Lu, P. H. 1988. Characterisation of chain pillar stability in a deep Western Coal Mine - a case study. *Min. Eng.* 40(12), 1115-1119.

Hendon, G., Carr, F., Lewis, A. C. & Cassie, J. 1997. A co-operative study of gate entry designs - Welbeck Colliery (UK) and Jim Walter Resources (USA). *Mining Technology.* 79(909), 115-121.

Holland, C. T. 1973. Mine pillar design. *SME Mining Engineering Handbook. Soc. Min. Eng. AIME.:* 1: 13/96-13/118.

Koehler, J. R., Demarco, M. J. & Wuest, W. J. 1996. Critical pillar concept in yield pillar based longwall gate road design. *Min. Eng.* 48(8), 73-78.

Kripakov, N. P., Sun, M. C. & Donato, D. A. 1994. Automation of a progressive failure procedure for analysis of underground mine pillar designs. *Proc. of IS'* Int. Conf. on Ground Control in Mining.,* 59-68.

Mark, C. 1990. Pillar design methods for longwall mining. *BuMines IC 9247.*

Newman, D. A. 1989. In-situ yield behaviour of a coal pillar. *Int. J. of Mining and Geological* Engineering. 7,163-170.

Obert, L & Duvall, W. 1967. *Rock Mechanics and Design of Structures in Rock. Wilev. New York.*

Salamon, M. D. G. & Munro, A. H. 1967. A study of the strength of coal pillars. *Journal of the South African Institute of Mining and Metallurgy.* 55-67.

Salamon, M. D. G. 1970. Stability, instability, and design of pillar workings. *Int. J. Rock Mech. Min. Sei. & Geomech. Abstr.l,* 613-631.

Salamon, M. G. D. 1992. Strength and stability of coal pillars. *Workshop on Coal Pillar Mechanics and Design.* 94-121.

Van Heerden, W. L. 1975. In-situ determination of complete stress-strain characteristics of large coal specimens. *J. S. Afr. Inst. Min. Metall.* 75(8), 207-217.

Wagner, H. 1974. Determination of the complete load-deformation characteristics of coal pillars. *Proc. 3rd Int. Cong. Rock. Mech.* 1076-1081.

Whittaker, B. N. & Singh, R. N. 1979. Design and stability of pillars in longwall mining. *The Mining Engineer.* 59-71.

Yavuz, H. 1999. *Physical and Numerical Modelling of Pillar* Protected Mine Roadways. PhD. Thesis, Leeds University.

1 /" International Mining Congress and Exhibition of Turkey- IMCET2Q01, © 2001, ISBN 975-395-417-4

Investigation into Relationship Between Cutting Depth and Vibration in Cutting Process

Y.Ozcelik, S.Kulaksiz & LC.Engin
Department of Mining Engineering, Hacettepe University, Ankara, Turkey
A.S.Eyuboglu
Department of Applied Science, University of Arkansas at Little Rock, AR, USA

ABSTRACT: Vibration occurs in disc cutter machine during the cutting process of hard rock. If the vibration frequency is high, cutting quality can decrease, the segments on disc can wear untimely, deteriorate rapidly, and energy consumption can be higher. The aim of the study is to measure the magnitude of vibration occuring in the equipment during the cutting process and to investigate the relationship between the cutting depth and vibration frequency. Experiments performed include the measurements of the components of the vertical, lateral and longitudinal particle velocity, effective frequency and highest vectorial resultant values as a function of the cutting depth. About 40 Hz average effective frequency value was measured. The only relationship was observed between the cutting depth and lateral particle velocity. Consequently, it was found that when the cutting depth increases, the lurching in the cutting machine decreases,

1 INTRODUCTION

Circular diamond saw blade used in the stone industry contains a steel core which has diamond impregnated segments brazed on the periphery (Fig. 1). The two basic functions of the segments (metal bonds) are to hold the diamond tight and to erode at a rate compatible with the diamond loss. Due to a large variety of sawing conditions many metal matrix compositions are in general use. Bonds based on copper, various bronze, compositions, cobalt, tungsten, tungsten carbide as well as combinations there of cover a wide range of stone sawing applications. Sometimes small amount of iron, nickel etc are added to aid the manufacturing process or in belief that the addition improves diamond retention or matrix wear properties; however, the complexity of compositions encountered in production practice, which in same cases comprise seven components makes a scientific approach to the total behaviour extremely difficult or even impossible (Konstanty 1991; Ozcelik et al. 2000;OzceIiketal.2001).

In general, stone cutting by circular saw blade method influenced by many factors. These factors are divided in to 3 groups (as shown in Table. 1) (Ozcelik et al. 2000; Eyuboglu, 2000; Kulaksiz et al. 2000; and Ozcelik et al. 2001).

Vibration occurs on a rock cutting machine during the cutting process of hard rock with circular blades. When the vibration frequency is high, cutting quality decreases, segments on disc can wear untimely, deteriorate rapidly, and energy consumption can be higher (Eyuboglu, 2000; Kulaksiz et al. 2000).

As seen from the Table 1, the technical properties of the working conditions such as cutting speed, peripheral speed, depth of cutting, water quantity and vibration of the machine are very important for stone cutting by circular saw blade.

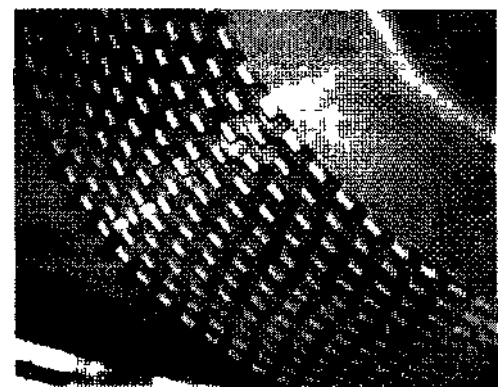

Figure I. Circular diamond saw blade

Table 1. Factors effecting the stone cutting by circular saw blade

Unchangeable Parameters	➢ Engineering Properties of Sawing Material
	⇒ Physico-Mechanical Properties
	⇒ Chemical Properties
	⇒ Mineralogical Properties
	⇒ Pétrographie Properties
	⇒ Particles Orbit and Filled Discontınıtİes
	⇒ Textural Properties
	⇒ Structural Properties
	⇒ Weathering Characteristics
Changeable Parameters	➢ Properties of Cutting Equipment
	⇒ Disc Diameter
	⇒ Blade Structure
	⇒ Metallurgical Structure of Matrix
	⇒ Tolerance Boundary
	⇒ Diamond Type
	⇒ Wear Types in Segment
	⇒ Peripheral Speed
	➢ Technical Properties of Working Conditions
	⇒ Feeding Forces
	⇒ Water Quantity
	⇒ Cutting Speed
	⇒ Power of the Machine
	⇒ Depth of Cutting
	⇒ Up and Down Cutting Parameters
	⇒ Traverse rate
	⇒ Vibration of the machine

Nowadays, there are different model seismographs with and without record unit. These are small, more powerful and so they are used easily and have a high capacity for recording of vibration. Generally they have a rechargeable accumulator İn their constitution. These equipments measure the particle velocity and also give the displacement and acceleration values by calculation. When displacement and acceleration are important parameters for the study, they should be measured directly in the study. The maximum particle velocity value measured by typical seismograph is 254 mm/s and frequency interval is 2-200 Hz (Erkoc & Esen 1998).

Particle velocity is defined as the movement velocity of particle on the ground. Initial particle velocity is zero and die particle velocity decreases after reaching the maximum velocity value. Frequency shows the number of vibrations of the particle on the ground per second. Frequency is expressed by Hertz (Hz)(Kulaksizetal.2000).

The scope of this study was to determine the existence of die relationship between vibration values and cutting depth.

2 EXPERIMENTAL STUDY

The seismograph machine (Fig 2) was taken from Middle East Technical University Mining Engineering Department (Ankara, Turkey) for determining the vibration frequencies occur during the cutting of andésites.

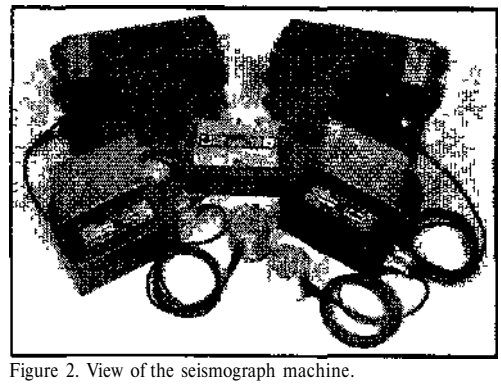

Figure 2. View of the seismograph machine.

Vibration (particle) velocity and frequency values were taken with seismograph at different cutting depth during the cutting process with disc cutter. Vertical, lateral and longitudinal velocities and highest vectorial resultant values were obtained during measurements. During the experiments, the velocity of 1200 mm in diameter circular saw blade was set at 13.1 m/rain and the cutting depth was set at 1.2 mm for forward motion and 1.1 mm for backward motion and also diamond impregnated segments in the circular saw blade were used. These constant operating parameters of this study are shown in Figure 3.

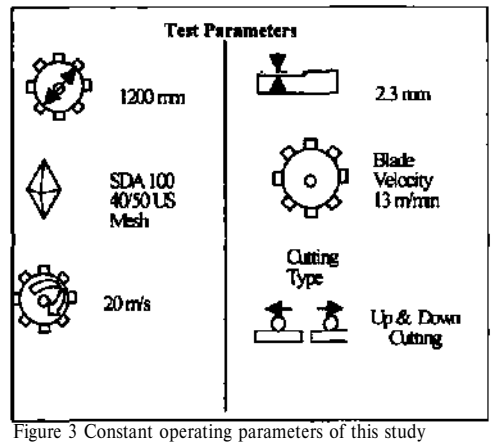

Figure 3 Constant operating parameters of this study

3 RESULTS AND DISCUSSION

Experimental values include vertical, lateral, longitudinal particle velocities (mm/s), effective frequency and highest vectorial resultant value (mm/s) as a fonction of cutting depth and results obtained were given in Table 2. Furthermore, the relationships among these properties and cutting depth were investigated and results were given in Figure 4.

When the relationship between particle velocity and cutting depth was investigated (Fig. 4), it was observed that there was no correlation between them. Lateral particle velocity varies among 0.5, 0.63 and 0.76 mm/s, vertical particle velocities were same (0.38 mm/s) except the 0.25 mm/s particle velocities at 22 cm cutting depth. Longitudinal particle velocity values vary between 0.5 and 0.63 mm/s and highest vectorial resultant value are determined among 0.63, 0.76 and 0.88 mm/s. When the relationship between lateral particle velocity and cutting depth was investigated (Fig. 4), decreasing of lurching was seen with increasing of cutting depth. Any relationship was not determined İn other figures. When the relationship between frequency values and cutting values was investigated (Fig. 4); it was determined mat lowest value of lateral effective frequency was 12.8 Hz, highest value of lateral effective frequency was 64 Hz, lowest value of vertical effective frequency was 25.6 Hz, highest value of vertical effective frequency was 51.2 Hz, lowest value of longitudinal effective frequency was 18.9 Hz, highest value of longitudinal effective frequency was 56.8. Any relationship can not be found between cutting depth and all effective frequency.

4 CONCLUSION

Many parameter affect the cutting process during sawing of rocks. These parameters are unchangeable properties related with rock, changeable and/or semi-changeable properties related with circular blade. Each variable should be controlled for economical cutting and desired capacity and it is necessary to perform the conception according to these.

During cutting process, approximately 40 Hz average effective frequency value was measured. During this process, only one relationship was determined, this was between cutting depth and lateral particle velocity. Increasing of cutting depth causes decreasing of lurching. Any relationship can not be found between other vibration values and cutting depth.

ACKNOWLEDGEMENTS

The authors would like to thank to Assoc. Prof. Aydin Bilgin and Research Assistant Sedat Esen for their kind help throughout the research.

REFERENCES

Erkoc O. Y., & Esen, S. 1998. Measurement of blast induced ground vibrations and the evaluation of the vibration recording device outputs, *3rd Drilling and Blasting Symposium,* Ankara, pp. 139-147, (in Turkish).

Eyuboglu, A. S., 2000. Investigation of segment wear on disc cutting machines in Ankara andésites, M.Sc. Thesis, Hacettepe University, Ankara, 133 p. (unpublished) (in Turkish).

ISRM, 1981. Rock Characterisation testing and monitoring; suggested methods: Oxford, 16 p.

Konstanty, J., 1991. The materials science of stone sawing, *Industrial Diamond Review,* No: 1, pp. 27-31.

Kulaksiz, S., Ozcelik, Y., Eyuboglu, A.S., Engin. I.C, Gene, Y., 2000. Statistical and microscopic investigations of diamond segment wear after sawing of hard rocks by circular disc, *Hacettepe University Research Fund,* Project No: 99 02 602 003 (unpublished).

T.S.E., 1987. Testing and examination methods of natural building stones, T.S. 669, TSE. Press, Ankara, 82 p. (in Turkish)

Ozcelik, Y., Eyuboglu, A. S., Kulaksız, S., Engin. I.C, Özgüven, A., 2000. Investigation of the affect of up and down cutting parameter on the current consumed in the process of cutting with disc in hard rocks, *V. National Rock Mechanics Symposium of Turkey,* pp. 123-128.

Table 2. Partical velocity (P.V.) and effective frequency values occurred during the rock cutting with disc cutter.

Record Number	Current (Ampere)	Recording Time	Cutting Depth (cm)	Lateral Partical Velocity, ppv, (mm/s)	Vertical Partical Velocity, ppv, (mm/s)	Longitudinal Partical Velocity, ppv, (mm/s)	Highest Vectorial Resultant Value, pvs, (mm/s)	Lateral Effective Frequency, (Hz)	Vertical Effective Frequency, (Hz)	Longitudinal Effective Frequency, (Hz)
2	124	10.57	0	0.50	0.38	0.50	0.63	64.0	39.3	36.5
3	148	10.59	1.0	0.76	0.38	0.50	0.88	17 0	36.5	20.4
4	148	10.59	1.3	0.63	0.38	0.50	0.63	18.9	36.5	18.9
5	152	11.00	1 5	0.63	0.38	0.63	0.76	17.6	30.1	30.1
6	152	11.02	2 0	0.76	0.38	0.63	0 88	18.2	34.1	19.6
8	154	11.10	5.0	0.63	0.38	0.63	0.76	25.6	46.5	30.1
9	154	11.10	5 0	0.63	0.38	0.63	0.63	26.9	39.3	26 9
10	157	11.21	10.0	0.50	0.38	0.63	0.63	19 6	32.0	34.1
11	157	11.21	10.5	0.63	0.38	0.63	0.63	12.8	36 5	34.1
12	158	11.32	15.0	0.50	0.38	0.50	0.63	28.4	34.1	30.1
13	158	11.39	18.0	0.50	0.38	0.50	0.63	23.2	36.5	32 0
14	158	11.43	20.0	0.50	0.38	0.63	0.63	32.0	25.6	56.8
15	160	11.45	21.0	0.63	0.38	0.63	0.76	21.3	34.1	32.0
16	161	11.47	22.0	0.50	0.25	0.50	0.63	64.0	51 2	32.0
20	161	11.50	23.0	0.63	0.38	0.50	0.63	23.2	34.1	34.1

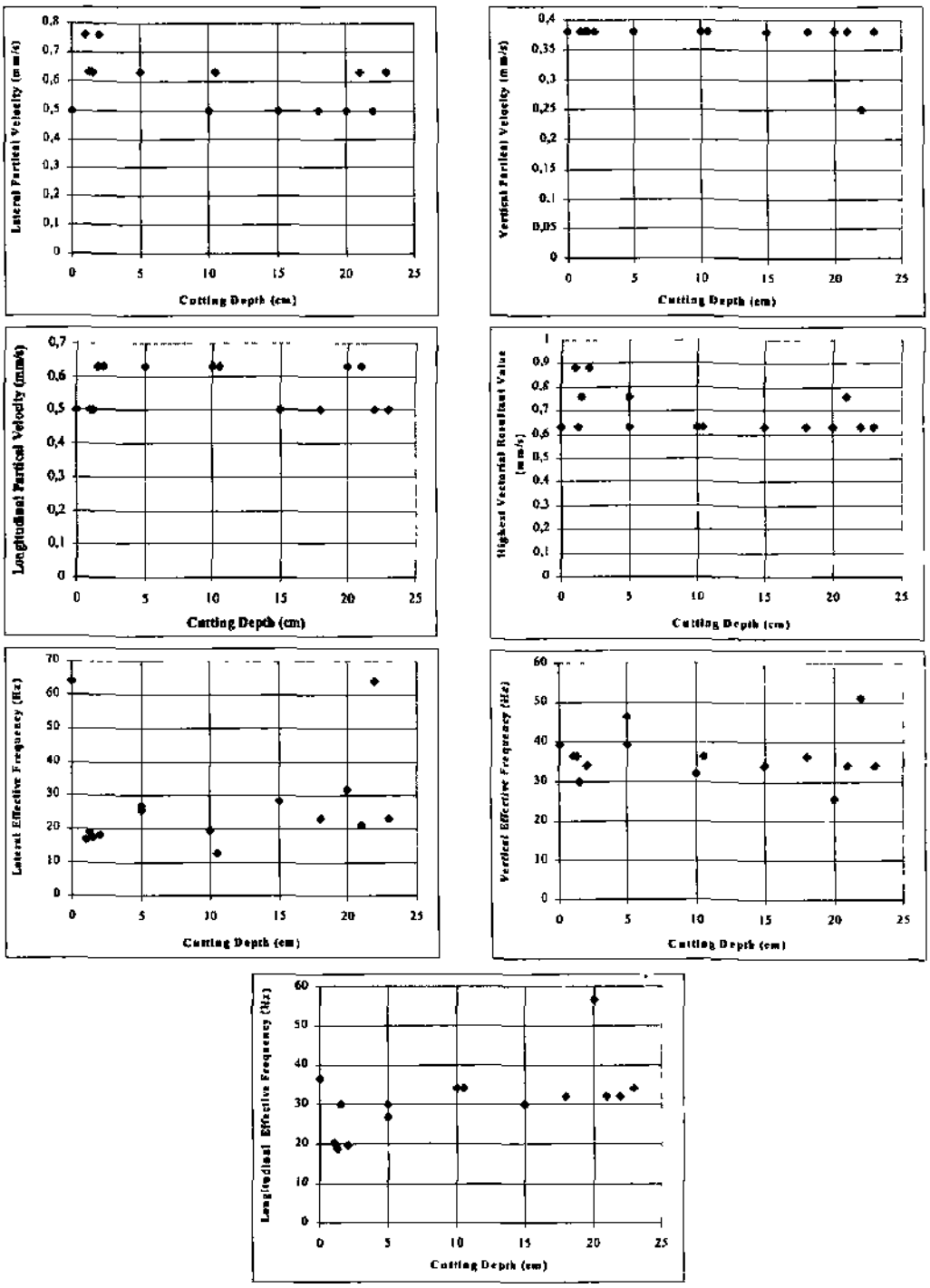

Figure 4 Relationships between particle velocity, effective frequency and cutting depth.

17* International Mining Congress and Exhibition of Turkey-İMCET 2001,® 2001, ISBN 975-395-417-4

The Effects of Specimen Volume, Temperature and Water Content on Shore Hardness

R.Altındağ
Department of Mining Engineering, Süleyman Demirel University, İsparta, Turkey

ABSTRACT: In this study, the effect of specimen size, temperature and water content on Shore hardness is investigated. With this objective, core samples of different sizes were prepared from nine different types of rocks. Firstly, Shore hardness (SH) tests on these samples were conducted and hardness values were determined using Shore scleroscope apparatus. Secondly, the same specimens were conditioned in a drying-out cupboard at different temperatures. Then, the Shore hardness values of the saturated specimens were obtained according to specimen volume. In order to determine die SH values of the rocks, the minimum test specimen volume required is suggested.

1 INTRODUCTION

Shore hardness (SH) value, one of the main physical properties of rocks, is essentially influenced by rock mineralogy, elasticity and cementation. The physical and mechanical properties of rocks are used for drillability analyses in laboratory and field studies. The SH values of rocks are used for various purposes. SH value is used in empirical equations in the literature with regard to drillability (Rabia & Brook, 1981), the efficiency of roadheaders and wearing of drilling tools. The SH value is also used to determine the uniaxial compressive strength of rocks (Wijk, 1980; Atkinson, 1993; Holmgeirsdottir & Thomas, 1998; Onargan et al. 1997).

Therefore, a reliable determination of the SH value of rocks is very important. The differences in the size of the specimens affect the Shore hardness value (Rabia & Brook, 1979; Misra, 1972; ISRM, 1978). Thus, it is impossible to compare test results presented in literature.

2 PREVIOUS WORK

Misra (1972) suggested that a specimen should have a diameter of 25 mm (surface area of 4.91 cm^2) and thickness of 5 cm for determining its Shore hardness value (Rabia & Brook, 1978).

According to the method proposed by the International Society for Rock Mechanics (ISRM, 1978), a test specimen with a minimum surface area of 10 cm^2 and a minimum thickness of 1 cm should be used.

Rabia & Brook (1978) suggested that die minimum specimen volume should be 40 cm^3 for determination of the Shore hardness of a specimen. They proposed that a minimum of 50 measurements should be made on 5 specimens and the arithmetical average of these measurements should be used for the determination of the SH value of a specimen.

3 THE EFFECT OF SPECIMEN VOLUME

In Üiis study, cores were drilled from nine different rocks at 54 mm in diameter. For each rock, approximately 7-8 specimens were prepared. Firstly, the SH values were measured for each rock of different volume. Then, the specimens were conditioned in a dry-out cupboard at temperatures of 20°C, 60°C and 120°C. The Shore hardness values of the specimens were measured for each temperature.

For the SH measurement, about 3500 readings were made using a C-2-type Shore scleroscope according to the suggested methods of the International Society for Rock Mechanics {ISRM, 1978).

The relationships between specimen volume and Shore hardness are illustrated in Figures 1-7. The Shore hardness values of the specimens were found to increase depending on the specimen volume up to the critical volume. Specimens with volume greater than 80 cm^3 did not show significant variations in SH value.

The arithmetical average of the SH values, which were measurements at the horizontal level of the

curve, was taken as the Shore hardness value of die specimen. The specimen volume curve at dus point, where it begins to extend horizontally, İs the volume for determining the SH value of the specimen. This point shows the necessary minimum specimen volume for determining SH. It was determined that the minimum specimen volume was 80 cm^3 in all the tests for nine different rocks. Therefore, it is suggested that die minimum specimen volume should be 80 cm^3 for the determination of the SH of a specimen. This finding is different from the specimen volume values suggested by previous workers.

Finally, the effects of the specimen volume and temperature on Shore hardness were investigated.

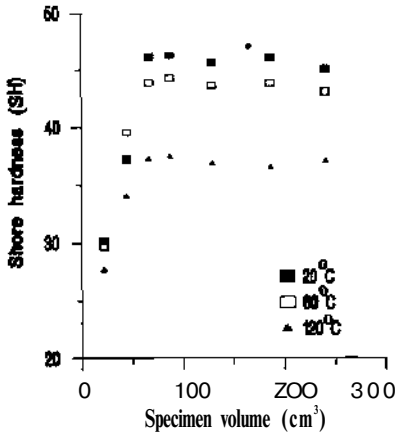

Figure 1. The relationship between specimen volume and Shore hardness value of the 1 st rock type

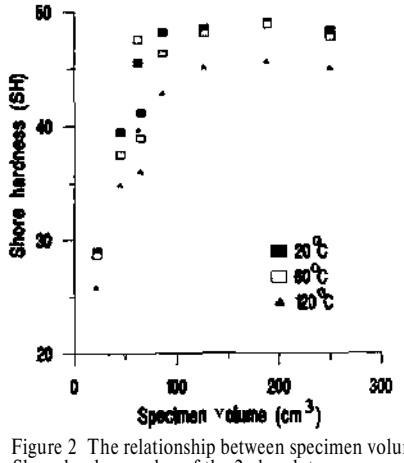

Figure 2 The relationship between specimen volume and Shore hardness value of the 2nd rock type

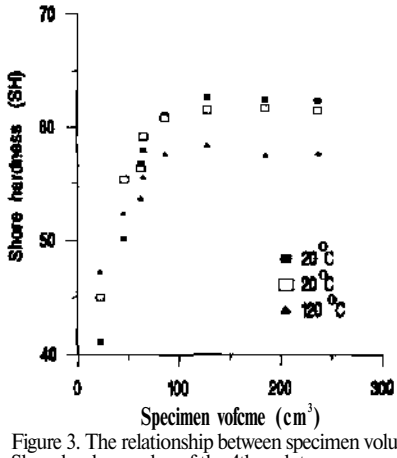

Figure 3. The relationship between specimen volume and Shore hardness value of the 4th rock type.

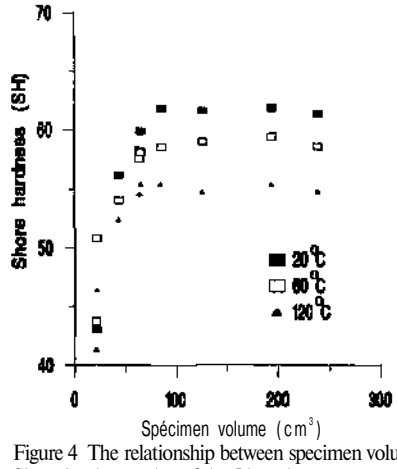

Figure 4 The relationship between specimen volume and Shore hardness value of the 5th rock type.

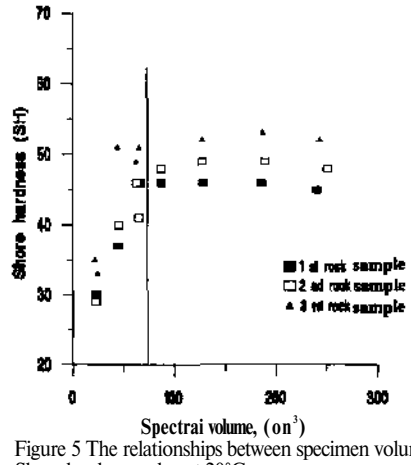

Figure 5 The relationships between specimen volume and Shore hardness value at 20°C

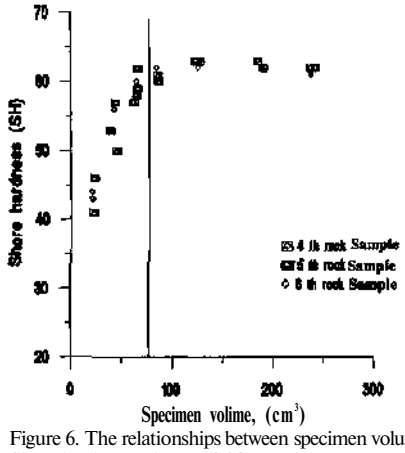

Figure 6. The relationships between specimen volume and Shore hardness value at 20 °C

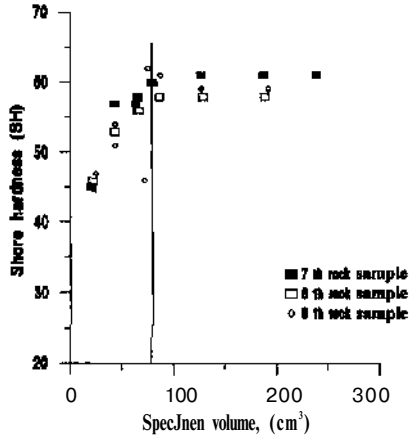

Figure 7 The relationships between specimen volume and Shore hardness value at 20 °C

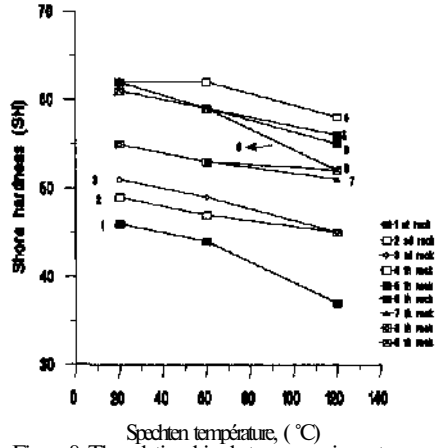

Figure 8. The relationships between specimen temperature and Shore hardness value (with 80 cm^3 volume)

It is not possible to compare the Shore hardness values obtained from previous methods suggested by various researchers. Therefore, the author believes that the standard test method suggested by the ISRM should be reviewed.

4 THE EFFECT OF SPECIMEN TEMPERATURE

In a previous study, it was observed that the mechanical parameters of the heated rocks decrease with temperature (Mahmutoğlu, 1998).

The relationships between SH and specimen volume at 20 °C are given in Figures 5-7.

The SH values of each rock were taken as the arithmetical average values of measurements which were made on volumes greater than 80 cm^3.

In this study, specimens of different volumes prepared from each rock were conditioned in a drying-out cupboard at 20°C, 60°C and 120°C in order to determine the effects of specimen temperature on Shore hardness. The relations of specimen volume vs. SH values were given in Figures 1-4 for some rock types.

It can be seen that the Shore hardness value decreases with increasing specimen temperature. Therefore, when the temperature increased in the specimens, the SH decreased. At each temperature, the Shore hardness values of the rocks did not exhibit significant differences at volumes higher than 80 cm^3. It can be seen that the minimum volume of specimens was found to be 80 cm^3.

The relationships between SH values and specimen temperatures with a volume of 80 cm^3 are illustrated in Figure 8. This figure shows that the SH value decreases with increasing specimen volume. Therefore, the SH values fall with increasing rock temperature.

The Shore hardness values of the rocks tested at different temperatures are given in Table 1.

Table 1. Average Shore hardness values of rocks at different temperatures (with 80 cm^3 volume)

Rock Number	Rock Sample	20°C	60°C	120°C
1	Marble	46	44	37
2	Marble	49	47	45
3	Marble	51	49	45
4	Limestone	62	62	58
5	Limestone	62	59	56
6	Limestone	61	59	55
7	Limestone*	55	53	51
8	Limestone**	55	53	52
9	Sandstone	61	59	52

* SH values of each test is given in the Appendix (Table A1)
** SH values of each test is given m the Appendix (Table A2).

5 THE EFFECT OF WATER CONTENT

During this stage of the investigations all the specimens were saturated by being kept in water for 72 hours. The Shore hardness values of all the specimens were determined by a Shore sclerescope as in the other tests. The relationships between the Shore hardness values of the saturated specimens and their varying values were examined graphically (Figure 9). Figure 9 shows that the Shore hardness values of specimens greater than approximately 80 cm^3 do not *have* recordable changes. According to this graph, the critical volume for saturated specimens can be taken as 80 cm^1.

However, the Shore hardness values of the saturated specimens were found to be lower than the original specimen values. Therefore, water content has a negative effect on the Shore hardness of specimens.

The Shore hardness values of saturated specimens, obtained nine different rock types, tested during this study are presented in Table 2.

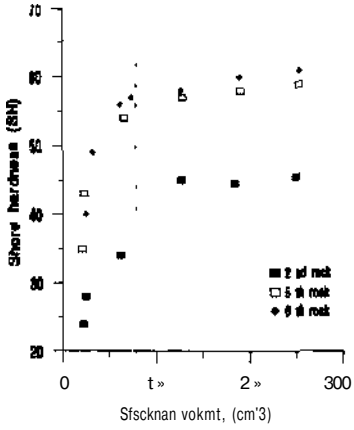

Figure 9. The relationship between specimen volume and Shore hardness value of some saturated rocks.

Table 2. Average Shore hardness values of saturated rocks (with 80 cm^3 volume)

Rock Number	Rock Type	Shore Hardness
1	Marble	42
2	ManMe	45
3	Marble	45
4	Limestone	58
5	Limestone	59
6	Limestone	60
7	Limestone	53
8	Limestone	53
9	Sandstone	58

6 RESULTS AND DISCUSSION

1. A minimum volume of 80 cm^3 is suggested in order to obtain a consistent Shore hardness value of a rock.

2. No significant variations were recorded with volumes larger than the suggested volume. The mean of readings taken from 5 specimens can men be taken as the Shore hardness of a rock.

3. An increase in the temperature of a specimen causes the Shore hardness value of the specimen to decrease. Therefore, increasing temperature has a negative effect on the SH values of rocks.

4. The Shore hardness values of saturated specimens are lower than original specimen values. For saturated rocks, Shore hardness tests should be conducted with a minimum specimen volume of 80 cm^3.

5. The method suggested by the International Society for Rock Mechanics should he rewieved.

REFERENCES

Atkinson, R H 1993. Hardness tests for rock characterisation. *In Comprehensive Rock Engineering, 3, Rock testing site characterisation,* ed. J A Hudson, 105 -117.

Holmgeirsdottir, TH. & Thomas, P.R. 1998. Use of the D-762 Shore hardness Scleroscope for testing small rock volumes, Technical Note, *Int. J. Rock Mech. Min & Geomech. Abstr.* 35, N.1, 85-92.

ISRM, 1978. Commission on standardisation laboratory and field results, Suggested methods for determining hardness and abrasiveness of rocks. *Int. J Rock Mech. Mm & Geomech. Abstr,* 15,89-97.

Mahmutoğlu, Y. 1998. Mechanical behaviour of cyclically heated fine-grained rock. *Rock Mech Rock Eng.,* 31, 169 - 179.

Misra, B. 1972. Correlation of rock properties with machine performance, Ph.D. Thesis, University of Leeds

Onargan, T., Delİormanlı, A. H., Saydam, S. & Hacımustafaoğlu, S. R 1997. An investigation the effects of surface hardness on strength of marbles (m Turkish), *Proceedings of 2nd marble symposium of Turkey* 29-34.

Rabia, H. & Brook, N 1978. The Shore Hardness of Rock, Technical Note, *Int. J Rock Mech Min* <£ *Geomech. Abstr.* 16,335-336

Rabia, H & Brook, N. 1981. The effects of apparatus size and surface area of change on the impact strength of rock, *Int J. Rock Mech Mm A Geomech. Abstr* 18,211-219

Wyk, G 1980. Sclerograph measurements on rock materials. *Geotech Testing J.* GTJODJ, 3(6), 55-65.

APPENDIX

Table AI Shore hardness values of Fethiye Bej (limestone)

	Shore Hardness Values		
V fem^3)	20JÇ	60JÇ	120 *C
85 63	57 71	55 90	54 45
66 23	56 20	52 40	5160
42 50	53 15	50 00	48 25
21 17	46 24	40 35	43 95
188 03	58 43	58 00	54 40
127 5	58 14	56 30	55 70
64 54	5552	5565	48 75
Average	55 06	52 66	5101

Table A2 Shore hardness values of Kennt (limestone)

	Shore Hardness Values		
V fem*)	20 °C	60 ^{D}C	120°C
19181	58 55	56 55	55 55
12649	5929	5841	5660
7195	4620	47 10	47 45
86 68	6120	59 10	58 20
74 48	62 10	57 55	57 70
44 06	54 40	54 05	53 80
25 19	46 70	45 20	45 60
4443	50 60	46 25	46 90
Average	54 87	53 01	52 73

17* international Mining Congress and Exhibition of Turkey- IMCET 2001, ©2001, ISBN 975-395-417-4

Failure and Failure Theories for Anisotropic Rocks

E. Yaşar
Department of Mining Engineering, Çukurova University, Adana, Turkey

ABSTRACT: This paper deals with the failure mechanism of sedimentary rocks in terms of underground stability. The engineering behaviour of anisotropic rocks and anisotropic influence needs further investigation with regard to stability analysis due to the different failure mechanisms. In order to understand the effects of anisotropy, laminated rocks were investigated. Laboratory test results for the anisotropic strength characteristics of sedimentary rocks in different directions were determined. The material selected for the tests was sandstone and siltstone from the Upper Miocene-Pliocene Handere Formation (Th) in n«>ithern Adana (Turkey). Samples were then prepared as test samples to ISRM standards with the samples ot stated at 10° increments to the lamination plane for the application of failure theories. The deft[1] mation characteristics of these anisotropic rocks in the application of the failure theories were determined by the lamination plane angle to the loading direction when applying the stress state. Various failure théorie», were applied to determine the anisotropic strength and deformation properties of these rocks. It is commonly assumed that bedding planes of sedimentary rocks exhibit homogeneous properties and it was found to be a transversely isotropic rock material.

1 INTRODUCTION

A great number of underground constructions are built in laminated sedimentary rock formations. Changes in the engineering properties of rock masses depend on the mineral content, mineral orientation and grain size, density, discontinuity, lamination and bedding planes. Experimental works show that the mechanism of failure varies according to the conditions of stress and loading angle to lamination in the specimen. Because of the different degrees of strength in respect of the loading direction to lamination, laminated siltstone and sandstone specimens were prepared with 10 different angles at 10° increments between 0° and 90°. Several uniaxial compressive, indirect tensile strength and triaxial tests were conducted for each angle. The engineering properties and failure mechanisms were determined with respect to the different directions of 0° to 90 in the laminated rock specimens. A complete picture of the laminated rock behaviour may be predicted from the different loading angles. The failure plane developed along the lamination and other discontinuities.

The laboratory test results for the anisotropic strength characteristics of sedimentary rocks in different directions were determined. A variety of failure criteria for anisotropic materials have been proposed. The applied theories have been classified into three groups: mathematical continuous criteria, empirical continuous models and discontinuous weakness plane theories. The deformation characteristics of these anisotropic rocks for application to the failure theories were determined by the lamination plane angle to the loading direction when applying the stress state. In order to obtain the friction (i>) and cohesion (Co) parameters required for each (ß) orientation, the empirical Hoek-Brown failure criterion was fitted to the triaxial data sets for each orientation. The corresponding Mohr-Coulomb failure envelope and friction and cohesion parameters were derived using Balmer's equations as per the procedure detailed by Hoek et al. (1980). The single plane of weakness theory proposed by Jaeger is the most widely known. In this theory, the classic Mohr-Coulomb criterion is used to describe the failure of both the bedding planes. Good results can be obtained for stratified rocks with this criterion.

2 METHODOLOGY OF MEASUREMENT

The material selected for the tests was sandstone and siltstone from the Upper Miocene-Pliocene Handere Formation (Th) in northern Adana (Turkey). It is characterised by lamination planes. The Handere Formation, which is whitish, yellowish, gray and black İn colour, consists mainly of four units: siltstone, sandstone, fossilized limestone and gypsum. The Handere Formation has concordance and transitive contact with the Kuzgun Formation, which is below it. Quaternary units have discordance and are above tie Handere Formation. Because of the covering of the Quaternary units, the thickness of this formation was not measured. The clastic grains consist predominantly of quartz (42%), rock fragments (22%) and feldspar (10%). The intergranular substance consists of matrix (18%), cement (4%), mica fragments (2%) and traces of coal fragments, altered feldspars and rock fragments. The size of the grains varies from 10 to 20 Jim. There were no signs of weathering on the rock specimens. The sandstone was generally weaker than the siltstone. The samples were taken from the more uniformly laminated sections.

The triaxial tests were applied to measure the variation in failure strength in different loading angle orientations and confining pressures for the analysis of structural anisotropy. A large laboratory testing programme was designed for this rock type in order to investigate the material strength anisotropy. A total of 400 tnaxial compression tests were performed for the loading orientations $\beta = 0$, 10, 20, 30, 40, 50, 60, 70, 80 and 90° and with the confining pressures σ_3= 0, 5, 10, and 15 MPa. The definition of the angle ß is given in Figure 1. Direct observation of the sample failure surfaces revealed that the failure mode had a strong dependence on loading orientation and confining pressure. Preliminary tests were performed to determine the degree of structural anisotropy of the material. First, wave velocities were measured along three identified structural axes of the rock (Fig. 1). According to the results, the lowest wave velocity occurred in the Z direction normal to the lamination, while the highest occurred İn one direction parallel to the lamination. Moreover, the difference between the velocities measured along two orthogonal directions (X, Y) in the lamination was very small. After calculating the anisotropy degrees from velocity data obtained from three cubic samples, it was concluded that the principal anisotropy of the material is related to the presence of bedding planes and the secondary anisotropy within bedding planes can be neglected. Therefore, the material behaviour can reasonably be considered transversely isotropic in nature. This can be summarised as follows.

Failure depends on confining pressure for the orientation ß = 0° and 90°. The sample failure takes place by bursting of the lamination under low confining pressures.

For orientations between $\beta = 20°$ and $\beta = 70°$, the failure is clearly controlled by sliding of the lamination.

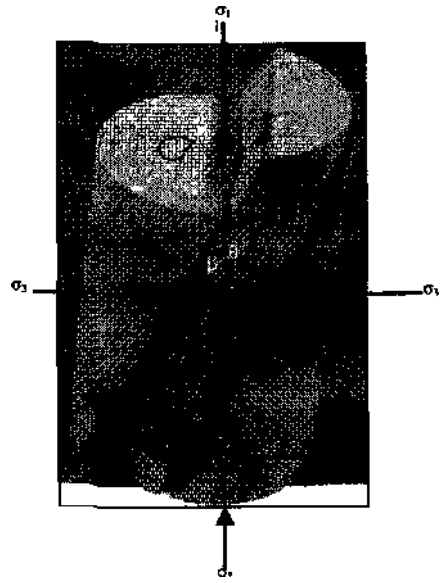

Figure 1. Loading direction on the samples.

The values of the failure strength defined at the peak point of stress-strain curves are presented both with loading orientation and confining pressure. There was a large variation in strength with the loading orientation for all the confining pressures tested. The material failure is due to sliding along the lamination for loading orientations between |$ = 20° and ß = 70°. The sudden decrease in strength at these angles in the rock samples represents the transition from parallel lamination failure to perpendicular lamination failure. The degree of material strength anisotropy is commonly quantified by the ratio of the largest and smallest values of failure stress for a given confining pressure.

$$\sigma_{an} = \sigma_c \max / \sigma_c \min \qquad 0)$$

The experimental values of this anisotropy ratio for various confining pressures are presented in Figure 2. The value of σ_{an} continuously decreases with confining pressure. This means that the material anisotropy İs smaller when the confining pressure is higher. However, the strength anisotropy ratio of the laminated rocks seems to show a tendency towards a constant value of about 1.1 even under high confining pressure.

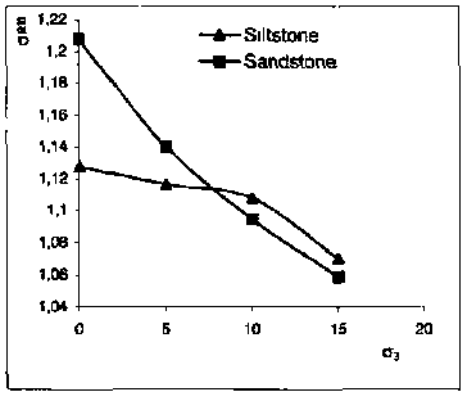

Figure 2. The ratio of anisotropy in the test material.

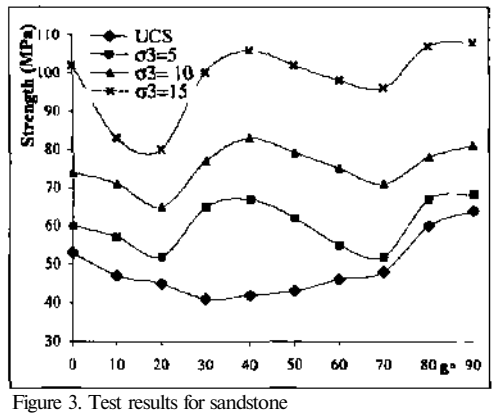

Figure 3. Test results for sandstone

3 TEST RESULTS

Sandstone and siltstone from the Hanaere Formation were studied in order to determine the geological, physical and mechanical properties of anisotropic rocks using a testing macnine. The samples were then prepared as test samples to ISRM standards with the samples orientated at 10° increments to the lammation plane for application to the failure theories. A series of triaxial and uniaxial tests were then conducted on each sample inclination, with repetition of the tests where matenal was available. A total of 400 sandstone and siltstone samples from the Handere Formation were tested. This study was concerned with the application of theories of anisotropic strength (Figures 3, 4 and 5). Tables 1 and 2 present a summary of the tests for sandstone and siltstone respectively.

Indirect tensile tests were also conducted using Brazilian discs. Here, the 90° core was prepared as a batch of discs which were then tested with the bedding at different inclinations. It was assumed that the induced tensile breaking stress generated m the test was at 90° to the applied load and, therefore, the tensile strength measured was also in this orientation.

Table 1 The results for sandstone

β	UCS (MPa)	σ3=5 (MPa)	σ3=10 (MPa)	σ3=15 (MPa)	ϕ°	τ0
0	53	60	74	102	37	13
10	47	57	71	83	36	12
20	45	52	65	80	32	II
30	41	65	77	1002	35	10.5
40	42	67	83	106	34	10
50	43	62	79	302	36	10
60	46	55	75	98	35	108
70	48	52	71	96	31	10 13
80	60	67	78	107	36	13
90	64	68.4	81	108	42	135

Table 2 The results for siltstone.

β	UCS (MPa)	σ3=5 (MPa)	σ3=10 (MPa)	σ3=15 (MPa)	ϕ°	τ0
0	76	86	102	129	45	14
10	69	79	87	100	43	13 5
20	67	74	80	92	39	12 52
30	67	87	101	115	41	13 48
40	72	88	105	112	42	125
50	74	93	112	124	41	12
60	76	87	103	120	40	14
70	68	79	97	116	41	145
80	87	101	120	131	46	15
90	85 71	96	113	138	49	14

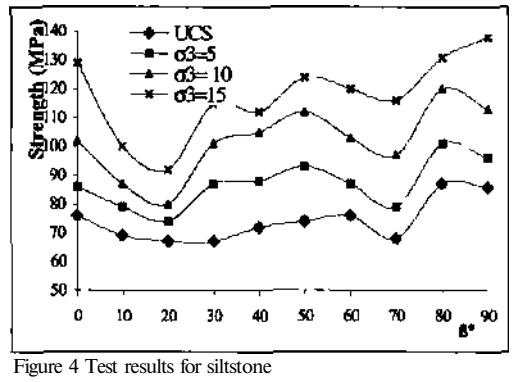

Figure 4 Test results for siltstone

4 APPLICATION OF THE TEST DATA TO THE THEORIES

Four failure theones were used for interpretation of the laboratory test results for the anisotropic rocks: the single plane of weakness theory (Jaeger, 1960); the continuously variable shear strength theory (Jaeger, 1960); the Walsh-Brace theoiy (1964); and the variable friction angle and cohesive strength

theory (Donath, 1972). The uniaxial test results for the anisotropic strength characteristics of the Handere Formation were determined and applied to the failure theories.

The single plane weakness failure theory for uniaxial conditions was determined from the following expressions (Jaegar and Cook, 1979)"

$$\sigma_1 = \frac{2\tau_0}{(1-\tan\phi\cot\beta)\sin 2\beta} \quad (2)$$

The failure stress di can be calculated by specifying τ_0' and $\tan\phi'$(constant for varying orientations of ß). It is necessary to evaluate two cohesive strength parameters and two coefficients of internal friction (τ_0', τ_0, $\tan\phi'$ and $\tan\phi$) for anisotropic materials.

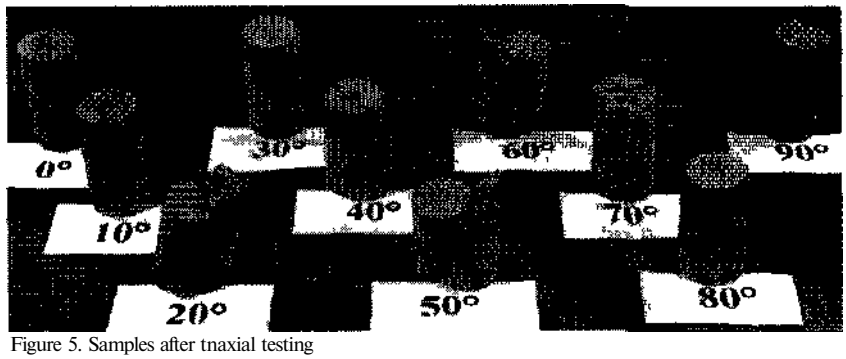

Figure 5. Samples after tnaxial testing

Walsh and Brace (1964) proposed a failure criterion which modified Griffith's tensile failure theory. The failure stress (0VÖ3) for a randomly oriented long crack is:

$$(\sigma_1-\sigma_3)_L = \frac{C_0[(1+\tan\phi_L^2)^{1/2}-\tan\phi_L]+2\tan\phi_L\sigma_3}{2\sin\alpha\cos\alpha(1-\tan\phi_L\tan\alpha)} \quad (3)$$

For calculating the weakest fracture strength, a friction angle of 45° was used.

The failure criterion for the continuously variable cohesive strength theory is as follows:

$$(\sigma_1-\sigma_3) = \frac{2\tau_0 - 2\sigma_3\tan\phi}{\sec\phi-\tan\phi} \quad (4)$$

where $\tau_0 = A\text{-}B\,[\cos 2(\beta'\text{-}\beta)]$

A and B are constants,

$\beta' = 45°$,

ϕ = angle of internal friction.

The variable friction angle and cohesive strength theory assumes that material fails in shear and has a variable cohesive strength (τ_0) and a variable internal friction angle, $\tan\phi$ (Donath, 1972).

The value of the internal friction angle ($\tan\phi$) may vary with respect to ß. The variation of the internal friction angle can be calculated by the following equation:

$$\tan\phi = C\text{-}D\,[\cos 2(\beta'\text{-}\beta)] \quad (5)$$

C and D are constants,

$\beta' = 45°$.

Figure 6 illustrates the application of the four failure criteria to test data for sandstone. Figure 7 illustrates the application of the four failure criteria to test data for siltstone. Tables 3 to 6 give the constants derived for each failure theory. The β orientation when the strength was at a minimum was found to be 70° for both sandstone and siltstone. The theoretical Walsh and Brace and single plane of weakness failure criteria, when applied to die test data, generated similar strength envelopes with both predicting a 'U'-shaped reduction in strength for failure along the weakness plane. At most confining pressures, these two criteria overestimated the strength in the regions where they predicted failure through the intact rock. However, for sandstone tested at confining pressures of 10 MPa and 15 MPa, these two theories produced a reasonable fit to the test data. This seems to indicate that at higher confining stresses there is a change in the failure mechanism of the sandstone and siltstone. The continuously variable cohesive strength criterion and the variable friction angle and cohesive strength criterion produced failure envelopes that predicted a continuous change İn strength in relation to the ß orientation. The variable cohesion theory tended to either underestimate or overestimate the strength at ß = 90° and β = 0°. The variable friction and cohesion theory provided a better fit to the data. It was also observed that generally σ_1 for β = 0° is

lower than CTi for ß = 90°, again except for sandstone tested at confining pressures of 10 and 15 MPa, Figures 3 and 4. In these cases, both of the empirical failure criteria underestimated the actual strength.

Table 3. Single plane of weakness parameters

	Weak Plane β = 70°		β = 0°		β = 90°	
	c (MPa)	ϕ°	c (MPa)	ϕ°	c (MPa)	ϕ°
sandstone	11.25	37	12	37	13.59	37
siltstone	13.78	45	15	45	17	41

Table 4. Walsh and Brace parameters.

	Weak Plane β = 70°		β = 0°		β = 90°	
	UCS (MPa)	ϕ°	UCS (MPa)	ϕ°	UCS (MPa)	ϕ°
sandstone	42.75	37	53	37	64	37
siltstone	68.81	45	76	45	85.71	45

Table 5. Continuously varying cohesion parameters.

	ϕ°	'A' constant	'B' constant
sandstone	37	15	3.5
siltstone	45	17	5

Table 6 Continuously varying friction and cohesion parameters.

	A	B	C	D
sandstone	15	3.5	42	6
siltstone	17	5	49	7

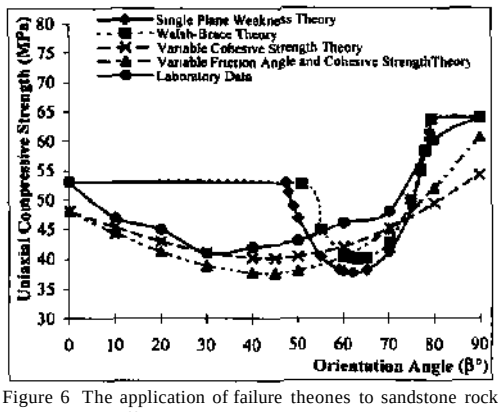

Figure 6 The application of failure theones to sandstone rock specimens in different bedding planes.

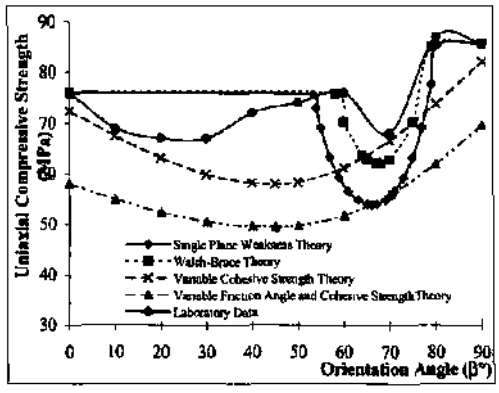

Figure 7. The application of failure theones to siltstone rock specimens m different bedding planes.

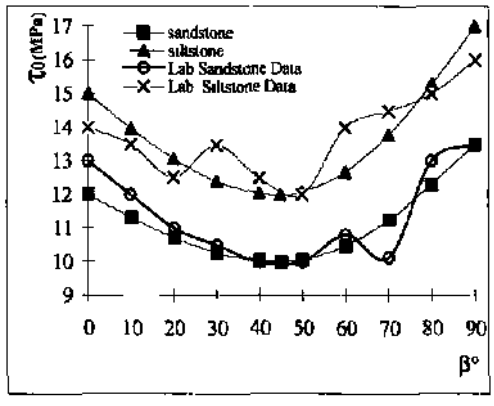

Figure 8. Cohesion strength versus bedding planes.

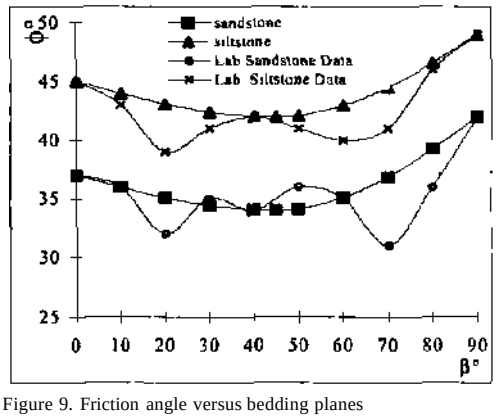

Figure 9. Friction angle versus bedding planes

When this theory was applied to both sets of sandstone and siltstone data, it was observed from Figures 6, 7, 8 and 9 that the method predicted the occurrence of the minimum fracture strength at a much steeper angle of anisotropy than the observed behaviour of the test data. This was also true of the Walsh-Brace failure theory, in which a similar description of failure was evident by the single plane of weakness theory.

However, when a spatially varying cohesion was introduced with a constant friction angle, the results indicated a closer theoretical evaluation of the measured minimum value of anisotropy at ß = 45° for each of the sandstone and siltstone data sets. The model, however, significantly underestimated the strength of both data sets at orientations of 0° and 90°.

The method that incorporated a variable friction angle as well as a variable cohesion in equation 4 produced the best overall fit to the sandstone and siltstone laboratory data. The model results predicted a minimum strength close to the test data at ß = 45° as well as producing a much improved estimation of the fracture strength at orientations of 0° and 90°.

4.1 *Effect of anisotropy on (ensile strength*

Figure 10 illustrates the change in tensile strength with respect to ß orientation for sandstone and siltstone. The figure illustrates that there is a decline in tensile strength from ß = 90° to ß = 0°. The scatter in the data precludes a close correlation of a regression curve to the data points; therefore, a linear trend line was fitted. The ratios between the tensile strength at ß = 90° and ß = 0° are 0.86 and 0.84 for sandstone and siltstone respectively.

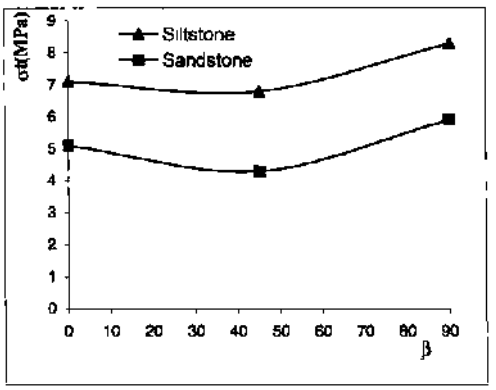

Figure !0. Change in tensile strength with respect to ß.

For each confining pressure, multiple tests were undertaken for any particular ß orientation. Multiple tests were also carried out at each ß orientation for the tensile and UCS tests. The data obtained from these tests exhibited variability in the strength of the rock tested at the same ß orientation and under the same conditions. This variability is a natural phenomenon of rock material and is attributed to the natural variation of rock strength and variation in lamination properties such as thickness, spacing, strength, orientation and form within each siltstone unit.

5 ANISOTROPIC STIFFNESS BEHAVIOUR

5.1 *Elastic properties and anisotropy*

The sandstone and siltstone of the Handere Formation are usually stratified deposits formed from sedimentation consisting of a cyclotherm sequence of various rocks with different material properties. The deformatipna! properties of diese rocks depend upon the orientation of die bedding planes and laminations to the major principal stresses. Since the siltstone and sandstone of die Handere Formation are located in stratified layers, it is reasonable to assume from the test data that such materials exhibit anisotropic elastic deformation behaviour that can be best approximated as a transversely isotropic material.

The transversely isotropic analysis represents a stratified elastic medium in which there are distinctly different elastic moduli perpendicular and parallel to tie layers. Five unique moduli are required to specify transversely isotropic material: E_{xz}, E_y, ν_{xz}, ν_y, G_{xy}. The shear modulus between the plane of isotropy and normal plane G_{xy} is very difficult to determine experimentally using direct testing metiiods (Chen et al., 1993). Laboratory data for sandstone and siltstone can be utilised for E^ and E_y with v_{X7}. and v_y assumed to be 0.2 to empirically determine $G_{„v}$ iteratively using a simple modelling technique. An example of the shear modulus calculated using the modelling method for sandstone is given in Table 7.

5.2 *Effect ofanisotropy on Young's modulus*

The laboratory test results show the change in Young's modulus with respect to ß orientation for sandstone and siltstone. A linear regression line to each set of data indicates a general decline in Young's modulus from ß = 90° to ß - 0°. Further testing is required to produce a better relationship between Young's modulus and ß orientation-

Table 7. Example of use of laboratory test data.

ß	UCS(MPa)	UTS(MPa)	E(GPa)	K(MPa)	τ_0(MPa)	ϕ	Gxy(GPa)
			Sandstone				
0°	53	5.1	16.8	169	13	37	
45°	42	4.3	14.2	131	10	34	5.047
90°	64	5.9	17.4	202.5	13.5	42	
			Siltstone				
0°	76	7.1	17.8	190.5	14	45	
45°	72	6.8	15.1	149.7	12	42	3.628
90°	85.71	8.3	18.3	227.8	14	49	

Young's modulus for rocks can be determined from failure stresses obtained in triaxial tests with ß = 90° and ß = 0°, as in these orientations, and the failure takes place in the rock matrix. However, according to experimental data for many anisotropic rocks, the strength with ß = 90° may be clearly different from that with ß = 0°. Therefore, it is useful to take different values of the cohesion and friction for the two principal directions. Experimental determination of these rocks' cohesion strength and friction angle in two principal orientations was carried out. However, the cohesion and friction of weakness planes have to be determined from failure stresses determined in triaxial tests with the loading orientation resulting in the minimum strength, generally for 20°< ßnn< 70°. At such an orientation, the material failure occurs along weakness planes.

6 CONCLUSIONS

The uniaxial compressive strength behaviour of siltstone and sandstone from the Handere Formation is dependent upon the orientation of the plane of anisotropy to the applied stress.

The maximum compressive strength occurred at an orientation of ß = 90° and 9 = 0° with a minimum value of strength occurring at ß = 68° and 8 = 22° for Jaegar's single plane of weakness theory and the Walsh-Brace criterion respectively.

The variable cohesive strength TO and the coefficient of internal friction tan0 vary with the orientation of anisotropy and they produced the best fit to the data obtained in the laboratory.

It was clear from the laboratory data that the modulus of elasticity varied with the orientation of the plane of anisotropy. The shear modulus between the plane of isotropy and the normal plane for both the siltstone and sandstone data sets had a reduction factor of 0.46 and 0.53 from the modulus of elasticity measured İn the laboratory for ß = 45° using transverse isotropy.

Triaxial testing and measurement of all directional deformation modulus properties are proposed and the anisotropic strength and elastic theories should be applied to more comprehensive and detailed data sets for all major Handere Formation lithology.

The variable friction and variable cohesion theory produced the best fit to the triaxial data, with the exception of sandstone and siltstone tested at confining pressures of 10 and 15 MPa. For these two cases, the single plane of weakness and Walsh-Brace criterion model best fitted the test data.

The maximum compressive strength for both the sandstone and siltstone occurred at an orientation of ß = 90° with a minimum value of strength occurring at ß = 70°. Jaegar's single plane of weakness criterion and the Walsh-Brace criterion do not have the flexibility and advantage of the variable friction angle and cohesive strength criterion, which is considered the most appropriate in most cases for modelling laboratory results. However, the test results for the sandstone and siltstone tested at confining pressures of 10 MPa and 15 MPa were best fitted by the single plane of weakness and Walsh-Brace theories. The sandstone was the weaker of the two lamination rocks tested and the test results may be a reflection of changing failure mechanisms at higher confinement. In order to validate this hypothesis, further triaxial testing at higher confining stresses is required.

It was observed from the laboratory data that the modulus of elasticity varied with the orientation of the plane of anisotropy. There was a large scatter in the test data and further testing is required to determine more accurately the influence of anisotropy.

This paper İs an introduction to the preliminary phase of a more detailed programme of research involving the detailed testing of a wide range of sandstone and siltstone samples.

REFERENCES

Chen, D.H., Zaman M.M. and Kukreti, A.R. (1993). Laboratory Testing and Constitutive Modelling of Coal Including Anisotropy, Structure and Properties of Engineering Materials. Vol. 48 pp 349-354.

Donath, F.A. (1972). Strength Variation and Deformational Behaviour in Anisotropic Rocks, State of Stress in the

Earth's Crust, American Elsevier Publ Comp, New York pp 281-298.
Hoek E. And Brown E T., (1980) Empirical Strength criterion for rock mass J. Geotech. Div. Am. Soc. Civ. Eng. 106. 1013-1035.
Jaeger, J.C. and Cook, N G W (1979) Fundamentals of Rock Mechanics, Chapman and Hall, London, Third Edition
Jeager, J C, (1960). Shear Failure of Anisotropic Rocks. Geological Magazine, Vol 97, pp65-72.
Walsh, J B. and Brace, W F , (1964). A Fracture Criterion for Brittle Anisotropic Rocks. Joum. Geophysical Research, Vol. 69(16), p3449

An Analysis of the Effect of Discontinuity Surface Matching on Shear Strength by Image Processing

M.Unal & B.Unver
Department of Mining Engineering, Hacettepe University, Ankara, Turkey

ABSTRACT: There are many factors affecting the shear strength of rock masses. The shear resistance of discontinuities could probably be regarded as the most critical factor in mis respect. As the roughness characteristics of discontinuity surfaces have a great influence on the shear behaviour of discontinuity, it is of primary importance to study the roughness characteristics of discontinuity surfaces. The shear resistance of a discontinuity is a function of the amount of friction created due to contact between two surfaces during shear displacement. Therefore, it is also necessary to analyse the contact characteristics, called the matching degree, together with the roughness properties of discontinuities. The effect of the degree of surface matching on the shear characteristics of a discontinuity has not yet been fully described. In this paper, the aim is to determine the degree of matching of surfaces under different normal loads and state its significance in the shear behaviour of discontinuities. In order to visualise the effect of the degree of matching, both surfaces were dyed with a low absorbable paint in the form of a thin film. The shear strength of discontinuities at different normal loads was determined and photographs of the surfaces were taken using a digital camera with 1600x1200 pixel resolution. The photographs were analysed on the basis of colour difference. Thus, the parts of the surface where the paint was eroded due to friction could be identified and analysed. This made it possible to isolate the effect of the degree of surface matching together with the discontinuity surface roughness characteristics.

1 INTRODUCTION

There is a significantly close relationship between the roughness of a discontinuity surface and interaction between two surfaces, which greatly influences the stability of rock masses. Therefore, visual observations and quantification of the characteristics of erosion and friction on sliding surfaces are of great interest in determining the shear behaviour of discontinuities. This is because the discontinuity surfaces are rough and contact areas between the two surfaces change during shearing. Contact areas, i.e., matching areas between two surfaces, essentially depend on the magnitude of normal load, shear displacements and the direction of sliding. The contact mechanisms of discontinuities have been studied by various researchers (Barton and Choubey, 1977; Kwafnievski and Wang, 1997; Re et al., 1997; Zhao, 1997).

Discontinuity surfaces should be kept as close as possible in order to increase the shear resistance of a discontinuity and, hence, to increase the strength of a rock mass. The loosening of surrounding rock around an excavation eventually leads to a decrement in the amount of matching degree of discontinuity surfaces. The purpose of support is to keep the rock mass in the vicinity of an excavation as close as possible to the original conditions. The main idea behind contemporary support strategy is to use the rock mass itself as a supporting element. This can only be achieved by preserving the strength of the rock mass. Fissures and cracks can be held tightly by preventing the loosening of the rock mass. This is of critical importance, especially in the case of the application of rock bolts, since rock bolts are very sensitive to deformation, having a lower deformation tolerance. Therefore, the degree of surface matching at different normal loads assumes critical importance İn terms of rock support design (Unver, 1999).

The purpose of this paper is to determine the degree of matching of surfaces with an analysis of damaged zones during shear tests under different normal loads. This analysis is based on the acquisition of grey level images of surfaces created by erosion as a consequence of friction. Segmentation of the images depends on the colour difference to identify the damaged zones clearly, and then calculation of the matching degree is performed by histogram analysis.

2 SAMPLE PREPARATION AND TESTING

*2.*1 *Preparation of specimens*

Two different kinds of marble sample having fine and coarse grains were used in this study. A senes of 8 x 8 x 12 cm^3 and 5 x 7.75 x 10 cm^3 prismatic marble specimens were used. The prismatic specimens were split into two pieces to get a 8 cm x 8 cm and 5 cm x 7.75 cm joint surface by applying an indirect flexure test.

2.2 *Acquisition of images of the sheared area*

The characteristics of contact areas between two surfaces cannot be clearly defined by an examination of the surfaces after shearing. In order to facilitate the visual identification of the degree of matching at different norma! loading conditions, the surfaces were painted prior to testing. Since the colour of the samples was white, a black paint was selected so as to increase the contrast. This process was repeated for every test before shearing.

Before and after shearing, photographs of the surfaces were taken with a PDC 2000/40 digital camera with V600xl200-pixe\ resolution Then the digital images were transferred to a computer using auxiliary software called TWAIN.

2.3 *Shear tests*

Shear tests were carried out by using standart portable shear box, under different normal stresses on marble specimens of different dimensions and degrees of roughness. The marble specimens had similar mechanical characteristics, with uniaxial compressive strength values of around 62 MPa. The magnitudes of the normal stresses were selected as 0 5, 1, 1.5 and 1, 2, 3 MPa for specimens with sizes of 8 x 8 cm and 5 x 7.75 cm respectively for the simulation of different loading conditions. The peak shear strength of the rock joint corresponding to each applied normal stress was measured during the shear test.

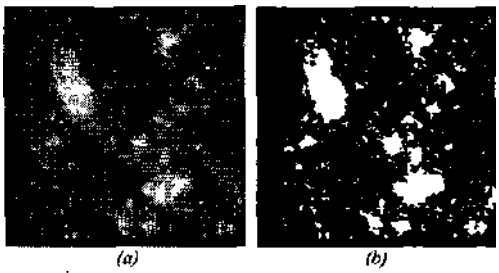

Figure İ Threshold filtering on the images of asheared joint surface a) before filtering b) after filtering

3 DETERMINATION OF DEGREE OF MATCHING

3.1 *Modelling of the surface topography*

In order to obtain 3-D models of the rock surface, a close-range digital photogrammetric technique was used. The test results show that it is possible to model the surface roughness of discontinuities by means of a digital photogrammetric method. The method is fast and of low cost. Details of discontinuity surface roughness determination by means of a photogrammetric technique can be found elsewhere (Unal et al., 2000; Ünal, 2000)

3.2 *Analysis of images*

The logic of the method for determination of matching degree depends on the fixing of the eroded area due to friction of the surfaces during shearing under different normal stresses and different shear displacements (Riss et al., 1997; Power and Durham, 1997; Reid and Harrison, 1997).

The degree of matching is the percentage of the part of the surfaces in contact. The ratio of the contact area to the whole area is defined as the coefficient of matching. Hence, the coefficient of matching takes a value between 0 and 1. (Zhao, 1997).

The eroded area can easily be identified by the removal of paint from the surface, creating a colour contrast. Advances in computer technology have reflected important improvements in the logic of image processing. These improvements provide a viable new approach for determination of the contact area of matching surfaces and now make it possible to calculate the contact area using simple and practical methods. In this study, the digital photographs of the surfaces were analysed in three stages'

- The photographs were dimensioned so as to include the surface for analysis, and colour images were converted into black and white.
- The contrast between the black and white regions was improved by the application of threshold filtering (Fig. 1). After threshold filtering, the ratio of the white regions as an indication of contact and change on the surface could be determined. Then, a histogram distribution of the change in colour was used to calculate the degree of matching of the two surfaces digitally. This analysis was repealed for each test. White regions on the photograph denote the eroded areas due to matching of the two surfaces, whereas black regions are the areas where there was no contact.
- The contour maps of the surfaces were drawn from the black and white photographs by

obtaining a threshold value, and these counter maps were superimposed with the contour maps obtained by means of digital photogrammetric maps. In this way, the eroded areas could be defined, as shown in Figure 2.

At the end of these analyses, the degree of matching (percentage of contact area) of the sheared surfaces and the peak strength values corresponding to these matching characteristics were determined. A summary of the results is presented in Table 1.

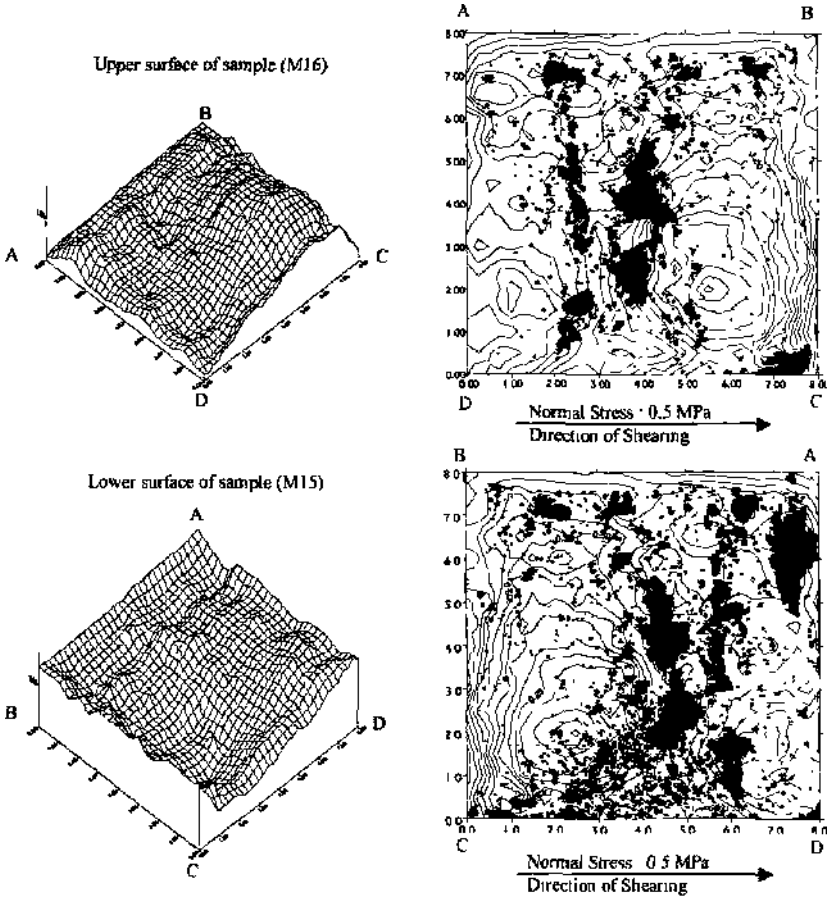

Figure 2. Determination of the topography and contour diagram of the sample joint surfaces together, black regions denote the contact area

4 DISCUSSION OF THE RESULTS

The effect and significance *of roughness* and the degree of matching on shear strength was demonstrated by employing a relatively simple method. The parameters that influence the shear strength of discontinuities are not independent of each other. There is interaction between these factors. The degree and nature of roughness have a great influence on the decree of matching.

As can be seen in Figures 3 to 5, there is a close relationship between normal stress, peak shear strength and the degree of matching. The relationship between normal stress and peak shear strength and the degree of surface matching in logarithmic scale (Figures 3-5 (a)) exhibits a similar trend. As the roughness of the samples increased, an eventual increase in the peak shear strength values was observed. On the other hand, the roughness and the degree of matching were found to be inversely proportional. In other words, as the roughness of the surfaces increased, interlocking of these rough surfaces became more difficult during shear displacement, as had been predicted. Due to dilatation, the degree of matching was decreased. However, the effect of normal stress on the peak shear strength value was greater. In addition, there seemed to be a difference between the degrees of matching of the lower and upper surfaces after shearing, as can be seen in Table I

Table 1. Summary of the results (Unal. 2000).

Specimen Code	Surface Dimensions (cm x cm)	^ JRC	Shear Displacement (mm)	Normal Stress(MPa)	Peak Shear Strength (MPa)	Contact Area (%)	
						Lower Surface	Upper Surface
*				0.5 -	1.055	11.83	10.66
Ml -M2	8 x 8	8-10	10.0	1.0	2.109	21.98	20.74
				1.5	2.617	34.21	27.56
*+				1.0	0.839	11.38	9.26
M4-M3	5x7.75	4-6	10.0	2.0	1.419	33.1	27.17
				3.0	2.065	48.43	42.71
+*				1.0	1.161	26.97	25.72
M6-M5	5 x 7.75	4-6	10.0	2.0	2.129	52.25	40.02
				3.0	2.839	68.55	63.14
**				1.0	0.981	20.14	17.61
M8-M7	5 x 7.75	4-6	10.0	2.0	1.742	35.79	35.54
				3.0	2.581	61.08	51.94
*•				1.0	1.032	22.49	18.8
MI0-M9	5 x 7.75	4-6	10.0	2.0	1.858	56.94	49.76
				3.0	2.348	64.73	54.95
*				0.5	1.016	14.62	5.86
Mil -M12	8 x 8	8-10	10.0	1.0	1.877	26.11	15.62
				1.5	2.422	33.97	25.32
*				0.5	1.250	17.69	14.44
M13-M14	8 x 8	8-10	10.0	1.0	2.1875	27.69	21.46
				1.5	2.539	35.11	30.81
**				0.5	0.820	23.98	13.43
MI5-M16	8 x 8	4-6	10.0	1.0	1.172	42.46	42.48
				1.5	1.484	58.42	57.35
**				0.5	0.703	15.57	10.47
M17-M18	8 x 8	4-6	10.0	1.0	1.016	41.06	25.38
				1.5	1.799	59.62	51.02
«w				0.5	0.703	16.4	11.8
M19 - M20	8 x 8	4-6	10.O	1.0	1.016	42.02	28.67
				1.5	1.289	51.02	39.05

* Coarse-grained marble
** Fine-grained marble
***Joint Roughness Coefficient

Examination of the lower and upper surfaces after shearing revealed that the amount of erosion due to friction was higher on the lower surfaces. Theoretically, surfaces of higher roughness are expected to show more erosion. This phenomenon could not be explained since the roughness of the upper and lower surfaces was almost identical. It was assumed that this occurred arbitrarily or due to difficulties experienced in keeping the rate of loading constant during the tests. The relationship between the peak shear strength values and the degree of matching is presented in Figures 3 to 5 (b).

As the figures show, the peak shear strength of discontinuities was found to be high at higher degrees of matching. The same trend was observed for all tests carried out on samples having various levels of roughness. It can be seen from a comparison of Figure 4 (b) and Figure 5 (b) that an increase in the joint roughness coefficient led to an increment in the value of peak shear strength.

During the calculation of normal stress on the shear surface, it is obvious that stress concentrations at different points are not constant. Therefore, the magnitude and nature of stress concentrations, especially at the tips of asperities, will be very high, eventually leading to failure of these parts. Therefore, depending on the value of normal stress, the dilatation of a discontinuity will be affected during shear displacement. At higher normal stress levels, better interlocking between discontinuity surfaces will obviously be achieved, and the stress concentration at the tips of asperities will tend to be lower due to the greater contact area. This phenomenon is thought to be the front line of support strategy for rock structures.

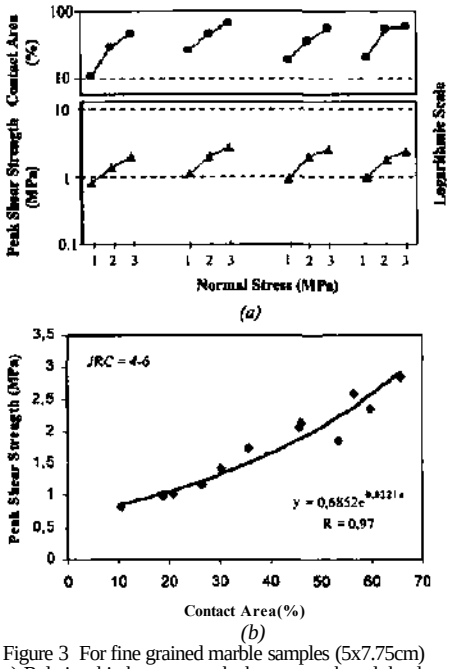

Figure 3 For fine grained marble samples (5x7.75cm) a) Relationship between peak shear strength and the degree of matching at different normal stress levels, b) Relationship between peak shear strength and the degree of matching

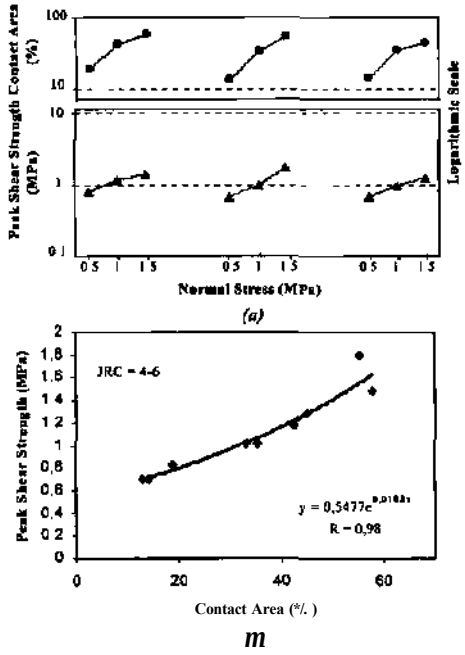

Figure 4 For fine grained marble samples (8x8 cm): a) Relationship between peak shear strength and the degree of matching at different normal stress levels, b) Relationship between peak shear strength and the degree of matching.

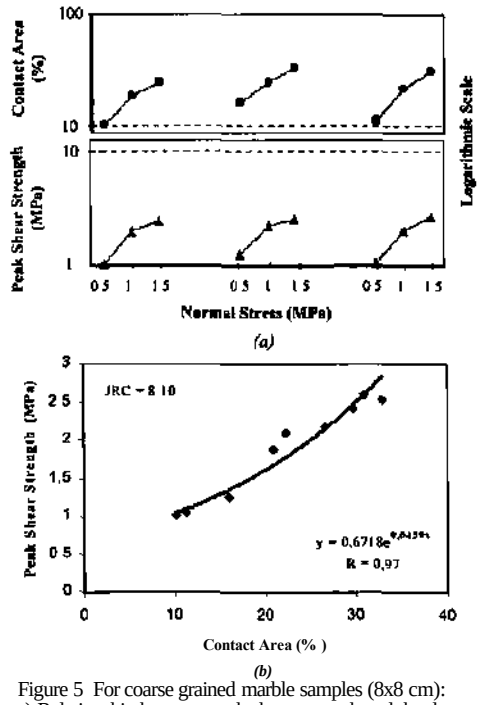

Figure 5 For coarse grained marble samples (8x8 cm): a) Relationship between peak shear strength and the degree of matching at different normal stress levels, b) Relationship between peak shear strength and the degree of matching

5 CONCLUSIONS

This paper reports part of a comprehensive research study carried out on the modelling of discontinuity surface roughness by the application of a digital photogrammetric technique and subsequent fractal and variogram analyses for significant and successful modelling of discontinuity surface roughness. The conclusions of the study presented in this paper can be summarised as follows:

- The value of the peak shear strength and the degree of matching of discontinuity surfaces are a function of normal stress.
- The peak shear strength of a discontinuity increases with an increase in the degree of matching.
- The degree of matching of surfaces assessed with a high roughness coefficient tends to be lower during shear displacement.

The relationship between the roughness, degree of matching and shear characteristics of discontinuities for different types of marble sample has been demonstrated in a quantitative manner. A numerical solution and the simulation of shearing activity in different conditions are suggested for further research.

REFERENCES

Barton, N. & Choubey, V. 1977. The shear strength of rock joints İn theory and practice *Rock Mechanics.* Vol: 10, pp.1-54.

Kwafhiewski, M. A. & Wang, J. A. 1997. Surface roughness evolution and mechanical behaviour of rock joints under shear. *Int. J. Rock Mech. Min. Sel,* Vol: 34 (3-4), pp. 157-161.

Power, W. L. & Durham, W. B. 1997. Topography of natural and artificial fractures in granitic rocks. *Int. J.Rock Mech. Min.* Sei.. Vol: 22, pp. 979-989.

Reid, T. R. & Harrison, J. P. 1997. Automated tracing of rock mass discontinuities from digital images. *Int. J. Rock Mech. Min. Sei.*. Vol: 34 (3-4): Paper no. 256.

Re, F., Scavia, C. & Zaninetti, A. 1997. Variation in contact areas of rock joint surfaces as a function of scale, *Int. J. Rock Mech. Min. Sei,* Voi: 34 (3-4): paper no. 254.

Riss, J., Gentier, S., Archaumbault. G. & Flamand, R. 1997. Sheared rock joints: dependence of damage zones on morphological anizotropy. *Int. J. Rock Mech. Min. Sei.,* Vol: 34(3-4), paper no. 258.

VJnal, M., Unver, B. & Tercan. A.E. 2000. Modelling of discontinuity surface roughness by digital phologrammetry and geostatistical methods, *Proc. of 9 Int. Symp. On Mine Planning and Equipment Selection,* Athens, Greece, pp. 391-396.

Unal, M. 2000. Modelling of discontinuity surface roughness and investigation of its effects on shear strength, PhD. Thesis, Hacettepe University, Ankara, 219 p. (in Turkish).

Unver, B. 1999. Methods related to use and performance of monitoring of rock bolts in underground coal mines. *Bulletin of Chamber of Mining Engineers of Turkey,* Vol: 28, No: 4, pp.3-20 (in Turkish with English Abstract)

Zhao, J. 1997. Joint surface matching and shear strength. *Int J. RockMech. Min. Sei.,* Vol: 36(2): pp. 179-185.

17th International Mining Congress and Exhibition of Turkey- IMCET 2001,© 2001, ISBN 975-395-417-4

Diversity of Electrical Conductivity in a Water-Bearing Rock Material

M.K.Gökay & İ. Özkan
Department of Mining Engineering, Selçuk University, Konya, Turkey

ABSTRACT: The electrical conductivity of rock materials was analysed in order to develop practical laboratory-based measurement equipment. In order to proceed with the selected aim, artificial rock materials were prepared by using plaster of Paris. Test samples were prepared in two categories: the first was the original material; the second group of samples contained glass pieces. Glass pieces were located in the test samples in a certain pattern to simulate random joint orientation in natural rock masses. The tests showed that, electrical fields around the joints are higher due to their high water-bearing characteristics. This property was used in the tests to determine hidden joint locations in the selected rock masses and model samples provided. Underground gas, water or petroleum storage excavations or excavations opened for waste dumping are all sensitive to seepage of the gases or liquids both into them and out of them. Evaluation of these rock masses for joint occurrence requires at least seismic and electrical conductivity measurements. In this research study, alternative measuring techniques were investigated for laboratory and field test procedures. The resulting graphics obtained in the laboratory tests illustrate how the joints in the rock masses were detected in the samples.

1 INTRODUCTION

Electrical conductivity depends on free electrons or ions in a material, which increase the conductivity. Metallic substances are conductive due to their free orbital electrons. Rocks, on the other hand, are known as isolating materials due to their very high resistance to electron passage. If electricity is supplied to such a rock, it can not pass through easily. This can be occur only at very high voltages, such as 25-50 kV. At normal voltages, 110-220V, electricity constitutes electrical potential differences in water-bearing rock materials. There can be sectional differences in rock material where resistivity varies according to property and water content differences in those sections. Water, as a supplier of free ions, is particularly important. The differences in water concentration in a rock denote irregular free ion distribution in the rock material. Therefore, electrical conductivity in different sections of,the same rock mass can be different. The water content of the rock material depends on the material characteristics, such as porosity, permeability, and mineralogical and structural properties. Since there İs no existing rock mass without weakness zones or discontinuities, capillary action takes water from any part of the rock section to the other side. In particular, discontinuities behave like water passageways in the rock mass and they contain more water than the massive parts of rocks. This also means that there are more free ions in/around discontinuities, so electrical resistance values at these sections are expected to be tow.

Electrical conductivity measurements have been used in mineral exploration, cavity localisation, exploration of water-bearing formations and many other engineering applications. This technique was recently used in Konya, Turkey by MTA, a state-owned organisation, for the evaluation of natural hot water reserve extensions in a host rock mass, providing very important information used to establish a thermal health centre. In the present study, however, laboratory investigations were carried out using similar techniques for laboratory-size samples. The aims of this research are the determination of the water content of the rock samples and location of the sectional variation of water concentration in the same specimens by using electrical conductivity measurements. In order to achieve this, special laboratory apparatus was designed and prepared.

Electrical resistance is a material property which is dependent on the type of material tested. If the material allows electric current to pass through, its

resistance (ohm) to electric current passage can be calculated by dividing the electrical potential differences (volt) between the material ends by the electric current flow rate (amper). If the test material is resistive to the passage of electrical current, when the current is applied to this material, there might be very low (or no) current passing through. However, if the required electrical potential differences are applied to these types of material, like rocks, electrical potential fields are created inside them. There are several measurement techniques that have been introduced to determine potential difference levels in the field. These are the gradient, dipole-dipole, pole-dipole, Wenner, and Schlumberger techniques (Long, etal., 1996).

The electrical potential field created by the given input voltage was then measured for different points. The electrical resistance of the tested sample was then calculated by following Ohm's law. The electrical resistance over a certain distance in sample *R* (Ohm.cm) is then equal to R=(Vp/I).(A/L). In this equation, Vp is the measured potential voltage (volt) between two selected points on the surface of the sample. The distance between the selected points is *L* (cm) and the current on the main input line is / (amper), which is very low in value. The label *A* stands for the-cross-section area (cm^2) in this equation.

The specific electrical resistivity of certain minerals has been determined using similar testing equipment (Figure 1). As can be seen in this figure, metallic material and minerals have relatively low resistivity values with respect to magmatic and silicified rocks.

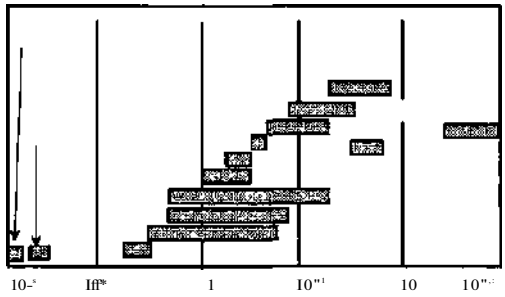

Figure 1. Specific electrical resistivity (Ωm) of certain rocks (Ergin, I973).

In fact, Ward (1990) listed the major effects of various geological processes on electrical resistivity. According to his study; clay alteration, dissolution, faulting, salt water intrusion, shearing and weathering decrease the specific electrical resistivity of the rock mass. He also listed the processes which increase electrical resistivity: induration, carbonate precipitation and sİlİcification. Metamorphism can result in either decreasing or increasing resistivity.

2 ELECTRICAL RESISTANCE MEASUREMENTS IN ROCK MATERIAL

During the preparation of the test instrument in this study, Wenner's four-point measurement technique was put into practice. As can be seen in Figure 2, the input DC voltage, which can be adjusted according to the rate required, was obtained by converting normal 220 ACV mains voltage in Turkey, This input voltage was applied to the selected samples as illustrated in Figure 2. The samples for this test were prepared so that they were cylindrical İn shape and the standard followed was similar to that for uniaxial compressive test sample preparation advised by the ISRM.

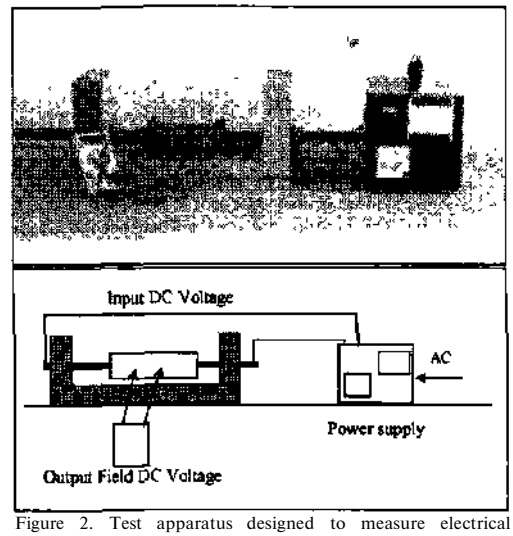

Figure 2. Test apparatus designed to measure electrical conductivity of the samples.

Since the resistance of dry rock İs so high, it was not possible to create an electrical field using normal input voltage (max. 350 DCV). In order to understand the conductivity of the dry rock, a 20cm-long cylindrical dacite sample (die diameter of the sample was 54mm) was tested for resistance to high AC voltages in the special test room of MED AS, the state-owned electricity distribution company for the Konya region. It was observed mat the test sample would resist 25-40kV AC. In order to facilitate electrical conductivity and enable the test to be conducted in normal laboratory conditions, the electrical conductivity measurements were performed with water-saturated samples. The

electrical conductivity measured on die sample surface is then dependent on the water content of the samples. Water ions in the sample aid the formation of electrical potential fields in the rocks. Research on water has demonstrated that saline water (sea water) increases the electrical conductivity of the medium. Schlumberger (1989) gave the results of a research showing a decrease in the electrical resistance of a medium when the temperature and NaCl solution are increased in that medium. Rock mass absorbs water and the water content depends on porosity characteristics.

Electrical conductivity tests were also performed previously in the Mining Engineering Laboratory of Selçuk University with actual rock samples, using the prepared test apparatus. The results obtained from these tests (Figure 3,4) have proved that discontinuities and water content in rock material cause differences in electrical resistivity (Gökay & Özkan, 2000).

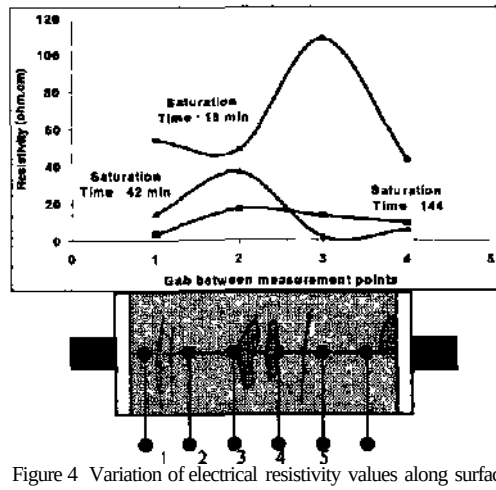

Figure 4 Variation of electrical resistivity values along surface of the limestone sample, discontinuities in the sample cause sudden increase or decrease at the resistivity, m between coincided measuring points (Gökay & Özkan, 2000).

3 ELECTRICAL RESISTANCE MEASUREMENTS IN MODEL MATERIAL

Since the actual rock mass consists of many irregulanties in the mineralogical and structural basis, it was decided that the same test procedures would be used with artificially prepared samples as well. In the research study presented here, the test samples were prepared artificially from plaster of Paris in order to control their structural homogeneity.

3.1 *Test sample preparation*

The test samples were prepared at the Rock Mechanics Laboratory of Selçuk University, Mining Engineering Department. In order to ensure the homogeneity of the prepared test sample, the following sample preparation steps were followed. First, moulds were prepared. Hard plastic pipe pieces

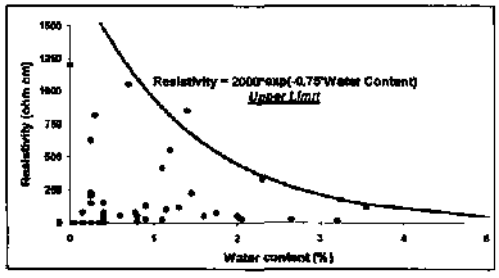

Figure 3. Relation between water content and electrical resistivity in a limestone sample (Konya region).

Second, special oily substances (wax)were used to grease the mould. This was to lessen the friction between the sample and the mould's inner surface. Thus, the samples would be removed from the moulds more easily. The main step in sample preparation was the mixing of homogeneous plaster of Paris powder with water so that liquefied plaster was obtained. This material was then poured into a specially prepared plastic mould and, once full, the mould was vibrated so that the material settled completely. The vibration and shaking actions forced any air bubbles present out of the mould. Then the mould and the material inside were allowed to dry for a short time (about two minutes). After this, the sample was forced out of the mould and put on a shelf in the laboratory. All the samples were then allowed to dry out completely on the laboratory shelves for as along as two weeks.

In order to create discontinuity surfaces in the prepared samples, glass pieces were used. They were selected because they can not absorb water. However, water fills the microvoids surrounding the glass plates when the samples are saturated. The glass pieces used for this purpose were 3mm thick with different dimensions according to the sample size. In general, they were rectangular and circular in shape. During preparation of the sample, the glass pieces were located horizontally or vertically in the sample. When the samples were removed from the mould for the final drying period, there was no sign of glass on the sample surface. They were totally hidden and buried in the samples.

After the samples had dried out, they were cut to required test size in the laboratory. All the samples, both with or without glass plates, were cut to 3 different sample sizes. These sizes were 46-127mm, 57-157mm and 71-196mm in diameter-length format. The samples were also labelled so that mey could be differentiated, label A was used for the samples without glass plates and labels B and C were used for the samples with glass plates.

3.2 *Mechanical characteristics behaviour of the model samples*

When all the samples were ready for electrical conductivity tests, some were separated for mechanical tests, while the others were tested for conductivity. During the test procedure, some of the test samples were destroyed" and it was not possible to obtain any measured values for them. However, most of the samples were tested as intended and the results were analysed for further engineering purposes. Therefore, the test samples prepared without glass plates were tested for their porosity, density and water absorption rate (Table 1,2). Since plaster of Paris is very sensitive to water, the test samples absorbed water very quickly as can be seen in Figure 5. Selected samples were also tested for their uniaxial compression and indirect tensile strength values, which were found to be in the ranges 0.54-3.79±1.10MPa and 0.10-0.33MPa respectively. The calculated average point load index, ïs{50), was 0.52 MPa and the anisotropy index was found to be 2.68.

3.3 *Electrical characteristic behaviour of the model samples*

After these mechanical characteristics had been determined, it was concluded that the prepared test samples were porous and their strength values were very low. Electrical conductivity tests were tien

Table 1 Density test results of model samples.

Sample #	Volume (cm^3)	Dry weight (Br)	Saturated weight (gr)	Dry density (gr/cm^3)
1	36.56	36 56	58 48	1.01
2	38 22	30.02	53.44	0.79
3	38.22	29.39	51.37	0.77
4	38.22	30.43	53 61	0.80
5	40.72	32.38	56 52	0.80
6	39.06	30.86	53 40	0.79
Average	38.50	3161	54 47	0.83

Table 2 Porosity test results of model samples.

Sample #	Sat. Density (gr/cm^3)	Σ (pore volume) (cm^3)	Water Saturation, (%)
1	160	21.40	58 52
2	1.40	23.42	61.26
3	1.44	21.98	57.50
4	1.40	23.18	60.63
5	139	24 14	59 29
6	137	22 54	57 72
Average	143	22 78	59 16

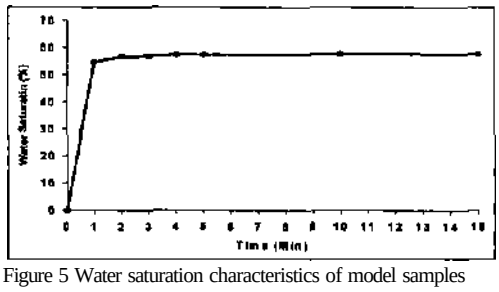

Figure 5 Water saturation characteristics of model samples

performed on test samples whose main strength characteristics had already been determined. Firstly, samples without glass plates (A group) were tested. A total of 12 samples were tested for electrical conductivity with 10 different levels of water content. Therefore, in these test a total of 1780 output voltage readings were measured and loaded into a data base using MS-Excel software. In the second group of tests, samples (total 11 samples) with horizontal glass plates (B group) were tested for electrical conductivity. Similarly, they were also tested with 10 different water contents, so a total of 1580 readings were taken for the purpose of characterising the second group of samples.

The result of the test readings were used to obtain characteristic features of electrical conductivity that could be used for further engineering purposes. Since the samples were specially prepared model material, the resulting electrical conductivity changes were determined exactly as the theoretical studies described. The samples without glass plates showed increased electrical conductivity only with increasing water content. The samples with glass plates, on the other hand, demonstrated valuable behaviour as previously obtained with limestone samples (Figure 4). Figure 6 shows one of the graphs obtaining from the test results of the B group samples, and it illustrates the relation between electrical conductivity and the saturation time of the sample. In this graph, it can be seem that there are two groups of curves. The curves situated in the upper part of the graph correspond to the measurements obtained from gaps which contain glass plates.

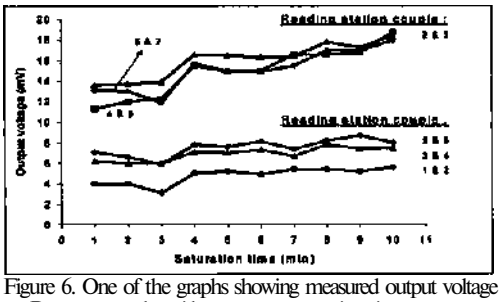

Figure 6. One of the graphs showing measured output voltage on B group samples with respect to saturation time

Thus, it was determined that the electrical conductivity was high compared to other gaps without glass plates. With regard to the curves in Figure 6, the reading points and input DC voltage were kept constant, while the water content of the tested models was increased. Then, as illustrated here, the measured output DC voltages increased as the water content increased.

If the same test data are plotted on a graph showing the changes in electrical conductivity along the surface of the test sample as output DC voltages between reading station points, it İs easy to evaluate the locations of discontinuities as seen in Figure 7. In this figure, modelled discontinuities (with glass pieces) corresponded to sudden conductivity increases between the readings of output potential field voltage. As shown in Figure 7, the glass piece locations in the sample appear with high peak voltage values. In addition, it was also determined that the water content increase in the test sample made the glass location on the resulting graphics more obvious. At the beginning of each conductivity test with samples (B group) of low water content, the resulting conductivity curves were smoother than those for values obtained from samples with high water content. These curves were rougher and conductivity values measured were high because water ions aid the formation of a high intensive electrical potential field.

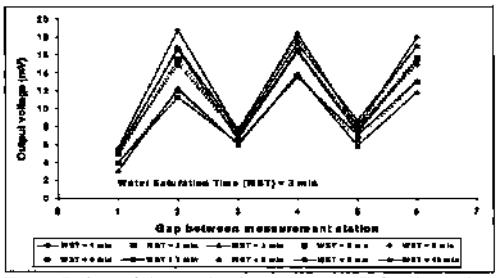

Figure 7. One of the graphs showing output DC voltage change in between the reading stations.

4 ENGINEERING USE OF ELECTRICAL CONDUCTIVITY

Electrical conductivity measurements in actual field work can be used in monitoring tasks. For example, country rocks surrounding galleries or 'equired excavations can be checked continuously by electrical conductivity props. After the idendification of problematic positions, these locations can be equipped with testing apparatus, as in the laboratory,

as shown in Figure 8. If readjusted measuring points on selected sample are connected to a computer base monitoring system which reads the output voltage between the station points and saves these data in a special database, the changes in output voltages in time can be obtained for any location whenever required. This helps engineers in field to visualise crack initiation and propagation through regular time base conductivity curves.

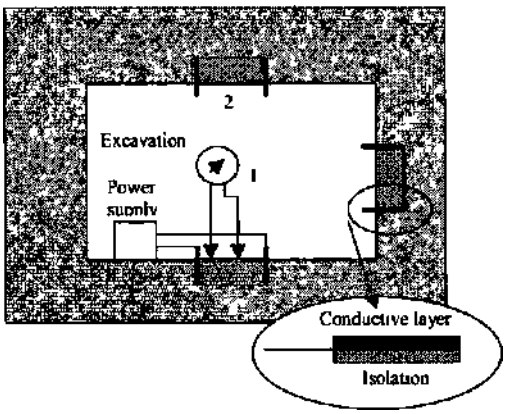

Figure 8 Momtonng task planned for excavation Any form of cracks initiated on excavation wall is detected through the output voltage (I), measured in continuous manner at problematic locations (2).

Cracks in any concrete blocks are also determined and monitored by designing special electrical conductivity measurement equipment. For this purposes, cracks in a concrete block which had been created through axial and lateral stresses in the Civil Engineering Laboratory of Selçuk University were analysed. It could also be supposed that these cracks are the result of a destructive earthquake. Electrical conductivity measurements were begun after permitting water absorption by the concrete block. Input DC voltages were supplied through metallic plates and the output voltages were

obtained through points arranged as a net {Figure 9). When the resulting output voltages were plotted, it was found that higher voltage outputs corresponded to visible and invisible joints on/in the concrete block. This means that joints which could not be located with the human eye were also determined and positioned. This is valuable information for mining and civil engineers as part of their repair programs.

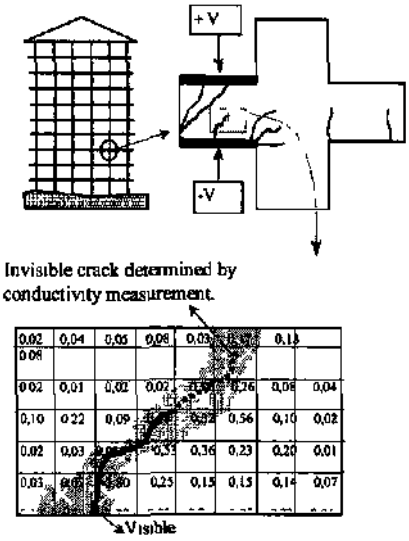

Figure 9. Monitoring of the cracks on concrete blocks.

5 CONCLUSIONS

In this research study, 81 test samples prepared from plaster of Paris were tested for electrical conductivity. Some structural and mechanical strength properties were also obtained for comparison with the test results. Since electrical conductivity measurements are not destructive in respect of test samples, this procedure has been used in many mining and civil engineering projects. Some research institutes have been using these measurement techniques for the localisation of the water-bearing strata or discontinuities. The measurement technique employed were implemented so as to develop laboratory-size apparatus for the localisation of inner joints in test samples. The aim was to apply the test procedure outcome during these works on artificial rock samples.

Since the original material (plaster of Paris, gypsum) in the sample İs sensitive to water, all the model samples reached maximum water content in a 4-5-minute time period. Strength test on the prepared model samples produced very low strength values, which is understandable if the porosity of the samples had been checked. The values were very high and influenced strength in a negative manner. The conductivity test results showed that when the water content in the model samples (A group) increased, electrical conductivity also increased. The relation between these two parameters depends on the porosity of the samples. The simulated discontinuity test samples (B and C groups) were also tested and the simulated discontinuity locations were estimated without mismatches. The graphics resulting from these tests indicated the location of the glass plates in the model samples. The test which were performed on concrete blocks were also found to be positive for determination of joint positioning. In addition, invisible joint surfaces were also determined from the electrical conductivity measurements. By applying electrical conductivity measurement techniques to mining and civil engineering projects more practically, engineers wilJ feel more confident in making engineering decisions.

REFERENCES

Ergin.K. 1973. Uygulamalı Jeofizik, I-T.Ü Maden Fakültesi, istanbul, Turkey

Gökay ,M.K. & Özkan, I 2000 Effects of water content on strength and electrical conductivity of rock material, *The* J'* *National Rock Meek Symp* : 145-151.

Long, CS.; Aydın, A.; Brown,S.R.; Einstein, A.H.; Hatir, K.; Hsieh.P.A.. Myer, L.R ; Nolte, K G , Norton, D L.; Olsson, O. L.; Paillet, F. L.; Smith, J L. and Thomson, L 1996. (Committe on Fracture Characterisation and Fluif Flow) *Rockfracturea and fluid flow; Contemporary understanding and applications.* National Reseacb Council, Geotechnical Board National Committee for Rock Mechamcs,US, National Academy Press, Washington, D.C.

Schlumberger. 1989 Log interpretation principles/applications, Schlumberger Ed Serv.

Ward, St. H 1990. Resisittvity and induced polarisation methods in *St Ward (ed.) Geotechnical and Environmental geophysics. Investigations in Geophysics,* NO 5 SEG, 169-189

1 7 International Mining Congress and Exhibition of Turkey- IMCET2001, © 2001, ISBN 975-395-417-4*

Estimation of Lining Thickness Around Circular Shafts

H.Öztürk & E.Ünal
Department of Mining Engineering, Middle East Technical University, Ankara, Turkey

ABSTRACT: In this paper, the broken zone developing, around a circular mine shafts and lining pressure is estimated by integrating the results of numerical analysis and the "cock-load height" equation derived from empirical analysis. During numerical modelling studies, the computer program FLAC^{2D} was utilized. In order to estimate equivalent Mohr failure Envelope from the generalised Hoek Brown failure criterion, a new FISH function was written within FLAC^{2D}. Parametric studies were carried out by considering mRMR (modified Rock Mass Rating) values, depth from surface, shaft diameter, ratio of horizontal principal-stresses and uniaxial compressive strength of intact rock. Finally, the computer program, "SHAFT" was also introduced. This program simplifies the lengthy and complex process of shaft-lining design.

1 INTRODUCTION

In literature, the lining thickness calculation for circular shaft is based on the assumption that the pressure on the rock-lining contact is known. This pressure is calculated analytically assuming hydrostatic state of stress, considering a failure criterion, and by determining the internal support pressure that will prevent the broken zone developing around the shaft. Consequently, wim the help of this value, the lining thickness is calculated from the thick-wall cylinder meory of elasticity. In this study, firstly, the broken zone developing around circular shafts were calculated, for different ratios of horizontal principal stresses, based on numerical studies. Secondly, considering these results and based on statistical analyses, Unal's (1983;1992) empirical rock-load height equation was calibrated, allowing for the effect of stress. Thirdly, the lining pressures was estimated. Lastly, by using the analytical thick-wall cylinder equation, the lining thickness was calculated.

2 ESTIMATION OF THE DISTURBED ZONE

Information on the extent of disturbed zones is one of the main required parameters in the design of shaft support system. This parameter can be estimated according to the induced stresses and an appropriate rock mass strength criterion. In this study, the numerical stress anaysis program FLAC^{2D} (Fast Lagrangian Analysis of Continua) (Itasca, 1993) and the empirical rock-load height equation derived by Unal (1983,1992,1999) were used.

2.1 *Numerical Studies*

In order to determine the extent of the failure zones developing around shafts, a two-dimensional finite difference program, FLAC^{2D}, was used. Parametric studies were carried out considering the ratios of horizontal principal stresses, uniaxial compressive strength of intact rock, mRMR (modified rock mass rating) (Unal, 1996), shaft diameter and depth from the surface. The unit weight of material was assumed to be 27kN/m^3. A total of 288 models were analysed. During modelling, only one-quarter of the cross-section of the circular shaft is modelled due to symmetry. As a failure criterion, Generalised Hoek-Brown Equation (Hoek and Brown, 1997), presented through Equations 1-4, was used. With the help of a new FISH function, an equivalent Mohr Envelope was derived and the tensile strength, cohesion and internal friction .angle were calculated. The Generalised Hoek-Brown criterion is presented in Equation (1).

$$\sigma'_1 = \sigma_3 + \sigma_{ci}\left(m_b \frac{\sigma_3}{\sigma_{ci}} + s\right)^a \qquad (1)$$

where
σ'_1= maximum effective stress at failure

σ'_3= minimum effective stress at failure
σ_{ci} = uniaxial compressive strength of the intact rock
mb,s,a = Hoek-Brown constants which depend on charecteristics of rock mass.

The material constant mb can be determined by Equation (2).

$$m_b = m_i \exp\left(\frac{GSI - 100}{28}\right) \quad (2)$$

where, GSI *is the* geological strength index and m,- İs the intact rock constant.

For GSI >= 25 the original Hoek-Brown criterion İs applicable with

$$s = \exp\left(\frac{GSI - 100}{9}\right)$$

and a=0.5 (3)

For GSI < 25

$$a = 0.65 - \frac{GSI}{200}$$

and s=0 (4)

For better quality rock masses(GSI>=25), the value of the GSI can be estimated directly from the 1976 version of Beniawski's Rock Mass Rating, with the ground water rating set to 10 (dry) and the adjustment for joint orientation set to 0 (very favourable). For very poor quality rock masses the value of RMR is very difficult to estimate and the balance between the ratings no longer gives a reliable basis for estimating rock mass strength. Consequently, Bieniawski's RMR classification should not be used for estimating GSI values for poor quality rock masses. If the 1989 version of Bieniawski's RMR classification is used, then GSI=RMRg9-5 where RMRgg has the groundwater rating set to 15 and the adjustment for joint orientation is set to zero (Hoek and Brown, 1997).

It should be noted, however that in order to provide a more quantitative basis for evaluating GSI values, the modifications were suggested by Sönmez and Ulusay (1999) should be considered. These modification include easily measurable parameters with their ratings and/or intervals which define the blockiness and surface condition of discontinuities.
An example of a failure zone developing around a circular opening is presented in Figure 1. In this example, the input parameters used are as follows: the depth is 300m, P_v=Ph2=8.1MPa uniaxial compressive strength of intact rock is 50 MPa, shaft radius is 3 meters, ratio of horizontal principal-stresses İs k=0.75 and mRMR is 60.

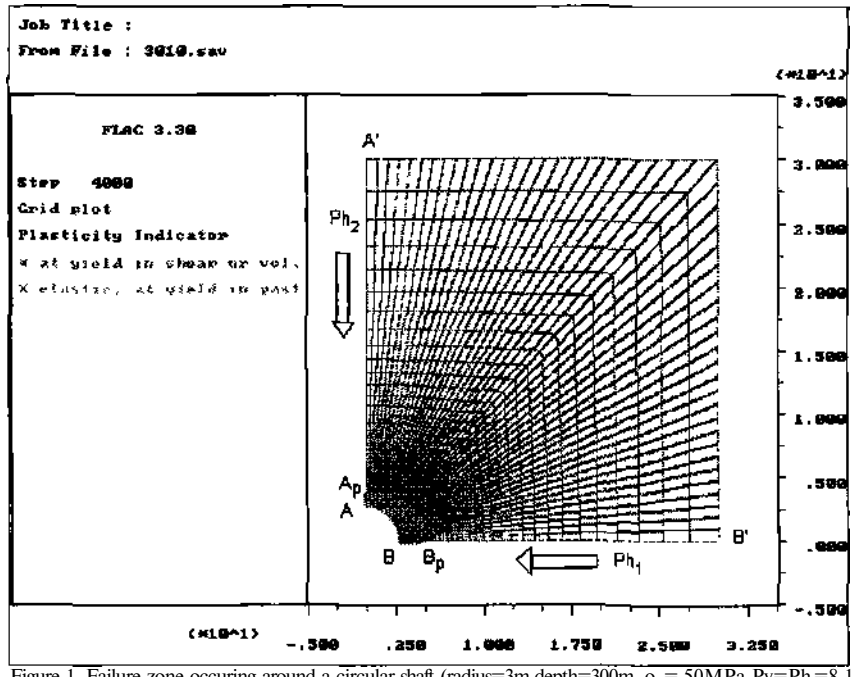

Figure 1. Failure zone occuring around a circular shaft (radius=3m,depth=300m, o_{ci}= 50MPa,Pv=Ph,=8.1 MPa,k= Ph(/Ph2=0.75, mRMR=60, m,=4) (Öztürk, 2000).

In order to check the validity of the model and to investigate the extent of the broken zone, the stress distribution presented in Figure 2 was analysed. This figure İs the result of a model having a principal horizontal-stress ratio of 0.75 and vertical in-situ stress of 8.1 MPa. As can be seen from this figure, at the roof and wall (when the shaft cross-section İs taken into account, the right side is called the wall) of the opening, the tangential stress jumps provides information about the extent of the disturbed zone. Another point that should be be mentioned is that as one goes away from the opening, stresses converge to in-situ stresses. In this study,the maximum extent of the broken zone was taken as the broken zone thickness.

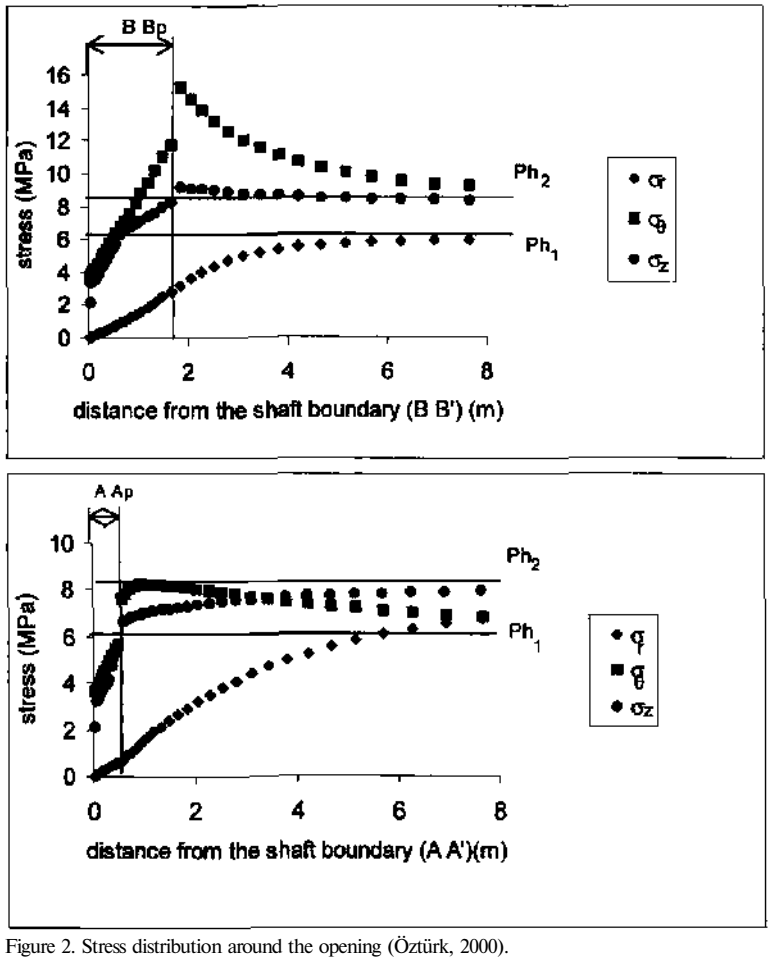

Figure 2. Stress distribution around the opening (Öztürk, 2000).

2.2 *Rock Load Height*

The rock-load height in underground openings can be calculated by using Equation (5), developed by Unal(1983; 1992).

$$ht = S * \left[\frac{100 - mRMR}{100}\right] * B \qquad (5)$$

where mRMR is the modified rock mass rating defined by the modified-RMR system developed on the basis of Bieniawski's RMR-system (Unal, 1989; 1996),B is the span, and S is the stress factor that should be determined by means of numerical studies.

Unal (1999) defines the rock-load height as the height of the potential instability zone around the opening which will exert pressure on the support.

This parameter is used, by the author, in the support design of roadways excavated at depuis of 50-500 meters.

3 COMPARISON OF THE ORIGINAL ROCK LOAD HEIGHTS AND FAILURE ZONES

In this study, the failure height {hfj is defined as the maximum extent of the failure zones around the circular shaft openings. During analyses, the failure heights were compared with the rock load heights (ht) obtained from the mRMR system. A typical plot obtained from the results of the empirical and numerical analyses is shown in Figure 3.

In Figure 3, the rock quality is kept constant (mRMR=60), while the broken zones are plotted as a function of various ratios of horizontal-principal-stresses (k) and shaft diameter. For h, calculations, "S" is taken as I. As can be seen in Figure 3, rock-load height is not sensitive to stress. Therefore, a stress factor (S) is necessary to calibrate the rock-load height. This process was realized by regression analyses, explained in Section 4.

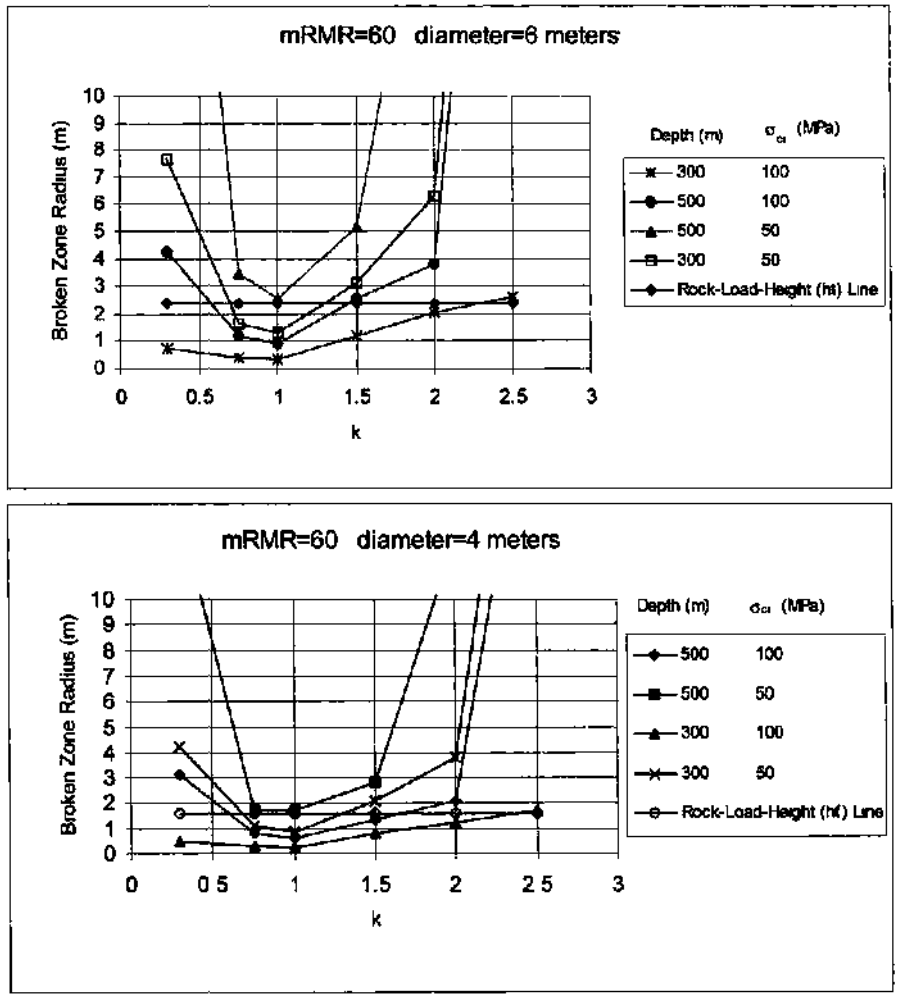

Figure3 Variation of broken zone radius with the ratio of horizontal-principal stresses (k) (Öztürk, 2000).

4 REGRESSION ANALYSES

Regression analyses were carried out by taking 288 models into account. These models were derived from combinations of ratio of horizontal-principal stresses with (0.3, 0.75, 1, 1.5, 2, 2.5), mRMR values (26, 35, 45, 60, 75, 85), depths of 300 and 500 meters and uniaxial compressive strength of intact rocks of 50 and lOOMPa and spans of 4 and 6 meters. Regression Equation (6) relates the numerical broken zone radius to empirical rock-load height (Öztürk, 2000).

$$S = Ae^{Bk} + Ck + D\frac{\sigma_{ci}}{P_v} \quad (6)$$

where,

k = ratio of horizontal principal-stresses

σ_{ci} = uniaxial compressive strength of intact rock (MPa)

P_v = vertical in-situ stress (MPa)

$A.B.C.D$ = regression constants which are presented in Table 1.

Table 1. Regression constants

RMR	A	B	C	D	R*
26	19.772	0.605	-24.727	-1.438	0.73
35	14.882	0.588	-17.814	-1.106	0.76
45	11933	0.59	-14.25	0.928	0.74
60	8.584	0.58	-10.042	-0.661	0-67
75	4.89	0.564	-5.79	-0.335	0.68
85	1.693	0-52Ş	-1.615	-0.078	0-5

For circular shafts, the rock-load height equation can be presented as shown in Equation (7).

$$ht = S * \left[\frac{100 - mRMR}{100}\right] * 2R_i \quad (7)$$

ht = 5*

where, = inner shaft radius

Ri

5 DETERMINATION OF LINING PRESSURE AND THICKNESS

For determination of tiie pressure exerted on die rock-lining contact, Equation (8), suggested by Unal (1999), can be used.

$$P_i = ht * \gamma * TS \quad (8)$$

where,

ht = rock-load height

y = unit weight of rock material

TS = support constant changes between 1 and 2.25 (Unal, 1999)

A comparison of Pressure Equation (8) with values reported in die literature is presented in Figure 4.

As can be seen from Figure 4, there is a good agreement witii observed values. The modified equation forms the upper limit for die values of mRMR smaller than 30; for other values of mRMR, the associated graphs are between die upper and lower bounds.

After finding the pressure, for the calculation of lining thickness, Lamé's thickwall cylinder theory (Timoshenko, 1976) can be used as shown in Figure 5 and Equation (9).

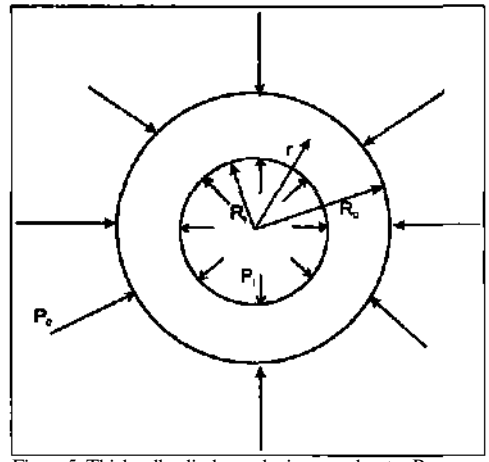

Figure 5. Thickwall cylinder under inner and outer Pressure (Timoshenko, 1976).

$$t = R_i\left(\left(\frac{\sigma_{\theta\,max} / SF}{\sigma_{\theta\,max} / SF - 2P_i}\right) - 1\right) \quad (9)$$

where,

$R\backslash$ =shaft radius

t =lining thickness

SF =safety factor applied to the ultimate compressive strength of the concrete

$\sigma_{\theta max}$ =tangential stress at the inside face of the lining prior to failure inside lining radius

Po =uniformly distributed hydrostatic pressure at the rear of the lining.

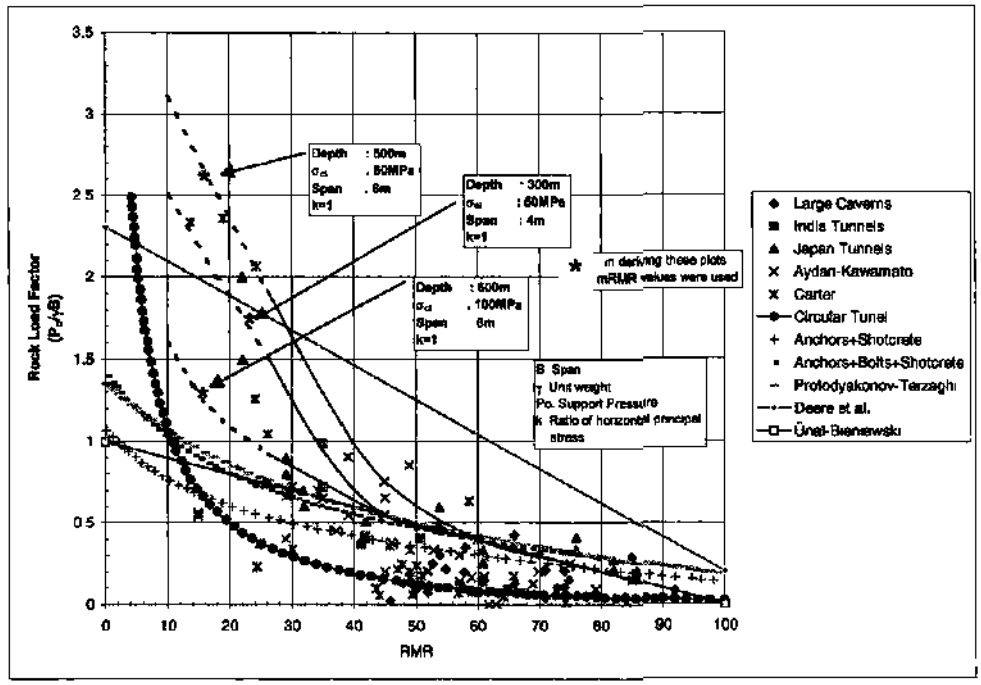

Figure 4. Comparison of pressure equation with reported values (modified after Aydan, 1999).

6 COMPUTER PROGRAM SHAFT

The computer program SHAFT (Öztürk, 2000) has been developed by the authors for determination of shaft support requirements. The program is written in Quick-Basic and consists of several sub-programs.

The required data to be provided by die user are listed below.

1. Radius of the shaft.
2. The number of regions (each region is a section of me rock mass which may respond to the shaft excavation in the same manner).

For each region the required data are:

3. RMR value or GSI value.

NOTE: RMR can be used considering the RMR classification system of Bieniawski 1989. However,the ground water index should be taken as IS and the joint orientation index should be taken as 0. If the RMR value is less than 40, which is usually the case for weak stratifying and clay-bearing rock, then it is suggested that Unal's mRMR index value be used.

4. The depth of each region from the surface (bottom depth of each region).
5. Uniaxial compressive strength of intact rock material.
6. Unit weight of rock material.
7. Ratio of horizontal principal stresses.
8. Compressive strength of the concrete.
9. Required minimum factor of safety.
10. Compressive strength of steel (when required).
11. Required minimum factor of safety for steel.

The program provides the design outputs in graphical form. The total depth of the shaft is drawn on the screen. The cursor can be moved vertically along the shaft langth to obtain information for the required location. Moving this cursor to the desired point and progressing "ENTER" key will open a window on the screen. The design requirements for that particular point can be seen on the screen and can be printed if desired.

Example output data are shown in Figure 6. The following parameters were used for this example.

Shaft diameter	:3m
Number of zones having the same properties: 2	
For zone number 1	
mRMR	:26
Depth	:200m
Unit Weight	:27kN/m^3
Uniaxial Compressive Strength	:25 MPa
Ratio of horizontal principal-stresses	:3
For zone number 2	
mRMR or GSI	:85
Depth	:500m
Unit Weight	:27 kN/m^3

Uniaxial Compressive Strength :50 MPa
Ratio of horizontal principal-stresses :1
Concrete Properties:
Strength 50 MPa
Safety Factor : 1
Steel Properties:
Strength : 200 MPa
Safety Factor : 1
Outputs:
Sample outputs are presented in Figure 6.

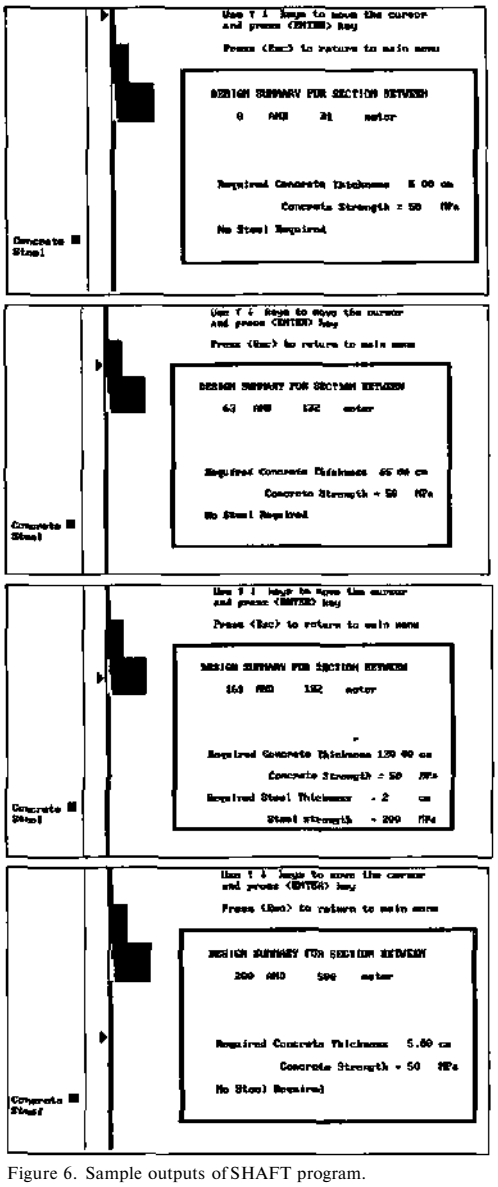

Figure 6. Sample outputs of SHAFT program.

7 CONCLUSIONS

According to the results of this study, the following conclusions were drawn.

1. The preliminary requirement for a support design in a shaft is knowledge of the extension of the broken zone. This parameter can be obtained from numerical analysis or simply from the following equation proposed in this study:

$$ht = S * \left[\frac{100 - mRMR}{100}\right] * 2R,$$

where

ht =rock-load height representing broken zone radius
$R,$ = shaft radius
$mRMR$ = modified Rock-Mass Rating
S = stress factor

2. It was observed from the regression analysis that die stress factor "S" is a function of the uniaxial compressive strength of intact rock, ratio of horizontal stresses and vertical stress in the form of:

$$S = Ae^{Bk} + Ck + D\frac{\sigma_{cf}}{P_v}$$

where:

k = ratio of horizontal principal-stresses
c_c, = uniaxial compressive strength of intact rock
P_v = vertical in-situ stress
A,B,C,D = regression constants

3. The pressure on the support can be found simply by multiplication of ht with the unit weight of the material and the support constant.
4. With the help of the computer program SHAFT, complex shaft lining design calculations were simplified. By providing information on the geometry and the properties *of* material through the shaft-driven zones, detailed information on lining requirements throughout the pre-entered successive zones of a driven depth can be obtained.

REFERENCES

Aydan, Ö. 1999. Support System of Large Underground Openings According to RMR Classification System *Yeraltı Yapılarında Mühendislik Jeolojisi Kollokyumu,* s. 103-110.

Bieniawski, Z.T 1989 *Engineering Rock Mass Classification.* Me Graw Hill, New York

Hoefc, E. and Brown, E.T 1997. Practical Estimates of Rock Mass Strength. *Int J. Rock Meek Min. Sei.* Vol.34 No.8. pp. 1165-1186

Itasca, 1993. FLAC Code, 3 Vol, Minneapolis, USA

Öztörk, H. 2000. *Prediction of Broken Zone Radius and Lining Thickness Around Circular Mine Shafts* M. Sc. Thesis, 136 pages, METU, Turkey.

Sönmez, H., Ulusay, R. 1999. Modifications to the geological strength index (GS!) and then" applicability to stability of slopes. *International Journal Of Rock Mechanics And Mining Sciences.* Vol. 36: (6) pp. 743-760.

Timoshenko, S. 1976. *Strength of Materials, Part II, Advance Theory and Problem.* 3rd Edn. Van Nostrand Reinhold^ New York.

Unal, E. 1983. *Development of Design Guidelines and Roof-control Standards for Coal Mine Roofs,* **Ph.D.** Thesis, Penn State Univ., USA.

Unal, E. 1992. Rock Reinforcement Design and Its Application m Mining. *Proceedings of the International* Symposium on *Rock Support, Canada,* pp. 541-547.

Unal, E. 1996. Modified Rock Mass Rating M-RMR System. *Milestones in Rock Engineering: A Jubilee Collection; Z. T. Bieniawski, Editor,* A.ABalkema,pp, 203-223.

Unal, E. 1999. Personal Communication

17 International Mining Congress and Exhibition of Turitey- IMCET2001, ©2001, ISBN 975-395-417-4*

New Anchorage Capacity Testing System and Pull-Out Applications in Yeniçeltek Coal Mine

E.Taşel & T.T.Ozan
Atlas Copco Makinaları İmalat A.Ş., Istanbul, Turkey
E.Ünal
Department of Mining Engineering, Middle East Technical University, Ankara, Turkey
MBildik
Yeniçeltek Kömür ve Madencilik A.Ş., Merzifon, Amasya, Turkey

ABSTRACT: A unique 45-ton-capacity, pull-out testing system was developed in METU Mining Engineering department. This system is capable of testing different types of rock bolts and cable bolts. In-situ pull-out tests were carried out in Yeniçeltek Coal Mine using Standard Swellex bolts. A 20-m section of this roadway was successfully supported by these bolts. It was shown that the cost of roadway support can be reduced by about 50%.

1 INTRODUCTION

In recent years, the range of applications of rock bolts has widened due to advances in rock mechanics, developments in rock reinforcement concepts, and better understanding of rock mass and rock bolt interaction mechanisms. Consequently, the use of rock reinforcement systems in underground excavations has increased as an alternative to more traditional forms of support.

Several types of rock bolt testing systems, such as destructive, non-destructive and overcoring techniques, have been developed for understanding the working principle of a rock bolt in different rock masses. The pull-out test is a typical destructive test performed for determining the anchorage capacity of rock bolts. During pull-out tests, bolt displacement is measured as a function of the applied bolt load. The anchorage capacity is one of the input parameters used İn rock reinforcement design. It is also used for controlling the quality of bolt material and installation method.

Currently, it is not possible to test all rock bolt types utilising a single pull-out testing system. Usually a special type of pull-out test device has to be prepared for each kind of rock bolt since the head and manufacturing principles of each type of rock bolt are different.

In this paper, a unique 45-ton-capacity, pull-out testing system that can be used for all rock bolt types İs introduced. The pull-out tests carried out İn Yeniçeltek Coal Mine are also presented.

2 NEW ANCHORAGE CAPACITY TESTING SYSTEM

This system was developed İn METU Mining Engineering department.

2.1 *General layout of the testing system*

In general, the anchorage capacity testing system consists of three main parts, namely, mechanical, hydraulic and electronic.

2.1.1 *Mechanical part*

The mechanical part of the system consists of four main components, namely the *(i)* pull collar, *(ii)* connector, *(Hi)* pull bar, and *(iv)* reaction frame. The pull collar, connector and pull bar are installed onto each other such that they can pull the rock bolt out of the hole İn the direction of the bolt's centerline. The reaction frame was designed to fit the dimensions of the pulling unit and hollow ram. It has four adjustable legs. These legs can be adjusted on a rough surface to keep the pulling direction on the longitudinal axis of the rock bolt. An engineering drawing and a photograph of the mechanical parts installed on each other are shown in Figures I and 2 respectively.

2.1.2 *Hydraulic Part*

The hydraulic part of the system comprises: *(i)* hydraulic hand pump and manometer, *(ii)* hydraulic hose, and *(Hi)* hydraulic hollow ram havmg a capacity of 60 tons.

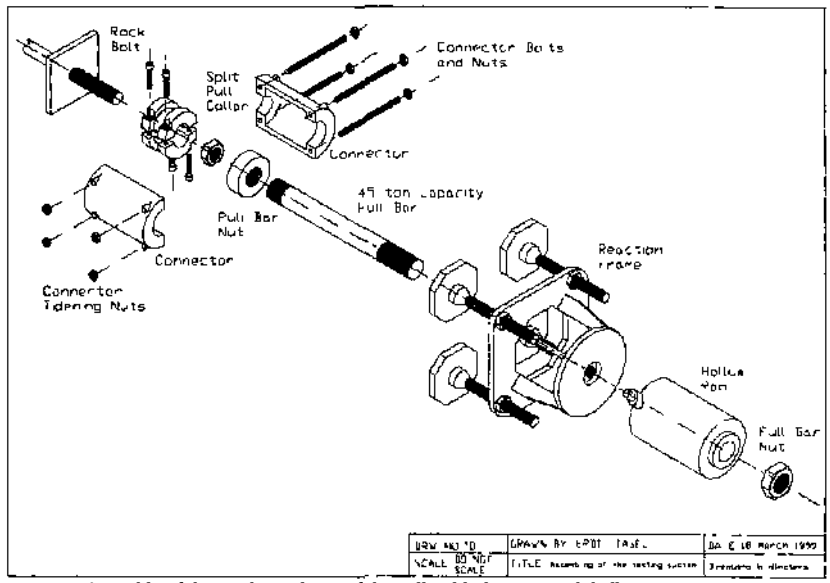

Figure 1. Assembly of the mechanical part of ihe pull-oul lesl system with hollow ram

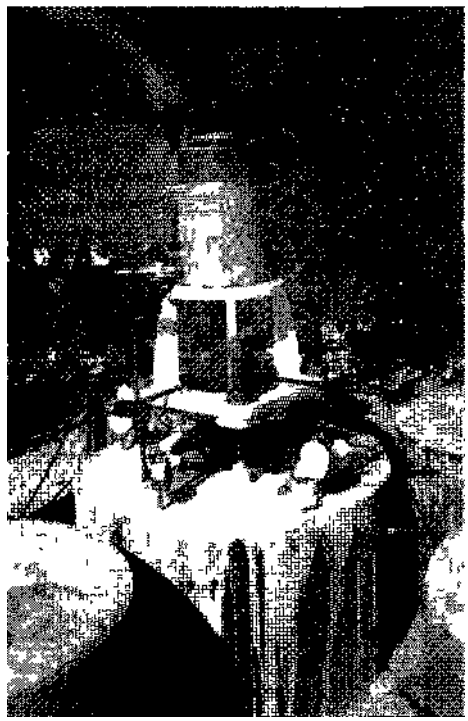
Figure 2. Mechanical part of the pull-out test system

A simple sketch of the hydraulic part of the system is shown in Figure 3. The hollow ram and the hydraulic pump can also be seen in Figures 2 and 5.

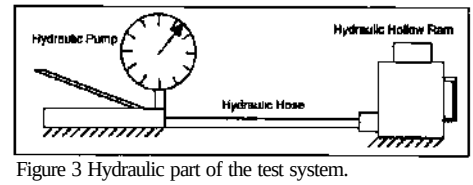

Figure 3 Hydraulic part of the test system.

2.1.3 *Electronic part*

A data acquisition system is essential to handle the massive amount of data obtained during testing and to be able to plot the load-displacement curves.

This system is installed onto the connector with the help of gauge connection bars. The system is capable of taking either electronic or mechanical readings. This is essential because of the limitations in use of A.C. in some underground coal mines. In the METU testing system, the data acquisition part consists of the following components: *(i)* pressure transducer, *(it)* electronic or electromechanical dial gauges or LVDTs, *(Hi)* signal conditioner (input voltage source, filter), *(iv)* strain indicator (amplifier), and *(v)* recorder (personal computer with A/D converter card).

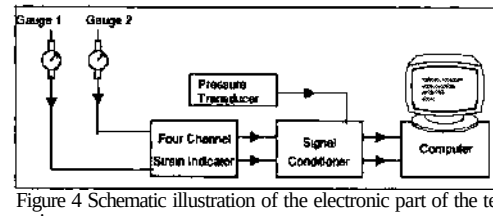

Figure 4 Schematic illustration of the electronic part of the test sysiem.

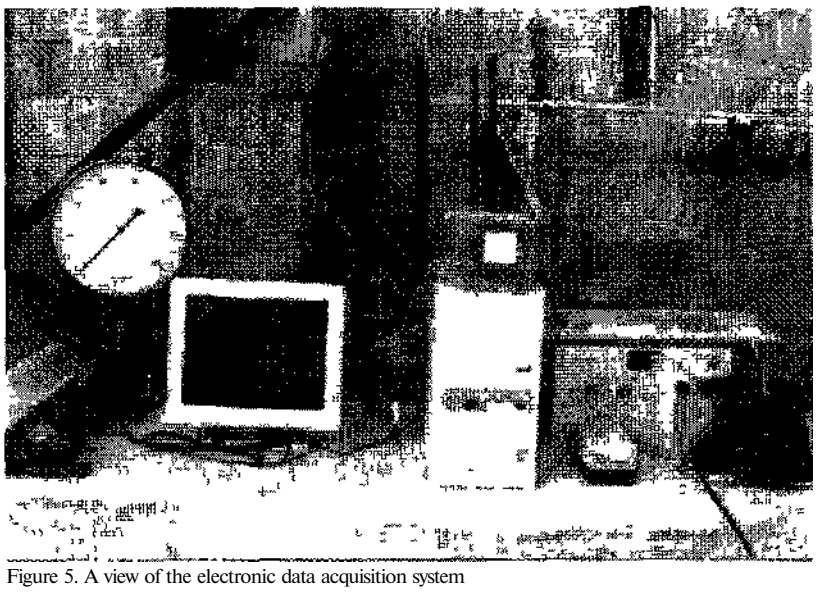

Figure 5. A view of the electronic data acquisition system

3 PERFORMANCE TESTING

During the development of the anchorage testing system, two types of tests were carried out. The "stability tests" provided information about the stability of the mechanical, hydraulic and electronic components. The capability tests provided information about the suitability of the system for testing different types of rock bolts in various rock-mass conditions. The stability tests were carried out İn the METU rock mechanics laboratory and the whole system was checked with a 200-ton-capacity hydraulic testing machine. During these tests, the behaviour of each component of the system was monitored under specific loads. The "capability tests", on the other hand, were performed on different types of rock bolt installed in large-diameter confined hollow specimens made of different qualities of concrete. The confinement was provided by means of steel cells. During these experiments, the testing difficulties were identified.

The anchorage testing system and the confined and bolted specimens are shown in Figure 6.

4 PULL-OUT TESTS IN YEN1ÇELTEK COAL MINE

4.1 *Yeniçeltek underground coal mine*

Yeniçeltek lignite mine is near the Merzifon-Samsun highway, located about 15 km east of Merzifon, 35 km northwest of Amasya and 90 km south of Samsun

In general, the thickness of the coal seam ranges from 8 to 12 meters However, only the upper portion of this seam is mined due to the higher calorific value, determined as 4100 kcal/kg (Gıiyagüler and Ünal, 1998).

In Yeniçeltek Lignite Mine, the retreat longwall mining method is used. The length of the longwall faces is about 80 meters. The faces are supported by two or sometimes three rows of 40-ton-capacity individual hydraulic props, installed under steel caps 1.25 meters long. The excavated coal is transported by double-chain conveyors in the face, by band conveyors in the gate roads, and by loco-trains in the mine roadways. Finally, after travelling a long distance, the coal is transported to the surface with the help of a skip.

4.2 *Test site*

The anchorage capacity tests were carried out in a new haulage way known as "256/210 inclined". This incline is at a distance of about 1 km from the skip bottom, and will connect the +256 level to the +210 level. It will be used to transport the coal that will be produced from new panels of the 302 region A schematic illustration of the test location is shown in Figure 7.

4 3 *Test equipment*

During underground tests, only the mechanical-hydraulic system was used. This system consists of the following parts:

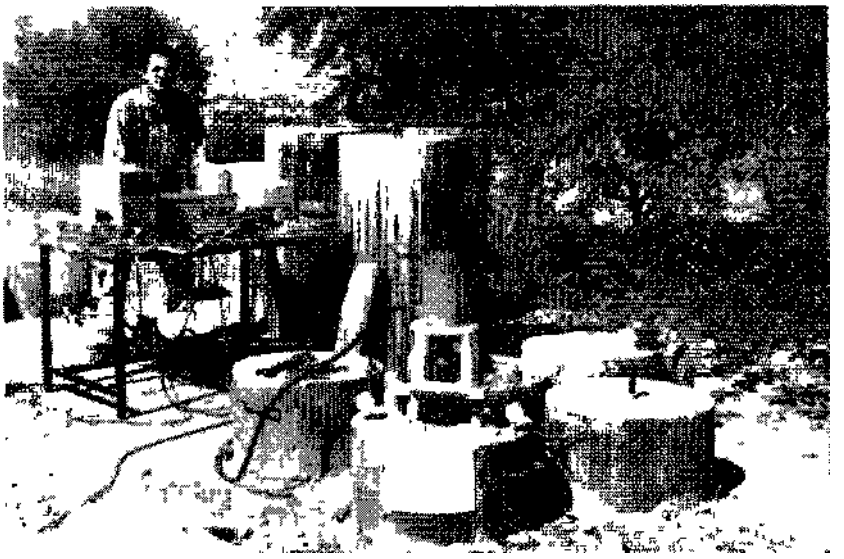

Figure 6. Pull-out tests were simulated on mechanicaly anchored rock bolts and swellex bolts.

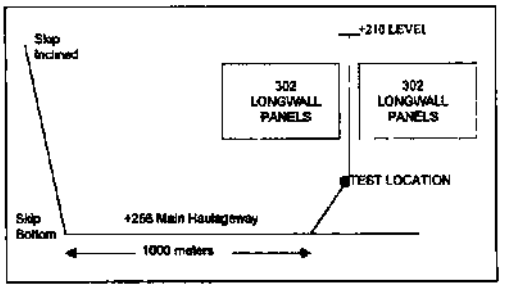

Figure 7. Schematic illustration of the test location at Yeniçeltek coal mine

1. Mechanical Part.
   a) 26-mm split pull collar.
   b) Connector.
   c) 25-ton-capacity pull bar.
   d) Reaction frame.
   e) Dial gauge connection bars.
   f) Extensometer.
2. Hydraulic Part.
   a) 60-ton-capacity hollow ram.
   b) Hydraulic hose.
   c) Hydraulic hand pump.
   d) Manometer.

Anchorage capacity tests were carried out on 2.4-meter-long Standard Swellex bolts. During the first series of tests, a hole about 2.4 m long was drilled in the roof of the haulage way. After the drilling operation, the 26-mm split pull collar was connected to a bolt head and a Swellex bolt was inserted into the drillhole and inflated at a pressure of 280 bar. Following this step, the mechanical components and the 60-ton-capacity hollow ram, hydraulic hand pump and a calibrated manometer were installed. Finally, a telescopic extensometer was placed under the pull-out test system to measure the displacement data.

During die second series of tests, the same equipment was used. However, instead of the extensometer, two mechanical dial gauges were connected to the connector body with the help of the dial gauge connection bars. Thus, displacement measurements were taken between the roof and the bolt. This system can be visualised by turning the pull-out system, shown in Figure 2, upside down. In both tests, safety changes were made to prevent a sudden drop of the system from the roof.

4.4 *Test results*

4.4.1 *First series*

A general view of the testing system and the test location is shown in Figure 8. During testing, an initial arbitrary load of 5 kN was applied to take up the slack in the equipment. Following this step, the load was increased in steps of 5kN. The resolution of the displacement dial gauge was 0.01mm. A typical load-displacement plot obtained from the first series of measurements is shown in Figure 9. As a result of these tests, the anchorage capacity of the Standard Swellex bolts was found to be 90.5kN.

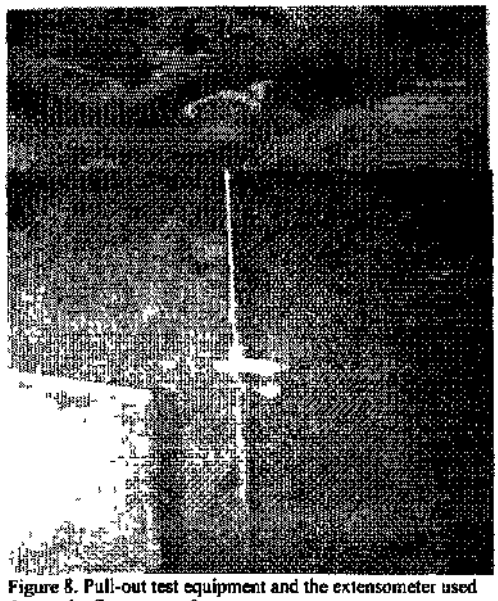

Figure 8. Pull-out test equipment and the extensometer used during the first series of tests.

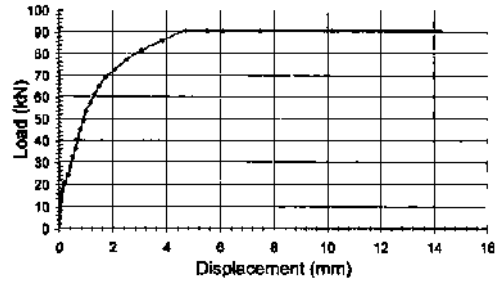

Figure 9 A typical load-displacement plot obtained during the first series of tests earned out in Yeniceltek underground mine.

4.4.2 *Second series*

During this series, instead of a telescopic extensometer, two mechanical dial gauges were used due to the low height of the roadway. A typical result obtained from these series is shown in Figure 10. As a result of these tests, the average anchorage capacity of the Standaid Swellex bolts was found to be lOkN.

5 ROCK REINFORCEMENT DESIGN

During the anchorage capacity tests, the test site was supported by traditional steel arches. Based on the results of these tests, the rock-mass classification studies carried out at the test site, and Ünal's rock reinforcement design codes (1983, 1990, 1999), a 20-m section of the roadway was supported with Standard Swellex bolts. Consequently, it was possible to compare the performances of the roadway supported by both steel arches and Swellex bolts.

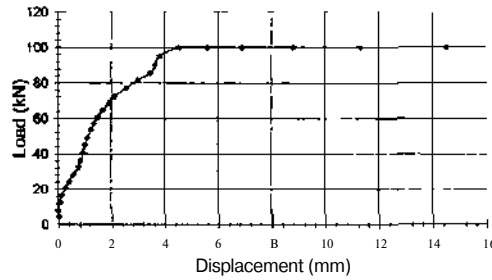

Figure 10. A typical load-displacement plot obtained during the second series of tests earned out in Yeniceltek underground mine

6 CONCLUSIONS

The main findings of this study are the following:

1. The METU pull-out testing system is capable of testing different types of rock bolt, such as mechanically anchored bolts, grouted rock bolts, frictional rock bolts (split-set and Swellex) and most cable bolts having capacities of less than 45 tons.

2. By evaluating the results of the anchorage capacity tests, the modified rock-mass rating (mRMR) values and the design method suggested by Ünal, a 20-m section of this roadway was successfully supported by Swellex bolts. This roadway has been stable ever since.

3. As a result of this application, it was shown that the cost of roadway support can be reduced about 50%.

4. Due to the simple installation procedure of the Swellex bolts, the time required to support the roadway can also be reduced considerably.

REFERENCES

Gıiyaguler, T. & Ünal, E I998. Yeniceltek ve Sorgun Linyit İşletmelerinin rezerv durumlannın belirlenmesi, ekonomik olarak işletilmesi ve yem teknoloji olanaklarının araştırılması projesi. *Proje kod no ODTÜ Agüdos, 98-03-05-01-05. Ankara. Orta Doğu Teknik üniversitesi Maden Mühendisliği Bölümü. Aralık 1998*

Taşel, E., 1999. *Development of a new pull-out testing system for rock bolts* M Sc. Thesis, Department of Mining Engineering, Middle East Technical University, Ankara, Turkey.

Unal, E-, 1983. *Design Guidelines and Roof Control Standards for Coal Mine Roofs.* Ph D Thesis, Pennslyvania State University, University Park, USA.

Unal, E, 1999. Special communication

Una!, E. and Ergür, K M., 1990. PC based modeling of rock reinforcement requirements in mine roadways. *Proc of 31" US Symp Rock Mechanics Contributions and Challenges,* 761-768.

17'" International Mining Congress and Exhibition of Turkey- IMCET2001, ©2001. ISBN 975-395-417-4

Studies in the Relationships between Hardgrove Grindability and Some Rock Index Tests on Çayırhan Coals

B.Tiryaki, KAtasoy, N.E.Yaşıth
Department of Mining Engineering, Hacettepe University, Ankara, Turkey
A.S.Eyüboğlu
Department of Applied Sciences, University of Arkansas at Little Rock, Little Rock AR, USA
M.Z.Ay din
Ministry of Energy and Natural Resources, Ankara, Turkey

ABSTRACT: The most economical and time-efficient method of assessing mechanical properties of coal in the field is rock index tests. The use of these is supposed to be limited to certain applications and rock types. This paper İs concerned with the investigations to determine the usefulness of some rock index tests in assessing mechanical properties of coal and to determine whether there were significant correlations between these tests and the Hardgrove grindability test. For these purposes, an extensive testing program for determining the mechanical and grindability characteristics of coals at Çayırhan Lignite Mine was conducted. Analyses of the test results indicated that, there were significant correlations between the Schmidt hammer, Shore scleroscope and NCB cone indenter hardness tests and the Hardgrove grindability test, while point load tests gave the uniaxial compressive strength values close to those determined through compression tests, revealing the practicability of these tests on coal.

1 INTRODUCTION

Coal, being a natural resource, is involved in several operations during the mining and processing stages, such as excavation by cutting machines or drill-and-blast technique, pillar support, crushing, and grinding. Selection and, when necessary, optimisation of the coal excavation machine, pillar design in room-and-pillar mining, and crusher and mill selection in coal-fired power stations or in coal preparation plants all basically depend on mechanical properties of coal such as strength and hardness. In operations where the physical structure of coal is destroyed, determination of the probable behaviour of coal in terms of cuttability and grindability is also of paramount importance.

Determining these properties through comprehensive laboratory studies is likely to be expensive and time-consuming. In particular, cuttability and grindability tests require complicated laboratory facilities. For the determination of mechanical properties of rocks, fast, easy, and cost-efficient methods and testing equipments have been developed and standardized through studies organized by the International Society for Rock Mechanics (ISRM). Although these tests can be applied both in the laboratory and in the field on various shapes of rock samples, their applicability and reliability for different rock types and fields of application are still matters for discussion (Bilgin & Shahriar, 1986; O'Rourke, 1989; Göktan & Ayday, 1993; Holmgeirsdottir & Thomas, 1998). Furthermore, the literature does not seem to contain any comprehensive in-situ or laboratory studies on the relationships between the cuttability or grindability of coal with the most common tests in relation to rock excavation.

This paper is concerned with detailed laboratory and in-situ investigations on coals from the Çayırhan district, carried out during a research project on the performance optimisation of coal shearers employed at Çayırhan Lignite Mine (Tiryaki, 1998). A series of mechanical and grindability tests were made in-situ and on laboratory samples in an attempt to investigate the relationships between rock and coal index tests when employed in evaluation of coal properties, and to determine their reliability in predicting the uniaxial compressive strength of coal. For these purposes, Schmidt hammer, Shore scleroscope, NCB cone indenter, point load, and Hardgrove grindability tests, along with uniaxial compression and Brazilian tests were conducted on coal samples taken from the upper and lower coal beds of the A-05 and F-02 longwall panels. The results from both the laboratory and in-situ experiments were analysed statistically and are discussed.

2 DESCRIPTION OF THE STUDY AREA

Çayırhan Lignite Mine is the first fully mechanized underground coal mine in Turkey. Formerly operated by Turkish Coal Enterprises (TKJ), it is now run by Park Enerji, a joint venture of Park Holding and SaarTech, with a planned annual production of about 5 Mt with a view to feeding a coal-fired power station of 4 x 150 kW. The panel layouts of the A and F fields of the mine are given in Figure 1. The shaded areas in Figure 1 indicate panels A-05 and F-02 from which coals were tested in this study. The Çayırhan coal basin contains two coal seams separated by the interburden sediments. The total thickness of interburden sediments varies from 120 to 150 m. The upper coal seam that has been extracted is separated into two coal beds by a siltstone interlayer varying from 0.4 to 1 m in thickness. The average thickness of the upper coal bed is 1.5 m, while that of the lower coal bed is 1.7 m. These are extracted individually using a fully mechanized retreat longwall method with caving. The upper coal seam, which is 1.45 t/m^3 in density, contains 23.94% carbon, 22.06% moisture, 30.17% ash, and 4.02% sulphur, with an average heating value of 2868 kcal/kg (TKI1987).

3 DETAILS OF TESTS

3.1 *Specimen preparation*

All index tests, with the exception of the Schmidt hammer test were carried out in laboratory conditions. Numerous coal block samples were taken from the upper and lower coal faces of the A-05 and F-02 panels. They were packed tightly İnside double-polyamide sample bags underground and were then transported to the Rock Mechanics Laboratory at Hacettepe University Mining Engineering Department, and the Mineral Analysis and Technology Division Laboratories at the General Directorate of Mineral Research and Exploration of Turkey (MTA). Only coals from the face sections close to the main entries to the four longwall faces were evaluated in this study, taking into consideration the prevailing stress conditions along the faces. Irregular coal specimens with parallel ends were used for Shore scleroscope and point load tests, whilst specific specimen preparation steps were followed for the compression, Brazilian, NCB cone indenter, and Hardgrove grindability tests. Cylindrical core specimens for uniaxial compression tests were obtained by drilling the sample in such a way that the drill bit's longitudinal axis was perpendicular to the bedding planes of the sample. For the Brazilian tests, additional cylindrical core specimens that have longitudinal axes parallel to the bedding planes were obtained by drilling. Disc specimens for the Brazilian test were then machined from these cylindrical core specimens.

Some difficulties were encountered during the specimen preparation stages of the mechanical tests due to the brittle and friable nature of the coal. The coal specimens tended to disintegrate, either it the core drilling stage while attempting to obtain required sizes, or at the cutting stage while trying to ensure parallel ends for the compression and Brazilian tests. Therefore, compression and Brazilian tests were achieved only with samples from the F-02 panel where in-situ coal cutting tests were conducted. The standard testing procedures suggested by the ISRM for testing mechanical properties of rock were followed throughout the tests, except in the NCB cone indenter tests. These tests were conducted on small coal specimens, following the instructions given by the National Coal Board (NCB) of the UK. Hardgrove grindability tests were carried out according to ASTM (American Society for Testing and Materials) standard D 409-71 (NCB, 1977; ASTM, 1983).

3.2 *Uniaxial compression test*

Cylindrical specimens BX in diameter x 10 cm in length, for both the lower and upper coal beds of the F-02 panel, were loaded in such a way that the direction of loading was perpendicular to the bedding planes, using a stiff testing machine with a capacity of 3000 kN at a loading rate of 0.05 kN/s. The uniaxial compressive strength of the test specimens was calculated from the load at failure (ISRM 1979). The average compressive strength for the lower coal bed was found to be 8.6 MPa and for the upper coal bed, İt was 7.9 MPa. These values are close to those obtained in a previous study by Ünal (1974); 9.19 MPa for the lower coal bed and 8.35 MPa for the upper coal bed.

3.3 *Brazilian test*

Disc specimens BX in diameter x 2 cm in thickness, for both the lower and upper coal beds of the F-02 panel, were loaded in such a way that the direction of loading was perpendicular to the bedding planes, using a MTS-type hydraulic press with a capacity of 10 tons at very low machine-controlled loading rates (ISRM 1978b). The average uniaxial tensile strength for the lower bed was found to be 2.1 MPa, while this figure was 2.6 MPa for the upper bed.

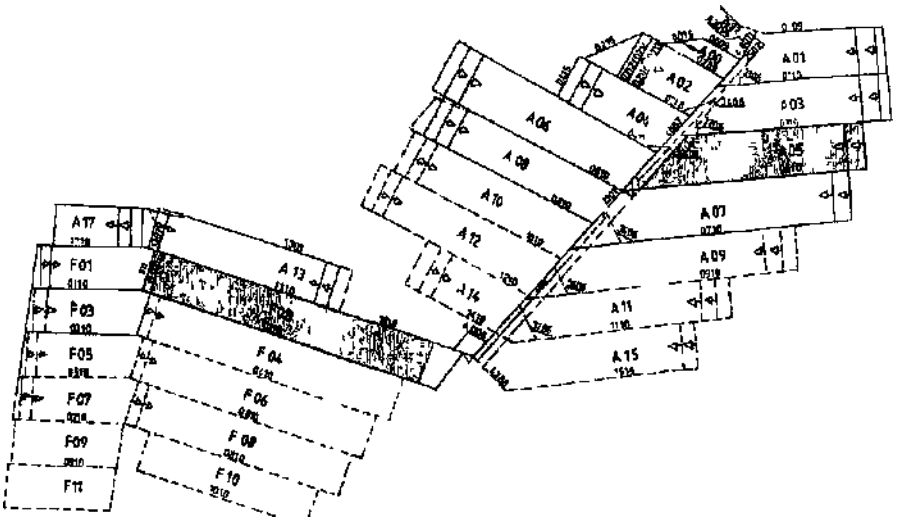

Figure 1. Panel layouts of A and F fields at Çayırhan Lignite Mine

3.4 *Schmidt hammer test*

The Schmidt hammer rebound test was developed to determine the compressive strength of concrete, and has been used to determine the hardness and compressive strength of rock material (ISRM 1978a). This equipment is portable, easy to use, and can be applied both in die laboratory and İn tihe field. It has also been reported that the Schmidt hammer has a possible use in the prediction of die performance of mechanical excavators considering the mechanical properties rock if proper testing, recording, and data processing methods are used (Göktan & Ayday, 1993).

Schmidt hammer rebound tests were carried out directly on the faces of the lower and upper coal beds at both the A-05 and F-02 panels by using a calibrated L-type hammer (Fig. 2). Face areas close to die main entries to four Iongwalls corresponding to die first 15 shield supports in these Iongwalls, each wim a width of 1.5 m, were adopted as die

Figure 2. Schmidt hammer.

measurement areas. At least 20 individual tests were conducted on diese areas, separated by at least a plunger diameter, in which die longitudinal axis of the hammer was perpendicular to the face plane. Following die determination of individual Schmidt rebound hardness values for the longwall faces, corresponding uniaxial compressive strength values were calculated according to me calibration curves supplied by the hammer manufacturer (Table 1).

3.5 *Shore scleroscope test*

The Shore scleroscope rebound test was originally designed to determine the hardness of metals, and then a procedure was suggested by the ISRM with which to utilize this test for determining the hardness of rock materials (ISRM 1978a). Previous studies have revealed me potential of dûs test in the assessment of *the* plasticity and uniaxial compressive strength of rocks (McFeat-Smith 1977, Holrageirsdottir & Thomas 1998).

A senes of rebound tests were conducted on die flat surfaces of coal specimens from the lower and upper faces of the A-05 and F-02 panels using a Model C-2 Shore scleroscope (Fig. 3). At least 20 tests were conducted on each specimen, separated by at least 0.5 cm, in which the longitudinal axis of the glass tube was perpendicular to the bedding planes of me specimens. The Shore scleroscope hardness of each coal bed was determined by averaging die arimmetic mean values obtained from individual test specimens (see Table 1).

Table 1. Measured index values and predicted uniaxial compressive strengths for A and F field coals.

Indices	Measured Index Values				Predicted Uniaxial Compressive Strengths (MPa)			
	A-05 Panel		F-02 Panel		A-05 Panel		F-02 Panel	
	Upper Bed	Lower Bed	Upper Bed	Lower Bed	Upper Bed	Lower Bed	Upper Bed	Lower Bed
Schmidt Hammer	47.43	52.98	40.42	52.19	53.00	63.00	43.00	61.00
NCB Cone Indenter	1.2123	1.2090	1.1785	1.1781	20.00	19.95	19.44	19.44
$I_{a(50)}$ Perpendicular	0.39 MPa	0.28 MPa	0.76 MPa	0.48 MPa	8.58	6.16	16.72	10.56
$I_{a(50)}$ Parallel	0.36 MPa	0.27 MPa	0.38 MPa	0.31 MPa	7.92	5.94	8.36	6.82
$I_{a(50)}$	1.08	1.04	2.0	1.55	–	–	–	–
Shore Scleroscope	43.34	47.85	40.18	46.03	–	–	–	–
Hartigrove	49.28	34.57	64.80	40.71	–	–	–	–

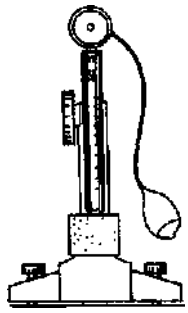

Figure 3. Shore scleroscope.

3.6 *NCB cone indenter test*

The NCB cone indenter test apparatus was developed at the NCB to determine the hardness and umaxial compressive strength of rock that may be cut by a mechanical excavator by measuring its resistance to indentation by a hardened tungsten carbide cone (Fig. 4). The basic principle of this apparatus is to measure the penetration depth of the cone into rock for a known applied force. Details of the testing, recording and data processing methodologies for the NCB the cone indenter test can be found elsewhere (NCB, 1977; Bilgin & Shahriar, 1986). It has been reported mat there is a high correlation between the NCB cone indenter hardness and the performance of mechanical excavators, especially for coal measures strata. In addition, the equation proposed by the NCB for predicting uniaxial compressive strength of rock in relation to the NCB the cone indenter hardness value gives satisfactory results in the extent of sedimentary rocks tested (NCB, 1977).

NCB cone indenter tests were conducted on the small pieces of coal 12 x 12x6 mm in size taken from the lower and upper coal beds of the A-05 and F-02 panels. An average of at least 10 measurements was considered to characterize the coal beds in terms of NCB cone indenter hardness. The average NCB cone indenter hardness values of each coal bed were then employed for the determination of the corresponding uniaxial compressive strength values using Equation 1 (see Table 1).

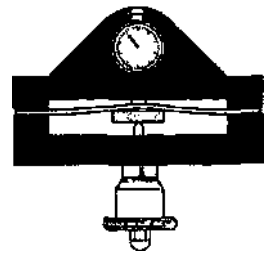

Figure 4. NCB cone indenter.

$$UCS = I_w \times 16.5 \quad (1)$$

where *UCS:* uniaxial compressive strength of coal and I_w*:* NCB the cone indenter hardness of coal.

3.7 *Point load test*

The Point load test has been widely used as a rock strength index for many years with great accuracy (Broch & Franklin 1972, Bieniawski 1975). The test apparatus is portable and can be applied either in the field or in the laboratory, on rock specimens that are in the form of a core, disc, or irregular lump (Fig. 5). The point load strength index (I450)) and the strength anisotropy index (I»<so)) values of rock specimens are determined by compressing the rock specimens between two standard conical platens. The strength index is calculated considering the load and the distance between the platens at failure (ISRM, 1985). Point load strength values are known to correlate well with the uniaxial compressive and tensile strengths of a wide range of rocks.

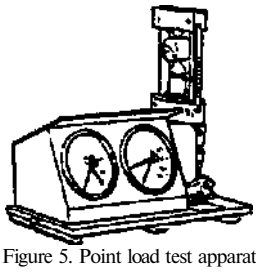

Figure 5. Point load test apparatus.

Point load strength tests were conducted on irregular coal lumps from the lower and upper coal beds of the A-05 and F-02 panels. Tests were carried out both in the perpendicular and parallel directions to the bedding planes of coal lumps. At least 10 tests were made in each loading direction for each coal bed. Anisotropy index values for each coal bed were calculated by dividing the average strength index values found during perpendicular loading by those found during parallel loading. The average $I_{s(50)}$ values found in both perpendicular and parallel loading directions, and average $I_{a(50)}$ values for each coal bed are given in Table 1. The average $I_{s(50)}$ values found during perpendicular loading were then employed for the prediction of the corresponding uniaxial compressive strength values using Equation 2 (see Table 1).

$$UCS = I_{s(50)} \times 22 \quad (2)$$

where *UCS:* uniaxial compressive strength of coal and $I_s fso)$- point load strength index found during perpendicular loading.

3.8 *Hardgrove grindability test*

With the development of pulverized coal-fired power stations, there was a need to evaluate the different coals in terms of resistance to grinding for use in pulverized fuel furnaces. The Hardgrove grindability test was developed to determine the relative grindability or ease of pulverization of different coals when compared to standard coals. A certain amount of coal is subjected to a grinding energy in a Hardgrove mill, and the change in the size of the coal particles is expressed as the Hardgrove grindability index by sieving. Lower index values correspond to a higher resistance to grinding (Hardgrove 1932, ASTM 1983, Szwilski 1985). Studies carried out at MTA on coals from different collieries in Turkey have shown that as the Vickers microhardness values of coals increase, corresponding Hardgrove grindability index values asymptotically decrease (Gencer 1986). Since the grindability of coal is mainly a function of mechanical properties of coal such as strength, hardness, elasticity and fracturing, it also has a close relationship with the cuttability of coal. It has been reported that the Hardgrove grindability method can also be adopted for determining the cuttability of coal (Evenden & Edwards 1985). Previous research by Roxborough et al. (1981) on the in-situ cutting performance of a continuous miner revealed that in all cases low Hardgrove grindability index values corresponded to high cuttability, i.e., high resistance to cutting action.

Hardgrove grindability tests were conducted on representative samples from the lower and upper coal beds of the A-05 and F-02 panels, İn the laboratories of the Mineral Analysis and Technology Division at MTA (see Table 1).

4 ANALYSIS OF TEST RESULTS

The data obtained from the laboratory and in-situ tests on the Çayırhan district coals were analysed in an effort to establish the correlation between the mechanical properties measured by rock index tests and the grindability of coal. These data were also analysed to investigate the reliability of some mechanical index tests in predicting the uniaxial compressive strength of coal, and to investigate the relationships between mechanical index tests. For these purposes, the test results were analysed statistically in series of pairs. In the analyses, the degree of the relationship between the variables investigated was explained in terms of the coefficient of regression.

Statistical analysis revealed that both the Schmidt hammer and Shore scleroscope hardness values were in very high correlation with Hardgrove grindability index values of four coal samples taken from different longwall panels of Çayırhan Lignite Mine. Figures 6 and 7 show the best-fit curves between the Hardgrove grindability index and Schmidt hammer and Shore scleroscope test results, respectively.

NCB cone İndenter tests showed that the coals of the A-05 panel were harder than those of the F-02 panel. According to the results of the Hardgrove grindability tests, coals of the A-05 panel are more difficult to grind than those of the F-02 panel. Since the Hardgrove grindability index is known to be indirectly proportional to the hardness of the material, NCB cone indenter tests can be considered to succeed in reflecting the differences found in the Hardgrove grindability values between the A-05 and F-02 panel coals (Fig. 8).

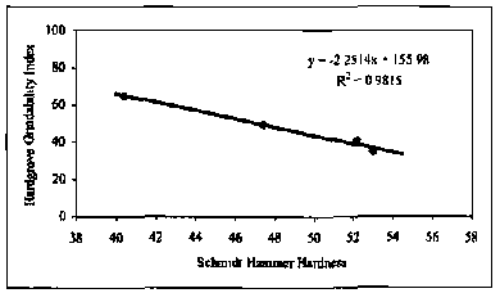

Figure 6. Relationship between Schmidt hammer hardness and Hardgrove gnndability index.

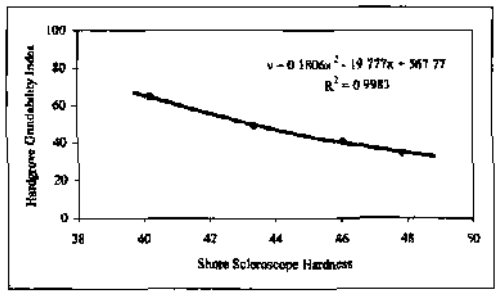

Figure 7. Relationship between Shore scleroscope hardness and Hardgrove gnndability index.

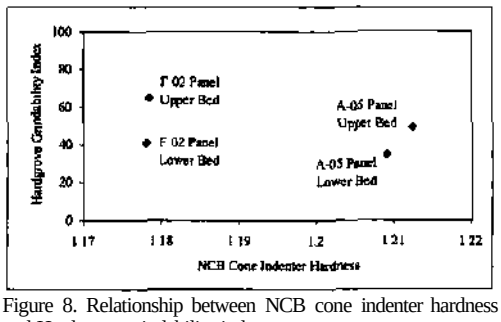

Figure 8. Relationship between NCB cone indenter hardness and Hardgrove grindability index.

However, NCB cone indenter tests did not reveal differences between the lower and upper coal beds for both the F-02 and A-05 panels in terms of NCB cone indenter hardness. This may be due to the lack of differences between the indentation hardness values of coals of the upper and lower coal beds for each longwall panel, which can be sensed by the NCB cone indenter test. According to the hardness scale for the standard NCB cone indenter test proposed by McFeat-Smith (1977), coals of the A-05 and F-02 panels can be considered moderately soft.

The Results of the point load strength tests for perpendicular and parallel loading directions showed that as point load strength index values for both loading directions increased, the Hardgrove grindability index values also increased (Fig. 9). This finding conflicts with the fact that, the Hardgrove grindability test suggests a decrease in grindability index values, i.e., increase in the power required to grind a certain coal, with increase in hardness and strength values.

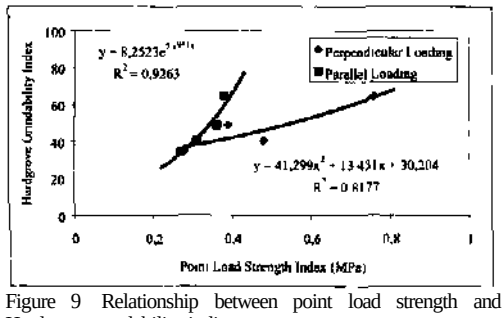

Figure 9 Relationship between point load strength and Hardgrove gnndability indices.

This situation may arise from the impracticability of point load strength test for characterization of rock materials with very low strengths with respect to their point load strength index values. Hoek (1977) pointed out that very soft materials, such as mudstones and claystones, with a compressive to tensile strength ratio of about 5 may not be tested accurately using the point load test.

Even if the correlation between the point load strength index values and Hardgrove grindability index values was regarded as unsatisfactory, the point load test seemed to be best as a prediction tool for the compressive strength of coal. For the strength classification of weak rocks by using point load test, it seems to be more realistic to use uniaxial compressive strength values rather than point load strength index values. However, for the strength classification of rock materials by using point load test, it is recommended to use point load strength index values rather than uniaxial compressive strength values (ISRM 1985). This is due to the fact that the correlations between the point load strength index and uniaxial compressive strength values are only approximate as seen in Equation 2. However, this approach is likely to be valid for the rocks with moderate and high strengths.

The point load test, being almost a simulation of a laboratory compression test intended for use in the field, is very useful for strength classification of

intact rocks. Therefore, this test should be adapted for use in the strength classification of weak rocks with respect to point load strength index values, through intensive theoretical, laboratory, and field studies.

The prediction of rock strength using the NCB cone indenter test has been recommended to be accomplished considering the region and type of rocks (Bilgin & Shahriar, 1986). It has been reported that, in order to have similar uniaxial compressive strength values to those determined by compression tests, the equation coefficient proposed by NCB should be changed depending on the region and type of rock tested (Bilgin & Shahriar, 1986). Investigations into the reliability of the NCB cone indenter test for the strength classification of coals from different collieries are expected to improve our knowledge of the prediction of strength properties of coals.

The Schmidt hammer, one of the simplest and easiest- to -operate rock testing methods, overestimated the uniaxial compressive strength of the coals tested in this study. This may be due to the data processing method suggested by ISRM, in which only the top readings are considered for determination of Schmidt hammer hardness. However, it showed a very close agreement with the Hardgrove grindabİlity test indicating its potential for use in testing coal properties. Empirical equations correlating Schmidt hammer hardness with uniaxial compressive strength for coal with an acceptable accuracy may be established through consistent efforts carried out in this field.

Statistical evaluation of the test results indicated that, there was a very high correlation between the Schmidt hammer and Shore scleroscope hardness values (Fig. 10). There found to be no other statistically significant correlations between the mechanical index tests.

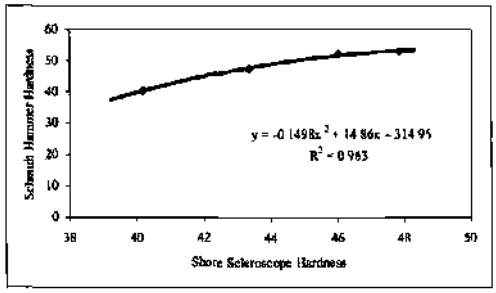

Figure 10. Relationship between Shore scleroscope and Schmidt hammer hardness.

Shore scleroscope and Schmidt hammer rebound tests seemed to be the most reliable means of hardness assessment for Çayırhan district coals.

5 CONCLUSIONS

Coal strength properties are known to affect the support capability of coal pillars and the cuttability and grindability of coal. However, these properties are difficult to determine, both in the field and in the laboratory, due to the brittle and visco-elastic nature of coal influenced by bedding planes and cleats. In this field, rock index tests can offer valuable data for strength characterization of coal in an economical and time-efficient manner.

Based on the results of comprehensive in-situ and laboratory rock and coal index tests described in this paper, the following conclusions can be drawn:

1. The Hardgrove grindability index, being an indicator of the ease of grinding or pulverization of coal, and being one of the significant parameters used in determining the capacity of a coal mill in a coal-fired power station, was found to be İn very high correlation with the results of Schmidt hammer and Shore scleroscope rebound tests for Çayırhan district coals. There is also a significant relationship between this index and NCB cone indenter hardness.

2. For the prediction of the uniaxial compressive strength of Çayırhan district coals, point load tests gave the most reliable results, similar to those determined by the compression tests conducted İn the laboratory. It seems to be more reliable to use point load strength test for weak rocks such like coal in order to predict their uniaxial compressive strength values, instead of characterizing these rocks with respect to their point load strength index values.

3. It was found to be possible, for the coals of Çayırhan Lignite Mine, to estimate the Schmidt hammer hardness from Shore scleroscope rebound tests, or vice versa, by using the regression equation given in Figure 10. However, if it is necessary to determine either of the two hardness properties, appropriate tests should be conducted.

The use of rock index tests for the classification of rock materials with respect to their strength properties largely depends on the statistical analysis carried out. Past experience and results of this study indicate that the equations proposed for the prediction of uniaxial compressive strength of rock are usually valid for specific site conditions and rock types. The rank, i.e., carbon content, ash content, density, and structural properties of coal should be taken into account when these tests are utilized for different coals.

ACKNOWLEDGEMENTS

The authors wish to thank Turkish Coal Enterprises (TKI) for permission to carry out in-situ investigations, Mr. Zafer Gencer from MTA of Turkey for his invaluable support during the Hardgrove grindability tests, and Prof. Dr. Osman Z. Hekimoglu from Dicle University for providing the NCB cone indenter test apparatus.

REFERENCES

ASTM, 1983. Standard test method for grindability of coal by the Hardgrove machine method. *Annual book of ASTM standards*. 05.05: 245-251.

Bieniawski, Z.T. 1975. The point load strength test in geotechnical practice. *Engineering Geology*. 9: 1-11.

Bilgin, N. & Shahriar, K. 1986. Evaluation of the indirect methods used in determination of some mechanical properties of rocks and coal seams. *Proceedings of the ht Turkish national symposium on rock mechanics*. 127-137.

Broch, E. & Franklin, J.A. 1972. The point-load strength test. *International Journal of Rock Mechanics and Mining Sciences and Geomechanics Abstracts*. 9: 669-697.

Evenden, M.P. & Edwards, J.S. 1985. Cutting theory and coal seam assessment techniques and their application to shearer design. *Mining Science and Technology. 2:* 253-270.

Gencer, Z. 1986. *The effect of physical and petrographical properties of coal on its binderless briquettabttity*. Technical report. Mineral Analysis and Technology Division of MTA of Turkey (Unpublished).

Göktan, R.M. & Ayday, C. 1993. A suggested improvement to the Schmidt rebound Hardness ISRM suggested method with particular reference to rock machineability. *International Journal of Rock Mechanics and Mining Sciences and Geomechanics Abstracts*. 30: 321-322.

Hardgrove, R.M. 1932. Grindability of coal. *Transactions of the American Society of Mechanical Engineers*. 54: 37-46.

Hoek, E. 1977. Rock mechanics laboratory testing in the context of a consulting engineering organization. *International Journal of Rock Mechanics and Mining Sciences and Geomechanics Abstracts*. 19:43-45.

Holmgeirsdottir, TH. & Thomas, P.R. 1998. Use of the D-762 shore hardness scleroscope for testing small rock volumes. *International Journal of Rock Mechanics and Mining Sciences and Geomechanics Abstracts*. 35: 85-92.

ISRM, 1978a. Suggested methods for determining hardness and abrasiveness of rocks. *International Journal of Rock Mechanics and Mining Sciences and Geomechanics Abstracts*. 15:89-97.

ISRM, 1978b. Suggested methods for determining tensile strength of rock materials. *International Journal of Rock Mechanics and Mining Sciences and Geomechanics Abstracts*. 15:99-103.

ISRM, 1979. Suggested methods for determining the uniaxial compressive strength and deformability of rock materials. *International Journal of Rock Mechanics and Mining Sciences and Geomechanics Abstracts*. 16: 135-140.

ISRM, 1985. Suggested method for determining point load strength. *International Journal of Rock Mechanics and Mining Sciences and Geomechanics Abstracts*. 22: 51 -60.

McFeat-Smith, I. 1977. Rock property testing for the assessment of tunnelling machine performance. *Tunnels and Tunnelling*. March: 29-33.

NCB, 1977. *NCB Cone indenter*. MRDE Handbook No.5. Staffordshire: Mining Research and Development Establishment.

O'Rourke, J.E. 1989. Rock index properties for geoengineering in underground development. *Mining Engineering*. 41: 106-110.

Roxborough, F.F., King, P. & Pedroncelli, EJ. 1981. Tests on the cutting performance of a continuous miner. *Journal of the South African Institute of Mining and Metallurgy*. January: 9-25.

Szwilski, A.B. 1985. Relation between the structural and physical properties of coal. *Mining Science and Technology. 2:* 181-189.

Tiryaki, B. 1998. *Optimisation of tool lacing parameters for drum shearers*. Ph-D. Thesis. Hacettepe University, Ankara, Turkey (Unpublished).

TKI, 1987. *Çayırhan Lignite Mine*. Introductory brochure. Beypazarı: Education centre at Çayırhan Lignite Mine.

Unal, E. 1974. *A study of load and convergence at two longwall faces and interpretation of strata behaviour at Orta Anadolu Linyitleri Collieries Beypazarı*. M.Sc. Thesis. Middle East Technical University, Ankara, Turkey (Unpublished).